Functional interchangeability of pharmaceutically equivalent oral controlled release dosage forms based on heterodisperse polysaccharides

Kelly, M. Louise

Award date:
1999

Awarding institution:
University of Bath

Functional interchangeability of pharmaceutically equivalent oral controlled release dosage forms based on heterodisperse polysaccharides

Submitted by
M. Louise Kelly BSc. Pharm., MPSNI
for the degree of Doctor of Philosophy
of the University of Bath

Louise Kelly
.....

ProQuest LLC
789 East Eisenhower Parkway
P.O. Box 1346
Ann Arbor, MI 48106-1346

Acknowledgements

I would like to thank my research supervisors, Dr Michael Tobyn and Professor John Staniforth, for their advice, bright ideas and friendship over the period of this work. I am grateful to have been able to avail of the excellent research facilities available in the department of Pharmacy and Pharmacology at Bath University and for the opportunities given to present my work at conferences.

I would also like to thank the technical staff and secretarial staff of the pharmacy department who were always willing to help in many ways. Special thanks to Jason McConville and Fraser Steele for their computer and technical expertise.

I can't forget all the postgraduate students and post doctoral staff of the Pharmaceutical Technology Group who provided lots of entertainment over the years. Very special thanks to Stanner's Soccer Superstars (SSS) for including me in their team line up. Thanks also to my flat mate Linda Cameron for her friendship and support.

This research would not have occurred without funding from Penwest Pharmaceuticals Co., Patterson, N.Y. to whom I am very grateful.

I am also indebted to Dr Ali Rajabi-Siahboomi for all his patience and co-operation in carrying out the gamma scintigraphy study and his assistance in analysing the results. Thanks also to Prof. John Staniforth for arranging funding for the scintigraphy study

Last but not least, I would like to thank my parents for all their help in many ways during the course of all my studies.

Summary

The release-controlling action of hydrophilic matrix tablets based on heterodisperse polysaccharides (HP) was investigated in relation to the initial physical characteristics of the tablets. Mercury intrusion porosimetry, surface area analysis by nitrogen adsorption, scanning electron microscopy and liquid penetration studies were used to characterise physical characteristics. Mercury porosimetry was selected as the primary source of physical data since reproducible and representative quantitative data were obtained.

HP-based granules were prepared and subsequently compacted into tablets under carefully controlled conditions. Quantification of porous structure showed that the tablets had different pore volumes and pore size distributions. The release of a highly water-soluble model drug from HP-based matrix tablets was found to be independent of initial dry matrix structure. A second model drug, having low water-solubility, was found to be released from HP-based tablets at a rate that was independent of the shape of the tablet and the force at which the tablet was compacted.

A theory of porosity-independent release was postulated and tested. The implications of this hypothesis are potentially far-reaching in relation to clinically and/or pharmaceutically equivalent controlled drug delivery systems. HP-based formulations were contained within hard gelatin capsules in the form of loose, uncompacted granules. This gave a very porous matrix system. The *in vitro* release profiles of slightly water-soluble and freely water-soluble model drugs from matrix capsules were similar to the release profiles obtained when the same materials were compacted into matrix tablets. Since capsule and tablet matrices had equivalent release profiles they were considered functionally interchangeable under the *in vitro* testing conditions employed. The dosage forms were also pharmaceutically equivalent since they contained the same formulation, processed in the same way. Such flexibility in oral controlled release systems has not been hither to described.

A gamma scintigraphy on pharmaceutically equivalent tablet and capsule matrices showed that capsule matrices fragmented earlier than tablets matrices but that capsule matrices still maintained a high degree of integrity as they passed down the GIT.

Table of contents

1. Introduction

1.1 Concepts of controlled release, hydrophilic matrices, functional interchangeability and pharmaceutical equivalence.

The majority of pharmaceutically active therapeutic agents are administered as solid oral dosage forms produced by the formulation and processing of powdered solids (1). For some drugs, delivery as an oral controlled release dosage form can provide greater safety and efficacy in therapeutics than conventional dosage forms. The purpose of controlled release systems is to optimise drug input rate into the systemic circulation in order to achieve a desirable and predictable pharmacodynamic response as well as to improve patient compliance, minimise side effects and maximise drug product efficacy. Controlled release dosage forms can have pharmacoeconomic value since they often lead to greater clinical effectiveness, fewer adverse side effects requiring treatment and economic benefits where increased patient compliance is associated with increased cure rates, reduced length of treatment and lower medical care costs (2). The majority of controlled release preparations are designed for prolonged release with prolonged therapeutic effect making them suitable for chronic administration.

The hydrophilic matrix (HM) is a popular and widely used strategy for achieving controlled release drug delivery. HM's can be easily prepared by distributing a drug through a hydrophilic carrier, frequently a polysaccharide, and either compacting the material into tablets or containing it within a hard gelatin capsule. This principle has been successfully applied for several drugs as exemplified by the marketed controlled release tablets of felodipine (Plendil®, Astra), nifedipine (Nifelan®, Elan) and alprazolam (Xanax®XR, Pharmacia/Upjohn). Some of the perceived advantages of HM over alternative controlled release technologies, such as reservoir, hydrogel and osmotic systems, are listed in table 1.1 (3).

HM formulations are more commonly presented in tablet than capsule form. Controlled released capsule formulations are often complex and generally consist of the active ingredient formulated as multiple unit dosage forms contained within a hard gelatin capsule. The sub-units are usually based on microgranules, spheroids, beads or pellets and can be produced using a wide range of technologies. In a review of controlled release delivery of some water-soluble drugs, Khan (4) described some methods that have been used to formulate controlled release sub-units. This included spheroids produced by loading a drug onto a water-insoluble but swellable non-ionic polymer then coating with a slightly water permeable polymer; microgranules produced

by granulating a drug with water-soluble polymers then coating the granules with wax like substances or with permeable hydrophobic polymers, and beads and pellets produced by attaching a drug to a solid inert carrier then coating with soluble film forming polymers such as polymethacrylates. Marketed controlled released capsule dosage forms based on multiple unit dosage forms contained within a hard gelatin capsule shell include Minocin MR® (minocycline HCl, Lederle) and Indomax 75 SR® (indomethacin, Ashbourne Pharmaceuticals Ltd.). Dilacor XR™, a proprietary formulation of diltiazem HCl, is more unusual in that it consists of 3 or 4 mini tablets contained within a capsule (5). Each tablet consists of three layers. The faster hydrating core layer contains 60mg of the active drug. Two external layers sandwiched around the core limit drug release from the lateral side of a cylindrical shaped tablet. The matrix is hydrophilic and releases through a swollen gel structure over 24hr (5).

In the U.K. it is common for drugs delivered as immediate release solid dosage forms to be formulated as capsule preparations at one drug strength and in tablet form at another drug strength. For example, the anti-depressant drug dothiepin, is marketed by Boots as Prothiaden® 25mg capsules and Prothiaden® 75mg tablets, while the anti-infammatory drug, mefenamic acid, is marketed by Parke-Davis as Ponstan® 250mg capsules and Ponstan® 500mg tablets. For controlled release products it is usual for any one company to manufacture a drug in either capsule or tablet form, but it is unusual for both controlled release tablets and capsules to be manufactured by the same company. This possibly reflects the high development and production costs involved in producing two controlled release dosage form technologies. However, for drugs that are no longer under patent protection, and have a high market share, it is common for one company to market the drug in capsule form and for another company to market the drug in tablet form. For example, the calcium-channel blocker diltiazem HCl is marketed by Lorex Pharmaceuticals Ltd. as Tildiem Retard® 90mg and 120mg tablets and by Napp Laboratories Ltd. as Adizem-SR® 90mg, 120mg and 180mg capsules. Similarly, the coronary vasodilator, isosorbide dinitrate, is marketed by Zeneca Pharma as Sorbid SA® 20mg capsules, and by Schwarz Pharma Ltd. as Isoket retard® 20mg tablets.

In the U.K, a pharmacist presented with a prescription for any generically written solid oral dosage form must dispense the dosage form presentation indicated on the prescription. This means that when a drug is prescribed the practitioner must specify whether a capsule or tablet dosage form presentation is required. Similarly, in the USA, a practitioner must specify the dosage form to be dispensed. However, in 1997 the standards division of the United States Pharmacoepia (USP) suggested that the concept

of functional interchangablility of solid oral dosage forms should be adopted by the USP (174). The division of standards recommended that USP general notices and requirements include the following statement; 'Unless otherwise stated in the individual monograph, tablets and capsules prepared with the same active substance and of the same release rate classification (e.g. prompt release) are considered to be functionally interchangeable'. This would mean that any specific official USP solid oral dosage form could be dispensed regardless of whether it was formulated as a tablet or a capsule. However, three criteria must be met:

(1) the articles contain the same active ingredients
(2) the articles contain the same amount of active ingredient
(3) the articles' release characteristics are the same

The practical implication of functional interchangeability means that either a capsule or tablet form could be dispensed, depending on the patients needs and/or desires, as long as the two preparations contained the same drug in the same quantity and had equivalent release profiles. However, there would be no requirement for the tablets and capsules to contain the same excipients or for the formulations to be processed in the same way. Functional interchangeability could for example, exist between a hydrophilic matrix tablet and a capsule containing the drug formulated as controlled release pellets, even if the formulations contained different excipients and were processed in different ways.

A new direction in oral controlled release technology would be solid oral dosage forms that could be considered functionally interchangeable and yet remain pharmaceutically equivalent. This would mean that the articles would contain the same active ingredient, the same amount of active ingredient, have the same release characteristics and also contain the same excipients, processed in the same way. The potential advantage of such a system would be the possible reduction in research, development and manufacturing costs involved in producing two dosage form presentations of the same active ingredient since capsules and tablets would be composed of the same formulation, processed in the same way. The possibility of achieving functional interchangeability and pharmaceutical equivalence in oral controlled release tablets and capsules using heterodisperse polysaccharides has been investigated here.

Perceived advantages of hydrophilic matrices over other controlled release dosage systems
Simplicity of formulation
High drug loading: their capacity to incorporate active principles is large, which makes them suitable for the delivery of large doses.
Economically efficient excipients
Wide range of carriers approved for oral use are available
Low capital equipment costs: the dosage forms may be manufactured using standard powder processing and tabletting equipment
The possibility of dose 'dumping' is low
Bioerodable: HM systems erode as they pass down the GI tract avoiding the potential accumulation of 'ghost' dosage forms in the body.
The systems depend on both erosion and diffusion, and therefore drug release is not entirely dependent on GI motility
Versatility: systems formulations can be formulated as 'mini-matrices' or floating tablets

Table 1.1 Perceived advantages of HM over other controlled release dosage systems (3).

1.2 Hydration of and drug release from hydrophilic matrices

When a dry (or glassy) HM comes into contact with an aqueous medium, the solvent (usually water) penetrates the free spaces between the macromolecular chains. A relatively impermeable gelatinous surface barrier develops, which retards further ingress of water and acts as a rate-controlling barrier to drug release (6). As water penetrates into the dosage form the thickness of the gel-like layer increases and the outer layers become progressively more hydrated. Movement of drug from an erodible swollen HM into the surrounding medium occurs in two ways. Water-soluble drugs undergo dissolution as they are exposed to an aqueous solvent front and begin to diffuse through the tortuous network of the swollen gel (6). As the solvent front moves further into the matrix the distance that the dissolved molecules must travel to reach the solvent-matrix interface increases. In addition, the progressive swelling leads to an increase in the volume of the swollen network and therefore a further increase in the diffusional pathway. Release by diffusion shows time-dependent kinetics with a high rate of release

observed at the beginning of the process, which decreases with time in an exponential way. Drug release can also occur via attrition of the outer surface of the swollen polymer (7). For poorly water-soluble drugs this is frequently the primary mechanism of release (6) although some degree of release by erosion will also exist for water-soluble drugs. The presence of a solvent front, the potential for unlimited swelling and the combined controlling mechanism of diffusion and erosion are the distinguishing features of HM's. Such dosage forms differ from the swellable but effectively insoluble cross-linked polymers commonly known as hydrogels.

Studies using cryogenic SEM have provided evidence that the gel-like layer within hydrated hydroxypropylmethylcellulose (HPMC) matrices might not be homogenous and may have a complex internal microstructure (8). It has also been shown that gas bubbles form an important structural feature of the hydrated surface layer of HPMC matrices (9). Direct visual evidence suggests that air bubbles originate from void spaces within the core tablet (10). The internal structure of the hydrated layer formed by sodium alginate matrices in simulated gastric fluid has been shown to differ markedly from the structure formed in simulated intestinal fluid (11). It has been suggested that the structure of the gel-like layer of hydrated HM's may be important in controlling drug release (10,11).

1.3 **Kinetics of drug release from hydrophilic matrices**

The overall rate of drug release rate from HM's generally follows first-order kinetics, a potential drawback of matrix systems that have conventional geometry such as spheres, cylinders and slabs (12). However, zero-order release profiles have been achieved (13-15) and even bimodal release kinetics have been reported (16). The kinetics of drug release is thought to be determined by the relative movements of boundaries that exist within a hydrated matrix (17). Up to three boundaries have been defined in hydrating matrices. The boundary that separates the swollen matrix from the dissolution medium is commonly known as the erosion front, while the boundary that separates swollen polymer from dry (or glassy) polymer is known as the swelling front (17). Lee *et al.* (18) and Colombo *et al.* (17) have described the possibility of the presence of a third front; the boundary between undissolved and dissolved drug. This front has been termed the diffusion front and can occur under certain conditions of drug loading and drug solubility and will only be observed when it is not coincident with the swelling front. Movement of the swelling front, diffusion front and erosion fronts are

thought to be associated with rate of water uptake, rate of dissolution and rate of matrix erosion, respectively (17). Colombo *et al.* (17) proposed that when a polymer is sufficiently soluble the erosion front can synchronise with the swelling front leading to zero-order release kinetics provided that the releasing area is constant. Drug release from such systems will be linear because the distance over which the drug molecules must diffuse to reach the tablet surface will remain roughly constant. Under certain conditions of drug solubility and loading the erosion and swelling fronts can move separately and the difference between the erosion and diffusion fronts is thought to be decisive for release kinetics (17). Zero-order dissolution profiles for water-soluble drugs are not generally obtained with gelling agents comprising non-ionic cellulose ethers alone. By mixing combinations of HPMC and the more water-soluble polymer, sodium carboxymethylcellulose, zero-order release kinetics have been achieved (13,14). This has been attributed to the rate of advancement of the swelling front being similar to the rate of erosion (19). However, after assaying tablet erosion Vazquez *et al.* (15) concluded that although erosion mechanism may contribute to the observed zero-order dissolution kinetics other factors are probably involved.

The apparent simplicity of the formulation and behaviour of HM devices belies the fact that the mechanism of drug release from matrices is probably a very complex phenomenon. Consequently, the process is difficult to model because so many different processes may be contributing. The mathematical analysis of release kinetics from HM's is also complicated by the presence of a moving diffusional front and an eroding polymer front. The mathematical descriptions of such mass transfer problems involving moving boundaries are known as Stefan problems (20). Simple pseudo-steady state approximations have been used to analyse the kinetics of release of a dispersed solute from a polymer matrix, the most common one being Higuchi's treatment for a non-erodible matrix under perfect sink conditions (21,22). This approach involves fitting cumulative release data to the square root of time, providing limited quantitative data. The pseudosteady state approach assumes a linear solute concentration profile, which is valid only when the solute loading is in excess of the solute solubility. However, in reality this is not always the case (20). Release data has also been analysed using the simple exponential equation developed by Ritger and Peppas (23), where the fraction released is proportional to t^n, n being a diffusional coefficient indicative of the mechanism of drug release. Although the Higuchi and Ritger treatments are widely applied in the literature to swellable matrix systems they are only approximations to complex moving boundary problems.

1.4 Hydrophilic matrix carriers

Rapid hydration and swelling of individual polymer particles, and their coalescence to form a gel matrix is the key to the successful performance of a HM. An ideal HM carrier would also behave independently of pH and ionic strength, would be inexpensive, cost effective, regulatory authority-acceptable, inert, easily processed and versatile so that a wide range of release profiles could be obtained. At present, no HM carrier fulfils all of the foregoing desirable qualities. The most widely used and the most intensely studied HM carriers are the cellulose ethers, in particular hydroxypropylmethylcellulose (HPMC). Grades of hydroxypropylcellulose (HPC) and sodium carboxymethylcellulose (NaCMC) are actively promoted as HM carriers for controlled release tablet formulations by their manufacturers. The low cost of thermally modified starches has prompted renewed interest in their use as HM carriers (24). Sanchez *et al.* (25) reported the use of a thermally modified wheat starch by a gelatinisation/freeze-drying technique. Chitosan has been shown to act as an effective carrier in acid conditions. However, in water or simulated intestinal fluid, disintegration and rapid drug release occurs (26). The release controlling action of polyvinylalcohol has been investigated (17,27). Xanthan gum is a more recent HM carrier and its behaviour as a sustained release excipient has been investigated extensively by Talukdar *et al.* (28-30). Scleroglucan successfully forms HM tablets at physiological pH's, and in many other aspects behaves as a nonionic polysaccharide carrier similar to the cellulose ethers (24). Te Wierik *et al.* (31) have shown that amylodextrins possess the characteristics of a controlled release excipient. Carbopol is a cross-linked polymer of acrylic acid that has also been used as a HM carrier (32,33). Under acidic conditions the material is unionised however, as neutral pH's the carboxylic acid groups ionise. This creates a low pH environment that has been used advantageously to control the release of a basic compound (33). A number of combinations of HM carriers have been studied in the literature. Combinations of HPMC/NaCMC have been used to optimise drug release profiles (14,19,34). A HM consisting of pectin and HPMC has been used to optimise the release of diltiazem HCl from a simple tablet matrix (5). Combinations of locust bean gum and xanthan gum have been investigated (35) and the technological characteristics and release retarding action of xanthan gum and guar gum have also been considered (36). The wide range of materials that have been investigated as potential HM carriers reflects the extensive and continued interest in HM dosage forms.

1.5 Structure and properties of heterodisperse polysaccharides

A controlled release tabletting excipient that utilises the synergistic interaction that occurs between the heteropolysaccharide, xanthan gum and the homopolysaccharide, locust bean gum in the presence of secondary and tertiary components has been developed by Penwest Pharmaceuticals Co., Patterson, NY, USA. The individual components are wet massed using a high shear mixer producing a heterodisperse (HP)-based material that is easily compacted into tablets (37). Some of the properties of this system (TIMERx™) have been described previously (38). A review of the characteristics of the individual components of the excipient and the possible nature of the synergistic interaction is given.

1.5.1 *Xanthan gum: structure and properties*

Xanthan gum (XG) is a water-soluble anionic polysaccharide produced on a commercial basis by viscous fermentation of the bacterium *xanthomonas campestris* (39). XG gained food approval in the United States in 1969 and is now widely used in the food industry because of its unique and useful properties (40). It also finds many applications in the textile and cosmetic industry (40).

The primary structure of xanthan, shown in figure 1.1, is a β (1→4)-linked D-glucose mainchain with a trisaccharide side-chain attached to the 3 position of every second glucose giving a pentasaccharide repeating unit. The trisaccharide side chain is made up of a β-(1→4) linked D-mannose, an α-(1→2) linked glucuronic acid and an α-D-mannose. The α and β linked mannose units are variably acetylated and pyruvylated respectively (41).

At temperatures greater than 60°C and at low ionic strength xanthan chains exist in aqueous solution in an essentially disordered state resulting in a solution that has a low viscosity (39). Reduction in temperature and/or the addition of salt induces a sharp transition to an ordered structure that has been identified by x-ray fibre diffraction analysis as a 5-fold helix (42). The negatively charged side chains align with the backbone and the overall structure is stabilised with hydrogen bonds (39).

XG molecules have a high hydrodynamic volume and even at low concentrations, XG exhibits weak gel features that are of considerable technological value in, for example, the suspension of solid particles or the stabilisation of emulsions (39). At low concentrations, solutions of XG exhibit high viscosity's compared to those of most other polymers (39). As the concentration of gum is increased, a peak viscosity is reached

owing to the high affinity of XG for water. The peak occurs at a relatively low concentration owing to XG having a high affinity for water (39). At all concentrations, solutions of XG are viscoelastic: they always have a degree of mobility and when the two are brought together, they coalesce (39). At rest, the molecules associate into complex aggregates stabilised by hydrogen bonding imparting a high elastic modulus to the material. When shear is applied, the aggregates are disrupted with a resultant decrease in viscosity. The process is reversible and when the shear is removed the system returns to its originally high viscosity (41). The degree of pseudoplasticity of XG is higher than that of any other FDA-approved gums (39).

The viscosity of solutions of XG have been shown to be almost independent of pH changes (43). The behaviour of XG solutions in the presence of salts has been shown to be complex and appears to depend on the concentration of the gum. Zatz and Knapp (44) reported that a 0.3% solution of XG exhibited negligible viscosity change when either calcium chloride, sodium citrate or sodium chloride was added. Solutions containing higher concentrations of XG showed increased viscosity while solutions containing lower concentrations of XG underwent a reduction in viscosity. As the quantity of salt added to solutions containing high concentrations of XG was increased, a limiting viscosity was observed. Each of the salts appeared to be equally effective in changing the viscosity, suggesting that intermolecular charge repulsion was not a primary factor in these salt effects on viscosity. These results confirmed the finding of Rocks (43) who reported that solutions containing greater than 0.5% XG increased in viscosity on addition of salt.

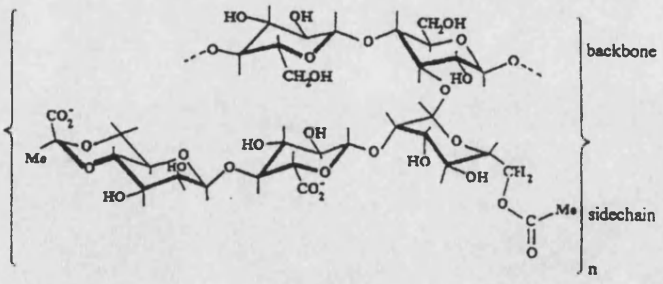

Figure 1.1 Primary structure of xanthan gum

1.5.2 *Locust bean gum: structure and properties*

Locust bean gum (LBG) is a galactomannan obtained from the species *ceratonia siliqua,* also known as the carob plant (45). The gum portion of carob pods is the endosperm, which is contained within the seeds of the pod. Specks of brown that may be seen in the gum are remains of the dark brown rusk that surrounds the endosperm. Galactomannans are polysaccharides that consist of a β-(1→4)-D-mannan backbone incompletely and irregularly substituted with single α-(1→6)-linked D-galactose side chains, (figure 1.2), with the galactose substituents occurring in cluster ('hairy regions') interspersed with unsubstituted mannan backbone ('smooth regions') (46). Locust bean gum has a molecular weight of approximately 2.6×10^6 and a mannose to galactose ratio in the region of 3.5:1 (47).

Solutions of LBG show characteristics of hyperentangled macromolecules (48). In contrast to XG, LBG is only slowly soluble and ungelled at low temperatures. Prolonged exposure to the dissolution media allows molecules to associate and undergo gelation as the result of intermolecular cross-linking in 'smooth' regions of the chain. Most of the gum will disperse in concentrations up to 5% but part remains as insoluble flocs that settle on standing (45). Dispersions that are first heated to approximately 95°C have a much higher viscosity than dispersions made in cold water so to obtain the greatest efficiency as a thickener dispersions are made in hot water and then cooled (45). LBG solutions are pseudoplastic (49) and since LBG is a neutral polysaccharide pH has little influence on the viscosity of solutions in the range pH 3 to 11 (49).

LBG is widely used in the food, textile and cosmetic industry. Its binding and stabilising properties are utilised in ice cream and sausage making, its heat-shock resistance is utilised in ice-cream making, while its thickening action is utilised in lotions, creams and print pastes (45).

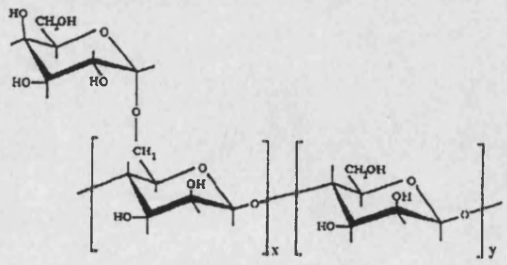

Figure 1.2 Primary structure of locust bean gum (x and y = 3 or 4)

1.5.3 *Xanthan gum/locust bean gum synergism*

When aqueous solutions of XG and LBG are mixed together, an interaction between the two polysaccharides occurs that results in the formation of a firm, thermoreversible gel with synergistic effects (47). Gels can be formed at room temperature using 0.2% total polysaccharide concentration (50). Solutions of mixed gums are associated with a high elastic modulus (50). The dynamic modulus of mixed gum systems is nearly independent of pH between pH values of 5 to 10 but decreases rapidly below 5 (40). Dynamic modulus is decreased in the presence of urea suggesting that hydrogen bonding is involved (40). Mixed systems are characterised by sharp setting and melting behaviour consistent with co-operative transitions and cross-linking by ordered non-covalent associations (51). The rheological behaviour of XG and all LBG/XG mixed systems is typical of weak gels (48). Various XG/LBG ratios have been suggested as optimal ratios. Copetti *et al.* (48) found that in mixed systems the maximum viscosity, and maximum elastic modulus occurred when the ratio of XG to LBG was 1:1, while Tako *et al.* (50) reported a maximum dynamic modulus at a XG:LBG ratio of 1:2. Mannion *et al.* (35) found that when XG and LBG were mixed in various proportions there was no significant effect on the viscous component, but significant increases in the elastic component with maximum synergy occurring at a polymer ratio of 70% XG to 30% LBG. This indicated that mixing the two polymers resulted in significant increases in gel strength but not in viscosity. HM tablets produced from the gums were shown to provide significantly slower release of a poorly water-soluble drug than from XG alone, with the greatest prolongation of release occurring at the polymer ratio corresponding to the greatest rheological synergy.

The synergistic interaction between galactomannans and XG was first reported by Rocks in 1971 (43), since when a large number of techniques have been used by various researchers to try and determine the precise nature of this interaction. The 'lock and key' model first proposed by Rocks (43) and supported by Tako (52) suggested that interaction occurs with xanthan molecules in a 5-fold, single-stranded helical structure with the side chains inserted into adjacent unsubstituted segments of the LBG backbone. A second model, proposed by Dea *et al.* (46), attributes the synergistic effect to an interaction between the xanthan helix and the unsubstituted or poorly substituted ('smooth') regions of the galactomannan. This was supported by the observation that the interaction between xanthan and galactomannans was heavily dependent on the amount and distribution of galactose. Cairns *et al.* (53,54) suggested that it was necessary for xanthan to be denatured before gelling would occur and suggested a sandwich model for

xanthan/galactomannan junction zones. In this model galactomannan chains are sandwiched between two xanthan chains the latter being in the disordered confirmation with the first xanthan chain running parallel to the second. Hydrogen bonding between OH-3 groups on the galactomannan and OH-4 of the inner mannose on the xanthan backbone and hydrophobic interactions at xanthan and locust bean contact points would stabilise the structure. From observations of mechanical spectra and rheological studies Copetti *et al.* (48) suggested the coexistence within the structure of mixed gels of both heterotypic LBG-XG and homotypic XG-XG junction zones, in which the xanthan chains retain their ordered helical conformation, thus supporting the original model described by Dea *et al.* (51) and Morris *et al.* (55). The exact mechanism of interaction between the two polysaccharides is still under debate but is important since the production of high gel strengths at low polymer concentrations has implications in the pharmaceutical, food and textile industries.

1.5.4 *Secondary and tertiary components of TIMERxN*

A secondary component, glucose, is dispersed throughout the polysaccharide network and is thought to potentiate the solubilisation of the gums (38). A percentage of calcium sulphate is added, which is believed to enhance gel rigidity. The role of calcium ions in the gelation of a number of polysaccharides has been documented. Calcium ions have been shown to favour the gelling of carrageenan solutions (56). The elastic modulus of water-soluble polysaccharides extracted from proliferating marine green seaweeds (*Ulva* spp.) was found to increase in the presence of calcium ion and boric acid (57). The addition of calcium chloride to matrices containing sodium alginate has been shown to prolong the release of chlorpheniramine maleate in simulated intestinal fluid (58). This was thought to be due to the interaction that occurs between sodium alginate and calcium ions at neutral pH (58). Contradictory results were reported by Stockwell *et al.* (59) who found that an alginate gel system without calcium, in the presence of acid, formed a compact rigid gel with a low water content. In the presence of calcium ions, a more open gel structure with a higher water content was formed, which was attributed to the formation of cross-linkages in the gel. The rate of release of three water-soluble model drugs from sodium alginate matrices was greater in the presence of calcium. It was thought that this was due to the more open diffusional pathway in the cross-linked gel.

Ethylcellulose is an inert, water insoluble, hydrophobic polymer. It has been used in conjunction with hydrophilic excipients to produce swellable matrix tablets (60). It is proposed that ethylcellulose can act as a binder and contribute to the structure of the hydrated layer.

1.6 **Factors affecting drug release from hydrophilic matrix tablets**

Factors affecting drug release from hydrophilic matrices have been the subject of many publications (eg 6). A complex situation exists in which the overall rate of release is dependent on many interacting factors operating in the system at any one time. As HPMC is extensively used as the base excipient for controlled release, most work in the area has been on this material. A review of the factors that have previously been investigated in relation to the release of solute from hydrophilic matrices is given.

1.6.1 ***Physical and chemical characteristics of the polymer***

1.6.1.1 *Viscosity*

The viscous properties of polymers in HM tablets have been shown to be important in determining the final release controlling action of the dosage form. Nakano *et al.* (61) found that the release of theophylline from hydroxypropylcellulose (HPC) matrices decreased as the viscosity grade of the HPC increased while Daly *et al.* (62) demonstrated the same effect for the release of chlorpheniramine from low viscosity grades of Methocel. Ford *et al.* (63) studied the release rates of aminophylline and propranolol hydrochloride from matrices containing HPMC K100, HPMC K4M, HPMC K15M and HMPC K100M (viscosity's of 2% aqueous solutions were 106, 3850, 12449 and 93000 cps, respectively). They found similar release rates from the K4M, K15M and K100M grades but under the same conditions K100, the lower viscosity grade gave consistently higher release rates. The idea of a 'limiting HPMC viscosity' was also proposed by Sung *et al.* (64) who, for the systems under consideration, found that drug release no longer decreased when the viscosity increased above 15000Pa. Interestingly, no 'limiting HPMC viscosity' was observed for HPMC dissolution from the series of formulations studied.

1.6.1.2 *Substitution type*

Three substitution types of HPMC (2906, 2910 and 2208) are described in the USP (65). Different proportions of hydrophobic methoxyl groups and of hydrophilic hydroxypropyl groups characterise the three polymer types. The three substitution types have been shown to control the release of water-soluble model drugs to the same degree (66,67). Differences in the release rate of a poorly water-soluble model from different polymer substituents have been observed (67). Drug release paralleled the erosion of polymer from matrix tablets but was not directly related to the rheological behaviour of the polymers. Dahl *et al.* (68) found that the dissolution of naproxen from different lots of HMPC 2208 was directly proportional to the hydroxypropyl content. The slower dissolution observed when tablets contained HPMC 2208 substituted with low quantities of hydroxypropyl groups was considered due to the greater hydrophobicity of the tablets.

1.6.1.3 *Polymer concentration*

It has been shown by a number of workers that as drug/polymer ratio is increased the rate of release of the drug decreases (6,25,63,69,70). This is likely to be due to an increased tortuosity in concentrated gel layers, which would increase diffusional path length and decrease release rates. It has also been proposed that increasing the total polymer content can influence the surface area of the matrix, which in turn controls the release rate (63). Mathematical relationships between polymer concentration and drug release have been proposed. Ford *et al.* (63) studied the rate of release of propranolol HCl and aminophylline from HPMC matrices of various grades at various concentrations. They found a linear relationship between the rate of release, calculated as the slope of square root of time versus percentage released curve, and the reciprocal of the tablet content of HPMC. Using four soluble drugs, Baveja *et al.* (34) concluded that a linear relationship existed between the time taken to release 50% of drug from the matrix ($t_{50\%}$) and the ratio of total gum to drug in the tablet (G/D). The relationship held for both HPMC alone and matrices containing a combination of HPMC and NaCMC.

1.6.1.4 *Particle size*

Particle size has been shown to be important in determining the release controlling action of HPMC and XG. The effects have been attributed to differences in hydration between coarse and finer fractions (6,71) and relative lack of carrier when coarse particle sizes are used (72). The effect of Methocel K15M particle size on release of promethazine HCl was found to depend on the percentage of HPMC in the matrix

(72). At a HPMC loading of 64% similar release profiles were obtained using particle size fractions ranging from greater than 355μm to less than 75μm. At a 26% HPMC loading, sieve fractions having a particle size greater than 355μm and 210 to 355μm gave a burst release of drug. It was proposed that increased dissolution rates were due to the relative lack of HPMC in the matrix. In tablets containing a low proportion of polymer in the form of coarse particles it was thought that distribution of the polymer around the drug was not sufficient to form a protective barrier. Areas poor in polymer were likely to leach drug quickly producing a burst effect and the absence of polymer facilitated the rapid penetration of water into the inner regions of the tablet. Water uptake studies, measured by differential scanning calorimetry, indicated that initially larger size fractions imbibed water faster than smaller size fractions. This was in contrast to the proposal by Alderman (6) that burst release of riboflavin from matrices containing a low proportion of coarse Methocel K4M granules, was due to slow hydration of these particles, although experimental data to confirm this was not presented. Similarly, burst release of acetaminophen from xanthan gum matrices prepared with relatively coarse particle size fractions (74 to 100μm and 177 to 420μm) was attributed to slow hydration of these particles (71). Particle sizes less than 74μm were effective in sustaining drug release. Again, the effects may have been due to relative lack of carrier, and not differences in hydration rates as proposed. Burst release due to coarse particles has been shown to be more pronounced for less hydrophilic grades of Methocel (73).

1.6.1.5 *Moisture content*

Mosquera *et al.* (74) showed that variations in the moisture content of HPMC matrices, despite having an effect on the compression behaviour of the HPMC itself and on the mechanical properties of tablets made from it, had no effect on the dissolution rate of the poorly soluble drug hydrochlorthiazide from the matrices.

1.6.2 ***Physical and chemical characteristics of the drug and other excipients***

The solute contained within a matrix can play an active role in determining its own release rate. Additionally, the presence of non-polymeric excipients can play a part in controlling the rate and kinetics of drug release.

1.6.2.1 *Drug solubility, particle size, molecular weight and wettability*

Drug solubility is important in determining release rates since water-soluble drugs must firstly dissolve before they diffuse through the matrix while water-insoluble drugs can only be released by erosion of the matrix (6,75). Although drug solubility is important, a review of the literature suggests that there is no direct relationship between drug solubility and release rates. Ranga-Rao *et al.* (76) studied the release of 23 drugs of various solubilities and molecular sizes through matrices of Methocel K4M and mixtures of Methocel K4M and NaCMC. It was concluded that the differences in profiles observed could not be explained based on those two parameters alone. Furthermore, the release phenomena observed for Methocel K4M matrices did not always apply to Methocel K4M/NaCMC matrices for the same solutes. It was concluded that other factors might be governing drug release including; interactions between the polymers and drug; penetration of the solvent into the matrix; erosion of the swollen gel; influence of the drug on gel erosion and solubilisation of the drug by the polymer. Baveja *et al.* (77) took a series of structurally related water-soluble bronchodilators and studied the dissolution from HPMC based matrices. Although the drugs had almost identical aqueous solubilities, they showed different release rates from the tablets. The difference was observed in all three grades of HPMC studied. Release rates were correlated with the accessible surface area of the drug, a parameter that was mathematically derived, and the relationship was tested with another similar chemical entity. Good agreement with the predicted result was obtained. Tahara *et al.* (78) found that with model drugs having solubilities between 0.05% and 0.5%, dissolution rates increased with drug solubility. For model drugs having solubilities greater than 0.5% dissolution rates were found to be less influenced by drug solubility.

Malamataris and Ganderton (79) looked at diffusion and erosion in a matrix consisting of an insoluble hydrophobic material (hydrogenated vegetable oil) and a hydrophilic gel forming material (carboxypolymethylene) using indomethacin, ibuprofen and diclofenac sodium as model drugs. They postulated that matrices containing the water-soluble, wettable diclofenac sodium could accommodate the swelling of the gel and release was achieved through diffusion and erosion of the gel. However, with the less wettable ibuprofen, the matrix eroded rapidly due to deaggregation caused by the inability of the matrix to accommodate the swelling of the hydrophilic part.

Different particle size fractions of propranolol HCl and aminophylline (63 to 90μm, 125 to 180μm and 180 to 250μm) have been shown to be released at equivalent rates from HPMC matrices (63). Ford *et al.* (80) indicated that as the particle size of

promethazine HCl (a highly water-soluble drug) was increased from 45 to 63μm to 500 to 750μm, only a 12% change in dissolution rate was observed. For the poorly soluble drug, indomethacin, release rates from HPMC matrices decreased as particle size of indomethacin increased (75).

1.6.2.2 *Drug loading*

Release rates can be affected by the total concentration of drug in the matrix. The dissolution of caffeine and potassium chloride (KCl) at different drug loadings from polyvinylpropylene matrices has been studied and percolation theory used to interpret the results (81). For all caffeine loadings there was a poor correlation when the percentage released was plotted against $\sqrt{t}$. With KCl the correlation was good when the drug loading was > 30%. For caffeine a better fit was obtained when the amount released (Q_t) was plotted against time. Using linear regression the slopes of the Q_t/t curves were calculated then normalised to give a theoretical release rate. For drug loadings of caffeine greater than 70% w/w, the experimental values were below the theoretical value. The 70% drug loading was regarded as the percolation threshold above which the polymer ceased to span the tablet and instead formed finite clusters which insulated the caffeine in those regions producing a slower than predicted release rate. The percolation threshold was lower for KCl (10% w/w), which was attributed to the larger particle size of this material.

Drug loading also influences release when the drug itself contributes to the hydration and swelling of the matrix. Mitchell *et al.* (82) showed that as the concentration of propranolol hydrochloride in HPMC matrices was reduced the ability of the matrices to sustain the release of drug decreased. The drug appeared to be involved in maintaining the integrity of the matrix probably by affecting the gelation temperature of the polymer (see section 1.6.3.3).

1.6.3 ***Matrix component interactions***

There is considerable potential for interaction between the polymer network, added excipients and drugs that may influence release profiles. The presence of drug or additive in the hydrophilic matrix is likely to influence release by two mechanisms

1. By changing the rate of hydration, swelling and/or erosion of the matrix
2. By altering the tortuosity of the swollen network thereby changing diffusional path length.

1.6.3.1 *Physical effects*

Highly swollen gel systems can be considered analogous to porous media with the permeable regions serving as the pores and the impermeable regions as the walls. If there is no interaction between the polymer chains and the drug then the effect of the polymer chains on the diffusion process may be one of geometrical obstruction. Areas of obstruction caused by insoluble excipients, amorphous polymeric areas or poorly hydrated regions potentially could increase the tortuosity. Alternatively, dissolution of soluble components could leave a matrix of high porosity and low tortuosity, which would allow rapid diffusion of drug and rapid matrix erosion.

Ford et *al.* (63) found that replacement of HPMC by a soluble or insoluble diluent increased dissolution rates of model drugs. Only at high diluent levels did differences become apparent between the soluble diluent lactose and the insoluble diluent calcium phosphate. The results confirmed the findings of Lapidus and Lordi (83) but contradicted the statement by Alderman (6) that as little as 10% insoluble solids such as calcium phosphate may destroy sustained release from HPMC matrices by producing a lack of content uniformity of the gel.

1.6.3.2 *Swelling effects*

It is known that drugs and additives can actively contribute to the swelling of hydrophilic matrices. The swelling of matrices of either Methocel K100MCR or polyethylene oxide have been shown to be greater in the presence of the water-soluble drug, propranolol HCl, than in the presence of the insoluble drug, flurbiprofen (84). The results were attributed to variations in the rate of water penetration. In polyethylene oxide matrices, which exhibited greater swelling than Methocel K100MCR matrices, release kinetics appeared to be affected to a greater extent by polymer hydration and swelling. The phenomenon was more profound with the soluble material propranolol HCl. Propranolol HCl and tetracycline HCl have been shown to play an active role in the swelling behaviour of HPMC matrices (82). The drugs were thought to enhance the solubility of the polymer causing it to hydrate and gel more rapidly. Talkudar and Kinget (28) postulated that sodium indomethacin contributed to the swelling of XG tablets by means of an osmotic or plasticising effect. Fluorescein has been show to increase the transient gel layer thickness of HPMC tablets because of the additional osmotic contribution (85).

1.6.3.3 *Thermal hydration*

Cellulose ethers exhibit the property of thermal gelation, which is often quantified using gelation temperatures, defined as the temperature at which the relative viscosity of a solution is at its minimum value on the viscosity-temperature curve (86). The gelation behaviour may be explained as follows: in a solution state at low temperature, molecules are hydrated and there is little polymer-polymer interaction. As the temperature of the solution or gel rises, the molecules gradually lose their water of hydration. When sufficient, but not complete dehydration of the polymer occurs, a polymer-polymer association takes place and causes a high viscosity gel to form. The temperature at which gelation occurs and the strength of thermal gels are affected by the type and degree of substitution present, the concentration of the polymer and the presence of other water-soluble materials in the solution (86). Added water-soluble components can compete for available water in the gel layer and thereby reduce the hydration of the polymer. This can lead to a stronger gel due to increased extent of hydrophobic polymer interactions primarily between methoxy-substituents (6). At further increased solute concentrations the integrity of the HM can be rapidly lost due to precipitation of the polymer (87). The effects of solutes can be important whether present in the dissolution medium, present in the matrix or both.

Touitou and Donbrow (86) found that while small organic ions caused dehydration or 'salting-out' of a methylcellulose matrix, large organic ions improved polymer hydration and stabilised the matrix. A hypothesis was put forward that the cohesiveness of matrices containing large organic ions was a function of increased hydration and stretching of the macromolecular chains. This theory was supported by viscosity measurements.

1.6.3.4 *Chemical interactions*

Chemical interactions could possibly occur between the drug and the polymer, the additive and the polymer or the additive and the drug. Instances of all three situations have been reported in the literature. The slower than expected release of chlorpheniramine maleate from matrices containing sodium carboxymethylcellulose was thought to be due to the formation of a complex between the chlorpheniramine cation and NaCMC backbone (88). A similar theory has been applied to explain why cationic drugs are released at different rates from non-ionic HPMC matrices and HPMC/NaCMC (anionic) matrices (76). Lubricants with high hydrophobicity will slow the dissolution rate with the effect being less pronounced when the polymer concentration is high (89).

Daly *et al.* (62) showed that gel viscosity of a modified HPMC could be increased using sodium lauryl sulphate possibly due to binding between the anionic surfactant and the non-ionic polymer.

1.7 *Tablet hardness, porosity and geometry*

A large number of studies have examined the relationship between release rates and tablet hardness, porosity and/or compaction force. Ford *et al.* (80) did not detect any relationship between compaction force and the release of promethazine HCl from HPMC K15M matrices. Bansal *et al.* (90) drew a similar conclusion from a study of a water-soluble drug in a mixture of alginate and hydroxypropylcellulose, while Bettini *et al.* (91) found that the initial porosity of Methocel K15M matrices did not influence the release of buflomedil pyridoxalphosphate. A number of papers however, have reported links between either tablet hardness, compaction force, or porosity in relation to drug dissolution from tablet matrices.

Korsmeyer *et al.* (92) studied tablet matrices containing potassium chloride and hydroxypropylcellulose and found that release profiles varied inversely with tablet porosity and mean pore diameter. It was proposed that air entrapped within the matrix was acting as a transport barrier thus tablets with higher porosity had more entrapped air and displayed slower release of drug. When the samples were prepared using a method to reduce entrapped air the release profiles changed from first-order to approximate zero-order for up to 70% release and the difference between release profiles from tablets compacted at high and low compaction forces was less marked. It was suggested that evacuating the tablets prior to dissolution lead to water being forced into the pores by atmospheric pressure producing a saturated aqueous phase throughout the tablet at the beginning of the experiment. The effect of entrapped air on dissolution behaviour has been deliberately exploited by Hashim and Li Wan Po (93) who incorporated effervescent mixtures into HM tablets in order to change release kinetics.

Pérez-Marcos *et al.* (32) observed that increasing the force used to compact frusemide, a drug of low water-solubility, in either 20 or 40% Carbomer lead to a rise in the dissolution rate. Release was postulated to be via erosion of the matrix. The significant effect of compaction force on release of this sparingly water-soluble drug was attributed to the effect of this variable on gel consistency.

The release of theophylline from amylodextrin tablets was controlled by altering the force used for compaction (94). Increasing the compaction force from 5 to 10kN

reduced the burst effect seen at 5kN, decreased the release rate and changed the kinetics to almost zero-order for up to almost 60% release. No further change was seen when the compaction force was increased from 10 to 15kN. The results were attributed to differences in the rate of solvent penetration into the tablet.

Rizk *et al.* (95) reported a scleroglucan/theophylline/lactose formulation that displayed a marked decrease in release rate with increasing hardness. The result was correlated with a seven-fold decrease in pore radius and not a decrease in pore volume. The effect was possible due to a change in the rate of water uptake and swelling.

The sustained release function of tablets prepared with low-substituted hydroxypropyl cellulose (L-HPC) granules was found to be affected by the internal pore size distribution of the tablet (96). Granules prepared by roller compaction using a high pressure were mechanically strong and resulted in matrix tablets having a high interstitial porosity. Drug release from matrices having high porosity, as determined from mercury porosimetry, was faster than from tablets having a lower porosity. The observations were attributed to faster rates of hydration and swelling in high porosity tablets.

Compaction force was found to influence the rate of release of a water-soluble drug from XG/guar gum matrix tablets (36). A faster release was observed in tablets having higher tablet porosity, the effects were more pronounced in a phosphate buffer. In acidic medium the release was influenced to a lesser extent by compaction pressure.

Relationships between release rate and tablet dimensions have been reported. Ford *et al.* (69) found that the √time release rate of promethazine HCl (a highly water-soluble drug) from HPMC matrices was proportional to the surface area of the tablet since release rates decreased as the tablet surface area decreased. Modification of the geometry of tablets based on retrograded pregelatinised starch was used to control the release of a water-soluble model drug (97). Dosage form presentations with a larger releasing surface area showed a faster release of drug than dosage forms with a smaller surface area. The results were attributed to the differences in surface area available for solvent penetration and to the distance that the solvent front had to travel within the tablet.

1.8 Factors affecting drug release from hydrophilic matrix capsules

HM capsules, containing formulations in powder or granule form, were originally introduced as 'hydrodynamically balanced systems' (HBS) for prolonging gastric residence time (98). The theory was that capsules having a specific gravity less than that

of gastric juice could float in the stomach and increase the residence time there. Research efforts that have focused on non-floating HM capsules have examined the effects of polymer type, microenviroment pH control and formulation variables on drug release (14,59,70,99,100).

The release of pseudoephedrine, a highly water-soluble model, from HM capsules based on HPMC was unaffected by variations in tamping force used to consolidate the powder within the capsule, within the range investigated (99). At least 25% polymer was required for cohesive powder plugs to be formed. Hussain *et al.* (14) found that blends of hydroxyethylcellulose and sodium carboxymethylcellulose could be used to obtain zero-order release kinetics from capsule matrices. This technique for obtaining time independent kinetics was previously applied to tablet matrices. It was found that slowly hydrating polymers such as methylcellulose, hydroxypropyl cellulose and sodium carboxymethylcellulose did not give sustained release from capsule matrices but grades of HPMC (F4M premium, E4M premium and K4M premium) were found to give sustained release action (6). The effect of capsule size on the dissolution of a soluble model from hydrophilic matrix capsules was investigated by Alderman (6). Hard gelatin capsules ranging from size 3 (0.36g) to size 0 (0.87g) controlled the release of the model to the same degree. It was also suggested that capsule forms required slightly more polymer to achieve the same dissolution times as tablets, possibly because of lower powder density. Data to substantiate this was not presented.

Although HM capsules have been considered as HBS no reports have been found in the literature regarding the use of HM capsules as simple hydrophilic matrix systems.

1.9 *In vitro* dissolution testing of hydrophilic matrices

The formulation development of any solid oral dosage form normally starts with dissolution testing. Dissolution testing is essential for screening and proper assessment of different formulations. Although standardisation of dissolution testing has been successfully implemented for immediate release dosage forms (65), enormous difficulties have been encountered in establishing proper dissolution test conditions and parameters for testing controlled release dosage forms. Formal guidelines to evaluate these products do not exist therefore the current trend is to evaluate every controlled release dosage form on an individual basis (101). One of the difficulties in generalising test conditions arises because many controlled delivery systems are designed to possess diverse physicochemical and pharmacokinetic properties. The majority of studies that

have focused on the dissolution profiles of controlled release solid oral dosage forms use USP dissolution apparatus with either paddle or basket method. Despite their widespread use, the USP paddle and basket methods are not ideal for testing extended release products. Firstly, the USP apparatus II does not allow an automatic flow of the dissolution medium with variable pH, which is desirable for evaluating and testing extended release products. Secondly, the system is not suitable for testing the dissolution of very low solubility drugs because of a limited ability to maintain sink conditions. Thirdly, dosage forms, such as floating capsules or tablets, can not be positioned appropriately in the system to test dissolution characteristics. To overcome some of these difficulties several modifications have been suggested in the literature (101). However, none of these are yet comprehensive enough to be adopted as a standard testing procedure.

Difficulties also exist in simulating *in vivo* conditions *in vitro*. Since most controlled release preparations are designed for prolonged release and therapeutic effect, variability in *in vivo* conditions over time (such as presence and nature of food in the GI tract, time of day that the dosage form is administered etc), can substantially affect the release profiles of a drug. The first challenge in predicting *in vivo* predictability is to select a suitable dissolution medium. In an ideal situation, an extended release system would be tested *in vitro* throughout the entire physiological pH of the GI tract. However, difficulties exist in determining the time intervals that would relate to a particular section of the GI tract. Since ionic strength can be important to dissolution behaviour of hydrophilic matrices (58,87,102), this should be a consideration when designing dissolution media. The exact physico-chemical properties of the GI contents is difficult to predict since it is determined by many factors including; (a) fed/fasted state (b) nature and quantity of food (c) excipients of the dosage form and co-current administration of other drugs (d) interpersonal variability due to for example, age and illness. The second challenge to selecting *in vitro* dissolution conditions is establishing dissolution test parameters. Knowledge about mechanical stress and hydrodynamic conditions within the GI tract is limited and difficult to simulate. Furthermore, the variability in motility patterns in fed and fasted conditions complicates the task of setting a unique agitation condition during *in vitro* testing. The difficulty in selecting appropriate *in vitro* agitation conditions to correlate with *in vivo* observations is exemplified by the findings of Shameem *et al.* (103), who compared *in vitro* and *in vivo* release behaviour of HPMC based tablet matrices in seven volunteers. They found that the fastest *in vivo* release under fasting and fed conditions was similar to the *in vitro* curve determined by the

rotating basket method at 150rpm. The slowest release from the tablets under a fasting condition was less than the *in vitro* dissolution curve by the paddle method at 10rpm. They attributed the large inter-subject differences observed to differences in the GI destructive force generated by GI motility and residence among subjects. This means that *in vitro* testing under highly destructive conditions may not necessarily be more physiologically meaningful than testing under less strenuous conditions. A difficulty with *in vitro* testing is that drug release influencing factors that are significant *in vitro* may be of limited importance *in vivo*. HM's that have been shown to be sensitive to changes in ionic strength of the medium *in vitro* have not shown the same sensitivity *in vivo* (60,104).

Although the ultimate test of product behaviour is *in vivo* pharmacokinetic and pharmacodynamic data it has been argued that a knowledge of the behaviour of a dosage form in the GI tract can be a useful step in formulation development (105). Gamma scintigraphy is a non-invasive imaging technique that has been widely used to study the behaviour of solid oral dosage forms in man (60,105,106). In this work, *in vitro* dissolution tests have been used as the first step in studying the functionality of controlled release formulations while a gamma scintigraphy study has been used to aid the evaluation of the behaviour of dosage forms based on heterodisperse polysaccharides *in vivo*.

2. Assessment and validation of methods for bulk physical characterisation of heterodisperse polysaccharide-based granules and tablets

2.1 Introduction

Physical characterisation of pharmaceutical solids can be carried out at three levels; the molecular level (properties associated with individual molecules), the particulate level (properties pertaining to individual solid particles) and the bulk level (properties associated with an assembly of particles) (107). This work is concerned with the bulk physical properties of heterodisperse polysaccharide (HP)-based granules and tablets. Bulk physical properties can be defined in terms of material density, porosity, pore size distribution, surface area and in the case of granules, flow properties. The parameters of specific surface area, bulk density, porosity, pore area and pore size distribution are considered here. Bulk density can be easily measured by determining the weight and apparent volume of solid samples. Specific surface areas can be measured using gas adsorption techniques, which depend on the ability to predict the number of adsorbate molecules required to exactly cover the surface of a material with a single molecular layer of inert gas (107). Accuracy of the technique is highly dependent on material characteristics and experimental conditions. Quantitative estimates of pore volume, pore diameter and pore area can be obtained using the technique of mercury porosimetry. This is based on capillary rise phenomena whereby a pressure is required to make a non-wetting liquid move up a narrow capillary (108). Quantitative data is obtained by relating pressure applied and volume of mercury intruded to pore size distribution, pore volume and pore surface area. Mercury porosimetry has gained popularity as a research tool due to the relative simplicity of the technique and the extensive range of data that can be generated (109). Due to its ease of use mercury porosimetry is often used as a black box which produces pore size distributions (110). However, basic limitations of the technique exist and problems may arise if it is applied to materials for which it has not been properly tested. To ensure that the data obtained is truly representative of the porous material potential sources of error need to be thoroughly evaluated and care must be taken with interpretation of results. For this purpose it is useful to compare mercury porosimetry results with results obtained using other methods of pore structure analysis.

In this study, HP-based granules and tablets were analysed using mercury porosimetry, gas adsorption measurements, scanning electron microscopy and liquid

penetration studies. The objective was to determine the suitability of these methods, alone and in combination, for characterising specific surface area, bulk density, porosity, pore area and pore size distribution of HP-based granules and tablets.

To achieve this it was necessary to; (1) ensure that the techniques gave information which was truly representative of the porous body; (2) determine the accuracy, precision and reproducibility of the methods; (3) ensure that the methods were suitable for the analysis of a large number of samples; (4) assess whether the measurements obtained would be potentially useful for physical properties/dissolution behaviour correlation studies.

2.2 Materials

Xanthan gum (Lot No. P5086), locust bean gum (Lot No. B7924), glucose (Lot No. CD4R02005), calcium sulphate (Compactrol NF, Lot No. 50320X) microcrystalline cellulose NF, BP (Emcocel 50M, Lot No. 3467) and TIMERxN (Lot No. NS664) were supplied by Penwest Pharmaceutical Co. (Patterson, NY, USA). TIMERxN is a proprietary formulation of heterodisperse polysaccharides, which contains two tertiary components, calcium sulphate and ethylcellulose, in addition to locust bean gum, xanthan gum and glucose. Mercury was obtained from Belgrave Mercury Ltd. (London, U.K.) and magnesium stearate (Batch No. 29846) from Fisons Scientific Equipment (Loughborough, U.K). Acetone, 2-propanol (HPLC grade) and cyclohexane (HPLC grade) were obtained from Fischer Scientific Ltd. (Loughborough, U.K.). Silica-alumina reference material (Lot No. A-501-23) was obtained from Norton Chemical Process Products Co. (Ohio, USA). The sintered glass disc was obtained from Amer Products Ltd. (Brimsdown, Enfield, U.K.) and silica gel from BDH Chemicals Ltd. (Poole, England). Ethylcellulose aqueous dispersion, NF containing 27% w/v ethylcellulose (Aquacoat, Lot No. J3381, FMC, USA) was obtained from Colorcon Ltd. (Dartford, Kent, U.K.). Dimethylyellow dye was obtained from Sigma Chemical Co. (Loughborough, U.K).

2.3 Methods

2.3.1 *Sample preparation*

HP-based material was either prepared by wet granulating the primary components or obtained pre-granulated from Penwest Pharmaceutical Co. To clearly distinguish between the materials, preparations obtained from Penwest Pharmaceutical Co. are referred to by their proprietary name, e.g. TIMERxN, while granules prepared at Bath are referred to as Bath heterodisperse polysaccharide (BHP)-based material. BHP-based granules have been allocated a three character alphanumeric code. The letter G, denoting granules is followed by a number that indicates the chapter in which the manufacturing process is described. A letter identifying the specific batch follows this (e.g. G3A). The preparation of two batches of granules (batches G2A and G2B) is described in section 2.3.1.2. Batch G2A was used for mercury porosimetry studies while batch G2B was used for gas adsorption studies. A number of other batches are referred to in this chapter since they were used to assess some of the analytical techniques however, their preparation is described in proper context in chapter 3. Both granule and tablet samples were used to assess the analytical techniques. Tablets were compacted from both TIMERxN and BHP-based granules. Tablets compacted from BHP-based granules are identified by the letter T followed by the remainder of the granule batch code (e.g. T3A are tablets compacted from granule batch G3A).

2.3.1.1 *Tablets*

TIMERxN has excellent compaction properties, which enabled tablets to be produced using a wide range of compaction forces. This would not have been possible using granules produced by wet granulation of the primary components. TIMERxN was compacted using a compaction simulator, which enabled compaction force and speed to be accurately controlled. An appropriate tablet weight was selected by determining the weight of material that would be required to produce a 3.5mm × 10mm compact at zero porosity. This is a standard procedure for compaction simulation work (111). To calculate this the true density of TIMERxN was required. A helium pycnometer (Ultrapycnometer 1000, Quantachrome Co., Greenvale, NY, USA) was calibrated immediately before use using a calibration sphere of known volume. TIMERxN was dried in an oven (Model 1H-150, size 2, Gallenkamp, Loughborough, U.K.) at 60°C for 24hr prior to analysis to reduce the moisture content of the sample. An accurately weighed sample (approximately 3g) was placed in a sample cell of known volume and

purged with helium for 15min to remove adsorbed gases and moisture. Pre-drying of the sample reduced the purge time required. 3 determinations of the volume of helium displaced by the sample were made and the corresponding sample density calculated. The mean value was found to be 1.596g/cm^3. To assess the performance of the pycnometer the same procedure was repeated on a sample of microcrystalline cellulose 50M (MCC). A value of 1.544g/cm^3 was obtained which corresponded closely to the value reported by Doelker (112) (1.543 g/cm^3). The product of the true density of TIMERxN and the apparent volume of a 3.5mm × 10mm tablet (0.275cm^3) gave the sample weight at a theoretical zero porosity (438mg). A compaction simulator (ESH testing Ltd., Machine No. 4287, Brierly Hill, U.K.) equipped with a regularly calibrated load cell (100kN) was fitted with 10mm flat-faced F tooling. Linear variable differential transformers attached to the upper and lower punches of the simulator were used to monitor the displacement of the punch tips from a reference position. This facilitated the determination of the separation of the punch faces at any point in time. The die and punches were cleaned with acetone and pre-lubricated prior to compaction with a suspension of 1.5% magnesium stearate in acetone. Accurately weighed samples (approximately 438mg) were introduced into the die cavity and compacted using a compaction speed of either 3mm/s or 100mm/s. A single ended sawtooth displacement/time profile was obtained. By adjusting the penetration distance of the upper punch into the die the force used to compact the material was controlled. Tablets were produced using target upper punch forces of 2, 4, 8, 12, 16 and 24kN. 2kN was the lowest force that still produced an intact tablet able to withstand gentle handling, while 24kN was the highest force achievable within the limits of the load cell.

BHP-based granules were compacted using a single punch tabletting press (Type F3, Manesty, Speke, Liverpool, U.K.) fitted with a 10mm flat-faced punch and die set. Accurately weighed sample, approximately 400mg were placed in the die cavity. The granules were compacted manually which allowed the weight and tablet thickness to be tightly controlled. The punch and die were not lubricated.

2.3.1.2 *Granules*

Batch G2A was prepared as follows: 25% locust bean gum (LBG), 25% xanthan gum (XG) and 50% glucose were dry blended for 5min using a high shear mixer (Cuisine Système Automatic 5000, Magimix, Surrey, UK.). Total batch size was 300g. The pre-blended solids were wet massed with 21% distilled water and tray dried at 60°C

in an oven (Model 1H-150, size 2 Gallenkamp, Loughborough, U.K.) producing material with a loss on drying (LOD) value of approximately 5%. LOD's were determined using an infrared moisture balance (Mettler LP16, Switzerland). The material was heated at 70°C until no further weight loss occurred (approximately 20min). The material was screened through a 0.63mm mesh using a mechanical granulator (Type MGL 4A, Frewitt, Switzerland). The granules were sieved for 30min (Endecotts Ltd., London, U.K.) through an I.S.O standard aperture diameter $\sqrt{2}$ sieve progression ranging from 710μm to 63μm. The sieves were agitated using a Fritsch sieve shaker (Type 03-502, Fritsch, Germany). To maintain a constant particle size the granules were size selected to give granules with a normal size distribution and a target median particle size of 182μm. Size selection was important since granules particle size can affect porosity (see section 3.4.3). Quantities from each sieve fraction were selected in the following proportions: 500 to 710μm (2%), 355 to 500μm (4%), 250 to 355μm (26%), 180 to 250μm (36%), 125 to 180μm (26%), 90 to 125μm (3%), 63 to 125μm (2%) and 0 to 63μm (1%). Sieve fractions were recombined using turbula rotation (Type T2C, Glen Creston Ltd., Stanmore, Middlesex, U.K.) for 5min at 50rpm.

Batch G2B was prepared as follows: 25% XG, 25% LBG, 35% glucose and 10% calcium sulphate were blended for 5min in a high shear mixer. Total batch size was 300g. A suspension containing 15% w/v ethylcellulose was prepared by diluting ethylcellulose aqueous suspension (Aquacoat™) with water. As the dry material was mixed 100ml of suspension was added slowly over a period of 4min. Mixing was continued for a further minute. The material was tray dried in an oven at 60°C for 24hr then hammer-milled (Type DHF48 Glen Creston Ltd., Stanmore, U.K.) using a 3mm screen. Particle size of the granules was determined using a Malvern Mastersizer (Type MSX02SM, Malvern Instruments Ltd., Malvern, U.K.) fitted with a dry powder feeder. The mean volume median diameter D[v, 0.5] (n=3) was 144μm.

2.3.2 *Mercury porosimetry*

Pore structure determinations were made using a Micromeritics Autopore II porosimeter (Type 9220, Micromeritics Instruments Co., Georgia, USA) capable of operating in the range of 3.4 to 414,000kNm^{-2}. The porosimeter was equipped with a low pressure chamber operating from atmospheric pressure (172kNm^{-2}) down to 3.4kNm^{-2} and a high pressure chamber operating from 172 up to 414,000kNm^{-2}. The

pressure at which mercury could be introduced into the penetrometer (fill pressure) could be controlled between 3.4 and 69kNm^{-2}. Assuming the contact angle of mercury to be 130° and the surface tension of mercury to be 485.0gcm/s^2 respectively, pores having median diameters in the range 360 to 0.003μm could be analysed. Pressure was generated by a hydraulic pump and the movement of mercury in the penetrometer stem was followed using a conductance detector. Samples were stored over dry silica in a vacuum dessicator for at least 24hr before analysis. Pre-treatment of the samples in this way removed moisture from the materials reducing the time required to evacuate the samples. Between 2.5 and 4g of granules were placed in a 15ml powder penetrometer that had a stem volume of 0.392ml. TIMERxN tablets were placed in a 5ml solid penetrometer (1.131ml stem volume) while tablets prepared from BHP-based granules were placed in a 5ml solid penetrometer (0.392ml stem volume). Between 2 and 5 tablets were used in each case. Samples were evacuated down to a pressure of 50μmHg to remove adsorbed gases and moisture. Penetrometers were filled with mercury at a pressure of 3.4kNm^{-2} for tablet samples and 69kNm^{-2} for granular samples. The penetrometer, fill pressure and sample size were carefully selected to ensure that between 10 and 90% of the stem volume was used. Measurements were carried at a consistent room temperature of 21°C using an equilibration time of 5s. The surface tension, contact angle and density of mercury at 21°C were taken to be 485.0gcm/s^2, 130° and 13.5438g/ml respectively. Between 30 to 50 points in the required range were taken. Porosimetry analysis was carried out on granule batches G2A, G3G, G3L and G3E and on tablets compacted from TIMERxN using a compaction speed of 3mm/s and compaction forces of 2, 4, 8, 12, 16 and 24kN.

The performance of the porosimeter was assessed using a silica-alumina reference material supplied by Micromeritics, taken from a portion of material that had been repeatedly analysed by the company using different instruments and various operators at a number of locations. Approximately 1g of material was analysed using a powder penetrometer with a 5ml bulb. An equilibration time of 10s was allowed and the fill pressure was set at 69kNm^{-2}. The results fell within the limits established by Micromeritics, indicating that the instrument was performing satisfactorily (Appendix I).

2.3.3 *Scanning electron microscopy*

Scanning electron microscopy was used to look at the surface of a number of batches of granules which had been produced using different granulation techniques (batches No. G3I, G3L G3K, and G3F). The granules were known to have different

porous structures as determined using mercury porosimetry. The preparation of these granules is described in chapter 3. Pores on the surface of TIMERxN tablets compacted using a range of forces at a speed of 3mm/s were also examined. Samples were stored in a vacuum dessicator over dry silica prior to examination. This removed moisture, which helped maintain integrity of the coating thereby preventing the material from charging (113). Granules were scattered onto adhesive, conductive mounting discs. Loose particles were removed by dusting with compressed air. Tablets were mounted on aluminium studs using carbon dag (a conductive paint). A layer of gold was deposited onto the sample surface using a sputter coater (Edwards high vacuum Model S150B, Sussex, U.K.) running at a voltage of 1.4kV for 8min. Samples were imaged with a scanning electron microscope (Jeol T6310, Japanese Electron Optics Ltd., Tokyo, Japan) using an electron beam potential of 5keV.

2.3.4 *Surface area analysis by nitrogen adsorption*

Nitrogen adsorption onto the surface of granule batch G2B was measured using a surface area analyser (ASAP 2000, Micromeritics Instruments Co., Georgia, USA). The instrument required a minimum total sample surface area of at least $20m^2$ for analysis. Since the surface area of the granules was predicted to be low (in common with many pharmaceutical excipients), it was estimated that at least 70g of sample was required for each analysis in order to meet the minimum surface area requirement. To accommodate this quantity of material the bulb of a standard glass sample tube ($25cm^3$) was expanded to a volume of approximately $128cm^3$. Outgassing of the sample was necessary to remove physio-adsorbed gases and vapours, which can alter surface potential and block or fill pores. To decrease the outgas time the material was dried in an oven at 80°C (Model 1H-10, Size 2, Gallenkamp, Loughborough, U.K.) which reduced the moisture content to 0.6% w/w. The sample was quickly transferred to the sample tube to prevent re-adsorption of atmospheric moisture. The sample was outgassed by vacuum pumping down to a pressure of 9mmHg. The sample tube was transferred to the analysis port and cooled to the boiling point of nitrogen (77K) by immersing the sample holder in a dewar filled with liquid nitrogen. The sample was exposed to increasing partial pressures of nitrogen and the volume of gas adsorbed was measured at each partial pressure. A series of 18 pressure/volume measurements were made over a sequence of ascending relative pressures from 0.00004 to 0.90263. A duplicate measurement on the same sample was carried out. To check the performance of the surface area analyser, the surface area of a

sample of microcrystalline cellulose 50M was also determined. Analysis was carried out on approximately 1g of dry material. The sample was heated to 60°C during degassing to reduce the degas time.

2.3.5 *Liquid penetration studies*

Analysis of liquid flow through complex pore systems is based on capillary theory (108). The rate of penetration of a non-wetting liquid is dependent on the contact angle θ between liquid and solid, the surface tension of the liquid and the viscous resistance exerted by the capillaries which is dependent upon the cross section of the pores, their total perimeter and size distribution (114). Tablets having a more coarse intergranular structure may permit a more rapid movement of liquid through the pores than a tablet with the same porosity but a more even pore structure (115). A piece of apparatus to determine the rate of penetration of cyclohexane, a liquid that did not appear to wet HP-based materials, into tablets and granules was constructed. The apparatus was based on a design by Shah *et al.* (73). Figure 2.1 shows the equipment used. A circular disk of sintered glass with a porosity value of P4 (16μm) was sealed into a 15ml glass funnel and connected to the centrepiece of 3-pronged piece of glass tubing using polytetraethylene tubing. A reservoir fitted with an on/off tap was connected to the right hand side of the glass tubing while a 0.2ml pipette with 0.01ml divisions was connected to the left hand side of the glass tubing. The glass tubing was fixed to a board and held vertically. The apparatus was filled with cyclohexane that contained a small amount of dimethylyellow dye to render the liquid yellow. This enabled the movement of cyclohexane in the pipette to be followed. Experiments were carried out in a controlled temperature environment (21°C) to ensure that any loss of cyclohexane by evaporation was kept constant. The level of cyclohexane in the apparatus was adjusted so that the pipette was filled with liquid up to the zero mark. The reservoir was closed of using the tap and the sample to be tested placed on top of the sintered glass. Granule samples (approximately 300mg) were placed in an open ended cylindrical container in order to maintain a constant contact surface area with the sintered glass. As cyclohexane was wicked by the sample the pipette gradually became depleted of liquid. The volume of cyclohexane removed from the pipette was followed as a function of time. Cycloheaxne penetration studies were carried out on (a) tablets that had been compacted from TIMERxN using a range of forces and a compaction speed of 100mm/s (b) on granules that were known to have a range of porosity's as determined by mercury porosimetry

(batches G3A, G3B and G3E) and (c) on tablets compacted to equivalent relative density from granule batches G3D, G3J, G3N, G3O and G3P (tablets T3D, T3J, T3N, T3O and T3P). These batches were expected to have different porosities despite having equivalent tablet thickness. Three samples were analysed from each batch of material.

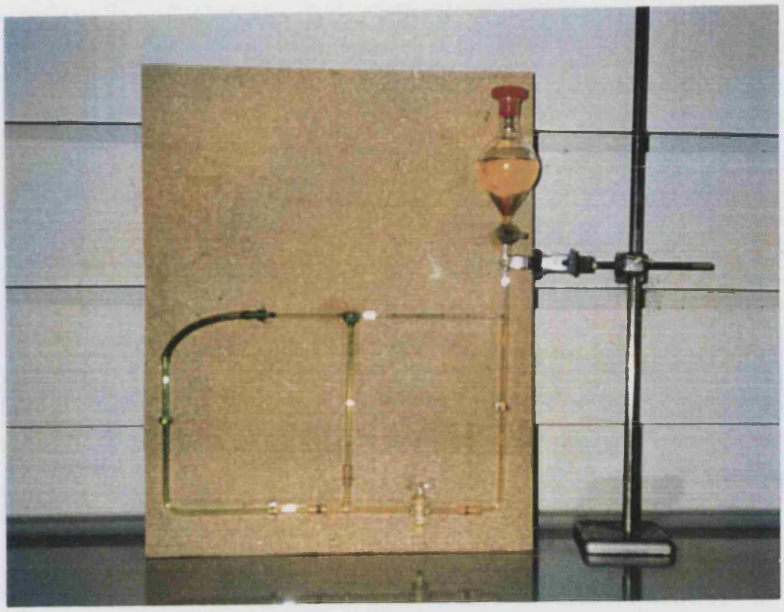

Figure 2.1 Apparatus used to determine cyclohexane uptake rates.

2.3.6 *Measurement of bulk density*

Bulk density was calculated by dividing the mass of a tablet or a sample of granules by its apparent volume. The apparent volume of a tablet was calculated using equation 2.1.

$$V = \pi r^2 h \qquad (2.1)$$

Where h was tablet height or thickness and r was tablet radius. Tablet dimensions were measured using a digital micrometer (Digit-cal electronic calipers, TESA S.A., Switzerland). To measure the apparent density of granules a sample of material (2 to 4g) was accurately weighed out and slowly poured into a 10ml graduated measuring cylinder. Care was taken to prevent consolidation of the particles. The volume of the sample was read from the cylinder. A mean of three determinations was found and the standard deviation from the mean calculated.

2.4 Results and discussion

2.4.1 *Mercury porosimetry*

The volume of mercury V penetrating tablet and granule samples was measured directly as a function of applied pressure P. This P-V information provided a unique characterisation of pore structure. Porosimetry results from granule batch G2A and from TIMERxN tablets compacted using a force of 4kN and a speed of 3mm/s were used as model sets of data. Various means of extracting quantitative information from the raw data were considered using graphical representation of the data to aid interpretation of the information. Regions of the P-V data that represented penetration of mercury into spaces between granules or tablets was distinguished from data that represented filling of pores within the actual material. Porosimetry profiles of granule and tablet samples were analysed to determine likely areas of misinterpretation and to identify the degree to which values obtained were likely to represent 'real' values. The performance of the porosimeter and the reproducibility and limitations of the technique were also assessed.

2.4.1.1 *Quantification of raw data*

Using the Washburn equation (116) (equation 2.2) pressure P was transformed into a pore diameter D:

$$D = \frac{4\sigma_{LV}\cos\theta}{P} \qquad (2.2)$$

where θ was the contact angle of mercury (130°) and σ_{LV} was the surface tension of mercury (485gcm/s^2). The P-D information was presented in a number of graphical forms. Figures 2.2 and 2.3 show incremental intrusion plots over the complete analysis range for model granule and tablet samples, respectively. Incremental intrusion volume (ml/g) was presented on a linear scale and pore diameter (μm) on a logarithmic scale. These incremental plots represent both the penetration of mercury into spaces between granules or tablets and also pore filling within granules and tablets themselves. The point at which inter-particulate or void filling ends and pore filling begins is indicated by a sharp rise in intrusion volume which occurs at around 4 to 7μm for the granule sample and at approximately 4.5μm for the tablet sample. Only data representing pore filling provides useful information. To analyse this data the void space was 'removed' and the cumulative volume of mercury intruded (ml/g) was calculated from the point of pore

filling down to a cut off point of 0.02μm. Selection of pore filling and cut-off points are considered in greater detail in sections 2.4.1.2 and 2.4.1.3, respectively. Cumulative intrusion volume on a linear scale was plotted against the logarithmic of pore diameter. Figure 2.4 shows cumulative intrusion plots over the range 6.5 to 0.02μm for granules and 4.5 to 0.02μm for tablets. Data from cumulative intrusion curves was quantified by determining the pore diameter which corresponded to 50% of the intrusion volume (median pore diameter) and, in some instances, the pore diameter which corresponded to 25% and 75% of the cumulative volume (first and third interquartile points). Median pore diameter based on volume distribution is the most common method of describing pore size distribution (109) however, peak values from other pore size distributions can be used. Diameter calculations based on volume were selected for this study, as this was appropriate for correlation with water penetration phenomena.

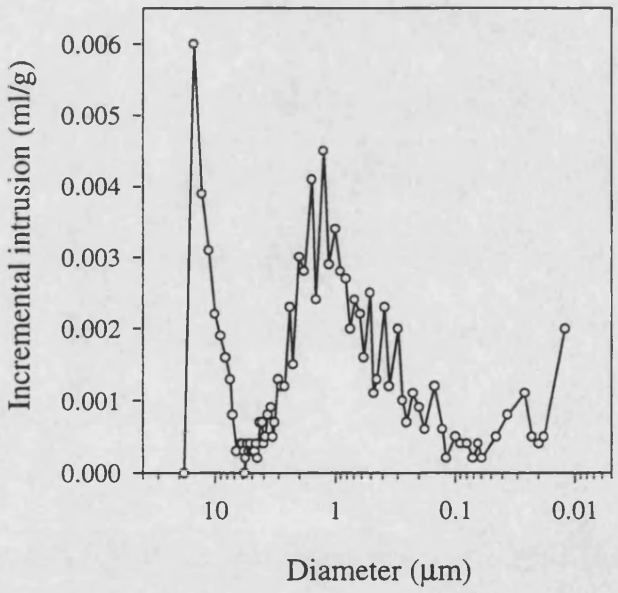

Figure 2.2 Incremental intrusion plot over pressure range 69 to 103400kNm^{-2} for model granules (batch G2A)

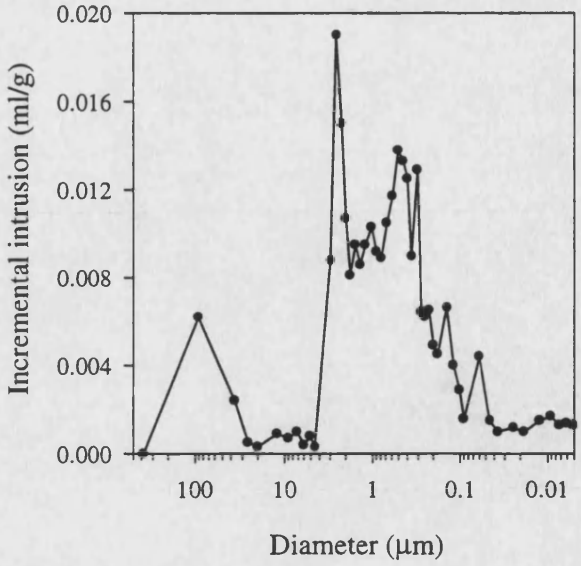

Figure 2.3 Incremental intrusion plot for model tablets over pressure range 3.4 to 241000kNm^{-2}

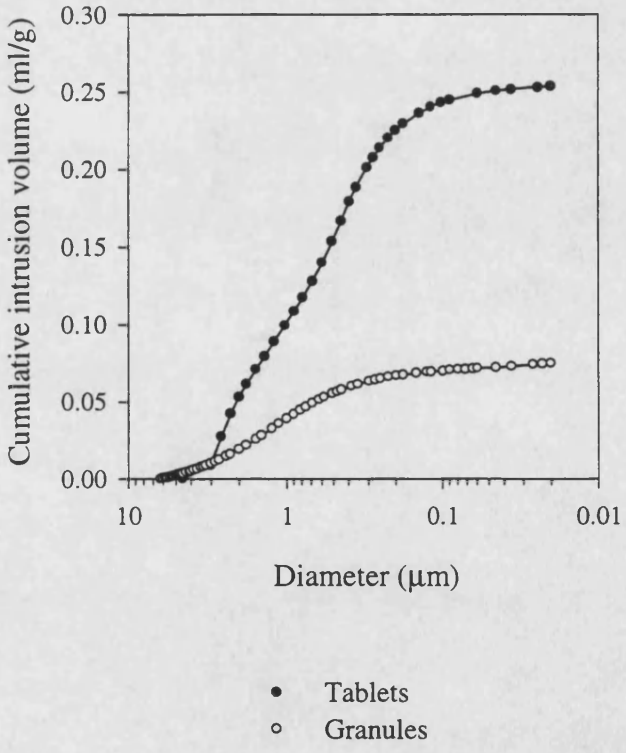

Figure 2.4 Cumulative pore size distributions of model granule and tablet samples.

In order to calculate sample porosity determination of the apparent volume and pore volume of each sample was necessary. The difference between the volume of mercury filling the empty penetrometer and the volume with the sample present gave the apparent volume of the sample. Empty penetrometer volume was determined by carrying out a blank run while the volume with the sample present was determined by weighing the penetrometer after the low pressure run, converting mass into volume using the density of mercury at 21°C (13.5438g/ml) and back calculating to a pressure below which the pores were filled. This point corresponded closely to the last pressure point of the low pressure run (172kNm^2). Using apparent volume, bulk density values for the samples were calculated. To confirm that values of bulk volume determined by porosimetry were acceptable, the values were compared to bulk density values calculated using bulk volumes determined from geometrical calculations. Table 2.1 shows bulk density values obtained for TIMERxN tablets compacted using a number of compaction forces and a speed of 3mm/s. Both methods of determining bulk volume produced similar results. Total porosity P of samples were determined using equation 2.3

$$P = \frac{V_P}{V_A} \times 100 \qquad (2.3)$$

Where V_P was the pore volume (total volume of mercury intruded) and V_A was the apparent volume of the sample.

Volume-pressure data was also used to obtain a pore area distribution using equation 2.4, which is commonly used to calculate pore area (110):

$$\Sigma \Delta A = \frac{\Sigma P \Delta V}{\gamma \cos\theta} \qquad (2.4)$$

Pore diameter was also described using an average pore diameter. This was calculated by multiplying pore volume by four and dividing by pore area (4V/A). This produced a value that took into account both pore volume and the number of pores (pore area values partly reflect the number of pores). Average pore diameters were useful when comparing pore size distributions of batches that had similar pore structures.

Compaction force (kN)	Bulk density (g/cm^3)	
	Determined from porosimetry	Calculated from tablet geometry
2	1.03	0.99
4	1.09	1.10
12	1.25	1.25
16	1.27	1.31
24	1.33	1.36

Table 2.1 Bulk density values of TIMERxN tablets compacted at a speed of 3mm/s. Values were calculated using apparent volumes derived from (a) mercury porosimetry and (b) geometrical calculations.

2.4.1.2 *Determination of pore filling point*

In order to calculate pore parameters a clear difference must exist between inter-particulate and intra-particulate pore space filling, in the case of granules, or void space filling and pore filling in the case of tablets. If a transition point cannot be clearly distinguished then calculation of values to describe porous structure becomes impossible. Transition points were determined by examination of incremental and cumulative intrusion plots. Plots included data collected over the completed range of penetrometer filling, which was 69 to 103400 kNm^{-2} in the case of the model granule sample and 3.4 to 241000 kNm^{-2} in the case of the model tablet sample. Cumulative intrusion curves for both granules and tablets (figures 2.5 and 2.6, respectively) showed a distinctive knee point or inflection on each curve. This occurred at a pore diameter of approximately 3 to 4 μm for the tablet sample and approximately 6 to 8μm for the granule sample. Incremental intrusion plots (figures 2.2 and 2.3) of the same samples showed difference in the plots before and after these points. In figure 2.3 the large intrusion volume before 4.5μm appeared to represent filling of the voids between tablets while the intrusion peaks after this point represented filling of pores within tablets. Similarly, in figure 2.2, intrusion at pore diameters greater than 7μm appeared to represent inter-particulate filling and intrusion of pores less than 4μm represented filling of pores within the granules themselves. Distinct inflection points in cumulative intrusion plots occurred in all subsequent granule samples which were analysed and in the majority of subsequent tablet samples analysed (Chapter 3). Only data collected from tablets that had been

compacted at very low forces (<2kN) using a high compaction speed failed to show a defined inflection point. It has been reported that in powder and granule systems it is often difficult to difficult to determine the point at which inter-granular filling stops and intra-granular filling begins (109). In BHP-based granules the defined inflection point observed could be a consequence of the relatively small pore size of this material. The largest pore diameter of BHP-based granules was approximately 7μm, much smaller than that reported for other pharmaceutical excipients. Ganderton and Selkirk (117) found that that 22% of the pores of lactose granules had diameters in the range 14 to 56μm, while Sheskey and Williams (118) reported that the median pore diameter of Methocel F4M granules was 15μm (median particle size was 267μm). Granules having large pore diameters are likely to be penetrated by mercury at low pressures including the penetrometer fill pressure. The smaller pore size of BHP-based granules meant that pore filling was unlikely to occur during penetrometer filling and applied pressures were

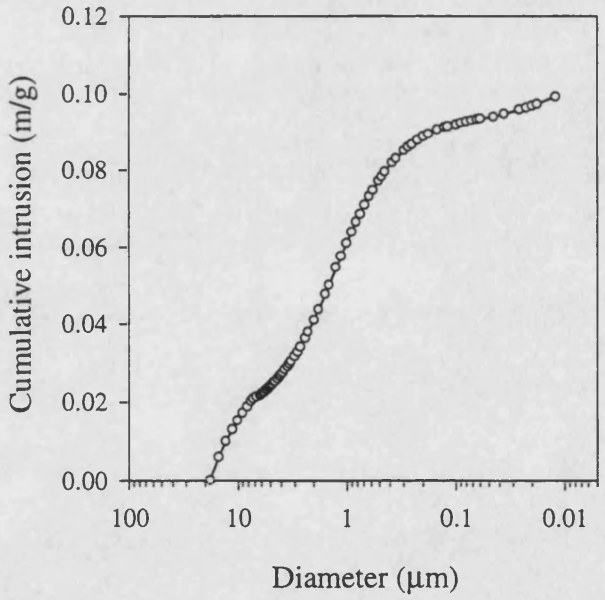

Figure 2.5 D-V data for model granules collected over the range 18 to 0.011μm presented as a cumulative intrusion plot.

needed to penetrate the largest pores. This meant that the point of pore filling could be readily identified. This is an unusual situation for pharmaceutical excipients (109). Possible reasons for the existence of very small pores in BHP-based granules is considered in section 3.4.1.2.

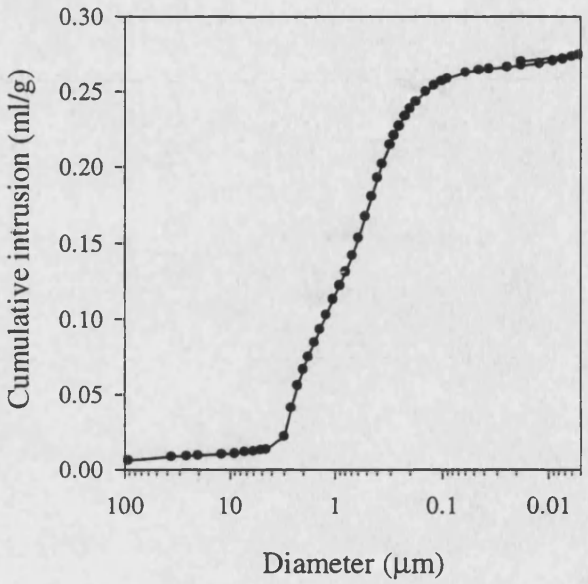

Figure 2.6 D-V data for model tablets collected over the range 100 to 0.005μm presented as a cumulative intrusion plot.

From intrusion curves it was estimated that the transition point (ie pore filling point) lay between 4 and 7μm for the granule sample and between 3 and 6μm for the tablet sample. It was not possible to select the exact point at which pore filling began therefore introduction of an error was unavoidable. To examine the effect of this on quantitative values, experimental data from model tablets was computed using a number of theoretical pore filling points. Theoretical fill points were selected above and below 4.5μm which was considered to be a reasonable estimated pore fill point (table 2.2). A comparison of pore parameters calculated using data collected over the pore diameter range 5 to 0.02μm with pore parameters using data collected over the pore diameter range 3 to 0.02μm showed that there was only a small difference between the results. It was concluded that a pore filling point selected anywhere within the estimated range would be acceptable. When pores larger than 5μm were included in the calculations the porosimetry data did not change substantially suggesting that there were effectively no pores greater than 5μm in the tablet sample. Interestingly, SEM's of model tablets showed the existence of surface pores greater than 5μm. It was concluded that these larger pores were predominately surface cavity windows and did not contribute largely to

total porosity. Other researchers have reported that for porous media in which a cavity-window structure can be recognised, it appears improbable to find agreement between mercury porosimetry and two-dimensional photographs (119). Bulk density data provided confirmation that pore filling points had been correctly identified. Comparison of bulk density data obtained from mercury porosimetry with bulk density values calculated from geometrical dimensions showed that the results were similar (table 2.1). This suggested that that the knee point on cumulative intrusion curves did correlated to the point at which pore filling began since accurate measurements of bulk density also depended on the correct identification of this point. For subsequent tablet and granule samples pore filling point was decided for each individual sample from visual examination of cumulative and incremental intrusion curves.

	Theoretical pore filling point (μm)					
Pore parameters	**20**	**10**	**5**	**4.5**	**3**	**1**
Specific pore area (m^2/g)	2.66	2.66	2.66	2.66	2.64	2.43
Median pore diameter (μm)	0.71	0.70	0.69	0.69	0.65	0.40
Porosity (%)	28.3	28.1	27.8	27.8	26.8	16.6

Table 2.2 Pore parameters of model tablets calculated using data collected from a range of theoretical pore filling points down to 0.02μm.

2.4.1.3 *Determination of cut-off point*

The Micromeritics Autopore II porosimeter is capable of operating up to a pressure of 414,000kNm^{-2}. However, since the materials being studied were not microporous and since mechanical damage to the material could, theoretically, occur at high pressures it was considered unnecessary to analyse up to the maximum achievable pressure. It was also known that the instrument itself can lose accuracy at high pressures and that the contribution made to the overall results can be substantially affected by the measurements of large quantities of small pores at high pressures (109). It was therefore important to determine a reasonable point at which the data could be truncated.

Data from the model tablet sample was computed between the diameter at which the pores began to be filled, taken as 4.5μm, and a range of minimum pore diameters. Figure 2.7 shows how calculated specific pore area values changed as the cut off point

moved towards larger pore diameters. Including pores of very small diameter in the analysis resulted in a very high pore area. As smaller pores were eliminated from the calculations the surface area values rapidly decreased. The rate of change of pore area with pore diameter began to fall as the truncation point moved towards pores greater than 0.015μm. This illustrated how small pores could substantially alter estimated pore areas because small volumes of small pores largely contribute to this value. Although selected cut-off points largely influenced pore area values, table 2.3 shows that estimates of median pore diameter and porosity were much less influenced by selected cut-off points. Smaller pores contributed little to total pore volume while median pore diameter calculations based on volume measurements were also more affected by large volume pores than by low volume pores (see section 2.4.1.4). A cut off point of 0.02μm was selected for subsequent studies since these were the smallest pores that could be included without adversely affecting the reproducibility of pore area estimates.

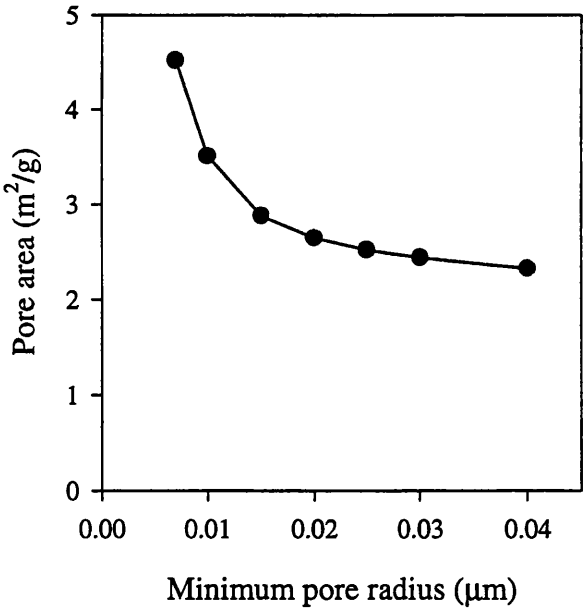

Figure 2.7 Variation of pore area with data cut-off point for model tablets illustrating the contribution of small pores to surface area.

	Minimum pore diameter (μm)						
Pore parameters	**0.007**	**0.01**	**0.015**	**0.02**	**0.025**	**0.03**	**0.04**
Median pore diameter (μm)	0.67	0.66	0.69	0.69	0.69	0.70	0.70
Porosity (%)	28.4	28.1	28.0	27.8	27.7	27.7	27.6

Table 2.3 Contribution of small pores to median pore diameter and porosity of a model tablet sample

2.4.1.4 *Interpretation and analysis of mercury porosimetry results using model data*

Table 2.4 shows values for total porosity, median pore diameter and specific pore area obtained for TIMERxN tablets compacted at a speed of 3mm/s and for granule batch G2A. Calculations were based on data collected from the estimated point of pore filling down to a minimum pore diameter of 0.02μm.

Pore parameters	**Tablets**	**Granules**
Pore area (m^2/g)	2.644	0.896
Median pore diameter (μm)	0.66	1.08
Porosity (%)	27.3	10.1

Table 2.4 Pore parameters of model tablets and granules.

Incremental intrusion plots of points within this range are presented in figures 2.8 and 2.9. Differential plots, derived from cumulative curves, gave a relative pore size distribution (figure 2.10). The visual impression of pore structure was assessed to examine how it related to the quantitative pore data given in table 2.4. Values for median pore diameter of tablets (0.66μm) and granules (1.08μm) were firstly assessed. Comparison of figures 2.8 and 2.9 showed that for both samples the majority of pores lay in the pore diameter range 0.2 to 3μm. Differential plots showed that the granules had a unimodal distribution of pores while the tablet sample had an essentially bimodal pore distribution (figure 2.10). The modal pore diameter in each case appeared to be approximately 0.3μm. However, the data in table 2.4 shows that the median pore

diameter of the tablets was much smaller than that of the granules. This reason for this discrepancy became apparent when the intrusion data was divided into groups of pores and the median diameter of pores within each group calculated. The intrusion plot was sub-divided into three regions: pores between the estimated pore filling point and 0.9μm, pores between 0.9 and 0.1μm and pores between 0.1 and 0.02μm. Tables 2.5 and 2.6 detail the porosity, median pore diameter and specific pore area of pores within each division for granule and tablet samples, respectively.

	Pore diameter range		
Pore parameters	**6.5 to 0.9μm**	**0.9-0.1μm**	**0.1 to 0.02μm**
Pore area (m^2/g)	0.094	0.303	0.499
Median pore diameter (μm)	1.90	0.49	0.04
Porosity (%)	5.7	3.7	0.7

Table 2.5 Sub-division of pore data from model granules into three pore diameter ranges. The characteristics of pores within each sub-division are detailed.

	Pore diameter range		
Pore characteristic	**4.5 to 0.9μm**	**0.9-0.1μm**	**0.1 to 0.02μm**
Specific pore area (m^2/g)	0.240	1.671	0.733
Median pore diameter (μm)	1.89	1.67	0.06
Porosity (%)	11.2	15.0	1.1

Table 2.6 Sub-division of pore data from model tablets into three pore diameter ranges. The characteristics of pores within each sub-division are detailed.

The quantitative data now gave a better indication of how the pore size distribution of the tablets and granules differed. This information could not be deduced from median pore diameters calculated over the complete pore range (table 2.4). The median pore diameter of pores in the range 0.9 to 0.1μm was much higher in tablets than

in granules. The percentage of total pore volume made up of pores within each range was calculated. This showed that 56% of granule pores had a median diameter greater than 0.9μm while only 41% of tablet pore volume was greater than this. As median pore diameters are calculated by volume values are biased towards larger pore diameters. Therefore, in this case, median pore diameters, as calculated in table 2.4, do not accurately reflect the pore size distribution of the tablets. These examples highlight the fact that differences between the pore size distributions of samples can be identified more effectively if the data is examined within different pore size distribution ranges. Examination of intrusion plots is essential in selecting areas to examine in more detail. Although not useful in these examples, first and third interquartile data points can also be used to give a better indication of pore size distribution (see section 3.3.4.1).

Overall, the median pore diameters obtained by mercury porosimetry were possibly lower than 'real' values due to the presence of structural hysteresis or 'ink-bottle' shaped pores. This describes a situation were the pores consist of an irregular network, with constrictions, cavities and junctions etc. However, equations 2.1 to 2.3 necessitated the assumption that pores in the material were cylindrical. Since this was unlikely, pore diameter values were not 'real' values but the best estimate of pore size distribution obtainable. Pore diameters can also be characterised by a hydraulic radius that is determined from a permeability coefficient obtained by measuring the rate at which dry air is drawn through a material (114). However, mercury porosimetry is considered a more effective way of characterising pore diameter (120).

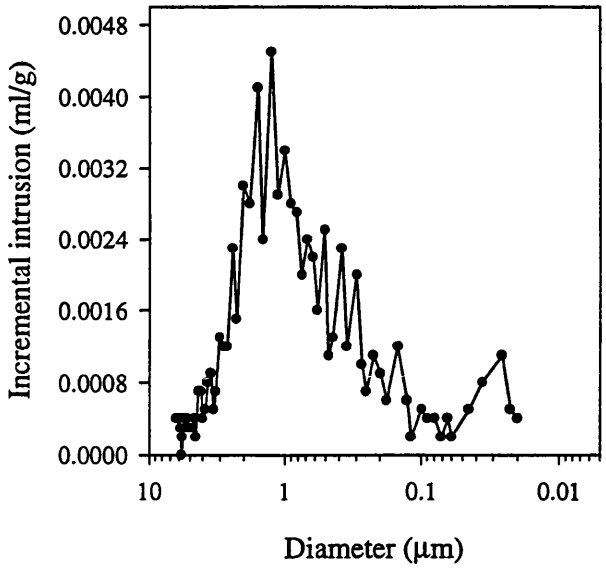

Figure 2.8 Pore distribution of model granules illustrated using an incremental intrusion plot.

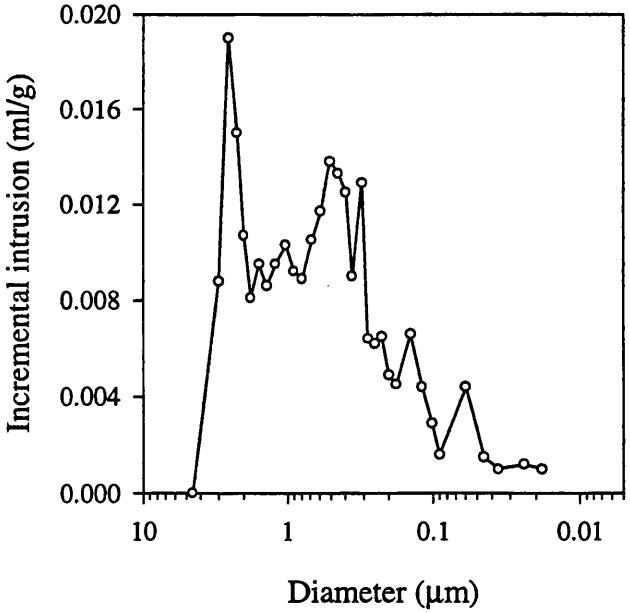

Figure 2.9 Pore distribution of model tablets illustrated using an incremental intrusion plot.

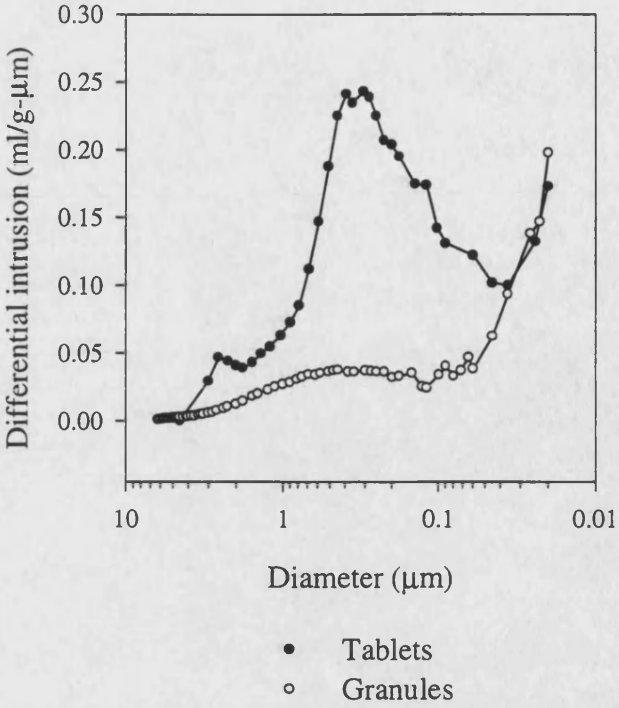

Figure 2.10 Differential plots showing the relative pore size distributions of model granule and tablet samples.

Considering the porosity of tablet and granules sample. Table 2.4 shows that the tablets were much more porous than the granules. From figures 2.8 and 2.9 it can be seen that pores of larger diameters accounted for the greater part of total porosity while small pores took up progressively less volume. Tablets had a bimodal pore size distribution while the majority of the pore volume of granules was accounted for by pores larger than 0.9µm. Tables 2.5 and 2.6 show pore volume distributions within each of the three pore diameter ranges selected for analysis. This quantitative information correlated well with the visual impression of pore volume distribution obtained from incremental intrusion plots. Porosity values calculated from mercury porosimetry were compared to porosity values obtained using the apparent volume and mass of the sample (table 2.7). In all cases porosity values determined from porosimetry were smaller, possibly due to the presence of closed pores that could not be accessed by mercury.

Compaction force (kN)	Porosity (%)	
	From porosimetry data	From geometrical calculations
2	31.2	39.3
4	27.8	31.8
12	22.0	21.6
16	18.4	20.2
24	11.9	16.3

Table 2.7 Porosity of TIMERxN tablets obtained from (a) mercury porosimetry measurements and (b) determinations of apparent volume from tablet geometry.

Pore area values determined using mercury porosimetry were examined using the model granule data. Using the data in table 2.5 it was calculated that although 56% of granule pores were greater than 0.9μm these pores only contributed to 10% of total pore surface area. In comparison, pores in the diameter range 0.1 to 0.02μm accounted for 6% of total porosity but made up 56% of total pore area. This again illustrated the fact that smaller pores contribute more to surface area than larger pores. The specific pore area of granules determined from mercury porosimetry ($0.896m^2/g$) was approximately three times greater than the specific surface area calculated from gas adsorption measurements on a similar batch of granules (see section 2.4.3). Although area determinations obtained from mercury intrusion are essentially pore surface areas they are often used as a measure of particle surface area (121). This difference between the values obtained in each case can be explained with reference to structural hysteresis. Surface area calculations based on intrusion of mercury into pores assume cylindrical pores, which have a larger surface area than a pore of equal volume displaying structural hysteresis. The phenomena of structural hysteresis means that values obtained from mercury porosimetry are likely to be less accurate than values obtained from gas adsorption techniques. Values obtained from mercury porosimetry tend to be higher than corresponding values obtained from gas adsorption measurements (110).

2.4.1.5 *Assessment of reproducibility*

It was anticipated that mercury porosimetry would be used to analyse a large number of granule and tablet batches. This meant that it would not feasible to carry out

replicate analysis on each batch of material. To ensure confidence in the results it was decided to carry out a number of replicate determinations on a selection of tablet and granule batches that had various pore structures. Manufacture of the granule batches used in these reproducibility assessments is described in chapter 3. Replicate values of porosity, median pore diameters and specific pore areas on tablets compacted from TIMERxN using a speed of 3mm/s and a range of compaction forces is illustrated graphically in figures 2.11, 2.12 and 2.13, respectively. Calculations were based on data collected from the estimated point of pore filling down to 0.02μm. For tablets compacted at each force the mean value of two determinations was found. The difference between the mean value and the individual values was calculated as a percentage of the highest value. The percentage difference was found to be 2.0% or less in the case of porosity values, 3.7% or less for specific pore area values and 4.0% or less for median diameter determinations. This showed that results obtained from mercury porosimetry were reproducible. Similarly, in the granule samples, (table 2.8) high reproducibility of each of the three pore parameters under consideration was obtained. Subsequently, only one porosimetry determination was made on each batch of material.

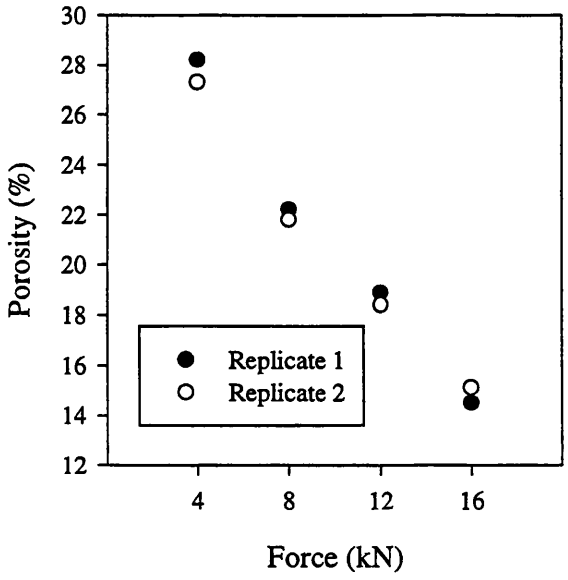

Figure 2.11 Porosity of samples taken from TIMERxN tablets compacted using pressures of 4, 8, 12 and 16kN.

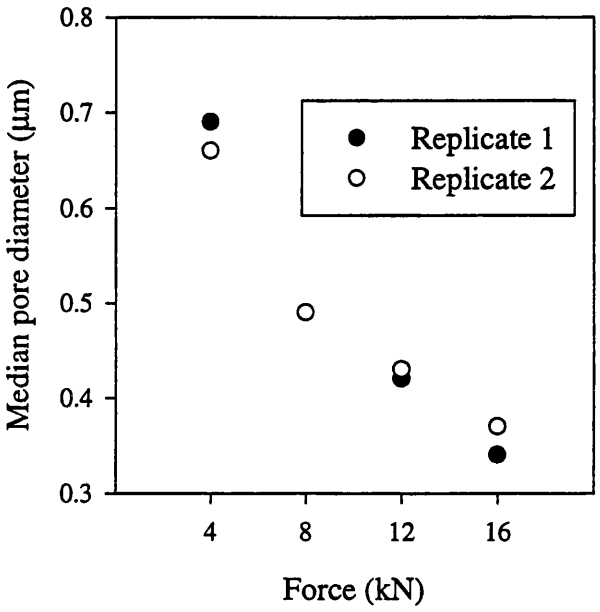

Figure 2.12 Median pore diameter determinations on TIMERxN tablets compacted using forces of 4, 8, 12 and 16kN

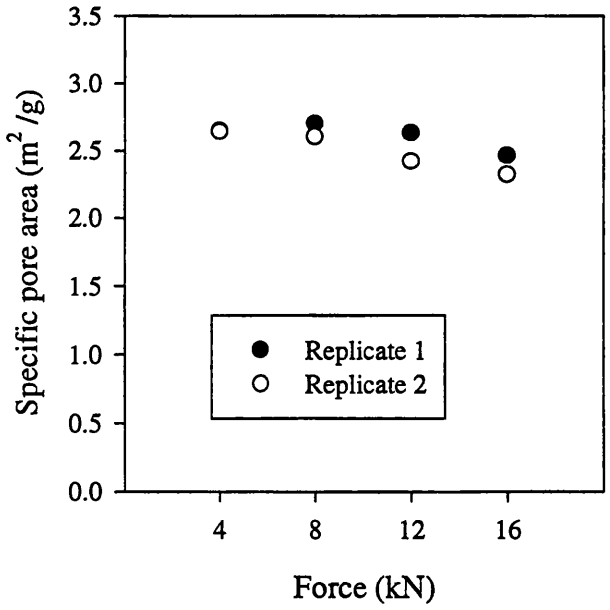

Figure 2.13 Specific surface area determinations on TIMERxN tablets compacted using forces of 4, 8, 12 and 16kN.

Pore characteristic	Batch No.					
	G3G		G3L		G3E	
Specific pore area (m^2/g)	0.699	0.635	0.392	0.405	0.871	0.893
Median pore diameter(μm)	1.82	1.75	2.18	2.01	0.99	1.08
Porosity (%)	4.95	4.13	3.45	3.40	9.83	10.11

Table 2.8 Replicate porosimetry determinations on three granule batches

2.4.1.6 *Limitations of mercury porosimetry*

Although reproducible results were obtained fundamental problems in the analysis of pore structure by mercury porosimetry were recognised. Firstly, the penetration of very large pores would be limited by the height of the sample, which determined a minimum pressure. However, scanning electron micrographs of the surface of tablets showed that only tablets compacted using a force of 2kN and a speed of 3mm/s had external cavity windows large enough to be penetrated at the pressure used to fill the penetrometer ($69kNm^{-2}$). It had also been shown that cavity windows did not contribute largely to pores volume therefore pore filling at very low pressures was unlikely to present problems. Secondly, accuracy of measurement of pore diameters was limited by the extent to which the contact angle selected represented the actual contact angle of mercury on the samples. Equipment to accurately determine the contact angle was not available however, for comparative purposes it was considered adequate to choose a reasonable value for the contact angle in order to ascertain whether or not two samples had the same pore size distribution and pore volume. For these studies a value of 130° was employed, which is one of the most frequently quoted values (110). Thirdly, compressibility of the dilatometer and mercury can occur causing base line errors. Carrying out blank runs and subtracting blank run data from the experimental run can eliminate this. Base line errors are only likely to be significant where the amount of sample to be analysed is very small, when tight levels of accuracy and reproducibility specifications are being imposed or if the porosity of the sample is very low. Since neither of these factors applied blank corrections were not carried out for this work. Fourthly, mechanical damage of samples can occur at high pressures. Taking the

relatively low pressure applied into account, compared with the forces applied during compaction, the occurrence of elastic deformation was unlikely. No signs of damage were observed when tablets were visually examined post analysis. It has been reported (109) that damage to pharmaceutical materials is unlikely to be observed. By eliminating many of the sources of error and with careful interpretation of the data it was considered that reproducible and representative results were being obtained.

2.4.2 *Scanning electron microscopy*

Figures 2.14, 2.15 and 2.16 show SEM's of three batches of granules that had different total pore volumes. The granule shown in figure 2.14 came from a batch of material having a porosity of 3.40% (batch G3L), the granule in figure 2.15 from a batch having a porosity of 4.64% (batch G3I) and figure 2.16 from material having a porosity of 10.36% (batch G3F). The granules selected were representative of the sample of material examined under the microscope. In these examples it appears that granules with the highest porosity had much more surface detail than granules with lower porosity. From this it could be concluded that SEM's could be used to rank samples in terms of porosity. However, an examinations of the granules in figure 2.17 shows that this material was made up of particles showing surface detail and particles showing little surface detail. The total porosity of this material was still relatively high at 11.14% (batch G3K). It was concluded that granule porosity for some samples was difficult to estimate because the total porosity was made up of the total porosity values of granules that had different porous structures. SEM's of tablet samples were useful for elucidating the compaction characteristics of granules (see Chapter 3) but were not useful for describing tablet pore characteristics.

2.4.3 *Surface area determination by nitrogen adsorption*

The volume of nitrogen adsorbed onto the surface of granule batch G2B and on to the surface of a sample of microcrystalline cellulose (Emcocel 50M) was plotted as a function of the relative pressure applied (P/P_0). Figure 2.18 shows the isotherms for batch G2B, which were Type II isotherms, typical for powdered relatively non-porous solids (107). Both isotherms possessed a defined knee point, which represented monolayer coverage of the adsorbate. The sorption isotherms were interpreted using the equation developed by Brunauer, Emmett and Teller (BET) (122). The BET equation (equation 2.5) was applied over the linear P/P^0 range, which was 0.07 to 0.4 for batch G2B and 0.03 to 0.2 for microcrystalline cellulose.

$$\frac{P}{V(P_0 - P)} = \frac{1}{W_m C} + \frac{(C-1)P}{V_m C P_o} \qquad (2.5)$$

Where V was the volume of gas adsorbed at pressure P, P was the partial pressure of nitrogen, V_m was the volume of nitrogen adsorbed in the monolayer, P_o was the saturation pressure of nitrogen at and C was a constant exponentially related to the heat of adsorption of the nitrogen gas on the sample. The surface area was determined as a product of the number of molecules in a completed monolayer and the effective cross sectional area of nitrogen (equation 2.6).

$$S_t = \frac{V_m N_0 A_{CS}}{M} \qquad (2.6)$$

Where S_t was the total surface area, N_o was Avogadro's number and A_{CS} was the cross sectional area of nitrogen ($0.1620 nm^2$).

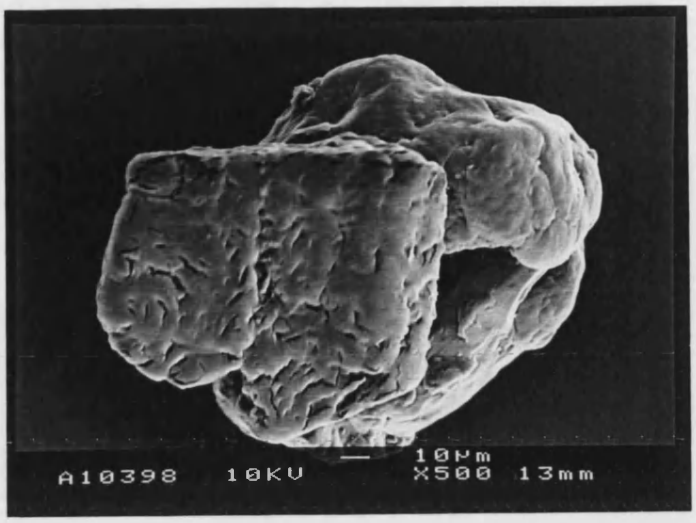

Figure 2.14 SEM of a granule taken from batch G3L which had a porosity of 3.40%. Shows a very smooth particle with little surface detail.

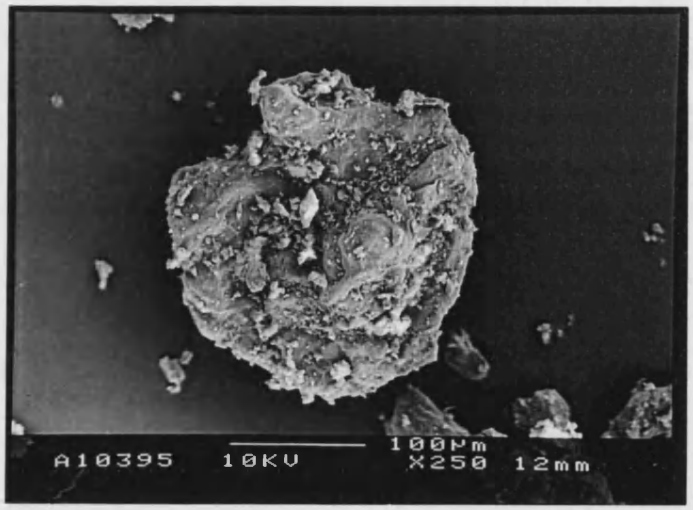

Figure 2.15 SEM of a granule taken from batch G3I which had a porosity of 4.64%. Some surface detail visible.

Figure 2.16 SEM of a granule taken from batch G3F which had a porosity of 10.36%. Degree of surface detail is greater than either batch G3L or G3I.

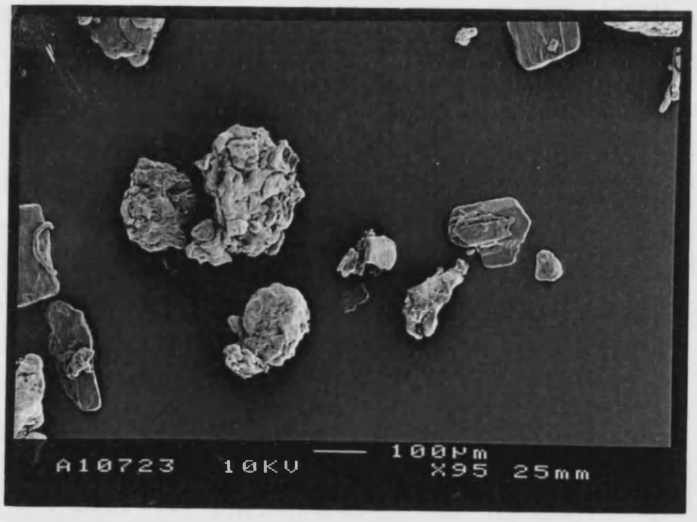

Figure 2.17 SEM of granules taken from batch G3K, which had a porosity of 11.14%. Both smooth and rough particles visible.

The results obtained for batch G2B are shown in table 2.10. Good reproducibility was observed along with low standard deviations. This is a low value typical of many other pharmaceutical excipients (e.g. lactose 0.53m^2/g (107)). The results were consistent with the observations made by electron microscopy, which indicated little surface detail. Correlation coefficients were on the limit or slightly below the accepted range (0.999 to 1) which can indicate that insufficient material has been used in the analysis (123). C values give a measure of the affinity of the adsorbate for the adsorbent. C values can range from 3 to 1000 depending on the adsorption isotherm of the material. In this case C values were toward the lower end of the acceptance range indicating that nitrogen had a relatively low affinity for the granules. This would have reduced the accuracy of the results. Although the standard deviation was low and the two results were similar the relatively small value of C and the low surface area of the material would indicate that krypton or xenon at the temperature of liquid nitrogen would be more suitable adsorbates. Krypton and xenon have lower vapour pressures, which would cause a larger amount of gas to be adsorbed onto the solid, resulting in more accurate measurements for materials with low specific surface area values. A further difficulty with measuring surface areas with this technique was the length of the analysis time. Due to the large sample weight the outgassing step took 24 to 36hr. Heating the sample can reduce the outgas time, but increased temperatures, especially under vacuum, can change the properties of organic materials (123). The results for Emcocel 50M are shown in table 2.11. Values quoted in the literature for Emcocel and similar grades of MCC range from 1.18 (124) to 1.27m^2/g (125), which suggested that values obtained may be highly dependent on analysis technique and experimental conditions. The results obtained here are higher than those reported elsewhere, possibly due to the low mass of material used for the measurement.

It was concluded that surface area determination by nitrogen adsorption would not be suitable for HP-based materials. However, the results were useful in that they had indicated that the surface area of the granules was low. To attempt to correlate surface area values with dissolution of model drugs from tablets or granules it would be necessary to produce materials that had largely different surface areas. If surface area values were low then physical modification of the material to produce batches with significantly different surface areas would be difficult. Attempts to correlate granule and/or tablet specific surface areas with dissolution profiles would be unlikely to

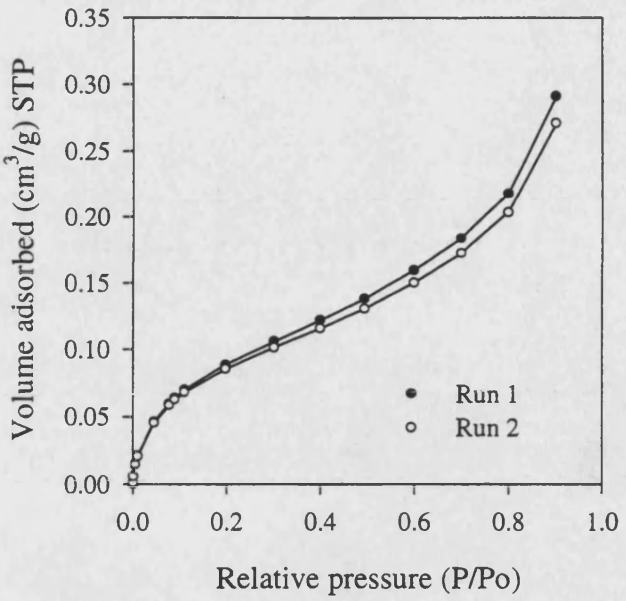

Figure 2.18 Type II isotherm of nitrogen adsorbtion onto batch G2B

succeed. In terms of bulk characterisation of HP-based granules and tablets it was concluded that determination of specific surface areas would not be useful.

	Run 1	**Run 2**
BET surface area ± SD (m^2/g)	0.338 ± 0.007	0.321 ± 0.007
C	32.36	37.57
Correlation coefficient	0.9917	0.9990

Table 2.10 Results from BET surface area analysis on granule batch G2B

	Run 1	Run 2
BET surface area ± SD (m^2/g)	1.581 ± 0.007	1.728 ± 0.009
C	70.51	50.19
Correlation coefficient	0.9998	0.9998

Table 2.11 Results from BET surface area analysis on Emcocel 50M

2.4.4 *Cyclohexane penetration studies*

Cyclohexane penetration into TIMERxN tablets compacted at a speed of 100mm/s using a range of forces is shown in figure 2.19. The porosity of the tablets as determined by mercury porosimetry and geometrical calculations is given in table 2.7. The graphs clearly showed that tablets having different pore volumes (i.e different tablet thickness) showed different rates of wicking, particularly between tablets compacted using the lower compaction forces. The data was quantified by calculating the slope of the linear region of each plot, which gave the rate of wicking into the tablets. The regression in each case was at least 0.99. Plotting compaction force against the inverse of the wicking rate enabled the relationship to be clearly examined (figure 2.20). The graph shows that measurement of wicking rates can distinguish between tablets which have largely different pore volumes, but does not substantially differentiate between those tablets compacted using forces of 2, 4, 8 and 12kN. Wicking studies on BHP-based granules that had different pore volumes but similar bulk volume showed that no difference in wicking could be observed between the batches (figure 2.21). The wicking of cyclohexane into BHP-based tablets that had equivalent relative densities is shown in figure 2.22. The tablets were compacted from granules that had various bulk physical properties (table 2.12). The graphs show that although differences can be observed in the wicking behaviour of some tablet batches the relatively high standard deviations made it difficult to obtain significantly different measurements. This method was not continued as a means of characterising tablet pore structure.

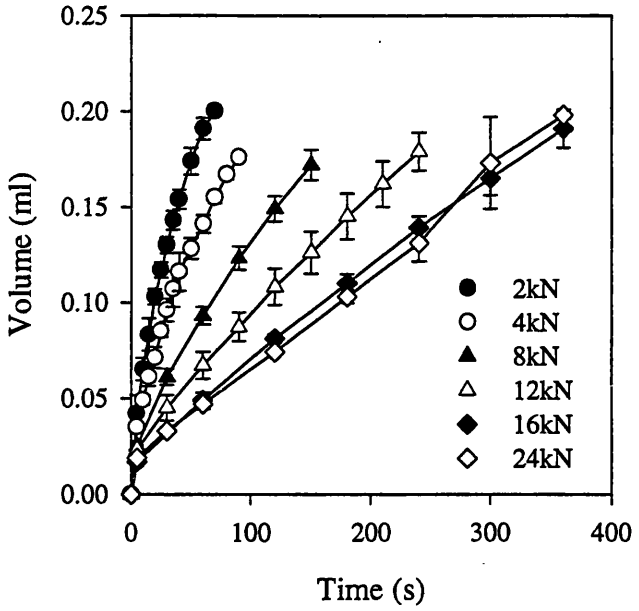

Figure 2.19 Cyclohexane penetration into TIMERxN tablets compacted using different forces at a speed of 100mm/s

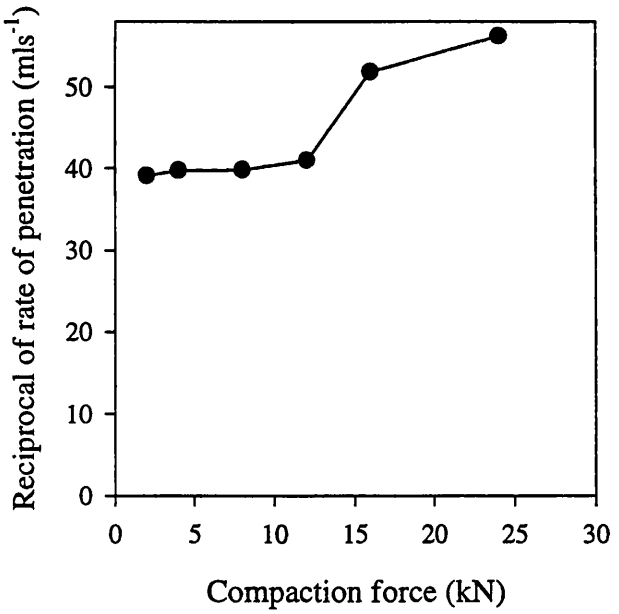

Figure 2.20 Effect of tablet porosity on cyclohexane penetration rates

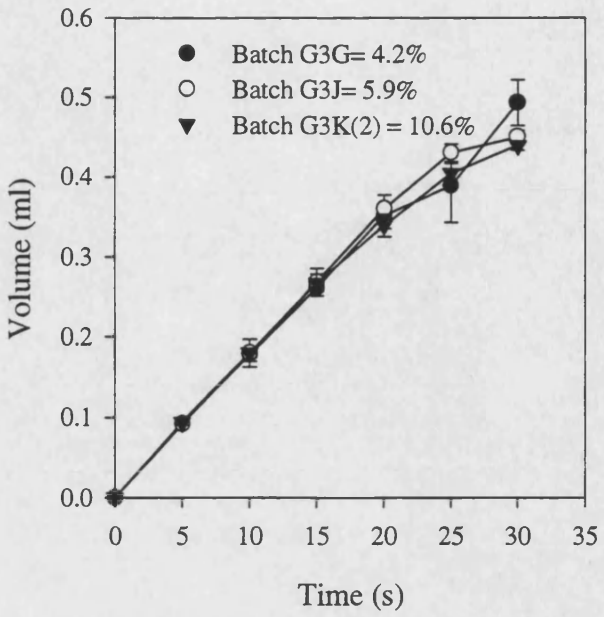

Figure 2.21 Cyclohexane penetration into HP-based granu

Pore parameters	**G3K(2)**	**G3N**	**G3L(2)**	**G3D**
Median pore diameter (μm) of pores >0.9μm	2.33	2.13	2.73	2.22
Porosity (%)	10.60	4.33	3.81	5.67
Bulk density (g/cm^3)	0.53	0.45	0.51	0.62

Table 2.12 Pore structure of granules batches G3K(2), G3N, G3L(2) and G3D

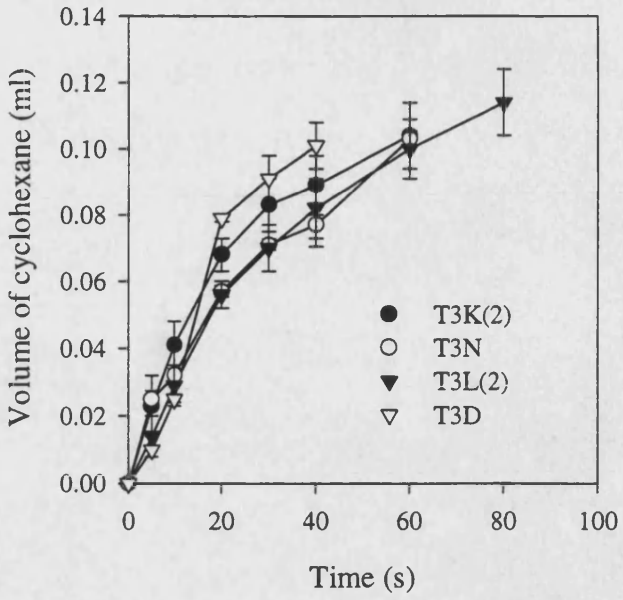

Figure 2.22 Penetration of cyclohexane into tablets compacted to equivalent relative densities

2.5 **Conclusions**

As a technique for determining the pore structure of HP-based granules and tablets, mercury porosimetry produced reproducible, quantitative information. With careful interpretation of the data it was felt that representative values of porosity and median pore diameter were being obtained. Examination of graphical presentations was essential to correctly interpret the data. The method was suitable for the analysis of both HP-based tablets and granules. The high degree of reproducibility provided confidence that sources of error had been avoided since these were likely to have become apparent in systematic reproducibility or repeatability experiments. Good reproducibility also gave confidence that one determination on subsequent batches of material would be satisfactory.

Measurements of surface area appeared to be less useful. Although determinations of surface area by gas adsorption appeared to yield reasonable surface area values the technique was not continued as a method of characterisation. This was due to three reasons; firstly, technical difficulties existed with the out gassing of such a large quantity of material which lead to very long experimental times. Determinations on large number of samples would therefore have been difficult. Secondly, although the two results obtained were very similar, the accuracy of the result was questionable

because of the very small surface areas involved. The use of krypton as the inert gas in place of nitrogen would improve the accuracy, but the small surface areas would still pose problems. Thirdly, since the material showed little surface detail and the particle size was relatively large then physical modification of the material to produce batches with significantly different surface areas was likely to be difficult. Attempts to correlate granule and/or tablet specific surface areas with dissolution profiles were unlikely to succeed. In terms of bulk characterisation of HP-based granules and tablets it was concluded that determination of specific surface areas was not useful. Determination of liquid penetration rates gave only a limited amount of quantitative information and was not useful for distinguishing porosity differences between tablets that had relatively large pore volumes. The method was not suitable for the bulk characterisation of granules. As scanning electron microscopy did not give quantitative data its use was limited on its own as a characterisation technique but was essential for using in conjunction with other methods.

3. Modification and characterisation of the bulk physical properties of heterodisperse polysaccharide (HP)-based granules and tablets

3.1 Introduction

One of the aims of this work was to obtain HP-based tablets that had substantially different porosities, pore size distributions and pore areas. It was considered that this could easily be achieved by compacting granules into tablets that had different tablet thicknesses. The only prerequisite was a material that would form intact tablets at high and low compaction forces. However, tablets having different tablet thicknesses have correspondingly different external surface areas. In the context of dissolution this means that the initial releasing surface area of the tablets differs. For the purposes of subsequent work it was necessary to produce tablets that had the same initial surface area yet different pore structures.

A tablet can be described physically as a large aggregate of small, strongly cohered granules (126). It was therefore proposed that the physical characteristics of the granules from which a tablet was compacted would affect the porous structure of the final tablet. Additionally, it was considered that tablet porous structure was likely to be dependent on the volume reduction behaviour of the material. This would be influenced to some extend by granule physical characteristics including bulk density (127).

It was considered that the pore structure of HP-based granules could be modified by controlling the processing conditions used to produce the granules. HP-based granules can be easily produced by wet massing the primary components, drying and size reducing the material. Many variables can be introduced into the various processing steps that could affect the particulate characteristics of the resulting material. The granulation of pharmaceutical materials has been extensively studied however, the majority of studies investigating the effect of processing conditions on the physical characteristics of granules have focused on lactose (128,131). A number of more recent papers have considered the granulation of glucose and mannitol (132,133) and HPMC (118). No literature could be found concerning the effect of processing conditions in relation to the physical properties of multi-component mixes. The initial part of this work therefore was concerned with assessing the effect of process variables on the pore structure and bulk density of HP-based material.

A study of the volume reduction behaviour of materials naturally splits into two parts: characterisation of the compaction process and characterisation of the finished

product. Investigations into compaction behaviour of pharmaceutical excipients have frequently centred on powder systems rather than granules, possibly because of the greater complexity of granular systems. Granular systems that have been studied have mainly been lactose based granulates (127,129,134,135). Little information exists on the compaction of multi component aggregates. The compaction of granules prepared by wet massing of HP-based material was considered here. BHP-based granules and TIMERxN (a proprietary formulation of HP-based material) were both used to obtain HP-based tablets having a range of physical characteristics.

3.2 Materials

Xanthan gum (Lots No. P5086 and 23071), locust bean gum (Lots No. B21577 and 22886), glucose (Lots No. CD4R02005 and CD6029107) and TIMERxN (Lot No. NS664) were supplied by Penwest Pharmaceuticals Co. (Patterson, NY, USA). Xanthan gum (Lot No. P5086), locust bean gum (Lot No. B21577) and glucose (Lot No. CD4R02005) were used to prepare all granule batches except G3K(2) and G3L(2). The latter two batches were prepared using xanthan gum (Lot No. 23071), locust bean gum (Lot No. 22886) and glucose (Lot No. CD6029107). Acetone and 2-propanol were obtained from Fisher Scientific Ltd. (Loughborough, U.K.). Magnesium nitrate hexahydrate (Lot No. KN09725JN) was obtained from Sigma Chemical Co. (Loughborough, U.K.). Calcium sulphate (Lot No. 92918620) was obtained from Mendell (Penwest Pharmaceutical Co., Patterson, NY, USA). Surelease™ E-7-19010 (Lot No. F7A0318), an aqueous solution containing 18.8% w/w ethylcellulose, 4.4% w/w ammonium hydroxide and 2.2% oleic acid, was obtained from Colorcon Ltd. (Dartford, Kent, U.K.).

3.3 Methods

3.3:1 *Characterisation of xanthan gum, locust bean gum and glucose*

The true density of each powder was determined using a helium pycnometer (Accupyc 1330, Micromeritics, Norcross, GA). A mean of 3 determinations was calculated (table 3.1). The aerodynamic particle size distribution was measured (Aerosizer, Amhesrt Instruments, Hadley, MA) using a low shear forces, a feed rate of 5000 particles/s and a 300s sample run time. Each raw material was analysed in

triplicate (table 3.1). Loss on drying (LOD) of the material was determined thermogravimetrically using an infra red balance. Approximately 5g, accurately weighed, was heated at 75°C until no further weight loss occurred (approximately 20min). The percentage weight loss was recorded.

	D [4,3] (μm)	True density (g/cm^3)	LOD (%)
Xanthan gum (P5086)	63.3 ± 8.6	1.54	9.4
Xanthan gum (23071)	70.9 ± 12.0	1.54	7.3
Locust bean gum (B21577)	72.3 ± 10.1	1.56	11.0
Locust bean gum (22886)	85.0 ± 8.9	1.53	7.1
Glucose (CD4R02005)	39.4 ± 7.5	1.53	8.6
Glucose (CD6029107)	45.3 ± 11.9	1.53	8.1

Table 3.1 Raw material characteristics

3.3.2 *Preparation of granules*

Batches containing 3-components (xanthan gum, locust bean gum and glucose) were prepared using 14 different sets of processing conditions. This included 8 batches of granules prepared as part of a factorially designed set of experiments. The aim was to obtain granules having different pore structures and bulk densities while evaluating the factors that were important in controlling bulk physical characteristics. The factorial design was used to investigate the effect of volume of water added, agglomeration time and drying temperature on pore structure and bulk density. Section 3.3.2.3 describes the preparation of 3 batches of granules containing calcium sulphate and/or ethylcellulose. These were prepared in order to investigate the effect of tertiary components on granule compactibility.

3.3.2.1 *Design of factorial experiment*

A three factor, two level factorially designed experiment was set up to evaluate the effect of agglomeration time (factor A), volume of water added (factor B) and drying

temperature (factor C) on the bulk physical properties of granules. The levels of each factor are detailed in table 3.2. The design of the study enabled the maximum information to be extracted from the data and reduced the total number of experiments needed to obtain the required information. Levels of factor A and factor B were determined by preliminary experiments and represented minimum and maximum levels achievable. 'Low' level of water was the minimum volume of water required to produce fine granules while 'high' level was the maximum volume of water which could be added before the granulation became unworkable. Following 'low' agglomeration time, added water appeared to be uniformly distributed through the material while 'high' agglomeration time was the maximum length of time that the wet mass could be mixed before mass agglomeration occurred. 'Low' temperature drying involved slow evaporation of water at room temperature (controlled at 21°C) until the material reached equilibrium moisture content (minimum of 48hr). 'High' temperature drying achieved a more rapid removal of water using elevated temperatures (60°C).

		Level	
Factor	**Description**	**Low**	**High**
A	Agglomeration time (min)	2	8
B	Volume of water added (%w/w)	15.9	20.6
C	Drying temperature (°C)	21	60

Table 3.2 Factors and levels selected for factorial design

The combination of factors and levels used to process the 8 granule batches is shown in table 3.3. The factors and levels were designated symbols traditionally used in experimental design with the letters indicating the factor at its highest level (136). For example, ab, indicated factors A and B at a high level (+1) and factor C at a low level (-1).

Treatment combination	Factor			Batch No.
	A	B	C	
(1)	-1	-1	-1	G3A
a	+1	-1	-1	G3B
b	-1	+1	-1	G3C
ab	+1	+1	-1	G3D
c	-1	-1	+1	G3E
ac	+1	-1	+1	G3F
bc	-1	+1	+1	G3G
abc	+1	+1	+1	G3H

Table 3.3 Treatment combinations used in factorially designed experiment

3.3.2.2 *Processing conditions*

Processing conditions used to produce the 8 batches of granules in the experimental design (batches G3A to G3H) and a further 6 batches, G3I to G3N, are described below. The treatment combinations used to produce batches G3I to G3N are shown in table 3.4. Batches prepared as part of the experimental design were carried out in random order to reduce bias. To look at reproducibility batches G3K and G3L were prepared again giving batches G3K(2) and G3L(2).

Dry mixing and wet massing was carried out in a uni speed high shear mixer (Cuisine Système Automatic 5000, Magimix, Surrey, U.K.). Xanthan gum (25%), locust bean gum (25%) and glucose (50%) were dry blended for 5min. Total batch size was 300g. As high shear mixing was continued the granulating fluid was added over a period of one minute. This ensured an essentially constant rate of addition for each experiment. A 'high' (20.6%w/w) or 'low' (15.9%w/w) volume of distilled water was added to batches prepared as part of the experimental design (table 3.2). Batch G3K was agglomerated using a mixture of distilled water (15.9%w/w) and 2-propanol (19%v/w). All other batches were agglomerated with 15.9%w/w water. The total volume of water added was maintained constant so that effects due to volume of water available for hydration were eliminated (excepts for batches G3B, G3D, G3F and G3H were the effect of increased water was specifically examined). For batches G3A to G3H mixing was continued for either a 'high' (7min) or 'low' (1min) mixing time. For all other batches

mixing was continued for 7min. Batches G3L, G3N and batches G3A to G3H were tray dried. The material was distributed on a tray into an approximately 1 to 2cm thick layer. The tray was either placed in an oven (Model 1H-150, size 2 Gallenkamp, Loughborough, U.K.) at 60°C for 24hr or left to dry in a temperature controlled room (21°C) for 48hr. The drying times selected were sufficient to ensure that the material had reached an equilibrium moisture content (approximately 7 to 11% at 21°C and less than 5% at 60°C). Fluid bed drying was used to obtain a higher rate of drying (batches G3I, G3J and G3K). This was achieved using a Uniglatt fluid bed drier (Uniglatt, Glatt AC, Switzerland) operating at either 60°C or 80°C for between 20 and 30min resulting in a LOD of less than 5%. Microwave drying was also used to achieve a rapid drying rate (batch G3M). Wet material was dried in batches of approximately 25g using a 750W domestic microwave (Type ST22 Proline Micro Chef, U.K.). 15min drying time per batch was required to obtain granules with a LOD less than 5%. During microwave drying heat was generated due to the high dipolar component of water coupling with the high frequency electromagnetic field. To dissipate generated heat and therefore prevent charring cold water was placed in the chamber.

Size reduction was carried out either when the material was wet or after it had been dried. Batches prepared as part of the experimental design were firstly dried then size reduced by passing the dry material though a hammer mill (Type 14-586, Glen Creston Ltd., Stanmore, Middlesex, U.K.) fitted with a 3mm screen. Hammer milling reduced particle size through high-velocity impact of the hammers against the powder. The remaining batches were size reduced using an oscillating granulator (Type MGL 4A, Frewitt, Switzerland), which reduced particle size by shear and attrition. Batches G3L and G3M were dried then passed through a 0.63μm screen (dry screening). Batches G3I, G3J, G3K and G3N were wet screened through a 0.32μm mesh and then dried. The rate of oscillation was constant in each case. To maintain a constant particle size the dry material was size selected to give granules with a normal size distribution and a theoretical median particle size of 182μm. Size selection was important since granule particle size can affect porosity (see section 3.4.3), compactibility (137,138) and ultimately, release controlling action (6,82). The granules were sieved through an I.S.O standard aperture diameter $\sqrt{2}$ sieve progression ranging from 710μm to 63μm (Endecotts Ltd., London, U.K.). The sieves were agitated using a Fritsch sieve shaker (Type 03-502, Fritsch, Germany) for 30min. No further change in weight of material retained on each sieve occurred when further sieving time was given. Quantities from each sieve fraction were selected in the following proportions: 500 to 710μm (2%), 355

to 500μm (4%), 250 to 355μm (26%), 180 to 250μm (36%), 125 to 180μm (26%), 90 to 125μm (3%), 63 to 125μm (2%) and 0 to 63μm (1%). Sieve fractions were recombined using turbula rotation (Type T2C, Glen Creston Ltd., Stanmore, Middlesex, U.K.) for 5min at 50rpm. Moisture contents were determined by loss on drying (LOD) measurements. LOD's were measured using an infrared moisture balance (Type LP16, Mettler, Switzerland). At least 5g of material was heated at 70°C until no further weight loss occurred (approximately 20min). Weight loss was recorded as a percentage of the original weight.

Granulating liquid	Drying conditions	Size reduction	Batch No.
Water	Fluid bed dried (60°C)	Wet screened	G3I
Water	Fluid bed dried (80°C)	Wet screened	G3J
Water/2-propanol	Fluid bed dried (80°C)	Wet screened	G3K
Water	Tray dried (60°C)	Dry screened	G3L
Water	Microwave dried	Dry screened	G3M
Water	Tray drying (60°C)	Wet screened	G3N

Table 3.4 Processing conditions used to prepare granule batches G3I to G3N

3.3.2.3 *Preparation of granules containing tertiary components*

One Patterson form of HP-based material, TIMERxN, contained 10% calcium sulphate and 5% ethylcellulose in addition to locust bean gum, xanthan gum and glucose (see Section 1.5.4). Batches of BHP-based granules containing one or more of these tertiary components was prepared according to the formulations shown in table 3.5. The dry materials were blended as before. Batches G3O and G3Q were prepared by adding 26.3%v/w of Surelease™ (an aqueous suspension containing 18.8%w/w ethylcellulose) over 1min. The granules were wet screened through a 0.32mm mesh using a mechanical granulator and tray dried for 24hr at 60°C. Batches G3N and G3P were agglomerated using 15.9%w/w water. The material was wet screened and tray dried for 24hr at 60°C. Particle size was standardised as described in section 3.3.2.2.

Components	Batch No.			
	G3N	G3O	G3P	G3Q
Xanthan gum (%)	25	25	25	25
Locust bean gum (%)	25	25	25	25
Glucose (%)	50	35	40	45
Calcium sulphate (%)	-	10	10	-
Ethylcellulose (%)	-	5	_	5

Table 3.5 Formulation of granules containing tertiary components

3.3.3. ***Standardisation of granule and tablet moisture content***

Under ambient conditions HP-based material retains approximately 4 to 9%w/w moisture. This is similar to the behaviour of cellulose ethers, which retain large amounts of water in their amorphous portions (137). Nokhodchi *et al.* (137) found that at any compaction speed and at a constant force an increase in the moisture content of HPMC K4M resulted in a decrease in porosity of the tablet. The presence of water also improved the mechanical properties of the tablet. For these studies it was therefore decided to control and standardise the moisture content of HP-based material. This was achieved by storing granules and tablets under controlled humidity conditions. A saturated solution of magnesium nitrate was prepared by adding an excess of magnesium nitrate hexahydrate to approximately 300ml of distilled water and agitating the solution overnight using a magnetic stirrer. The solution was prepared at room temperature. Sufficient solution was added to a glass chamber to cover the bottom of the vessel with a 2.5 to 5cm layer of solution. Samples of material to be compacted were distributed in a fine layer on weighing boats and supported above the saturated solution. The chamber was tightly sealed and allowed to equilibrate for at least 48hr at a controlled temperature of 21°C. 48hr was found to be the minimum time required for the samples to reach equilibrium moisture content. A saturated solution of magnesium nitrate produces an atmosphere that has a relative humidity of 55% at 20°C (139). Storage under these conditions resulted in material that had a final moisture content in the range 7 to 9%w/w. After compaction, tablets were returned to the chamber until further processing.

3.3.4 *Preparation of tablets*

Determination of the general compaction behaviour of each type of material, that is, the type of deformation and bonding that was occurring, was important in the characterisation of HP-based material. For TIMERxN this was achieved by compacting the material over a wide range of compaction forces using 3 different compaction speeds and characterising the resulting tablets using mercury porosimetry. For BHP-based granules the compaction behaviour of three batches of granules was examined. The granules were compacted using a range of compaction settings. To examine the effect of tertiary components on compactibility, batches G3N, G3O, G3P and G3Q were compacted to equivalent relative density (equivalent tablet thickness) and tablet mechanical strength was determined.

The second stage in tablet characterisation involved evaluation of the effect of initial granule physical structure on final tablet structure. Batches of BHP-based granules were (a) into tablets having equivalent relative density and (b) under constant applied force and compaction speed. The pore structure of the final tablets was assessed using mercury porosimetry. The granules compacted were selected on the basis of their physical characteristics and included batches with different pore structures and bulk densities. The physical characteristics of the batches chosen is discussed in section 3.4.5. The aim was to obtain tablets with largely different pore structures and to identify factors that influenced final tablet pore structure.

3.3.4.1 *Compaction to equivalent relative density*

Tablets compacted to equivalent relative density had the same external tablet surface area. To obtain tablets having equivalent relative density, selected batches of granules (see Section 3.4.5) were compacted using a single punch tabletting press (Type F3, Manesty, Speke, Liverpool, U.K.) fitted with a 10mm flat-faced punch and die set. The granules were compacted manually which allowed the weight and tablet thickness to be tightly controlled. Accurately weighed pre-conditioned samples (approximately 400mg) were hand filled into the die cavity and compacted by rotating the fly wheel manually. The punch and die were not lubricated. Tablet thickness was measured using a digital micrometer (Digit-cal electronic calipers, TESA S.A., Switzerland). The distance moved by the upper punch was adjusted so that the final tablet thickness was between 4.0 and 4.2mm. This was important since variations in tablet dimensions would

change tablet porosity. Final tablet weight was recorded. Tablet dimensions were re-measured prior to further analysis (at least 12hr after compaction).

3.3.4.2 *Compaction under controlled compaction force and speed*

A compaction simulator (ESH testing Ltd., Machine No. 4287, Brierly Hill, U.K.) equipped with a regularly calibrated load cell (100kN) was fitted with 10mm flat-faced F tooling. The die and punches were cleaned with acetone and pre-lubricated prior to compaction with a suspension of 1.5% magnesium stearate in acetone. To study the compaction properties of TIMERxN, accurately weighed samples (approximately 438mg) were introduced into the die cavity and compacted using three compaction speeds: 0.033mm/s, 3mm/s and 100mm/s. The distance moved by the upper punch was adjusted to produce tablets compacted with target forces of 2, 4, 8, 12, 16 and 24kN. Samples were taken from material that had been stored under ambient conditions. The LOD of the material was approximately 6%.

B-HP based granules were also compacted under conditions of controlled force and speed. A constant weight of approximately 439mg was maintained. Samples that had been conditioned at 55%RH for at least 48hr prior to compaction were introduced manually into the die cavity. The punch and die set were lubricated as before. Batch G3D was compacted at two target compaction forces (8 and 19kN) using target compaction speeds of 0.033mm/s, 3mm/s and 100mm/s. Batches G3K and G3L were compacted to target forces of 8kN and 19kN using a compaction speed of 3mm/s. 8kN was the minimum compaction force which would produce a intact tablet while 19kN was selected as an upper limit.

3.3.5 ***Analysis by mercury porosimetry***

Pore structure determinations were made using a Micromeritics Autopore II porosimeter (Type 9220, Micromeritics Instruments Co., Georgia, USA). Samples were stored over dry silica in a vacuum dessicator for at least 24hr prior to analysis to remove adsorbed moisture. Preconditioning in this way was shown not to affect the results obtained. Granule samples were analysed using between 3 to 5g of material per run. A 15ml powder penetrometer with a 0.392ml stem volume was employed and filled with mercury using a fill pressure of 68.9kNm^2. TIMERxN tablets were analysed using a 5ml solid penetrometer (1.131ml stem volume) using between 2 and 5 tablets per run and a fill pressure of 3.4kNm^2. Tablet batches T3L, T3D and T3K were analysed using a 15ml

solid penetrometer (1.131ml stem volume) using approximately 8 tablets per run. All other tablets were analysed using a 5ml solid penetrometer (0.392ml stem volume) using 2 to 3 tablets per run and a fill pressure of 3.4kNm^2. The penetrometer, fill pressure and sample size were carefully selected to ensure that between 10 and 90% of the stem volume was used. The surface tension, contact angle and density of mercury at 21°C were taken to be 485gcm/s^2, 130° and 13.5438g/ml respectively. Pore characteristics were calculated from P-V data that was collected from the filling of pores that had diameters of 0.02μm or greater. Results from one analysis on each batch of material are reported, except in the case of tablet batches detailed in section 3.4.5 were the mean of two determinations is given. Mercury porosimetry was used to characterise; (a) granule batches G3A to G3N, G3K (2), G3L(2); (b) TIMERxN granules; (c) tablets compacted from TIMERxN using different compaction speeds and forces; (d) tablets compacted from selected batches of BHP-based granules; (e) sieve fractions of batch G3G collected during size separation. This was carried out to assess whether granules having different particle sizes had different pore structures.

3.3.6 *Characterisation of the particle size, bulk density and flow properties of TIMERxN and BHP-based granules.*

A knowledge of the particulate characteristics of the powders compacted was important in understanding volume reduction behaviour. The particle size of TIMERxN was determined by sieve analysis. 300g of TIMERxN was passed through an I.S.O standard aperture diameter $\sqrt{2}$ sieve progression ranging from 710μm to 63μm as described in section 3.3.2.2. The weight collected in each sieve fraction was recorded. A cumulative percentage undersize plot was constructed and the first, second and third interquartile points were determined. A cumulative percentage undersize plot was also constructed for BHP-based granules using the weights selected from each sieve fraction. The interquartile coefficient of skewness (IQCS) was calculated using equation 3.1:

$$IQCS = \frac{(c-a)-(a-b)}{(c-a)+(a-b)} \qquad (3.1)$$

Where a, b and c were the second, first and third interquartile points, respectively.

Before determining bulk density the materials were firstly stirred to redistribute the particles. Between 2 and 4g of material was accurately weighed and slowly poured

into a graduated 10ml measuring cylinder. Care was taken to prevent agitation of the cylinder and consolidation of the particles. The volume of the sample was recorded. Bulk density was determined by dividing the weight of the sample by its volume. A mean of three determinations was recorded. Tapped density of the materials was found using a jolting volumeter (STAV 2003 JEL, Germany). The sample was tapped 300 times which was found to be sufficient agitation to obtain a maximum change in volume. The new volume was recorded.

3.3.7 *Determination of tablet hardness and mechanical strength*

Values of tablet mechanical strength were used as a measure of the effect of tertiary components on granule compactibility. A 1mm stainless probe was attached to a texture analyser (Type TA-XT2, Stable Microsystems, Surrey, England) that was fitted with a 50kg load cell. The tablet to be tested was placed underneath the probe, which was lowered at a speed of 1.0mm/s. The force (kN) generated as the probe penetrated the tablet was measured as a function of the distance moved by the probe (mm). The area under the curve between the minimum and maximum forces reached was calculated, which gave the work of failure. Six determinations on each batch were made and the mean value and standard deviation about the mean calculated.

Tablet crushing strengths were determined from the force required to fracture tablets by diametral compression on a motorised tablet hardness tester (Model 2E, Schleuniger, Switzerland). The mean value of six determinations is presented along with the standard deviation about the mean.

3.3.8 *Scanning electron microscopy*

Granules were scatted onto adhesive, conductive mounting discs. A layer of gold was deposited onto the sample surface using a sputter coater (Edwards high vacuum, Model S150B, Sussex, U.K.) running at a voltage of 1.4Kv for 8min. Samples were imaged with a scanning electron microscope (Jeol T6310, Japanese Electron Optics Ltd., Tokyo, Japan) using an electron bean potential of 5keV.

3.4 Results and discussion

3.4.1 *Effect of processing parameters on the bulk physical properties of BHP-based granules*

The results from the experimental design were analysed to determine significant and non-significant processing effects on granule characteristics. The information obtained from this was collated with information obtained from the analysis of batches G3I to G3N. The general characteristics of the granules were considered and parameters that appeared to affect physical characteristics evaluated.

3.4.1.1 *Determination of significant effects*

The responses of specific pore area, median pore diameter (of pores down to 0.9μm), bulk density and pore volume were selected for statistical analysis. The median pore diameter of pores having diameters 0.9μm and greater was chosen as a response. This was because visual examination of incremental intrusion plots showed that different methods of processing mainly affected larger pores. Table 3.6 shows the results (or yields) obtained for each response and for each treatment combination. A mean estimate of every effect on these physical characteristics was determined using the Yates technique, described recently by Davies (136). The data was first tabulated in standard order (see appendix II). The first and second yields ($y_{(1)}$ and $y_{(a)}$) were added and the sum entered as the first entry in column I. The third and fourth yields were added to obtain the second entry in column II. This was continued until the sum of all the pairs was obtained. The first yield was then subtracted from the second yield to obtain the fifth entry in column I. This was continued until the difference between all the pairs was obtained. The addition and subtraction process was repeated sequentially on n columns (n=3 for experiments with three factors). The first entry in column III gives the total of all the yields in the trial. The remaining entries gave the total effect for the main effects and interactions. The Yates technique was applied to the yields obtained for each of the four responses. For this 2^3 factorial design 4 estimates of every effect were obtained, therefore to calculate the magnitude of the effect the final value was divided by four. Table 3.7 gives the effect of each factor, or combinations of factors, for each of the chosen responses (porosity, pore area, median pore diameter and bulk density). P_i, a measure of the probability of the effect occurring, was calculated using equation 3.2.

$$P_i = \left(\frac{i-0.5}{n-1}\right)\times 100 \qquad (3.2)$$

Where i = i^{th} effect 1, 2, 3...etc.

When the effects in order of increasing magnitude were plotted on a probability scale, from the most negative to the most positive, against P_i on a linear scale, an idea of effects that were possibly statistically significant was obtained (136). Figures 3.1, 3.2, 3.3 and 3.4 show Yates plots for porosity, median pore diameter, pore area and bulk density, respectively. Effects that were merely random were expected to fall on a straight line, the effects that fell off it were possibly real and were examined further. The linearity of figure 3.1 indicated that changes in porosity were random and could not be attributed to any one factor or combination of factors. The deviation from linearity of point C on figure 3.2 indicated that using a lower drying temperature (factor C) might have significantly changed the median pore diameter of the granules. Drying temperature also appeared to affect pore area (figure 3.3) while factors A and C appeared to affect bulk density (figure 3.4). To determine the statistical significance of the effects the Yates table was further developed to produce an analysis of variance (ANOVA)

Treatment combination	**Pore area (m^2/g)**	**Median pore diameter (of pores > 0.9μm)**	**Porosity (%)**	**Bulk density (g/cm^3)**	**Batch No.**
(1)	0.448	3.10	5.85	0.54	G3A
a	0.486	3.14	4.22	0.56	G3B
b	0.819	3.38	6.12	0.54	G3C
ab	0.498	2.93	5.67	0.62	G3D
c	0.886	1.90	10.11	0.55	G3E
ac	0.833	1.75	10.36	0.63	G3F
bc	0.774	2.56	4.20	0.58	G3G
abc	0.819	1.79	6.12	0.62	G3H

Table 3.6 Results (yields) of 2^3 factorial experiment

Treatment combination	Specific surface area (m^2/g)	Median pore diameter (of pores > 0.9μm)	Porosity (%)	Bulk density (g/cm^3)
a	-0.0857	-0.333	0.532	0.055
b	0.0512	0.191	-1.597	0.020
ab	-0.0782	-0.276	1.222	0.005
c	0.2522	-1.138	2.742	0.030
ac	0.0557	-0.126	1.572	0.005
bc	-0.1402	0.158	-2.457	-0.010
abc	0.1012	-0.033	0.632	-0.025

Table 3.7 Effects and interactions from experimental design

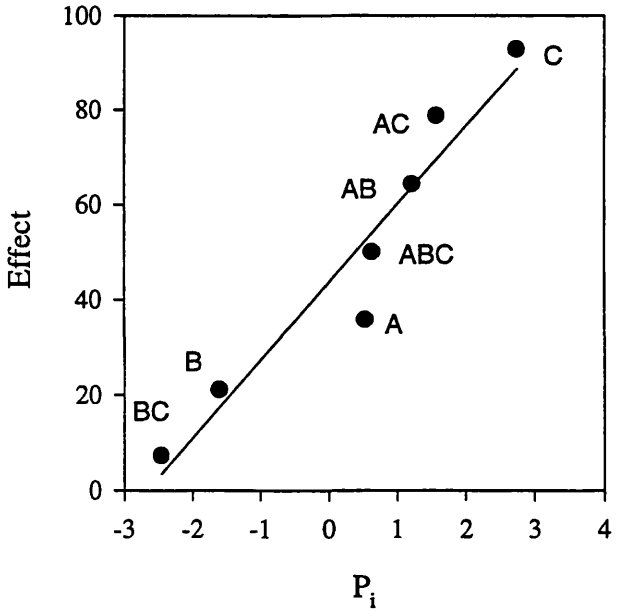

Figure 3.1 Identification of possible significant effects on porosity

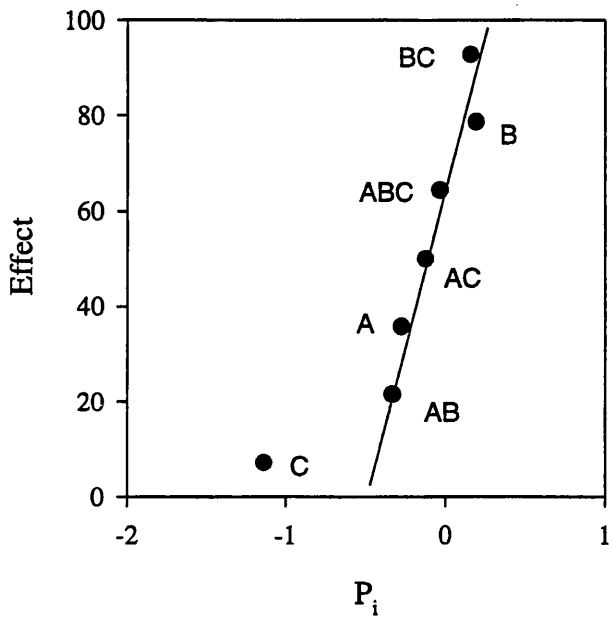

Figure 3.2 Identifcation of possible significant effects on median pore diameter

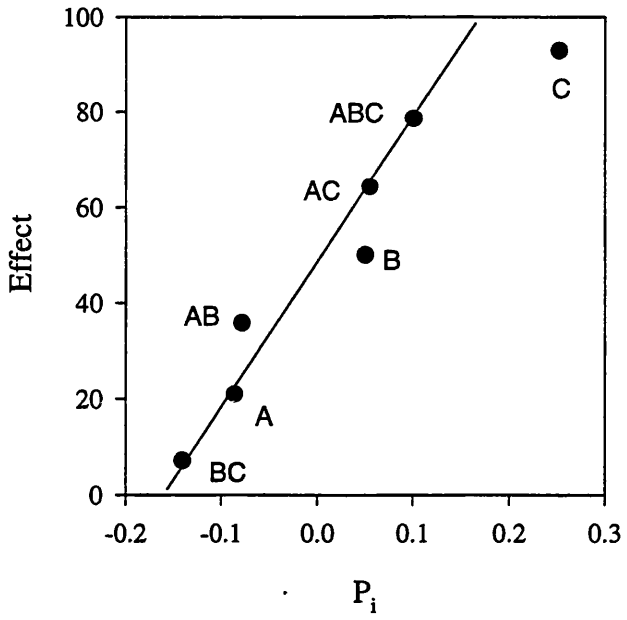

Figure 3.3 Identification of possible significant effects on pore area

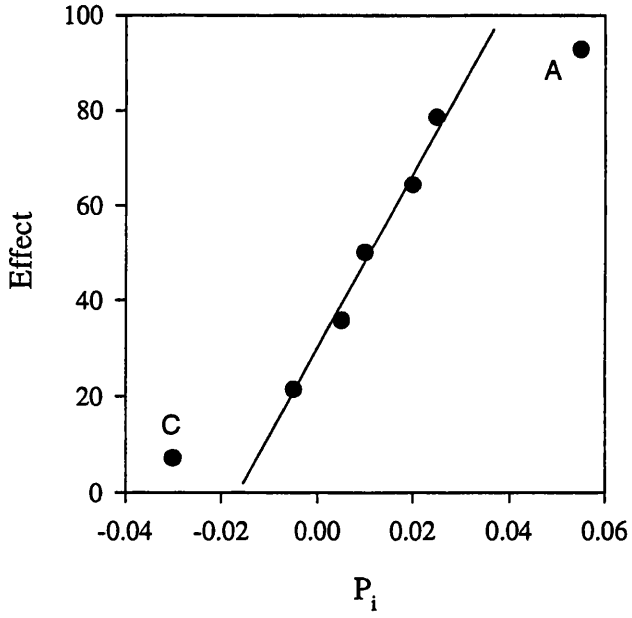

Figure 3.4 Identifaction of possible significant effects on bulk density

The sum of squares for the main effects and interactions was obtained by squaring the effect total and dividing this square by the number of observations in the experiment (ie, 8). When the sum of squares was divided by the appropriate degrees of freedom the corresponding variance of mean square s^2 was obtained. This divided the total variance of the results into the seven effects. Since the experiment was unreplicated each effect had one degree of freedom and the mean squares was equal to the sum of squares. To carry out an F test some effect or effects from the seven was required as an estimate of the error variance. The most satisfactory method would have involved running the experiment with replicates. However, this would have resulted in an excessively large number of experiments. In the absence of replication the experimental error was estimated by pooling the mean squares from higher order interactions. The two-way interactions AB, BC and AC, and the three-way interaction ABC were pooled. The ratio of the two variances was calculated using the error variance as the denominator and the observed values were compared to F tables at the 5% and 1% levels. Results from the analysis of variance on pore diameter data are presented in table 3.8. Comparing the experimental F values with F tables, F_C was significant ($\alpha_C < 0.01$) when df = 1,4. This meant that a high drying temperature (factor C) significantly decreased the median diameter of the larger pores. No other effects were significant. Analysis of

variance on bulk density data showed that factor A significantly affected bulk density when α_C <0.05 and d.f. = 1,4. Pore area and porosity were not found to be significantly affected by any factor or combinations of factors.

Factor	d.f	Mean square	F[a]
A	1	0.2220	3.74
B	1	0.0731	1.23
AB	1	0.1526	
C	1	2.5935	43.75*
AC	1	0.0318	
BC	1	0.0504	
ABC	1	0.0023	

Table 3.8 ANOVA table for median pore diameter data

[a]Error mean square based on AB, BC, AC and ABC interactions, 4 d.f

*α<0.01

3.4.1.2 *Effect of granulation conditions on bulk physical characteristics of BHP-based granules*

The bulk physical characteristics of granule batches G3A through to G3H and of batches G3I to G3N are detailed in tables 3.5 and 3.9, respectively. By changing the process conditions used to produce the granules, porosity could be varied between 3.23 and 11.14%. Overall, the variation in porosity achieved was relatively low compared with variations in porosity that has been obtained for other pharmaceutical excipients. By using different granulating techniques Wikberg and Alderborn (129) produced lactose granules that had porosity values ranging between 11.6 and 31.3%. Similarly, Sheskey *et al.* (118), using wet granulation techniques, produced HPMC granules that had substantially different pore volumes. The small variations in porosity observed for BHP-based granules could firstly be attributed to the presence of glucose in the formulation. Glucose is highly soluble in water (1:1) (139) and during wet granulation small glucose particles and the surface of large glucose particles can dissolve and recrystallise as glucose monohydrate (132). It has been shown that during wet

granulation of glucose, partly dissolved particles bond to each other through solid bridges formed during recrysallisation, producing granules that have low porosity (4 to 7%) (132). During wet granulation of XG, LBG and glucose a similar effect is likely to occur. Dissolved glucose is likely to form solid bridges with other glucose particles and with HP components resulting in the formation of very dense granules with low porosity. Pore diameters of BHP-based granules were much smaller than pore diameters that have been quoted for lactose granules (117,140). This again reflects the dense closed pore network that is formed.

Neither the volume of water added nor agglomeration time significantly affected any of the pore parameters measured. Increased moisture and increased agglomeration time had been expected to decrease granule porosity by affecting granule growth and densification. According to granulation theory, reviewed by Augsburger and Vappalla (141), low levels of moisture produce granules that consist of moist particles held together by liquid bridges in a pendular state. The pendular state refers to a situation were the water forms discrete lens shaped rings at points of contact. As more liquid is added nuclei agglomerate to the funicular state and coalescence of granules can occur. In the funicular state rings of water coalesce to form a continuous network of liquid interspersed with air. The action of the mixer brings the particles closer together so that internal pore space in the aggregates is reduced. Addition of a 'low' level of water to the dry blend produced nonspherical granules that were soft in texture, had a 'dry' surface, were light in colour and appeared to have a low density. Under these conditions the granules were probably in the pendular state. After the addition of a 'high' level of water granules were more spherical, firmer and denser in colour and in texture than at the 'low' level of addition. Coalescence of granules was observed probably due to increased plasticity imparted by the higher moisture content. As mixing was continued at the 'high' level of addition further coalescence occurred. However, despite the fact that material agglomerated with a 'high' volume of water differed visually in texture from that agglomerated with less water, no correlation was observed between volume of water added and/or mixing time and the final porosity of the dry material. The relationship between granule pore structure and amount of granulating liquid has also been studied for lactose and HPMC. Sheskey *et al.* (118) reported that the porosity and median pore diameter of HMPC decreased with an increased amount of granulating liquid (118). Tapper and Lindberg (130) and Jaegerskou *et al.* (140) found that the porosity of lactose granules decreased with increasing volumes of water added. Wikberg and Alderborn (142) however, did not find a correlation between porosity and volume of granulating

liquid added in lactose granulates. If final porosity was a function of densification during wet massing, screening and drying then this might account for the discrepancy in the results. In the case of BHP-based granules, final pore structure may not have been affected by mixing time and volume of granulating liquid because; (a) the effect of the hammer mill on the dry granules may have obscured any effects due to volume of water added and/or mixing time; (b) maximum densification may already have been reached at 'low' volume and 'low' mixing. Further addition of water and increased mixing may simply have produced aggregates of granules that were subsequently broken down during dry screening. Mixing time significantly ($p<0.05$) increased bulk density possibly due to rounding and smoothing of the particles over time.

The granules that were most porous were obtained when the components were granulated with an alcohol/water mix and dried rapidly by fluid bed drying. This could be due to reduced densification as a result of the surface tension of the granulating liquid. Wells and Walker (143) showed that the surface tension of a binding solution decreased as the proportion of alcohol in the solution was increased. Ritala *et al.* (144) found that the densification of dicalcium phosphate was greatest when the binding solution had a high surface tension. Increasing surface tension was thought to facilitate densification by increasing liquid bonding strength. As surface tension of the binding solution increased the agglomerates became stronger and more cohesive resulting in granules which had low porosity values. Wikberg and Alderborn (129) showed that the addition of alcohol increased the porosity of lactose granules.

The least porous material was batch G3L (3.23%). The processing condition likely to have caused this was the dry screening step. Dry screening was achieved using an oscillating granulator that reduced particle size through shear and attrition. This possibly resulted in breakage across granules rather that between granules. The abrasive action might also have smoothed the surface of the dry dense HP-based material producing granules with a relatively even and solid surface and a correspondingly low porosity.

Batches prepared as part of the experimental design were dried and then screened. For batches G3I, G3J, G3K and G3N, size reduction was the penultimate step while the final step was drying. The order of processing was considered relevant since the final granule pore structure was possibly a function of wet mixing, screening and drying. It was feasible that the effect of one step on pore structure may have been obscured by the effect of a subsequent step. It was considered that the effect of any one factor should be considered in relation to the order of processing steps. This was

relevant when considering the effects of drying temperature and drying method. In the experimental design drying temperature was found to significantly ($\alpha<0.01$) change the median pore diameter of the larger pores. At the higher drying temperature a decrease in pore diameter was observed. Batches G3I to G3N were dried using a number of different drying methods. The batches that were dried most rapidly were batch G3M (microwave dried), batch G3I (fluid bed dried at a high temperature) and batch G3K (contained alcohol in the granulating fluid, which increased the evaporation rate giving a high rate of drying). Examination of the data in table 3.9 shows that these batches were associated with relatively high median pore diameters. The conclusion that rapid drying produced granules having a higher median pore diameter was not in agreement with observations made from the factorially designed experiment where higher temperatures decreased median pore diameter. The differences between effects of drying may have been due to the order of processing. In the experimental design a variable introduced as a consequence of drying temperature was the final moisture content of the material. Batches dried at the high temperature contained less moisture after drying (less than 5%) than batches which had come to equilibrium moisture content under ambient conditions (7 to 11%). This may have affected the subsequent size reduction step. Hammer mills reduce particle size through high-velocity impact between rapidly moving hammers and the material particles. The dryness of the granules and the feed rate are important variables relative to the material (145). Drier granules were possibly more brittle and may have under gone greater attrition in the mill than granules containing a higher content of water. Water can act as a plasticiser in pharmaceutical excipients (137) and may have promoted plastic and elastic deformation during milling. In batches where drying preceded size reduction the observed changes in median pore diameter were probably due to the drying process itself rather than as a secondary effect to final moisture content. Drying rate may have been particularly important in these batches because of the presence of the water-soluble component glucose. It is possible that dissolution of glucose occurred during the early stages of drying as well as during wet massing. As water evaporates during drying glucose will recrystallise and the rate of drying may affect the degree of crystallisation. At slow drying rates larger crystals may develop while with faster drying rates smaller crystals are likely to be formed (132). Median pore diameters appeared to be larger when the rate of drying was faster. From incremental intrusion plots it could be seen that intermediate sized pores (0.9 to 0.1μm) were predominately affected by drying rates. With faster drying rates and the formation

of small crystals a more open network may have been formed producing a higher proportion of intermediate sized pores.

Batches with bulk densities ranging from 0.44 to 0.62g/cm^3 were obtained. The variation between multiple measurements was no greater than 0.02g/cm^3. High bulk densities were associated with a high agglomeration time. However, it was difficult to correlate any other factors or combination of factors to changes in bulk density. This may be because bulk density was affected by many particle characteristics including shape and apparent density.

Batch No.	Pore area (m^2/g)	Median pore diameter (μm) (of pores > 0.9μm)	Porosity (%)	Bulk density (m^2/g)
G3I	0.840	1.79	4.64	0.47
G3J	0.674	2.25	5.97	0.47
G3K	0.855	2.72	11.14	0.53
G3L	0.401	2.01	3.40	0.52
G3M	0.498	2.86	5.54	0.44
G3N	0.482	2.13	4.33	0.45

Table 3.9 Physical characteristics of batches G3I to G3N.

3.4.2 *Reproducibility of granule batches*

To thoroughly examine the effect of process variables on granule pore structure it would have been necessary to prepare more than one batch of granules under each set of processing conditions. However, this was not feasible due to the large number of batches involved. To ensure that the changes in pore parameter due to changes in processing conditions were not simply random, two batches were produced under similar conditions as previously. The pore characteristics of each batch of granules were very similar (table 3.10), which indicated that batches having high and low porosity could be reproduced. This gave confidence that the differences observed were not accidental. Average pore diameter was used in place of median pore diameter since this took into account both the volume and number of pores and therefore was a useful parameter for

comparative purposes. These batches were prepared using different lots of raw material from that used in previous batches. The particle size, density and moisture content of each lot was similar (table 3.1). Material lot did not appear to affect pore structure or bulk density.

	Batch No.			
Pore characteristics	**G3K**	**G3K(2)**	**G3L**	**G3L(2)**
Specific pore area (m^2/g)	0.851	0.749	0.401	0.426
Average pore diameter (μm)	0.444	0.426	0.233	0.249
Pore volume (%)	11.14	10.60	3.40	3.81

Table 3.10 Reproducibility of granule batches

3.4.3 *Effect of particle size on pore structure*

The results of mercury porosimetry analysis on sieve fractions of batch G3G are shown in table 3.11. Data in the last row came from granules that had been size selected and therefore consisted of particles having a wide size distribution. Examination of the data showed that the specific pore area of the granules increased as particle size increased, median pore diameter decreased with increasing particle size while porosity values remained similar within each size range. Granules that included particles taken from each of the sieve fractions had intermediate values of each pore parameter. To examine the data more thoroughly the characteristics of pores within 3 different pore size ranges was calculated. Tables 3.12 to 3.14 details the characteristics of pores within different pore diameter ranges for each of the sieve fractions. It can be seen that smaller pores contributed to the majority of specific pore area (table 3.12). The volume of pores (table 3.13) in the pore diameter range 0.2 to 0.02μm for particles with a size range of 355 to 500μm was more than double that for particles in the size range 125 to 180μm (table 3.13). This accounted for the observed increase in specific pore area with increasing particle size. Table 3.13 shows that the volume of large pores (>0.9μm) tended to decrease with increasing particle size while the volume of smaller pores (0.9 to 0.2μm and 0.2 to 0.02μm) increased. The net outcome was a minimal change in total

porosity but a shift in median pore diameter towards lower values. Overall, granules with a smaller particle size had a greater proportion of larger pores and a smaller proportion of smaller pores. The general conclusion was that for any batch of granules measured pore characteristics can vary depending on the particle size of the granules analysed. Therefore, when deciding whether or not a process variable affects the actual pore structure of the granules particle size should be considered. This is important since changes in process variables may also change the particle size distribution. For example, Sheskey and Williams (118) reported that the median pore diameter of Methocel K4M granules increased as the volume of granulating liquid was increased. An increase in granulating fluid added was also associated with a substantial increase in particle size, which could also cause an increase in pore diameter. Size selection of HP-based material prior to analysis ensured that changes in pore structure were not a consequence of changes in particle diameter.

	Pore parameter		
Sieve fraction (μm)	**Specific pore area (m^2/g)**	**Median pore diameter (μm)**	**Porosity (%)**
125 to 180	0.425	2.01	4.72
180 to 250	0.626	1.75	4.12
250 to 355	0.743	1.55	4.47
355 to 500	0.924	1.15	4.87
0 to 710	0.783	1.32	4.21

Table 3.11 Pore characteristics of different particle size fractions of batch G3G

Sieve fraction (μm)	Pore diameter range (μm)		
	> 0.9	0.9 to 0.2	0.2 to 0.02
125 to 180	0.049	0.046	0.334
180 to 250	0.032	0.042	0.567
250 to 355	0.035	0.052	0.660
355 to 500	0.033	0.067	0.830
0 to 710	0.033	0.051	0.703

Table 3.12 Specific pore area of sieve fractions of batch G3G

Sieve fraction (μm)	Pore diameter range (μm)		
	> 0.9	0.9 to 0.2	0.2 to 0.02
125 to 180	3.58	0.68	0.48
180 to 250	2.65	0.63	0.83
250 to 355	2.70	0.71	1.03
355 to 500	2.56	0.90	1.37
0 to 710	2.44	0.70	1.06

Table 3.13 Porosity of sieve fractions of batch G3G

Sieve fraction (μm)	Pore diameter range (μm)		
	> 0.9	0.9 to 0.2	0.2 to 0.02
125 to 180	2.60	0.55	0.047
180 to 250	2.92	0.50	0.045
250 to 355	2.72	0.46	0.053
355 to 500	2.77	0.49	0.057
0 to 710	2.54	0.47	0.049

Table 3.14 Median pore diameter of sieve fractions of batch G3G

3.4.4 *Characterisation of the compaction behaviour of TIMERxN and BHP-based granules*

3.4.4.1 *Compaction behaviour of TIMERxN*

The variation in porosity of TIMERxN tablets as a function of compaction force at 3 different compaction speeds is shown in figure 3.5. Mean compaction forces achieved did not differ from the target force by more than 10%. The variation from the mean force was not more than 0.4kN for forces less than 4kN and not more than 1.4kN for tablets compacted at forces greater than 4kN. Porosity decreased as the compaction pressure was increased. The reduction in porosity was dependent on the velocity of the upper punch. Compaction at low speed (0.033mm/s) produced a tablet that had a lower porosity than tablets compacted at a higher speed (100mm/s) when a similar compaction force was applied in each case. In order to understand the effect of compaction speed on porosity the sequence of events that occurs during a compaction process must be considered. When a force is applied on a powder or granule bed, a number of mechanisms become involved in the transformation of the loose particles into a porous, coherent compact. The compaction process, reviewed by Nystrom (146), can be described by a number of sequential phases. Initially, the particles in the die rearrange to give a closer packing structure. At a certain load, the packing characteristics of the particles or interparticulate friction between the particles prevent any further interparticulate movement. The subsequent reduction of compact volume is accompanied by reversible (elastic) deformation and irreversible (plastic) deformation of the whole or part of a particle. The degree of irreversible and reversible deformation can be characterised by the viscoelastcity of the material (147). For many materials fragmentation of particles also occurs (146). When the applied pressure is further increased the particle fragments can rearrange to form new positions and can also undergo deformation, which can further decrease compact volume. As a consequence of the compression of a powder, particle surfaces are brought into close proximity to each other and can form bonds. Intermolecular bonding (van der Waals forces, electrostatic forces and hydrogen bonding) constitutes the dominating bond mechanism for pharmaceutical materials (146). When the applied force is removed relaxation of the material occurs and the compact is ejected from the die. The actual porous structure is formed because of stress relaxation phenomena. Stress relaxation can be defined as the relative increase in volume after compression and occurs because the elastic component of the material can store mechanical energy when a stress is applied and release it when

the stress is removed (147). When TIMERxN was compacted at low compaction speeds the amount of stress relaxation relative to the creation of stress was high. After compaction, the newly formed tablet contained low internal stresses therefore the increase in volume was low which resulted in a lower porosity. In contrast, at high compaction speeds stress relaxation during compression was lower, so immediately after upper punch release the tablet still contained a lot of internal stress, which resulted in tablets having higher porosities. The fact that tabletting speed affected the consolidation behaviour of TIMERxN was a function of the viscoelasticity of the material (147). At low compaction speeds the viscous component dominated, which resulted in irreversible deformation while the elastic component was relatively unimportant due to stress relaxation. At higher compaction speeds the elastic component dominated total rigidity, which resulted in a considerable volume increase after compression. The final porosity of the tablet was the result of a balance between viscosity and elasticity (i.e irreversible and reversible deformation). TIMERxN can be described as strain-rate sensitive since it shows time-dependent deformation (148). This suggests that it deforms by plastic flow. Substances that consolidate principally by fragmentation show relatively little velocity dependence (148). SEM's of the upper surface of TIMERxN tablets supported the theory of plastic deformation. Figures 3.6 (a) to (c) show the surface of TIMERxN tablets compacted at different compaction forces using a speed of 3mm/s. Marked changes in the surface of the tablet occurred as the compaction force was increased. At low compaction pressures discrete granules could be identified. As the compaction pressure was increased the primary particles became fused so that boundaries became undetectable. The high plasticity of the material facilitated the formation of permanent particle-particle contact regions.

The change in median pore diameter of TIMERxN tablets as a function of compaction force is shown in figure 3.7. As expected, median pore diameter tended to decrease with increasing compaction force. Higher compaction speeds generally resulted in tablets having larger median diameters. Since median pore diameter gives only limited information on pore size distributions (see section 2.4.1.4), incremental intrusion plots were also examined. Figure 3.8 shows incremental intrusion plots for TIMERxN tablets compacted using forces of 4, 8 and 24kN. It can be clearly seen that as compaction force was increased the pore size distribution shifted towards smaller pores. Volume reduction occurred largely through reduction in size of larger pores while the smaller pores were less affected. This is characteristic of plastic deformation (149). For materials that deform mainly by fragmentation, porosimetry data would be expected to

show the existence of new populations of pores rather than a shift in existing pore size distribution. The shift in pore size distribution was also well illustrated by plotting the first, second and third incremental points from the cumulative intrusion plot (figure 3.9). This clearly identified the pores that disappeared when a force was applied.

The change in pore area of TIMERxN tablets with increasing compaction force is shown in figure 3.10. A trend of decreasing pore area with increasing compaction force was observed. This was likely to be due to plastic deformation and to a general decrease in pore volume. Pore areas were higher in tablets compacted at the higher compaction speed probably due to the greater pore volume of these tablets.

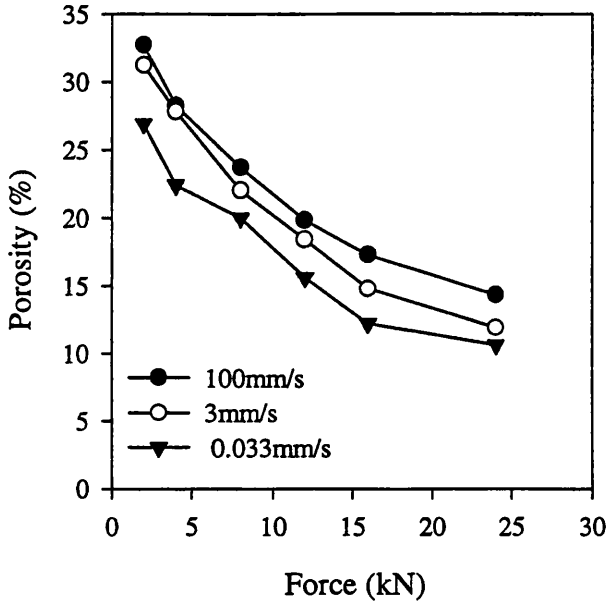

Figure 3.5 Variation of porosity of TIMERxN tablets with compaction force and speed

(a)

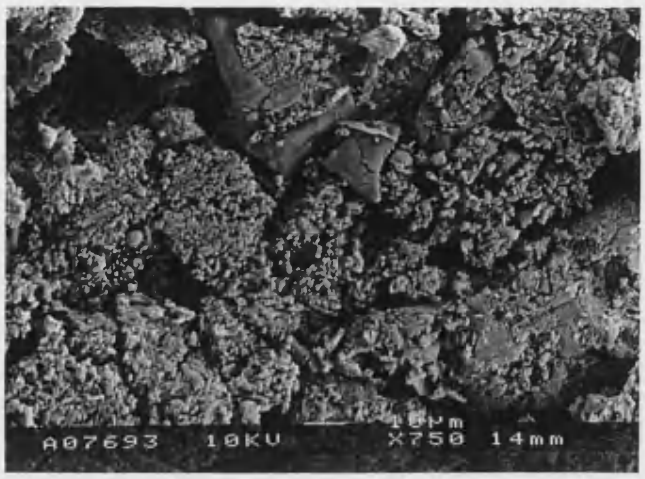

(b)

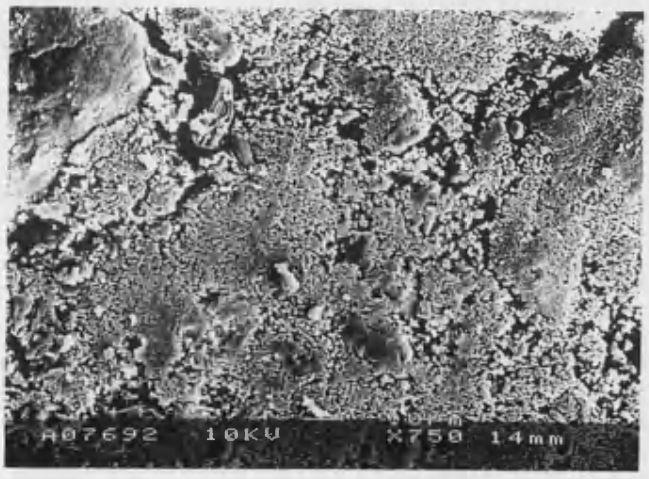

(c)

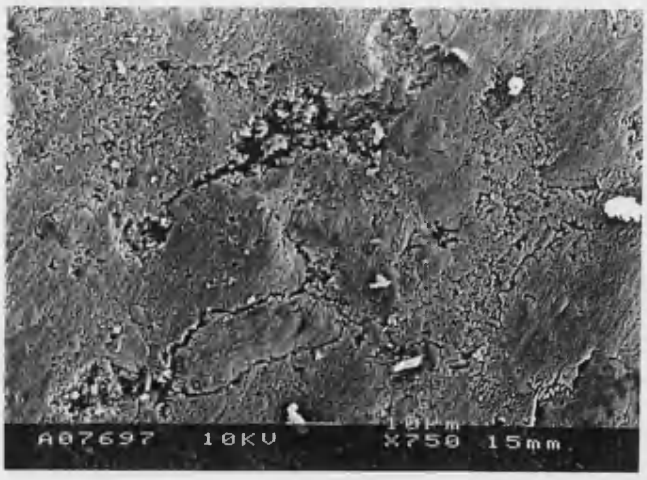

Figure 3.6 Scanning electron micrographs of TIMERxN tablets compacted using a speed of 3mm/s and compaction forces of (a) 2kN (b) 8kN and 24kN

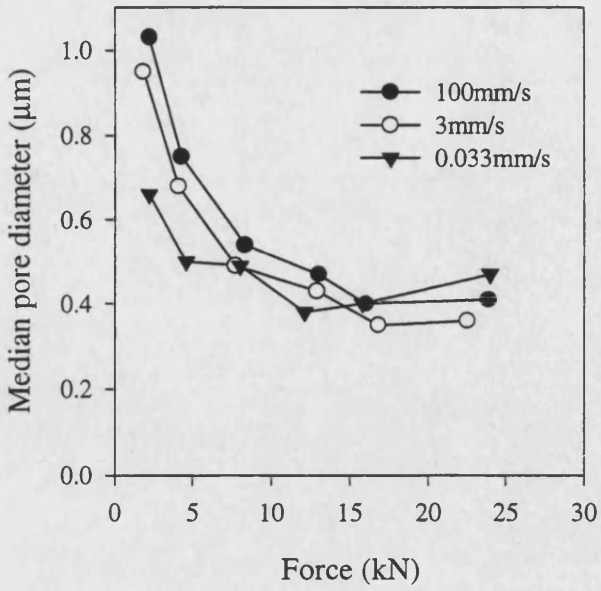

Figure 3.7 Variation of median pore diameter of TIMERxN tablets with compaction force and speed

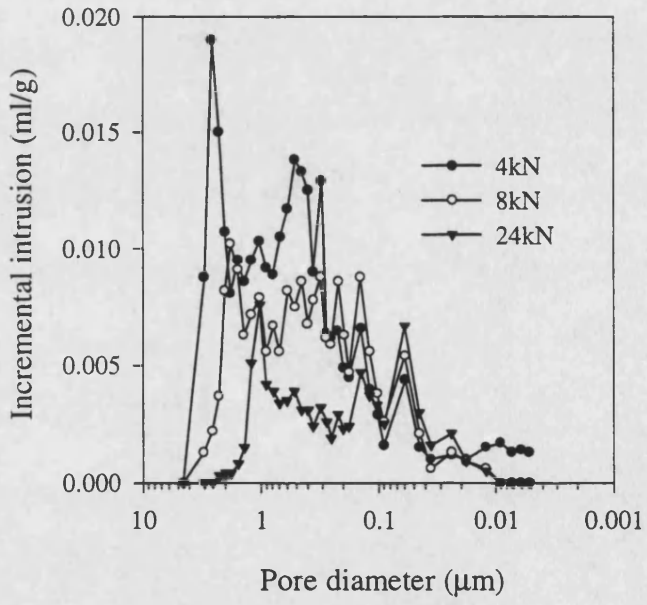

Figure 3.8 Incremental intrusion into TIMERxN tablets compacted using a speed of 3mm/s.

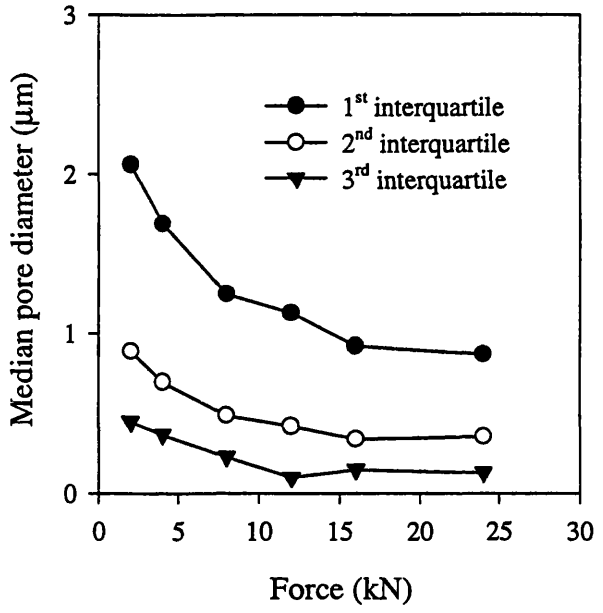

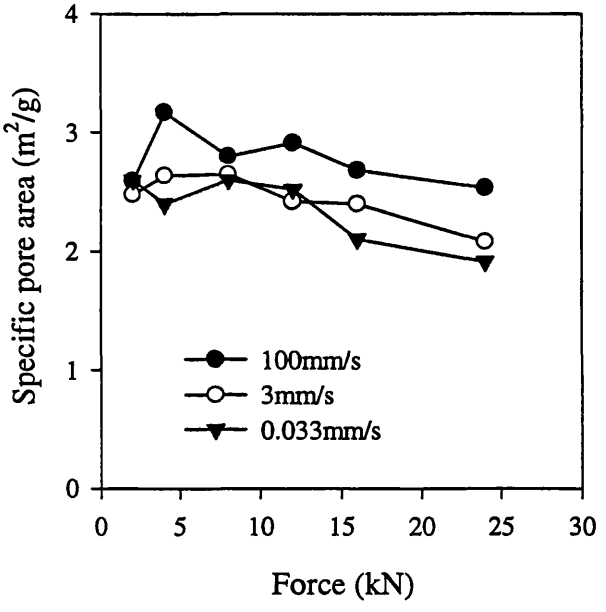

Figure 3.10 Variation of specific pore area of TIMERxN tablets with compaction force and speed

3.4.4.2 *Compaction behaviour of BHP-based granules*

BHP-based granules compacted very differently to TIMERxN. Table 3.15 shows the pore characteristics of tablets that were compacted from granule batch G3D. The granules were compacted using two compaction speeds to two target forces: high (19kN) and low (8kN). Actual mean forces reached ranged between 18.9 and 19.0 (maximum standard deviation from mean values was 1.3kN) for the 'high' force and 8.0 to 8.2kN (maximum standard deviation from mean values 0.25kN) for the 'low' force. Large differences in applied force and compaction speed produced only small variations in tablet porosity and median pore diameter. Similar observations were made for batches G3L and G3K (tables 3.16 and 3.17). Compaction forces less than 8kN and a faster compaction speed (100mm/s) failed to produce intact tablets. This high resistance to deformation was in contrast to TIMERxN, which compacted easily under a wide ranges of tabletting conditions. It was considered that the differences could be due to the excipient composition of each material and/or material physical characteristics. TIMERxN and BHP-based granules both contained 50% heterodisperse polysaccharides and a large proportion of glucose. However, TIMERxN also contained the tertiary components calcium sulphate and ethylcellulose. It was considered that the presence of ethylcellulose might have improved compactibility by promoting plastic deformation (126). To evaluate this, the compactibility of batches of BHP-based granules containing none, one or both of these tertiary components was studied using tablet mechanical strength as a measure of compactibility (see section 3.3.7). The presence of ethylcellulose and/or calcium sulphate in the granules was found to result in only a minor increase in diametric crushing strength and visual observations suggested that the presence of tertiary components did not substantially improve the compactibility of BHP-based granules. Therefore, to try and account for the difference in compactibility between these two materials the physical characteristics of batch G3D and TIMERxN were considered. Table 3.18 summarises some of these characteristics. It was noted that batch G3D had a larger median particle size than TIMERxN. The particle size in each case followed a normal distribution. Although the degree of deformation or compactibility in relationship to particle size is not fully understood (126), it is thought that a reduction in particle size reduces the effect of the rate of compaction on the relationship between tablet porosity and applied compaction pressure (150). This can be interpreted as a reduced viscoelasticity of particles with a reduced particle size and may explain why BHP-based granules could not be compacted into intact tablets at high compaction speeds. However, the differences in particle size between the batches was

not considerable and was unlikely to account for the large difference in compaction behaviour. The substantial difference in porosity between the two materials was considered to be the key to differences in compactibility. TIMERxN particles had a relatively high porosity (19.7%) while batch G3D had a relatively low porosity (5.7%). As previously discussed, wet granulation of the dry blend probably contributed to the formation of dense, low porosity granules through partial dissolution of the glucose component. The high resistance to deformation of BHP-based granules under an applied load granules was likely to be a consequence of the high granule strength of the material due to recrysallisation of dissolved glucose and the formation of solid bridges. This meant that the breaking of such a dense structure required the application of very high pressures. Therefore, the granules probably deformed plastically at their contact points rather than fragmenting to a large extent. The compaction of glucose granules has been studied by Juppo (133) who reported that glucose granules were more resistant to densification than either mannitol or lactose and attributed this to the strength of the glucose granules. TIMERxN possibly had a higher porosity because the components are agglomerated using an alcoholic slurry containing ethylcellulose. In the absence of water minimal dissolution of glucose would occur resulting in less crystalline, more porous granules. For porous particles it is thought that repositioning of the primary particles constituting the granule can occur under an applied load resulting in granule deformation (i.e, a change in granule shape) (126). For TIMERxN this might account for the degree of plastic deformation that was observed. For BHP-based granules, low porosity and a likely high granule strength meant that deformation within granules was difficult to achieve even under high applied force. From studies on the compaction behaviour of lactose and dipentum granules Wikberg and Alderborn (129,142) suggested that the degree of deformation that granules undergo during compaction is governed by the original granule porosity. A reduced granule porosity was thought to reduce the void space between the particles and hence increase the bonding force of the interparticulate attraction. However, although porosity difference may partly explain the difference in compactibility between TIMERxN and BHP-based granules the data presented in section 3.3.4 suggested that within different batches of BHP-based granules differences in porosity did not largely affect compactibility.

Compaction speed (mm/s)	Compaction force (kN)	Porosity (%)	Median pore diameter (μm)
3	8	7.94	1.65
0.033	8	7.35	1.68
3	19	6.57	1.84
0.033	19	6.15	1.91

Tables 3.15 Variation in porosity and median pore diameter of tablet batch T3D with compaction force and speed

	Porosity (%)	
Compaction force (kN)	**T3L**	**T3K**
8	7.94	6.57
19	7.35	6.15

Table 3.16 Variation in porosity of tablet batches T3L and T3K with compaction force

	Median pore diameter (μm)	
Compaction force (kN)	**T3L**	**T3K**
8	1.85	2.06
19	1.73	2.12

Table 3.17 Variation in median pore diameter of tablet batches T3L and T3K with compaction force

Characteristic	TIMERxN	Granules G3D
Porosity (%)	19.30	5.67
LOD (%)	5.7	7 to 9
Particle size (μm)	98	184
Median pore diameter (μm)	0.39	2.22
Bulk density (g/cm^2)	0.77	0.62

Table 3.18 Some physical characteristics of TIMERxN and granule batch G3D

Incremental intrusion into granule batch G3D and into tablets compacted from G3D is shown in figure 3.11. The pore size distribution of the tablets was essentially bimodal with the larger pores being predominantly intergranular pores and the smaller pores arising from both inter- and intragranular pores. The absence of new populations of smaller pores suggested that the material did not fragment to a large extent. Table 3.16 shows that the median pore diameter of the tablets did not substantially change as compaction force was increased. The median pore diameter of all tablets compacted from G3D was smaller that that of the granules themselves (2.22μm) although incremental intrusion plots clearly showed that the greater proportion by volume of pores generated during compaction had pore diameters larger than 2μm. The lower median pore diameter of the tables probably reflects the fact that a large number of smaller pores were formed as a result of compaction although this was not clear from intrusion plots. Therefore, some degree of fragmentation was probably occurring. Fragmentation during compaction is often identified using surface area values determined from air permeability measurements (128,129). Quantitative values for pore area derived from mercury porosimetry data are not ideal for characterising the volume reduction behaviour of HP-based granules. Pore area values from mercury porosimetry are biased towards very small pores and the existence of structural hysteresis may largely influence the values obtained. Difficulties in obtaining consistent values of specific pore area for HP-based tablets probably reflects these problems (see section 3.4.5) Values obtained from air permeability measurements relate more to overall pore size distributions which makes the technique more suitable for analysing volume reduction behaviour (129).

The difference between the compaction behaviour of TIMERxN and BHP-based granules illustrated the fact that compaction behaviour was a function of both the inherent properties of the material and its physical form. The compaction mechanism of TIMERxN was relatively easy to define. The material was viscoelastic and under an applied load deformed both plastically and elastically. A degree of fragmentation possibly occurred since this is common to most pharmaceutical excipients. The compaction behaviour for TIMERxN was similar to that reported for xanthan gum (29) and HPMC (137). Classification of the compaction mechanism of BHP-based granules was more difficult since the material was very resistant to densification. A high applied load possibly resulted in some granule repositioning but since the granules were relatively coarse this was likely to have resulted in a small contribution to total porosity reduction. As a consequence, irreversible changes in the physical characteristics of granules possibly constituted the major part of the volume reduction process. This probably consisted of a small amount of fragmentation along with plastic deformation of the granules themselves at points of contact. The poor compactibility of BHP-based granules limited the range of tablet thicknesses that could be obtained. In contrast, TIMERxN could be used to obtain tablets having a wide range of tablet thicknesses.

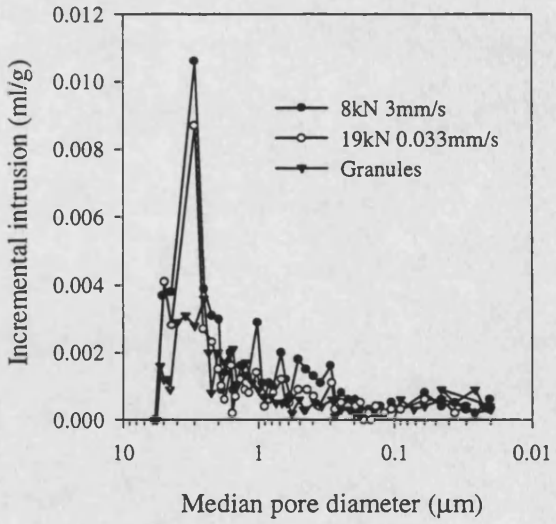

Figure 3.11 Incremental intrusion into granule batch G3D and into tablets compacted from the granules

3.4.5 *Effect of initial granule characteristics on tablet pore structure*

A number of granule batches having a range of physical characteristics were selected for compaction studies (table 3.19). These batches were selected for compaction studies because they had a range of physical characteristics. Granule batch G3K(2) had a high porosity (10.6%) while batch G3L(2) had a low porosity (3.8%). Batch G3J was selected because it was a batch with intermediate porosity (6.77%) and had a relatively large median pore diameter (3.09μm). The compaction of batch G3E was studied because its porosity was similar to G3J but it had a much lower median pore diameter. Batches with high and low bulk density were represented by batches G3D and G3N, respectively. Table 3.20 shows that compaction of these granules produced tablets that had different porosities and median pore diameters. A range of porosities from 18.6% down to 9.8% was observed. Considering the fact that the tablets were only between 4.0 and 4.2mm in thickness this was a notable difference in porosity. Initial granule characteristics obviously dictated the pore structure of the resulting tablets. This situation is not always observed. With some materials profound differences in tablet properties have been found to be largely obscured after compaction (128,131,143,151). It is possible that granules with a lower mechanical strength will lose much of their pore structure under applied loads, while stronger granules will exert a greater influence on final tablet structure. No correlation was observed between the initial median pore diameter or porosity of BHP-based granules and the median pore diameter and porosity values of the final tablets. This observation was in contrast to that made by Wikberg (134) who found that an increased porosity of lactose and dipentum granules before compaction promoted the formation of a more closed tablet pore structure. This effect of porosity on deformation is probably not seen in BHP-based granules because the resistance to densification in both high and low porosity batches is very high. It is possible that the granules had reached a threshold strength below and above which variations in granule porosity did not affect compaction behaviour. Therefore granule strength might play a part in dictating the relationship between porosity and deformation. For BHP-based granules initial granule bulk density appeared to be a major factor influencing tablet porosity. Table 2.21 details the change in porosity (that is the difference between granule and tablet porosity), during compaction, as a function of the bulk density of the initial granules. As a general observation, the difference between the porosity of the starting granules and the porosity of the final tablet decreased as bulk density of the initial granules increased. When the granules were compacted under constant force and speed, rather than to equivalent relative density, a similar conclusion

was drawn. Figure 3.12 shows granule and corresponding tablet porosity of four batches compacted using a force of 8kN and a speed of 3mm/s. Three batches had similar bulk densities (0.48 to 0.53g/ml) while the fourth batch had a higher bulk density (0.62g/ml). A greater increase in porosity occurred for the batches with lower bulk density values. Bulk density values were likely to reflect differences in particle shape of each batch of granules. More irregularly shaped particles were likely to have a larger bulk volume and pack less effectively during compaction producing a compact with comparatively large pore spaces. The fact that only a rough relationship appeared to exist between bulk density and change in porosity may have been due to other participating factors, some of which may have been interdependent. Particle shape and/or porosity may have affected the propensity of the particles to fragment. Particle shape might have affected bonding during compaction since irregular particles with an irregular surface geometry might have bonded more effectively than smooth particles. Bulk density values will have been influenced by particle porosity as well as particle shape since presumably high porosity, irregular granules would have a lower bulk density than low porosity, irregular granules. Mechanical strength could be a function of porosity and shape. Overall, the granule physical characteristics affecting tablet structure appeared to be complex, although bulk density appeared to be an important factor in determining tablet pore structure.

Compaction of the granules thus produced tablets with different porosities and different pore size distributions. Pore area values calculated for BHP-based tablets were found to be non-consistent and therefore were not used. The variation in pore areas could reflect the type of packing that was occurring, that is irregularly shaped pores displaying structural hysteresis. This can largely affect pore areas derived from mercury porosimetry data (see section 3.4.4.2).

Batch No.	Median pore diameter of pores > 0.9 μm	Porosity (%)	Bulk density (g/ml)
G3K(2)	2.33	10.60	0.53
G3J	3.09	6.77	0.47
G3E	2.22	5.67	0.55
G3L(2)	2.73	3.81	0.51
G3N	2.13	4.33	0.45
G3D	2.22	5.67	0.62

Table 3.19 Bulk physical characteristics of granules

Tablet Batch No.	Median pore diameter (μm)	Porosity (%)
T3K(2)	1.73	18.6
T3J	1.60	15.3
T3E	1.40	11.8
T3L(2)	2.30	9.8
T3N	2.21	16.4
T3D	1.55	9.8

Table 3.20 Pore structure of tablets having equivalent tablet thickness

Batch No.	Bulk density (g/ml)	Porosity increase (%)
G3N	0.45	12.0
G3J	0.47	8.5
G3L(2)	0.51	6.0
G3K(2)	0.53	8.6
G3E	0.55	1.7
G3D	0.62	4.1

Table 3.22 Change in total porosity as a result of compaction as a function of granule bulk density

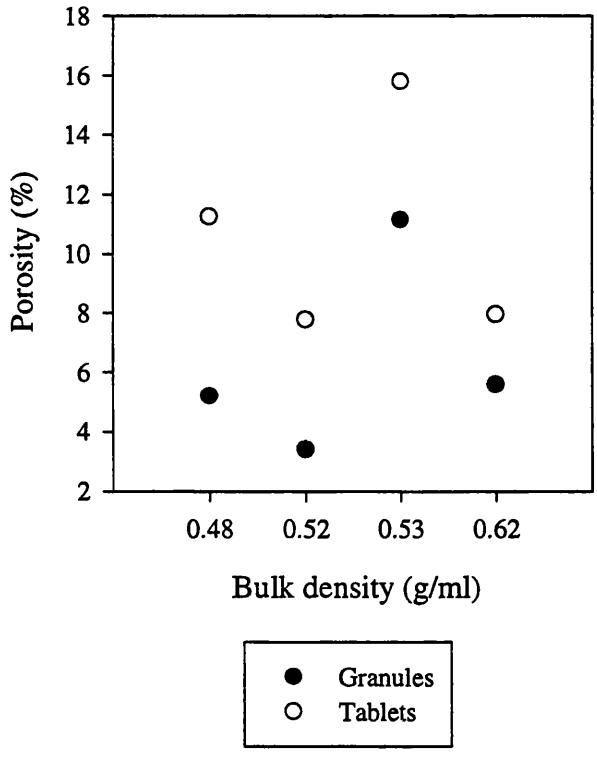

Figure 3.12 Granule and tablet porosity as a function of granule bulk density

3.4.6 *Effect of tablet shape on tablet pore structure*

Table 3.22 shows the pore characteristics of three differently shaped tablets compacted from granule batch G3L(2). Porosity and median pore diameter only differed slightly despite tablet shape being substantially different. The complex stress patterns that develop in a mass of particulate material when compacted in a cylindrical die have been mapped by Train (1957) (152). A close relationship was found to exist between the pressure response and the apparent density produced at a given point within the compacting mass. It might be expected that the pressure applied on regions of the powder bed would vary depending on die geometry. Therefore regions of densification would differ between different table shapes. Only small differences in pore structure was observed between each tablet possibly because of the resistance of this particular material to densification.

	16mm disk	**10mm cylinder**	**caplet**
Median pore diameter (μm)	2.08	2.28	2.21
Porosity (%)	8.34	9.38	10.87

Table 3.22 Variation of pore structure with tablet shape

3.4.7 *Effects of tertiary components on mechanical properties of tablets*

Table 3.23 shows the work of failure and hardness of tablets compacted from BHP-based granules formulated with and without tertiary components. The granules were produced under similar processing conditions. Tablets containing ethylcellulose had higher work of failures and associated lower standard deviations than tablets that did not contain ethylcellulose. The high standard deviation of tablets formulated without ethylcellulose suggested that these tablets were failing by brittle fracture. The work required to fracture the tablet probably varied depending on the fracture plane penetrated as the probe entered the tablet. Ethylcellulose possibly enhanced the plasticity of the granules so that the resulting tablets were less brittle. Both calcium sulphate and ethylcellulose appeared to increase the compactibility of the granules to some extent since the inclusion of these components produced tablets with higher tablet strength. Although the presence of tertiary components appeared to slightly improve the

compactibility of BHP-based granules the material was still more difficult to compact than TIMERxN.

Tertiary component	Batch No.	Work of failure (N/s) ± S.D	Hardness (kN) ± S.D
None	G3N	115.4 ± 79.6	2.65 ± 0.17
Ethylcellulose	G3Q	162.8 ± 35.6	5.60 ± 0.21
Calcium sulphate	G3R	115.2 ± 79.6	8.00 ± 3.05
Ethylcellulose + calcium sulphate	G3S	147.5 ± 32.8	5.27 ± 0.18

Table 3.23 Mechanical properties of tablets with and without tertiary components

3.5 Conclusion

Variation in the processing conditions used to produce BHP-based granules produced granules that had varying pore structures. Porous granules were produced by wet granulating with an alcohol mix and fluid bed drying the wet mass. Relatively non-porous granules were produced by passing dry material through a screen using an oscillating granulator. Median pore diameter was significantly altered by changing the drying conditions. This was thought to be a consequence of the residual moisture content on milling. TIMERxN was easily compacted into tablets that had different porosities by altering the compaction force and speed used to produce the tablets. Although pore structures were substantially different, the tablets had different thickness and therefore different initial releasing surface areas. To obtain compacts that had the same tablet surface area but different pore structures BHP-based granules were compacted into tablets that had a constant thickness. These granules were resistant to densification but this was advantageous in that the physical characteristic of the initial tablets strongly dictated the pore structure of the resulting tablets. Tablets with different porosities and different pore size distributions were produced in this way. The bulk density of the initial granules appeared to largely influence the porosity of the final tablet.

Tablets having different porosities, pore size distributions and bulk densities were obtained. This enabled a study to be initiated on the influence of tablet pore structure on the release retarding ability of HP-based matrices.

4. Investigation of the release-controlling action of tablets and granules comprised of swellable hydrophilic materials in relation to the initial bulk physical characteristics of the materials

4.1 Introduction

A number of studies have reported correlations between the initial bulk characteristics of swellable hydrophilic matrix tablets and the release controlling action of the matrices (31,32,69,92,94,96). It has been proposed that initial matrix porous structure can influence drug release by affecting the rate of solvent penetration into tablets (31,95); the susceptibility of the swollen matrix to erosion (32); the rate of matrix swelling (95); the degree of matrix swelling (96); the diffusion pathway through the matrix (92) and the releasing surface area of the swollen material (69). Other studies have found no correlation between initial bulk characteristics and dissolution profiles (63,90,91). It appears that parameters such as porosity, pore size distribution, tablet size and shape affect the rate of dissolution of model drugs from some matrices but are not important in determining drug release from other matrix systems.

In this study the release controlling action of swellable hydrophilic tablets and granules, including HP-based and non HP-based formulations, was examined as a function of the bulk physical characteristics of the initial dry material. Variations in tablet bulk characteristics have often been achieved by changing tablet thickness (63,94) and compaction studies had shown that TIMERxN granules could be compacted into tablets of varying tablet thickness. These tablets were known to have different initial releasing surface areas, porosity's and pore size distributions. Since it was considered that tablet thickness could theoretically influence dissolution rates, the release of model drugs from hydrophilic matrices having different initial tablet thickness was evaluated. It was also known that HP-based granules could be produced that had a range of bulk physical characteristics and that these granules could be compacted into tablets that had equivalent tablet thickness but different porous structures. These matrices had similar initial releasing surface areas however, it was considered that differences in porous structure could affect the rate of water penetration into the tablet, the rate of swelling and/or the tortuosity and mechanical strength of the swollen matrix. The release of model drugs from HP-based tablets and granules was therefore examined as a function of porous

structure. The release-controlling action of hydrophilic matrix tablets having different porous structures but equivalent tablet thickness had not previously been studied in detail.

4.2 Materials

Benzamide (Lot No. 6366081) was obtained from Aldrich Chemical Co. (Loughborough, U.K.). Xanthan gum (Lot No. P5086), locust bean gum (Lot No. B21577) glucose (Lot No. CD6D29107) and TIMERxN (Lot No. NS664) were supplied by Penwest Pharmaceuticals Co., (Patterson, NY, USA). Microcrystalline wax (Lot No. 3749) was obtained from Poth, Hille & Co. Ltd (U.K.). Acetone, 2-propanol, dichloromethane, magnesium stearate (Lot No. 30120362) and polyethylene glycol 4000 were obtained from Fisons Scientific Equipment Ltd. (Loughborough, U.K.). Anhydrous lactose 50M (Lot No. 8NC03A) was obtained from Kraft Inc. (Norwich, N.Y.). Diclofenac sodium (Lot No. 94-01342) was obtained from Heumann Pharma GmbH (Nurenberg, Germany). Sodium stearyl fumarate (Lot No. 212-01X) was obtained from Mendell (Penwest Pharmacuticals Co., Patterson, NY, USA). Polyvinylpyrollidone (PVP K29/32 Lot No. TX30118), frusemide (Lot No. 36H30119) and monobasic anhydrous potassium phosphate (Lot No. 106H0476) were obtained from Sigma Scientific Equipment Ltd. (Loughborough, U.K.). Sodium hydroxide solution (Lot No. 9627477A456) was obtained from Fischer Chemicals Co., (Loughborough, U.K.). Carbomer 934P (Carbopol 934P NF, Lot No. B981083) was obtained from BF Goodrich (Brecksville, Ohio, USA). Methocel K15M Premium EP (Lot No. KJ26012N01) was obtained from Colorcon (Kent, U.K). Lactose (Microtose 200mesh) was obtained from Meggle GmbH (Wasserburg, Germany). 1μm cellulose nitrate filters were obtained from Whatman International Ltd. (Maidstone, U.K).

4.3 Methods

4.3.1 *Characterisation of benzamide, diclofenac sodium and frusemide*

Benzamide and diclofenac sodium were selected as model drugs. The USP (65) classifies the aqueous solubility of drugs according to the number of parts of the drug required for dissolving one part of drug: < 1 for very soluble, 1 to 10 for freely soluble, 10 to 30 for soluble, 30 to 100 for sparingly soluble, 100 to 1000 for slightly soluble and

1000 to 10,000 for very slightly soluble drugs. Using this classification diclofenac sodium falls into the category of slightly soluble and benzamide as soluble. The percentage solubility (w/v) of each model drug in water (pH 7) and the drug loadings used in this study are given in table 1. Figures 4.1 and 4.2 show the molecular structure of benzamide and diclofenac sodium, respectively. Benzamide (benzoylamide) has a strong UV absorbance at low concentrations. The loss on drying value, determined thermogravimetrically by heating the sample at 70°C for 5min using an infrared moisture balance (Type LP16, Mettler, Switzerland), was approximately 0.3%. Benzamide was screened through a 180μm mesh before use. A low drug loading was used in order to minimise the extent that the model interfered with (a) granule compactibility and (b) the pore structure of the resulting matrices. Diclofenac sodium also has a high UV absorbance at relatively low drug concentrations. It retains approximately 2% of moisture under ambient conditions and, since it is highly cohesive, was not sieved before use. The drug loadings selected enabled the formulations to be conveniently assayed by UV detection in 1000ml of water.

Frusemide was used as a model drug to study the release controlling action of Carbopol formulations, which were reported to be sensitive to changes in tablet thickness (32). Frusemide is insoluble at pH 7.0 but is soluble in pH 5.8 phosphate buffer (32). Its molecular structure is shown in figure 4.3 and its solubility and the drug loading used are shown in table 4.1.

Model drug	**Solubility (%w/v)**	**Drug loading (%)**
Benzamide	1.35*	2.67
Diclofenac sodium	0.187**	5 and 10
Frusemide	Soluble at pH 5.8	5

* (153), ** (154)

Table 4.1. Water solubility and drug loading of benzamide, diclofenac sodium and frusemide

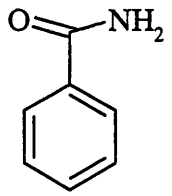

Benzamide

Figure 4.1 Molecular structure of benzamide

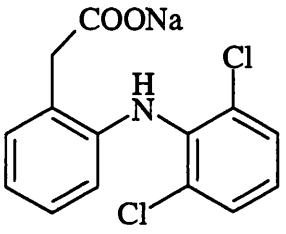

Diclofenac Sodium

Figure 4.2 Molecular structure of diclofenac sodium

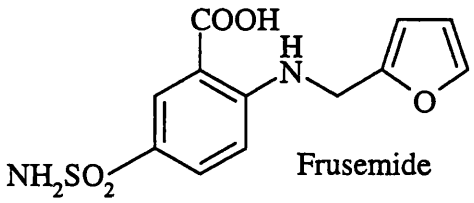

Frusemide

Figure 4.3 Molecular structure of frusemide

4.3.2 *Assay of benzamide, diclofenac sodium and frusemide*

The model drugs were assayed by detection of UV absorbance in aqueous solution at the λmax of each drug. The UV absorption of solutions of benzamide and diclofenac sodium in distilled water was scanned in the range 200nm to 350nm using a UV/VIS spectrophotometer (Lambda 3B, Perkin-Elmer Ltd., Beaconsfield, U.K.). The λmax was found to be 228nm for benzamide and 273nm for diclofenac sodium. A stock solution of benzamide (0.02%) was prepared by dissolving 50mg of benzamide, accurately weighed, in 250ml of distilled water. Aliquots of the stock solution were diluted to produce a

series of solutions having target concentrations of 0.0004%, 0.0008%, 0.0012% and 0.0016% (w/v) benzamide. The absorbance of each solution at 228nm was determined using a UV/VIS spectrophotometer (Unicam 8625, Cambridge, U.K) against a distilled water blank. The procedure was repeated twice using a new stock solution in each case so that three sets of calibration data from three different stock solutions were obtained. A stock solution of diclofenac sodium (0.1%) was prepared by dissolving approximately 500mg of diclofenac sodium, accurately weighed, in 500ml of distilled water. Aliquots of the stock solution were diluted to produce a series of solutions having target concentrations of 0.0005%, 0.0015%, 0.0030% and 0.0045% diclofenac sodium. The procedure was repeated twice using a new stock solution in each case. The UV absorbance at 273nm of each solution was determined against distilled water. 3 calibration plots were constructed for each model drug. Linear regressions were carried out using a computer graphics package (MicroCal Origin, MicroCal Software Inc., Northhampton, USA). A t-test was used to determine whether significant differences existed between each set of calibration data.

A stock solution of frusemide (0.025%) was made up by dissolving 125mg of frusemide, accurately weighed, in 500ml of pH 5.8 phosphate buffer. Aliquots of stock solution were diluted with buffer to produce a series of solutions having target concentrations of 0.0005%, 0.0010%, 0.0020% and 0.0030%. The UV absorbance of the solutions at the λmax of frusemide (271nm) (154) were determined using pH 5.8 phosphate buffer as a blank. The procedure was repeated twice using a fresh stock solution in each case. Calibration plots were constructed and analysed as described above.

The absorbance of a solution of each model drugs was determined before and after filtration by cellulose filters to determine if the filters retained any of the model drugs. No decrease in absorbance at the λmax of each model was observed. The maximum variation in absorbance before and after filtration was 3.3% of the unfiltered solution (n=3).

4.3.3 *Assessment of model drug stability*

It was important that the model drugs remained stable in solution at 37°C over the period of dissolution. The UV absorbance of solutions of benzamide, diclofenac sodium and frusemide maintained at 37°C was monitored at the λmax of each model drug. No

loss of absorbance at the λmax of the drug occurred over a 24hr period. The absorbance of benzamide varied by a maximum of +0.7%, the absorbance of diclofenac sodium by a maximum of +5.6% and the absorbance of frusemide by a maximum of +3.2%.

4.3.4 *Preparation of HP-based tablets and granules*

The effect of tablet thickness on the release of benzamide and diclofenac sodium from tablets that contained a high proportion of TIMERxN (48.6%) and tablets that contained a low proportion of TIMERxN (10%) was investigated. TIMERxN was used as the release controlling material because it was easily compacted into tablets having high and low tablet thickness (see section 3.4.4.1). Drug release from tablets that had different pore structures but equivalent tablet thickness was studied using benzamide as a model drug. The tablets were compacted from granules that had been prepared using a range of processing conditions and were known to have different porous structures. The effect of tablet shape on release rates was studied using diclofenac sodium as a model drug. The dissolution behaviour of benzamide from uncompacted granules was examined as a function of granule porosity.

4.3.4.1 *Tablets compacted to equivalent tablet thickness*

Benzamide was distributed extragranularly through four batches of granules (batch no's. G3E, G3L(2), G3K(2) and G3J). The preparation of these batches was described in Chapter 3. 2.67% benzamide was mixed with 97.33% granules using turbula rotation at 30rpm for 5min (Type T2C, Glen Creston Ltd., Stanmore, Middlesex, U.K). A single-punch tablet press (Type F3, Manesty, Speke, Liverpool, U.K.) was fitted with a 10mm flat-faced punch and die set. Granules that had been preconditioned at 55%RH prior to compaction were manually filled into the die and compacted to equivalent relative density. The tablet press was hand operated, which enabled tablet thickness and weight to be accurately controlled. A constant weight of approximately 400mg was maintained and tablet thickness was measured using digital calipers (Digit-Cal, TESA S.A, Switzerland). Tablets compacted from granule batches G3E, G3L(2), G3K(2), and G3J(2) are identified by the batch no's, T3E, T3L(2), T3K(2) and T3J, respectively.

The porosity of one batch of tablets was reduced by using polyethylene glycol (PEG) as a pore filler. PEG is a hydrophilic material that is readily soluble in dichloromethane (124). Tablets compacted from granule batch G3L(2) were immersed in

a 10% solution of PEG 4000 in dichloromethane for 5s. Following evaporation of dichloromethane the tablets were re-immersed for a further 5s. When the dichloromethane had evaporated PEG was left in the pores, thereby reducing the porosity of the tablets.

4.3.4.2 *Tablets compacted to different tablet thickness*

A formulation containing a high proportion of TIMERxN was prepared by blending TIMERxN (97.3%) with benzamide (2.67%) by geometric trituration. Tablets were compacted from the blend using a single-punch tablet press, which was operated manually. The press was fitted with a 10mm flat-faced punch and die set, which was lubricated with a 1.5%w/v suspension of magnesium stearate in acetone prior to compaction. A constant weight of approximately 400mg was maintained. The distance moved by the upper punch was adjusted to produce tablets having high and low tablet thickness.

Tablets containing a low percentage of HP-based material were prepared by blending TIMERxN (10%), diclofenac sodium (7.5%) and lactose (81.5%) by geometric trituration. Magnesium stearate (1%) was added as a lubricant and distributed using turbula rotation for 5min at 30rpm. The tablets were compacted using a single-punch tablet press fitted with 10mm flat-faced punches. The distance moved by the upper punch was adjusted to produce tablets having three different tablet thicknesses.

The effect of restricted matrix swelling on dissolution profiles was examined using tablets coated with a water impermeable barrier. Tablets having high and low tablet thickness were compacted from a TIMERxN/benzamide blend that contained 47% HP material (97.3% TIMERxN). Molten microcrystalline wax, which is water-insoluble, was applied to one base and to the lateral surface of each tablet and allowed to dry. This left one base free for drug release during dissolution.

4.3.4.3 *Tablets compacted to different geometrical shapes*

XG (25%), LBG (25%), glucose (45%) and diclofenac sodium (5%) were blended for 5min in a high shear mixer (Cuisine Système Automatic 5000, Magimix Ltd., Surrey, U.K.). Total batch size was 300g. The blend was wet agglomerated for 5min using 21.6% distilled water and tray dried at 60°C in an oven (Model H-150, Size 2, Gallenkamp, Loughborough, U.K.) for 24hr. The dry material was passed through a 0.63mm mesh using an oscillating granulator (Type MGL 4A Frewitt, Switzerland). The

granules were sieved for 30min (Endecotts Ltd., London, U.K.) through an I.S.O standard aperture diameter $\sqrt{2}$ sieve progression ranging from 710μm to 63μm. The sieves were agitated using a Fritsch sieve shaker (Type 03-502, Fritsch, Germany). Quantities from each sieve fraction were selected in the following proportions: 500 to 710μm (2%), 355 to 500μm (4%), 250 to 355μm (26%), 180 to 250μm (36%), 125 to 180μm (26%), 90 to 125μm (3%), 63 to 125μm (2%) and 0 to 63μm (1%). Sieve fractions were recombined using turbula rotation (Type T2C, Glen Creston Ltd., Stanmore, Middlesex, U.K.) for 5min at 30rpm giving particles with a median particle size of 184μm. Accurately weighed samples (approximately 373mg) were compacted using flat faced 8mm circular punches, flat faced 9.5mm × 9.5mm square punches and 5mm × 16mm caplet shaped punches. The tablet press was operated manually. The dimensions of the tablets were measured prior to dissolution using a digital micrometer and used to calculate average tablet surface area, tablet volume and bulk density. The bulk characteristics of caplet shaped tablets were calculated by assuming a cylindrical shape of similar dimensions.

4.3.4.4 *Preparation of reference tablets*

In order to compare dissolution profiles that had been obtained from different dissolution experiments it was necessary to ensure that the dissolution conditions were similar in each case. This was achieved by using reference tablets containing the appropriate model drug. The dissolution profile of one reference tablet was followed during each dissolution experiment. If the dissolution of the reference tablet fell within set limits at the 2hr and 6hr time points then this gave confidence that the dissolution conditions in each experiment were consistent. The limits were established by measuring the release profiles of between 6 and 12 reference tablets and determining the highest and lowest percentage released at each time point.

A reference batch of tablets containing benzamide was prepared by blending benzamide (2.67%) and TIMERxN (96.32%) by geometric trituration. Magnesium stearate (1%) was added as a lubricant and distributed by turbula rotation (Type T2C, Glen Creston, Middlesex, U.K.) at 30rpm for 3min. The blend was tableted using a single punch tablet press fitted with 10mm concave punches. The target weight was 450mg.

Reference diclofenac sodium tablets were prepared by blending TIMERxN (94%) and diclofenac sodium (5%) by geometric trituration. 1% sodium stearyl fumarate was added as a lubricant and distributed using turbula rotation for 5min at 30rpm. The blend

was compacted on a single-punch tablet press using 10mm flat-faced punches. The target weight was 400mg.

4.3.4.5 *High and low porosity HP-based granules*

The dissolution of benzamide from HP-based granules was examined using granules that contained benzamide distributed intragranularly. A 'low' porosity batch (batch No. G4A) and a 'high' porosity batch (batch No. G4B) were prepared.

Batch G4A: XG (24.25%), LBG (24.25%), glucose (48.50%) and benzamide (3%) were blended for 5min using a high shear mixer. The dry blend was agglomerated using 17.8% distilled water, which was added over 1min. Total mixing time was 5min. The wet material was tray dried in an oven at 60°C for 24hr giving material with an LOD of less than 5%. The dry material was screened through a 0.63mm mesh using an oscillating granulator and size selected as described in section 4.3.4.3, giving granules with a theoretical median granule size of 184μm.

Batch G4B: The dry materials were blended as described for batch G4A. The dry blend was agglomerated using a 1:1 mixture of 2-propanol and distilled water (27.8%w/w). The wet material was screened through a 0.32mm mesh using the oscillating granulator. The granules were then dried using a fluid bed drier (Uniglatt, Glatt AC, Switzerland) operating at 80°C for 20min. This reduced the LOD of the material to less than 5%. The granules were size selected as described in section 4.3.4.3, giving material with a theoretical median granule size of 184μm.

4.3.5 ***Preparation of Carbopol and Methocel tablets***

Carbomers (Carbopol™) are synthetic high molecular weight polymers of acrylic acid. They disperse in water to form acidic colloidal solutions of low viscosity that when neutralised produce highly viscous gels (124). Carbomer grades with a low residual benzene content 934P or 974P are sometimes used in oral preparations (124,155). The material has a relative high bulk density (1.76g/cm^2) and an average particle size of 2 to 7μm (124). Peréz-Marcos *et al.* (32) found that the rate of release of frusemide from Carbopol™ matrices was sensitive to the force used to compact the matrices. The release of frusemide from Carbopol matrices was therefore evaluated here. The effect of compaction force on the dissolution of frusemide from frusemide/Methocel matrices and frusemide/TIMERxN matrices was also examined.

A frusemide/lactose granulate was prepared using the method described by Peréz-Marcos *et al.* (32). 5% PVP K29/32 was dissolved in distilled water. Frusemide (39.5%) and lactose (59.4%) were blended in a mini high shear mixer (CH100 mini chopper, Kenwood Ltd., Surrey, U.K). Total batch size was 25g. 22%v/w of PVP solution was added and the materials were agglomerated for 2min. The wet mass was tray dried in an oven (Model 1H-150, Size 2, Gallenkamp, Loughborough, U.K) at 50°C for 3hr. The granulate was ground in a pestle and mortar and passed through a 250μm mesh. The granulate (12.56%) was blended by geometric trituration with (a) Carbopol 934P (87.44%), (b) Methocel K15M (87.44%) and (c) TIMERxN (87.44%). The blends were conditioned at 55%RH prior to compaction. Methocel K15M was selected as a hydrophilic matrix component as it is a high viscosity grade of HPMC that is frequently studied as a controlled release matrix excipient (63,64,91). The bulk density was found to be 0.29g/cm^2 and the true density determined by helium pycnometry (see section 2.3.1.1) was found to be 1.41g/cm^3. The mean particle size of Methocel K15M as determined by time of flight of flight measurements (see section 3.3.1) was 28.4 ± 0.5μm. A second granulate containing diclofenac sodium in place of frusemide was prepared using the method described above for frusemide. The diclofenac sodium granulate (12.6%) was blended with Carbopol 934P (87.4%). The blends were compacted using a single-punch tablet press fitted with 10mm flat-faced F tooling. The punch and die were lubricated with a 1.5% suspension of magnesium stearate in acetone prior to compaction. Compaction settings were adjusted to produce tablets having high and low tablet thickness and a target weight of 400mg. Each tablet contained approximately 20mg of drug.

4.3.6 ***Dissolution***

4.3.6.1 *USP II conditions*

Dissolution studies using USP II apparatus were carried out at 37°C ± 0.2°C in a Pharmatest dissolution apparatus (Type PTW S3C, Pharmatest Ltd., Gwent, U.K) with paddles positioned 3cm above the point of curvature at the bottom of the vessel. The speed of paddle rotation was 50rpm, 100rpm or 150rpm, as indicated under the appropriate figure. The tablets to be analysed were supported in stainless steel wire cages (approximately 3.5cm × 2.5cm) to allow both axial and radial swelling and to ensure

release from all surfaces. The dissolution medium was either 1000ml of distilled and degassed water or, in the case of frusemide formulations, 1000ml of degassed pH 5.8 phosphate buffer. A standard solution containing a known concentration of the active material was used as a reference. Distilled water or, in the case of frusemide formulations, pH 5.8 phosphate buffer was used as a blank. Sampling of the dissolution medium was carried out either manually, using filters with an average mesh size of 1μm to filter the medium, or automatically, when the medium was passed through 20μm mesh filters. Manual sampling was appropriate when a fine mesh filter was required to limit the interference of tablet excipients on the UV assay of the drug. The dissolution of diclofenac sodium from tablets having different geometrical shapes was followed by manual sampling: at predetermined intervals samples of dissolution medium were withdrawn using a syringe and filtered through 1μm cellulose nitrate filters. An equal volume of fresh distilled water heated to 37 ± 0.2°C was added to each dissolution vessel following sampling to maintain constant volume. The filtrate was analysed using an UV spectrophotometer (Unicam 8625, Cambridge, U.K.) at 273nm. It was shown that the cellulose nitrate filters did not decrease the absorbance of a solution of diclofenac sodium. The quantity of drug released at each time point was calculated taking into account the amount removed by sampling and the progressive dilution of the dissolution medium. The dissolution of all other batches was followed using automatic sampling: at programmed intervals the dissolution medium was pumped automatically through 20μm filters (Pharmatest Ltd., Gwent, U.K.) using a peristaltic pump (IsmaTec SA, Type MS-CA, Glattbragg, Switzerland) to a flow cell were spectrophotometric measurements were made (Unicam 8625, Cambridge, U.K.) at the appropriate wavelength. An 8-way valve (MS-FX, Twist Technologies, Cambridgeshire, U.K.) sequentially directed medium from each vessel to the flow cell. The percentage drug released was calculated at each time point using Pharmatest software (Pharmatest Ltd., Gwent, U.K). Drug release was expressed as a percentage of the total drug present in the dosage form, as determined from content uniformity measurements (see section 4.3.8). The mean of either 3 or 5 determinations was reported, with error bars representing the standard deviations from the mean. Linear regression analysis on dissolution data was carried out on approximately the first 70% of drug released (SigmaPlot Scientific graphical software, version 2.01, Jandel Scientific, San Rafael, CA, USA).

4.3.6.2 *Low agitation conditions*

A standard USP II dissolution set up was not suitable for determining the dissolution of granules as the high degree of agitation caused aggregation of the granules and a high variability in the results. To obtain very low agitation conditions the paddles from the USP II apparatus were replaced with baskets normally used under USP I conditions. The baskets were then removed leaving the shafts, which were rotated at 25rpm. The granules were finely distributed over the surface of the dissolution medium. Samples were analysed automatically as described in section 4.3.6.1. Low agitation conditions were also used when studying the dissolution behaviour of a number of tablet batches. This was to examine the release behaviour of formulations having different bulk physical characteristics, under low hydrodynamic flow conditions.

4.3.7 ***Assessment of excipient interference***

As dissolution of a drug from a HM occurs progressive quantities of the inert matrix can also undergo dissolution. Soluble and insoluble matrix excipients can potentially interfere with the UV assay of model drugs. During the dissolution of model drugs from Carbopol, TIMERxN and Methocel K15M formulations the dissolution medium remained clear and was easily filtered through 20μm Pharmatest filters. Dissolution tests on placebo formulations showed that the excipients did not interfere with the UV assay of the model drugs. During the dissolution of drugs from BHP-based matrices the medium became viscous and opaque. 20μm filters effectively filtered the medium for up to approximately 10hr dissolution however, for longer dissolution runs filtration through 1μm was necessary to limit interference by excipients. This necessitated manual sampling of the dissolution medium. UV absorbance measurements were carried out during the dissolution of a placebo formulation. This showed that the absorbance of filtered solutions containing HP-based material at the λmax of diclofenac sodium, was less than <6% of the total drug absorbance after complete dissolution of the tablet matrix.

4.3.8 ***Determination of content uniformity***

Prior to dissolution experiments the initial drug content of the formulations were determined. Samples were stirred with a spatula prior to sampling. 10 accurately weighed samples (approximately 100mg) were removed from regions within the powder

bed using a spatula. The samples were dispersed in 250ml of distilled water and allowed to equilibrate for 5 to 6hr. A sample of the solution was filtered through a 1μm cellulose nitrate filter and the UV absorbance of the solution at the appropriate wavelength was determined. The readings were converted into concentration values using the calibration data.

4.3.9 *Analysis using mercury porosimetry*

The pore structure of tablets and granules was quantified by mercury porosimetry using the methods described in section 3.3.4.

4.4 Results and discussion

4.4.1 *Calibration data*

Calibration data for benzamide, diclofenac sodium and frusemide are shown in tables 4.2 to 4.4, respectively. Calibration curves are given in appendix 2. Calibration plots for benzamide were found to be linear in the range 0 to 0.0016%, calibration plots for diclofenac sodium were found to be linear in the range 0 to 0.0035% and calibration plots for frusemide were linear in the range 0 to 0.0030%. Calibration plots encompassed a concentration range of 0 to 125% of the maximum concentration achievable after 100% dissolution. Student's t-tests showed that there were no significant differences within each set of calibration data ($p<0.05$).

	Calibration plot No.			
	1	**2**	**3**	**Mean (n=3)**
Intercept	0.0022	0.0038	-0.0010	0.0017
Slope	719.75	705.00	698.75	707.83
Standard deviation	2.32	11.07	10.91	-
Regression (r^2)	0.9999	0.9996	0.9996	-

Table 4.2 Calibration data for benzamide

	Calibration plot No.			
	1	2	3	Mean (n=3)
Intercept	0.0028	0.0010	0.0022	0.0020
Slope	300.93	294.40	297.76	297.70
Standard deviation	1.66	3.06	3.00	-
Regression (r^2)	0.9995	0.9998	0.9998	-

Table 4.3 Calibration data for diclofenac sodium

	Calibration plot No.			Mean (n=3)
	1	2	3	
Intercept	0.0229	0.0232	0.0021	0.0161
Slope	519.30	535.50	539.41	531.40
Standard deviation	13.32	12.06	25.41	-
Regression (r^2)	0.9990	0.9991	0.9967	-

Table 4.4 Calibration data for frusemide

4.4.2 *Dissolution of model drugs from HP-based tablets and granules containing a high proportion of HP material*

Figure 4.4 shows benzamide release profiles from TIMERxN tablets containing 48.6% HP and 48.6% glucose, compacted to high and low tablet thickness (5.17 ±. 0.04mm and 3.72 ±. 0.04mm, respectively). Although the thickness, and therefore the porosity and pore size distribution of the tablets were largely different (table 4.5) the

release profiles were very similar. The dissolution profiles followed approximately zero-order release kinetics (r^2 = 0.998) for the first 70% of drug released. Figure 4.5 shows the release of benzamide from tablets that had different pore structures but equivalent tablet thickness. The porosity of the tablets ranged from 4.8% to 18.6% while the median pore diameter ranged from 1.42μm to 2.87μm (table 4.6). Tablets that were immersed in PEG had the largest median pore diameter and this reflected the observation from the incremental intrusion plot that the smaller pores had largely disappeared in these tablets. Despite the pore structures being substantially different, the tablets released benzamide at similar rates. The large variations in standard deviation observed were due to poor distribution of benzamide within the granules arising from the difficult in distributing a small quantity of finely graded benzamide within relatively large granules. However, a low dose model drug was deliberately selected to minimise the extent to which the model changed tablet porosity. The mean time taken for 25%, 50% and 75% of benzamide to be released was calculated for tablet batches T3K(2), T3J, T3E and T3L(2). Statistical analysis using Student's t-tests showed that the means were not significantly different from each other ($p<0.05$).

The release profiles from each batch approximated to zero-order release kinetics (r^2 = 0.987 to 0.998), similar to the release kinetics observed for TIMERxN based tablets. Simple monolithic matrices are commonly associated with first-order release kinetics, that is, decreasing release rates with time (6), however, zero-order kinetics have sometimes been observed. For water-soluble drugs time independent release is thought to occur when the swelling and erosion fronts become synchronised thereby maintaining a gel-like layer of constant thickness (19). Zero-order kinetics have also be reported when the rate of release is erosion controlled, which can occur when the viscosity of the polymer is very low (27), or when the formulation contains a very low proportion of gum (156). However, since most of the drug was released while a large proportion of the matrix remained intact this suggested that diffusion was an important mechanism of release in these matrices. This is usually the case for water-soluble materials (6). Zero-order release of water-soluble drugs from xanthan gum matrices has also been reported (28).

Figure 4.6 shows that under conditions of low agitation no effects due to pore structure became apparent. Figure 4.7 shows the dissolution profiles of benzamide from granules when the granules were scattered over the surface of the dissolution medium. It can be seen that granules having 'high' and 'low' porosity (table 4.7) controlled the release of benzamide to the same degree. Dissolution from granules was rapid compared

with tablets because of the shorter diffusion pathway that the benzamide molecules needed to take to reach the dissolution medium.

The results suggested that the release controlling action of HP-based material was not dependent on tablet porosity, pore size distribution or tablet thickness. It was considered that this was because of the swelling characteristics of the material. In contact with aqueous medium the outer surface of the tablet rapidly hydrated, and swelled forming a gel-like barrier that limited water penetration. It is proposed that the formulation had a high affinity for water due to the high proportion of glucose and the hydrophilic nature of xanthan gum, and that this affinity for water, not initial porosity or pore size distribution, determined the rate of hydration of the dry matrix. As water penetrated through the outer hydrated layer into the core of the tablet a thick swollen layer developed. It is considered that the extensive swelling of the material meant that differences in initial pore structure and/or tablet thickness became negligible so that the tortuosity of the matrix was similar in each case. Therefore, each matrix limited the rate of water penetration to the same extent and presented a similar diffusional resistance to the solute. The results suggested that for these systems the initial porous structure of the matrix did not affect the propensity of the hydrated matrix to erode. Drug release from swellable matrix systems is thought to depend on the relative importance of tablet relaxation and drug diffusion rates (157). Within each HP-based tablet matrix drug diffusion rates are likely to be similar and it is the swelling of the matrix that dominates release behaviour. It appeared that any initial differences in tablet pore structure was outweighed by the extensive swelling of the system and that the rate of swelling was independent of initial tablet pore structure or bulk volume. It was thought that if matrix swelling dominated release behaviour then changes in release rates could be introduced by physically controlling matrix swelling. By coating one base and the lateral surface of tablets with an impermeable barrier the swelling of the matrix was restricted while the releasing surface area was maintained constant. Figure 4.8 shows that under conditions of restricted swelling release rates were faster in thinner (less porous) tablets. This was due to the longer diffusion pathway that existed in the thicker, more porous tablets. The high standard deviations observed could be due to be differences in tablet thickness within each set of tablets (3.62 ± 0.11mm, 5.20 ± 0.08mm).

Comparing figure 4.6, which shows the dissolution of benzamide from high and low porosity tablets under conditions of low agitation, with figure 4.5, which shows dissolution profiles at paddle speed 50rpm, it can be seen that the rate of release of

benzamide was much slower under low agitation conditions. Thermodynamic conditions could effect either the rate of erosion of the matrix or the rate of water penetration and solute movement within the tablet. Since diffusion of the drug through the matrix is likely to be the main releasing mechanism for water-soluble drugs (6), then it proposed that the speed of agitation predominantly affected diffusitivity with the tablets rather than the rate of erosion of the outer hydrated layer.

The kinetics of drug release from swellable hydrophilic matrices have often been modeled mathematically (27,28,69). The mathematical analysis of release is complicated by the presence of moving boundaries: the diffusion front, the swelling from and the erosion front, therefore mathematical solutions to release kinetics are complex (20). An simple empirical equation, developed by Ritger and Peppas (23), can be used to describe the degree of Fickian and non-Fickian release behaviour of some swellable polymeric excipients. However, the method is only suitable for modeling systems that do not swell to more than 25% of their original volume. Since HP-based matrices swell extensively (see section 5.4.2), no suitable models existed for modeling the release behaviour of these systems.

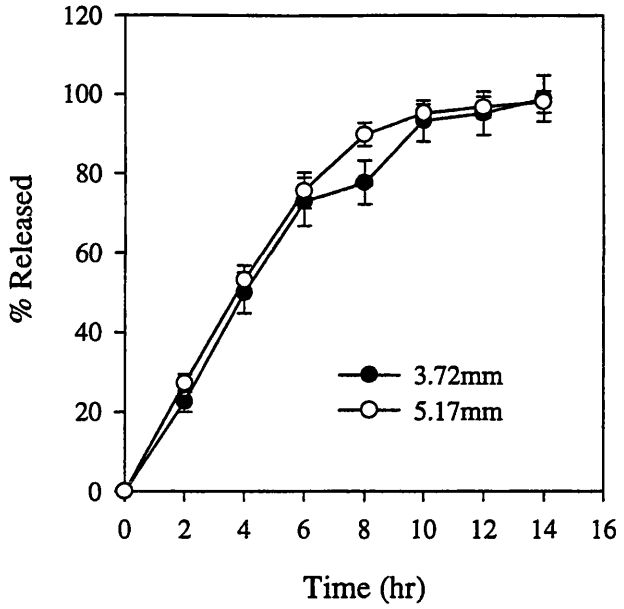

Figure 4.4 Dissolution of benzamide under conditions of low agitation from TIMERxN tablets compacted to different thicknesses (n=3)

	High thickness	**Low thickness**
Tablet thickness ± S.D (mm)	5.17 ± 0.04	3.72 ± 0.04
Specific pore area (m^2/g)	2.53	2.60
Median pore diameter (μm)	1.03	0.24
Porosity (%)	30.8	12.2

Table 4.5 Pore characteristics of TIMERxN tablets compacted to 'high' and 'low' tablet thickness.

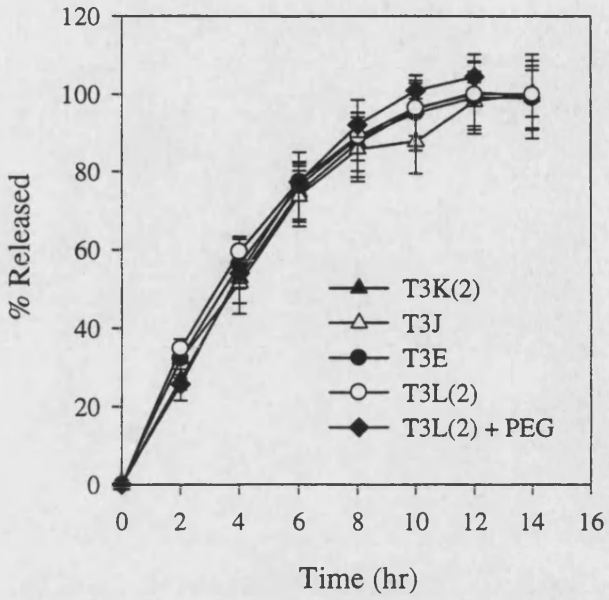

Figure 4.5 Dissolution of benzamide from tablets having different porous structures but the same tablet thickness (paddle speed 50rpm, n=5)

Tablet batch No.	**Median pore diameter (μm)**	**Porosity (%)**	**Thickness ± S.D (mm)**
T3K(2)	1.73	18.6	4.17 ± 0.12
T3J	1.60	15.3	4.12 ± 0.03
T3E	1.42	11.8	4.12 ± 0.05
T3L(2)	2.30	9.8	4.11 ± 0.03
T3L(2) + PEG	2.87	4.8	4.25 ± 0.07

Table 4.6 Pore characteristics of HP-based material compacted to equivalent tablet thickness

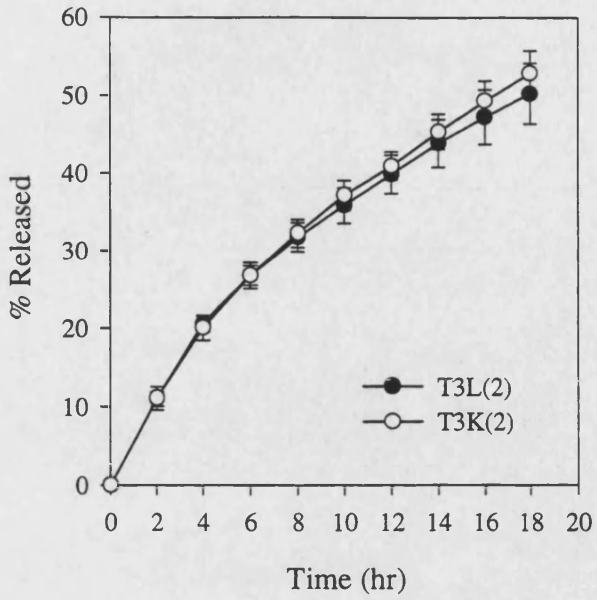

Figure 4.6 Dissolution of benzamide under conditions of low agitation. Tablets had equivalent thickness but 'high' and 'low' porosity (n=5)

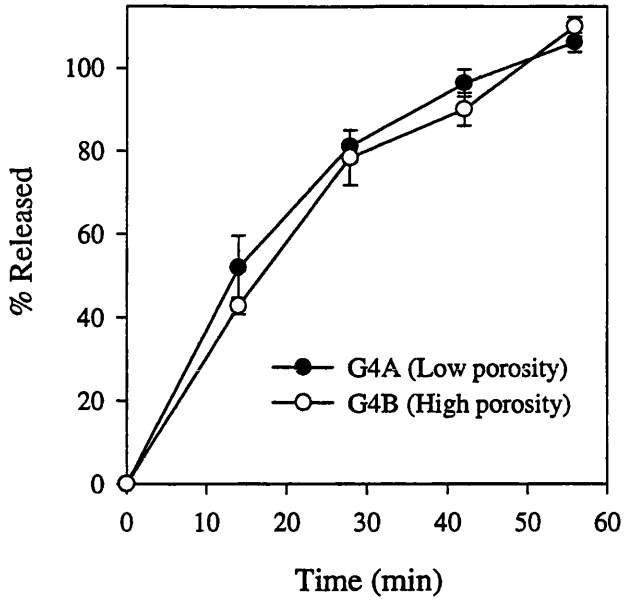

Figure 4.7 Dissolution of benzamide from high and low porosity granules under conditions of low agitation (n=3)

	G4A	G4B
Specific pore area (m^2/g)	0.390	0.163
Median pore diameter (μm)	2.33	3.16
Porosity (%)	2.73	8.38

Table 4.7 Pore characteristics of granules containing benzamide distributed intragranularly

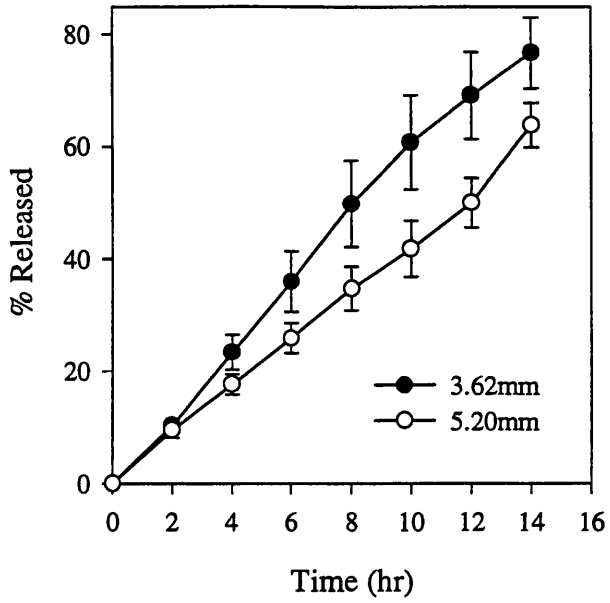

Figure 4.8 Dissolution of benzamide from a single surface of TIMERxN tablets under conditions of low agitation (n=3)

Figure 4.9 shows the dissolution profiles of diclofenac sodium from tablets that had different geometrical shapes and therefore different initial bulk densities, bulk volumes and initial releasing surface areas (table 4.8). Although initial bulk characteristics were different, release rates were similar. A statistical comparison of the mean percentages released at each time point was made using Student's t-test. This showed that there was no significant difference between the mean percentage released from 8mm cylindrical tablets and the mean percentage released from square tablets at each time point ($p<0.05$). The mean percentages released from 8mm tablets and caplets were not significantly different at the 2, 8, and 10hr time points ($p<0.05$) while the mean percentages released from square and caplet shaped tablets were not significantly different at the 2, 6, 8 and 10hr time points ($p<0.05$). Although some of the means were statistically different at a number of time points, overall the release profiles could not be considered practically different. Although a correlation between tablet shape and dissolution profile was not observed here, a relationship between shape and release profiles has been reported for other systems. Ford *et al.* (69) found that the root time release rates of promethazine HCl (a highly water-soluble drug) from HPMC K15M matrices was proportional to the initial

surface area of the tablets. Release rates decreased as tablet surface area decreased. It is possible that observations of correlation or lack of correlation will depend on many parameters including the model drug selected, test conditions and the nature of the hydrophilic excipient.

Visual observations showed that each geometrical form swelled extensively producing tortuous swollen bodies. Since a large proportion of the dose was released while most of the matrix remained intact it appeared that release of diclofenac sodium was primarily controlled by diffusion through the swollen matrix. It is proposed that where a very tortuous matrix exists, as a result of high matrix viscosity and extensive swelling, then slight difference in the shape of the hydrated matrix becomes negligible. The diffusion path length becomes similar in each matrix and therefore, for models that are primarily released by diffusion, similar release profiles are observed.

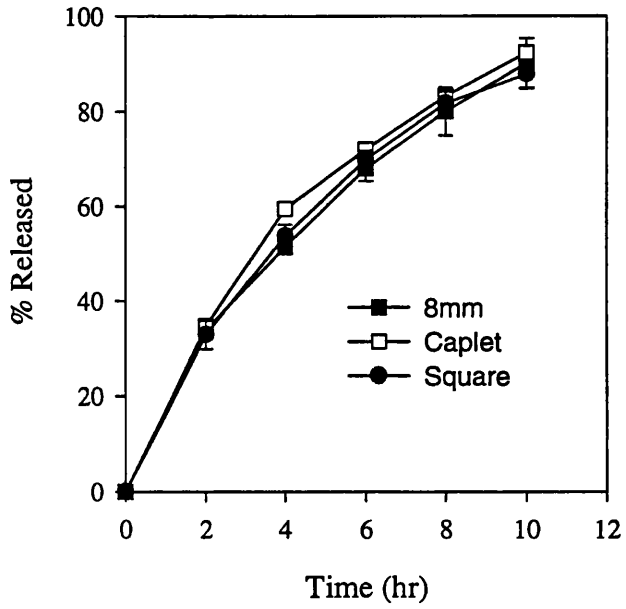

Figure 4.9 Dissolution of diclofeanc sodium from tablets having different geometrical shapes (paddle speed 50rpm, n=3)

	Cylindrical	Caplet	Square
Volume (cm^3)	0.387	0.327	0.279
Bulk density (g/cm^3)	0.97	1.23	1.33
Tablet surface area (cm^2)	2.93	3.63	2.08

Table 4.8 Volume, bulk density and tablet surface area of diclofenac sodium tablets compacted to different geometrical shapes

4.4.3 *Effect of tablet thickness on dissolution of diclofenac sodium from Carbopol and Methocel matrices*

Although release of diclofenac sodium and benzamide from HP-based matrices was independent of tablet pore structure, size and shape this situation has not always been observed in other hydrophilic matrix materials. Kawashima *et al.* (96) found that the sustained releasing action of low-substituted hydroxypropylcellulose (L-HPC) was determined by a function of internal pore size distribution and the swelling properties of the tablet. Van der Veen *et al.* (94) found that the release of theophylline from tablets containing 70% amylodextrin was dependent on the compaction pressure used to produce the tablets. Tablets compacted at a lower force had faster release rates. The results were attributed to difference in the rate of solvent penetration into the tablets. Korsmeyer *et al.* (92) found that the release of potassium chloride from hydroxypropylcellulose (HPC) matrices was found to vary inversely with tablet porosity and mean pore diameter. It was proposed that air entrapped within the matrix was acting as a transport barrier. Tablets with higher porosity had more entrapped air and thus released the drug at a slower rate. Rizk *et al.* (95) reported a scleroglucan/theophylline/lactose formulation that displayed a marked decrease in release rate with increasing tablet hardness. Peréz-Marcos *et al.* (32) observed that an increase in the force used to compact a frusemide/Carbopol formulation lead to an increase in of dissolution of the drug from the matrix. Drug release was thought to occur through erosion of the matrix and susceptibility to erosion was thought to change with tablet thickness. The result was correlated with a seven-fold decrease in pore radius. The work carried out by Peréz-Marcos *et al.* (32) was re examined here to determine whether the observations made for Carbopol could be extended to HP-based material. When the formulation containing frusemide prepared according to Peréz-Marcos *et al.* (32) was reproduced it was found that under the conditions reported by

these authors the dissolution profiles were sensitive to changes in tablet thickness (figure 4.10). When Carbopol was replaced with Methocel K15M, it was observed that again, tablets having different thicknesses released frusemide at different rates (figure 4.11). The difference between the profiles was less prominent than that observed with the Carbopol formulation. When Carbopol was replaced with HP-based material it was found that dissolution profiles were very variable because under the high agitation conditions employed, TIMERxN tablets did not remain stationary during the test. It was observed that formulations containing Carbopol and Methocel K15M did not swell to the same extent as HP-based tablets. Extensive swelling of HP-based material produced a large swollen mass that had sufficiently low density to become buoyant under the dissolution conditions. Figure 4.12 shows that when diclofenac sodium was used as a model drug in place of frusemide, then release rates ceased to be sensitive to tablet thickness. In this case very slow release rates were observed possibly due to an interaction between diclofenac sodium and Carbopol. When dissolution of the Carbopol/frusemide formulation was studied under more standard dissolution conditions, that is at a paddle speed of 50rpm rather than 150rpm, the release of drug from tablets was found to be independent of tablet thickness (figure 4.13). Overall, the sensitivity to compaction of the formulation used by Peréz-Marcos *et al.* (32) was a function of a number of interacting factors: the drug used, thermodynamic conditions and hydrophilic excipient used.

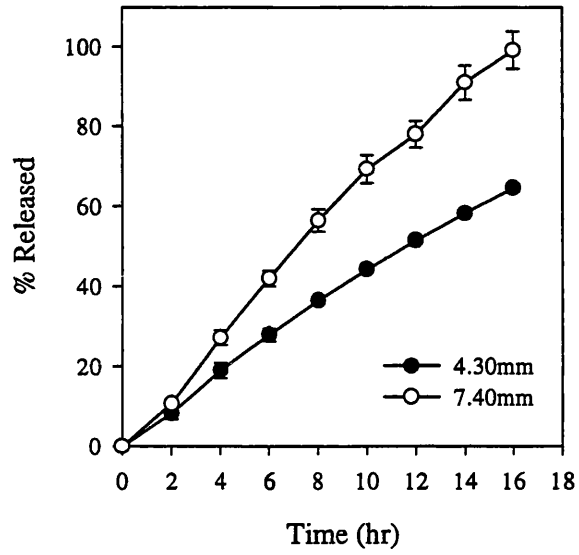

Figure 4.10 Dissolution of frusemide from Carbopol tablets compacted to different tablet thickness
(paddle speed 150rpm, n=3)

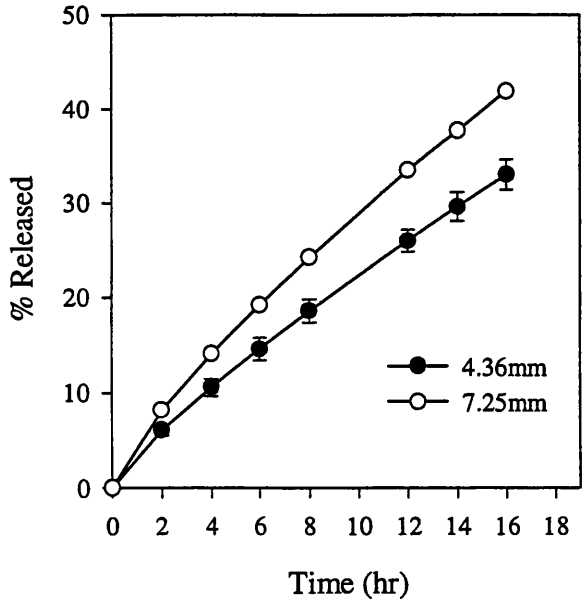

Figure 4.11 Dissolution of frusemide from Methocel K15M tablets compacted to different tablet thicknessess
(paddle speed 150rpm, n=3).

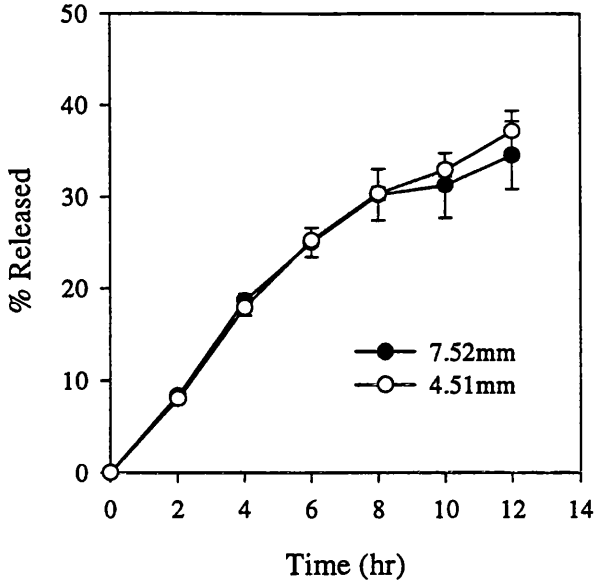

Figure 4.12 Dissolution of diclofenac sodium from Carbopol tablets compacted to different tablet thicknesses (paddle speed 150rpm, n=3).

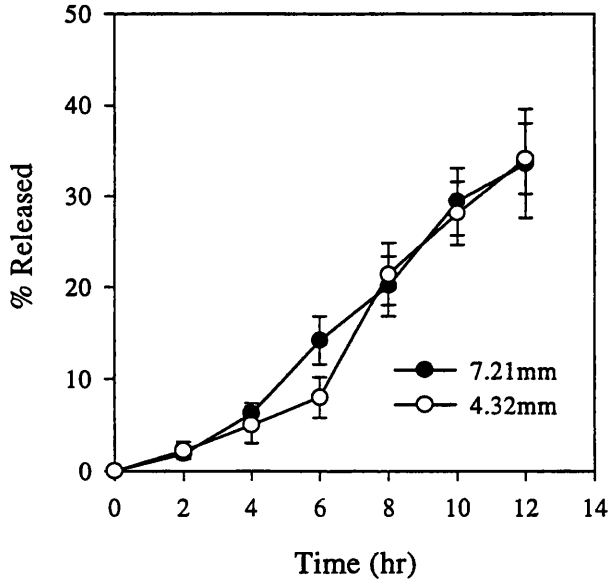

Figure 4.13 Dissolution of frusemide from Carbopol tablets compacted to different tablet thicknessess (paddle speed 50rpm, n=3)

4.4.4 *Effect of tablet thickness on dissolution profiles from tablets containing a low proportion of HP.*

Dissolution tests on tablets containing 5% HP compacted to four different tablet thickness showed that two very different release profiles were obtained (figure 4.14). In the case of tablets compacted to 7.40 ± 0.11mm rapid dissolution was observed leading to 90% release in approximately 15min. In the case of tablets compacted to 5.34 ± 0.09mm and 6.17 ± 0.02mm, sustained release of diclofenac sodium was observed. The effect of tablet thickness on the release of drug from matrices containing low gum loading can be explained by percolation theory. Percolation theory was introduced into the pharmaceutical field when Leuenberger *et al.* (158) employed this theory in the characterisation of solid dosage forms. The theory supposes the existence of a regular lattice underlying the system. In a binary mixture A/B, the sites of the lattice can be occupied by the component A or the component B. In random percolation models the occupation of the sites is random. A cluster is defined as a group of neighbour occupied sites in the lattice and the probability at which a cluster just percolates a system is called the percolation threshold. In HP-based matrices, HP-based granules can be considered as one component and the blend of diluent and drug can be considered a second component. When a tablet of low thickness (or low porosity) swells a network of gel-like material is formed which spans the tablet keeping it intact and sustaining the release of the drug. At higher tablet thickness swollen HP particles become isolated within the matrix and therefore the integrity of the matrix is lost leading to disintegration of the tablets and rapid drug release. The effect appears to be an "all or nothing" phenomena since no intermediate profiles were observed. Percolation theory has been used to explain the effect of drug loading (81,159) and polymer loading (160) on drug release from polymeric matrices. This work shows that the theory can also be used to explain the effect of tablet thickness (or compaction force) on the release controlling action of a tablet containing a low proportion of hydrophilic material.

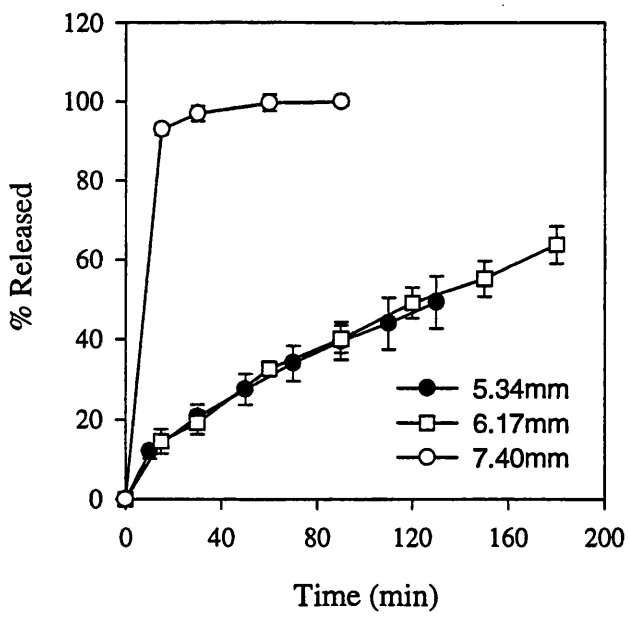

Figure 4.14 Dissolution of diclofenac sodium from tablets containing 5% HP (paddle speed 50rpm, n=3)

4.4.5 *Comparison of the release controlling action of TIMERxN and BHP-based tablets*

Figure 4.15 shows that the release profiles of benzamide from TIMERxN and BHP-based tablets were similar. In comparison, the rate of release of diclofenac sodium from TIMERxN tablets was much slower than from BHP-based tablets. Benzamide, being highly water-soluble, will have left the tablet matrix principally by a diffusion process. The fact that TIMERxN and BHP-based granules sustained the release to the same extent suggests that the diffusitivity of benzamide in theses two materials was similar. Being less water-soluble, the release of diclofenac sodium from the swollen material was likely to occur to some extent by attrition of the swollen material. Since TIMERxN sustained the release of diclofenac sodium longer than BHP-based tablets this suggests that matrices composed of TIMERxN were more resistant to erosion. This might possibly have been due to the presence of the tertiary components ethylcellulose and calcium sulphate in the TIMERxN matrix. Ethylcellulose is sometimes used as a binder in tablets where it reduces the rate of drug dissolution by virtue of its insoluble nature (161). The importance of calcium ions in the formation of firm gelatinous

networks of polysaccharides has been documented (56,57). These may play a part in holding the matrix together and preventing attrition and matrix dissolution. It was observed that even after 24hr of agitation at 37°C a swollen body of TIMERxN still remained in the dissolution vessels and the dissolution medium remained clear. In contrast, after approximately 24hr of dissolution BHP-based tablets had completely eroded. It is also possible that diclofenac sodium interacted with one or more of the tertiary components in TIMERxN resulting in a slower than expected release rate.

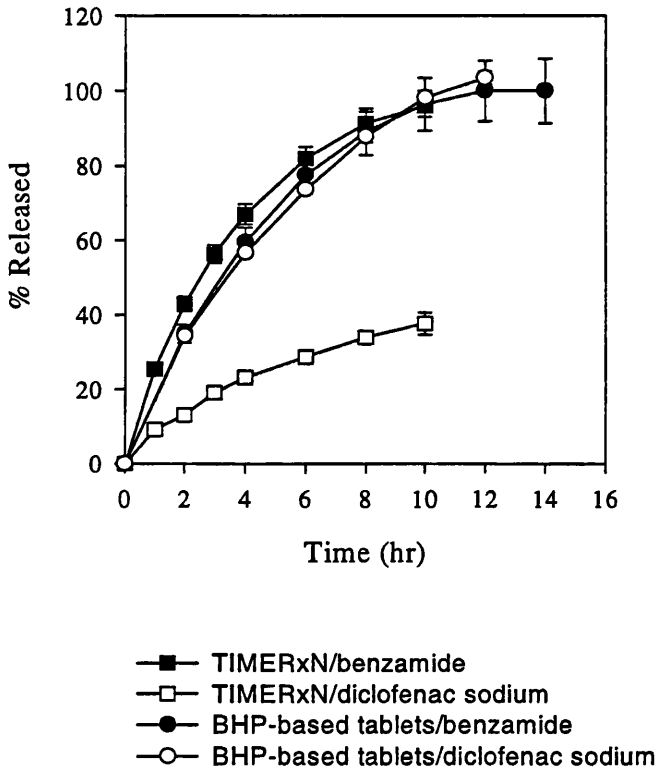

Figure 4.15 Comparison of the release controlling action of TIMERxN and BHP-based tablets (paddle speed 50rpm, n=5)

4.5 Conclusion

It appears than under certain conditions correlations between porosity, pore size distribution and release rates may be observed. However, for hydrophilic matrices that swell rapidly and extensively it seems likely that release rates will be generally be independent of the initial bulk physical characteristics of the matrix. The extensive swelling of HP-based matrix tablets meant that initial tablet porosity, pore size distribution

and initial release surface area were not important in determining drug release rates for the formulations studied. The swelling characteristics of the matrix meant that even when the tablets had initially different geometrical shapes, the release profiles of a slightly water-soluble drug were similar.

5. Functional interchangeability and pharmaceutical equivalence in HP-based tablet and capsule matrices: *in vitro* observations

5.1 Introduction

The rate of release of the model drugs benzamide and diclofenac sodium from HP-based tablets was found to be independent of the initial bulk characteristics of the dry tablet. A theory of porosity-independent release was postulated and tested using capsule matrices. Hard gelatin capsules containing uncompacted granules were considered analogous to tablets, the difference being that capsule matrices had a high interparticulate porosity. Assuming porosity-independent release then theoretically, capsules and tablets were expected to have equivalent rate controlling action. This was considered a novel concept since not only would the two dosage forms be equivalent in terms of release controlling action but they would also be equivalent in terms of formulation composition. The use of capsule matrices as an alternative to tablet matrices without formulation modification has not previously been reported. Capsule matrices have predominately been investigated as hydrodynamically balanced systems for prolonging gastric residence time (98,162). Only a limited number of studies have considered hydrophilic matrix capsules as simple hydrophilic matrix systems (14,31,70,99) and no studies have been reported that have compared the release controlling characteristics of swellable hydrophilic tablet with capsule matrices containing the same formulation.

5.2 Materials

Diltiazem HCl (Lot No. 970611) was obtained from Seloc AG, SIFA Ltd., Shannon, Ireland). Propranolol HCl (Lot No. 1067B193) was obtained from Industrie Chemiche Italiane, S.p.H. (Milan, Italy). Hard gelatin capsules, DBCAPS™ size A, were obtained from DAVCAPS (Capsugel, Belgium). Xanthan gum (Lot No. P5086), locust bean gum (Lot No. B21577), glucose (Lot No. CD6D29107) and TIMERxN (Lot No. NS664) were supplied by Penwest Pharmaceuticals Co., (Patterson, NY, USA). Diclofenac sodium (Lot No. 94-01342) was obtained from Heumann Pharma GmbH (Nürenberg, Germany). Benzamide (Lot No. 6366081) was obtained from Aldrich Chemical Co. (Loughborough, U.K.). Hydroxypropylmethylcellulose (Methocel K15M Premium EP, Lot No. KJ26012N01) was obtained from Colorcon (Kent, U.K). Acetone

and magnesium stearate (Lot No. 30120362) were obtained from Fisons Scientific Equipment Ltd. (Loughborough, U.K.). 1μm cellulose nitrate filters were obtained from Whatman International Ltd., (Maidstone, U.K).

5.3 Methods

5.3.1 *Characterisation of diltiazem HCl and propranolol HCl*

Diclofenac sodium, propranolol HCl, diltiazem HCl and benzamide were selected as model drugs. According to the USP solubility classification (65) diclofenac sodium can be described as being slightly water-soluble, benzamide and propranolol HCl as water-soluble and diltiazem HCl as freely water-soluble. The percentage solubility (w/v) of each drug in distilled water (pH 7.0) and the drug loadings used in this study are shown in table 5.1.

Model drug	Solubility in water (%)	Drug loading (%)
Diclofenac sodium	0.187*	5 and 7.5
Propranolol HCl	5*	20
Diltiazem HCl	Freely soluble**	30
Benzamide	1.35**	3

*(154), **(153)

Table 5.1. Solubility and drug loading of model drugs

The chemical structures of propranolol HCl and diltiazem are shown in figures 5.1 and 5.2. The chemical structures of benzamide and diclofenac sodium are given in section 4.3.1.

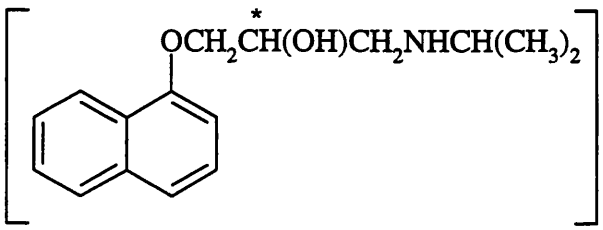

Propranolol hydrochloride

Figure 5.1 Molecular structure of propranolol HCl

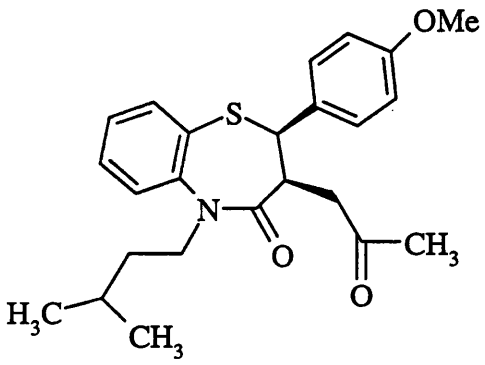

Diltiazem

Figure 5.2 Molecular structure of diltiazem

5.3.2 *Assay of diltiazem HCl and propranolol HCl*

Diltiazem HCl and propranolol HCl were assayed by UV detection at the λmax of each drug. The assay of diclofenac sodium and benzamide is described in section 4.3.2. Dilute solutions of propranolol HCl and diltiazem HCl were scanned between 200nm and 350nm using a UV/VIS spectrophotometer (Lambda 3B, Perkin-Elmer, Beaconsfield, U.K.). The λmax were found to be 288nm for propranolol HCl and 236nm for diltiazem HCl. A stock solution of propranolol HCl (0.075%) was prepared by dissolving 375mg of propranolol HCl, accurately weighed, in 500ml of distilled water. Aliquots of the stock solution were diluted to produce a series of solutions having target concentrations of 0.0015%, 0.0030%, 0.0045%, 0.0060% and 0.0075%. The absorbance of each solution was determined at 288nm using a UV/VIS spectrophotometer (Unicam 8625, Cambridge, U.K.) against a distilled water blank. Using the same stock solution a second series of dilutions was prepared and analysed in the same way. Using a fresh stock solution a third

series of solutions were prepared and the UV absorbance determined. A stock solution of diltiazem HCl (0.025%) was prepared by dissolving 125mg of diltiazem HCl, accurately weighed, in 500ml of distilled water. Aliquots of the stock solution were diluted to produce a series of solutions having target concentrations of 0.0005%, 0.0010%, 0.0015% and 0.0020%. A second set of dilutions was prepared from the same stock solution and a third set of dilutions was prepared from a fresh stock solution. The UV absorbance of the solutions at 236nm was determined against distilled water. 3 calibration plots were constructed for each model drug and linear regressions were carried out using a computer graphics program (MicroCal Origin, MicroCal Scientific Inc., Northampton, MA, USA).

5.3.3 *Sample preparation*

Each model drug was distributed in one or more HP-based formulations, in powder and/or granule form. Diclofenac sodium was also incorporated into HPMC based granules. The gelatin bodies of size A hard gelatin capsules were filled to capacity with powder or granules, the fill weight used depending on the bulk density of each formulation. A similar weight of material was compacted into 5mm × 16mm caplet shaped tablets using a single-punch tablet press (Type F3, Manesty, Speke, Liverpool, U.K.). The geometry of the capsules and tablets meant that each dosage form had a similar shape and length prior to dissolution. Table 5.2 gives approximate volumes, initial surface areas and dimensions of size A gelatin capsules and caplet shaped tablets. The mean weight (n=5) of each batch of tablets and the mean weight (n=5) contained in each batch of capsules are given in table 5.3.

	Capsule	**Caplet**
Bulk volume (cm^3)	0.97	0.44
Outer surface area (cm^2)	5.77	3.91
Diameter (mm)	8	5
Length (mm)	18	16
Thickness (mm)	-	5.5

Table 5.2 Bulk volume, surface area and dimensions of capsules and caplets

5.3.3.1 *Diclofenac sodium distributed intragranularly*

XG (25%), LBG (25%), glucose (45%) and diclofenac sodium (5%) were blended for 5min in a high shear mixer (Cuisine Systémè Automatic 5000, Magimix, Surrey, U.K.). Total batch size was 300g. The blend was wet agglomerated with 21.6% distilled water and tray dried at 60°C in an oven (Model H-150, Size 2 Gallenkamp, Loughborough, U.K.) for 24hr giving material with an LOD <5%. The material was screened through a 0.63mm mesh using a mechanical granulator (Type MGL 4A, Frewitt, Switzerland). The granules were sieved for 30min (Endecotts Ltd., London, U.K.) through an I.S.O standard aperture diameter $\sqrt{2}$ sieve progression ranging from 710μm to 63μm. The sieves were agitated using a Fritsch sieve shaker (Type 03-502, Fritsch, Germany). Quantities from each sieve fraction were selected in the following proportions: 500 to 710μm (2%), 355 to 500μm (4%), 250 to 355μm (26%), 180 to 250μm (36%), 125 to 180μm (26%), 90 to 125μm (3%), 63 to 125μm (2%) and 0 to 63μm (1%). Sieve fractions were recombined using turbula rotation (Type T2C, Glen Creston Ltd., Stanmore, Middlesex, U.K.) for 5 minutes at 30rpm giving particles with a theoretical median particle size of 182μm.

5.3.3.2 *Diclofenac sodium distributed extragranularly*

XG (25%), LBG (25%) and glucose (50%) were blended in a high shear mixer for 5min. This gave a simple, non-granulated, HP-based blend. The true density of the blend determined by helium pycnometry (Accupyc 1330, Micromeritics, Norcross, USA) using the method described in section 2.3.1 was found to be 1.52g/cm^3. The aerodynamic particle size distribution of the blend was measured using the method described in section 2.3.1 (Aerosizer, Amherst Instruments Inc., MA, USA). The D[4,3] was found to 59.6 ± 5.6μm (n=3). Diclofenac sodium (7.5%) was distributed through the blend (92.5%) by geometric trituration.

A formulation containing diclofenac sodium distributed extragranularly in pre-granulated HP-based material was also prepared. XG (25%), LBG (25%) and glucose (50%) were blended in a high shear mixer for 5min. The material was wet agglomerated with 15.9% distilled water, tray dried at 21°C for 48hr and hammer-milled (Type DFH 48, Glen Creston Ltd., Stanmore, U.K.) using a 3mm screen. The sieve fraction less than 180μm was collected (Endecotts Ltd., London, U.K.). The aerodynamic diameter of the granules (D[4,3]) was found to be 61.9μm ± 6.2μm, similar to the aerodynamic diameter of the simple HP-based dry blend. 92.5% of the pre-granulated material was blended with

7.5% diclofenac sodium by geometric trituration. Both extragranular diclofenac sodium formulations contained the same proportion of drug and excipients and had similar particle sizes.

5.3.3.3 *Propranolol HCl granules*

XG (25%), LBG (25%), glucose (30%) and propranolol HCl (20%) were blended in a high shear mixer. The materials were wet agglomerated with 21% distilled water for 5min then tray dried at 60°C in an oven for 24hr giving material with an LOD of less than 5%. The material was passed through a 0.63mm screen using an oscillating granulator and size selected as described in section 5.3.3.1, to give granules with a theoretical median particle size of 182μm.

5.3.3.4 *Diltiazem HCl dry blend*

XG (25%), LBG (25%) and glucose (50%) were blended in a high shear mixer for 5min. The simple dry blend of HP components was mixed, by geometric trituration, with diltiazem HCl in the ratio of 70% HP-based dry blend to 30% drug. The punch and die were lubricated with a suspension of 1.5% magnesium stearate in acetone prior to compaction of caplets.

5.3.3.5 *Benzamide granules*

XG (24.3%), LBG (24.3%), glucose (48.4%) and benzamide (3.0%) were blended for 5min using a high shear mixer. The dry blend was agglomerated using 17.8% distilled water, which was added over 1min. Total mixing time was 5min. The wet material was tray dried in an oven at 60°C for 24hr giving material with an LOD of less than 5%. The dry material was screened through a 0.63mm mesh using an oscillating granulator and size selected as described in section 5.3.3.1, giving granules with a theoretical median particle size of 182μm.

5.3.3.6 *Methocel K15M matrices*

Methocel K15M is a grade of HPMC that has often been studied as a hydrophilic swellable excipient (82). It has a nominal apparent viscosity of 15000cp (163) and a mean aerodynamic diameter of 28.4 ± 0.5μm (determined using the method described in Section 4.3.5). A formulation containing diclofenac sodium in a Methocel K15M matrix was prepared using a similar formulation and method used to produce the HP-based diclofenac

sodium formulation. Diclofenac sodium, glucose and Methocel K15M were blended for 5min in a high shear mixer. Batch size was 200g. The material was wet agglomerated with 33.3% distilled water for 5min. The material was tray dried for 24hr in an oven at 60°C and passed through a 0.63mm screen using an oscillating granulator. The dry material was size selected as described in section 5.3.3.1, giving granules with a theoretical median particle size of 182μm.

5.3.3.7 *Placebo granules and tablets*

Placebo capsules and caplets were prepared for use in mechanical strength studies. XG (25%), LBG (25%) and glucose (50%) were dry blended in a high shear mixer for 5min. The blend was wet agglomerated with 20.6% distilled water for 8min, dried at 21°C for 48hr and hammer-milled (Type 14-586, Glen Creston Ltd., Stanmore, Middlesex, U.K.) using a 3mm screen. The granules were size selected as described in section 5.3.3.1. The final LOD of the material was 6.5%.

	Weight in capsule (mg)	Weight of caplet (mg)
Diclofenac Na distributed intragranularly in HP-based granules	386.4 ± 5.9	372.9 ± 3.6
Diclofenac Na distributed in simple HP-based dry blend	471.5 ± 5.9	453.5 ± 12.8
Diclofenac Na distributed in pre-granulated HP-based material	477.3 ± 19.1	469.7 ± 8.7
Propranolol HCl distributed intragranularly in HP-based granules	380.7 ± 5.0	386.3 ± 1.3
Diltiazem HCl distributed in a simple HP-based dry blend	431.4 ± 14.0	433.8 ± 4.6
Benzamide distributed intragranularly in HP-based granules	396.9 ± 9.2	399.5 ± 2.8
Diclofenac Na distributed intragranularly in Methocel K15M granules	251.0 ± 4.7	252.3 ± 0.8

Table 5.3 Weight of material constituting tablet and capsule matrices.

5.3.4 *Dissolution testing*

Dissolution of model drugs from matrices in 1000ml of distilled water heated to 37°C ± 0.2°C was determined using a USP II dissolution apparatus (Type PTW S3C, Pharmatest Ltd., Gwent, U.K.) with paddles positioned 4cm above the point of curvature at the bottom of the vessel. Paddle speed was 50rpm or 100rpm. The dosage forms to be analysed were supported in stainless steel wire cages (approximately 5cm × 2.5cm) to allow unrestricted swelling, ensure release from all surfaces and to prevent the capsules from floating. To assay drug release from HP-based matrices samples of dissolution medium were withdrawn at intervals using a syringe and filtered through 1μm cellulose nitrate filters. An equal volume of distilled water heated to 37.0 ± 0.2°C was added to each dissolution vessel following sampling to maintain constant volume. The absorbance of the filtrate at the appropriate λmax was measured using an UV spectrophotometer (Unicam 8625, Cambridge, U.K.). Medium containing diltiazem HCl was diluted 1:5 with

distilled water prior to filtration to bring the absorbance within the linear range of the calibration plot. The quantity of drug released at each time point was calculated taking into account the amount removed by sampling and the progressive dilution of the dissolution medium. Drug release was expressed as a percentage of the initial drug content while error bars represented the standard deviation from the mean. It was shown that no loss of UV absorbance occurred at the λmax of each model when solutions of diltiazem HCl, propranolol HCl, diclofenac sodium and benzamide were passed through cellulose filters. This suggested that the models did not adsorb on to the cellulose filters. The UV absorbance of approximately 373mg of a placebo formulation contained in a hard gelatin capsule, completely dispersed in water, was found to be less that 6% of the maximum drug absorbance after the medium was filtered through 1μm filters.

To follow the release of diclofenac sodium from Methocel K4M matrices samples were removed and analysed using the automated set up described in section 4.3.6.1. Automatic sampling was possible with these matrices as excipient interference could be minimised by passing the medium through the 20μm filters fitted for the automatic sampling method.

5.3.5 *Determination of content uniformity*

The drug content of each diclofenac sodium formulation was determined. Accurately weighed samples (approximately 100mg) were distributed in either 200ml or 250ml of distilled water. The solutions were allowed to equilibrate for at least 6hr and sonicated (FS2006, Deacon Laboratories Ltd., U.K.) for 15min. Samples of the solution were filtered through 1μm cellulose nitrate filters and the UV absorption at 273nm was determined. The drug content of the diltiazem HCl formulation was determined by distributing approximately 70mg of powder, accurately weighed, in 500ml of distilled water. The samples were allowed to equilibrate for at least 6hr and filtered as described above. The UV absorbance at 236nm was determined. Six determinations were made on each batch of material and the mean drug content was calculated using the appropriate calibration data. The amount of drug release during dissolution was expressed as a percentage of the initial drug content. For the remainder of the formulations the drug released was expressed as a percentage of the theoretical drug content.

5.3.6 *Determination of drug stability*

The UV absorbance of solutions of diltiazem HCl and propranolol HCl maintained at 37.0 ± 0.2°C was measured at the λmax of each model drug at intervals over a 24hr period. The absorbance of a diltiazem HCl solution varied by + 5.2% over this period and the absorbance of a solution of propranolol HCl varied by up to + 4.3%. No loss of absorbance at the λmax occurred. This indicated that the model drugs would remain stable over the dissolution period.

5.3.7 *Preparation of reference tablets*

Reference tablets were used to give confidence that the dissolution conditions used in each experiment were consistent (see section 4.3.4.4). Diltiazem HCl reference tablets were prepared by blending diltiazem HCl (3.75%) and TIMERxN (95.25%) by geometric trituration. Magnesium stearate was added as a lubricant and distributed by turbula rotation at 30rpm for 5min. The blend was compacted on a single-punch tablet press using 8mm flat-faced F tooling. The preparation of diclofenac sodium and benzamide reference tablets is described in section 4.3.4.4.

5.3.8 *Determination of the mechanical strength of hydrated matrices*

A measure of the mechanical strength of placebo swollen capsule and tablet matrices was obtained by measuring the work done as a probe penetrated the swollen material. Dosage forms to be tested were placed in 3.5cm × 2cm mesh baskets, which allowed both axial and radial swelling. The baskets were placed in dissolution vessels that contained 750ml of distilled water heated to 37.0 ± 0.2°C. The water was agitated using paddles, positioned 4cm above the bottom of the vessels, rotating at 50rpm. At each time point the basket was removed, drained and the swollen gel-like material was placed directly under a 6mm stainless-steel cylindrical probe attached to a texture analyser (TA-XT2 Texture Analyser, Stable Microsystems, Surrey, England) fitted with a 5kg load cell. The probe was lowered at a speed of 1mm/s into the sample to a depth of 4mm. Measurement of force was triggered when the probe detected the surface of the material. The force generated was recorded over the period of movement of the probe and the work done was calculated as the area under the force (g)/distance (mm) plot. Six samples were tested at each time point using a fresh set of samples in each case.

5.3.9 *Imaging of tablet and capsule swelling*

Images were taken of hydrating capsule and tablet matrices prepared from granule batch G3B (see section 3.3.2). The granules were hand filled into a size A gelatin capsule (weight 460.7 ± 11.3mg) and compacted into a 5 × 16mm caplet shaped tablet (weight 467.7 ± 9.9mg). A flat-bottomed stainless steel vessel was filled to a depth of 4cm with distilled water. The vessel was heated with a hot plate (Model MR 3022, Heidolph, Germany) to 37°C ± 0.5°C and agitated using a magnetic flea rotating at 150rpm. The dosage forms to be imaged were anchored between two coils of a helical wire. This prevented the matrices from floating but put a minimum restriction on swelling. The dosage forms were imaged at pre-determined time intervals using a digital camera (DX-7, Fuji Photo Film Ltd., China) that was positioned directly above the vessel. A grid was used to provide a scale from which the dimensions of the swollen body could be determined. The images were processed using photoenhancer software (Pictureworks Technology Inc., Danville, USA).

5.4 Results and discussion

5.4.1 *Calibration data*

Tables 5.4 and 5.5 show calibration data for propranolol HCl and diltiazem HCl, respectively. Calibration plots, given in appendix 2, were found to be linear in the concentration range 0 to 0.075% for propranolol HCl and 0 to 0.020% for diltiazem HCl. Student's t-tests showed that there were no significant differences between the calibration plots for each drug ($p<0.05$).

	Calibration plot No.			
	1	**2**	**3**	**Mean (n=3)**
Intercept	0.0062	0.0122	0.0145	0.0109
Slope	178.44	177.92	182.17	179.51
Standard deviation	0.81	2.21	2.16	-
Regression (r^2)	0.9999	0.9997	0.9997	-

Table 5.4 Calibration data for propranolol HCl

	Calibration plot No.			
	1	2	3	Mean (n=3)
Intercept	-0.0072	-0.0040	0.0014	-0.0006
Slope	520.80	513.43	507.42	513.88
Standard deviation	2.8	3.5	3.1	-
Regression (r^2)	0.9999	0.9999	0.9999	-

Table 5.5 Calibration data for diltiazem HCl

5.4.2 *Dissolution from HP-based tablet and capsule matrices*

Figure 5.3 shows the release profiles of diclofenac sodium from capsule and tablet matrices that contained the drug distributed intragranularly. It can be seen that the release profiles obtained from capsules and tablets were very similar. Statistical analysis using Student's t-test showed that the mean percentage released from capsule matrices was not significantly different from the mean percentage released from tablet matrices at the 2, 4, 6 and 10hr time points ($p<0.05$). Although a statistical difference between the means existed at the 8hr time point this was not considered practically significant. Figures 5.4 and 5.5 show the release of propranolol HCl from capsule and tablet matrices and the release of diltiazem HCl from capsule and tablet matrices, respectively. Despite the high water-solubility of the models, capsule and tablet matrices controlled the release to a similar degree. Statistical analysis of the mean percentages released at each time point using Student's t-test showed that for tablets and capsules containing propranolol HCl the data was significantly different only at the 7hr time point ($p<0.05$). For diltiazem HCl statistical differences were calculated at the 1 and 3hr time points ($p<0.05$). Again, although statistically significant the differences were considered insignificant in practice. Although porosity independent release was predicted the results were interesting since it would have been conceivable that granules contained uncompacted in gelatin capsules would de-aggregate to some degree during the early stages of dissolution resulting in a burst release of drug. This was not observed with the capsule matrices studied.

It was also interesting to find that disintegration of the capsules did not occur when the degree of agitation in the dissolution medium was increased. Figure 5.6 shows that when the paddle speed was increased from 50 to 100rpm, capsule and tablet matrices

still controlled the release of diclofenac sodium to the same extent. Additionally, the release profiles obtained were very similar to the release profiles observed at 50rpm (figure 5.3). By increasing the paddle speed the hydrodynamic flow in the dissolution medium was increased. Paddle speed may also have affected the hydrodynamic stresses to which the dosage forms were subjected. However, the influence of paddle speed on hydrodynamic stress could not be quantified. An increase in paddle speed may not have caused a sufficient increase in hydrodynamic stress to affect the erosion of the matrices. Therefore, dissolution profiles remained similar. Alternatively, the fact that no differences in release profiles were observed when the paddle speed was increased was possibly due to the rheological properties of the swollen gel-like material formed in each case. Aqueous mixed solutions of XG and LBG are associated with high elastic moduli (50). In the context of dissolution from matrices this means that the matrices are likely to have a high resistance to erosion, as compared to purely viscous materials, which are likely to be washed away more quickly by the dissolution medium (39).

The absence of a burst release from capsule matrices was attributed to the hydration and rheological properties of HP-based material. When the capsules were placed in the dissolution vessel the gelatin shell slowly began to dissolve, gradually exposing the granules to the dissolution medium. The granules hydrated rapidly and began to swell, the rapid hydration probably being facilitated by the high proportion of glucose in the formulation and by the hydrophilic nature of the XG component. Swelling ensured that initially well separated particles came into contact. XG/LBG solutions are viscoelastic, which means that when the molecules come together they coalesce (50). This is in contrast to predominantly elastic solutions, which do not coalesce (39). It is this property that probably resulted in coalescence of the swollen particles producing a continuous viscoelastic matrix, which filled the interstices, maintaining the integrity of the capsule matrix. The digital images presented in figures 5.7 and 5.8 show that although hydrated capsule matrices appeared to be more diffuse than hydrated tablet matrices, hydrated capsules did not disintegrate and maintained an intact body over the six-hour period that the matrices were imaged. The gelatin shell modified the release profiles by allowing the polymer to gel prior to dissolution of the gelatin. The gelatin shell also appeared to be responsible for imparting a cylindrical shape to the powder plug.

Mechanistically, two distinctive processes, namely swelling and true dissolution, generally occur during the overall dissolution of polymers (164). Drug release occurs by a combination of diffusion through the swollen gel and erosion of the matrix (6). The

independence of diclofenac sodium release rates on paddle speed indicated that the transfer of drug from the matrix into bulk solution due to dissolution of the actual matrix was less important than diffusion of the drug from the matrix. The fact that, for each formulation a large proportion of the dose was released while most of the matrix remained intact, also indicated that, under the test conditions employed, transfer of drug from the matrix was predominately a diffusion process. This observation is in agreement with that of Pharm and Lee (165) who found that the effect of HPMC dissolution on drug release was insignificant and the release kinetics were mostly regulated by a swelling-controlled diffusional process, particularly for higher viscosity grades of HMPC. Based on the findings described in chapter 4, where release from tablet matrices was found to be independent of initial matrix porosity, it is proposed that the propensity of the hydrated layer to erosion and the diffusitivity of drug in the hydrated layer was the same for both capsule and tablet matrices under the *in vitro* conditions evaluated. Therefore, the diffusional path length presented by both matrices must have been similar in order to account for the equivalent release profiles observed. This could be as a result of a similar degree of swelling by each matrix. Digital images of a hydrating caplet and capsule (figures 5.7 (a) to (h) and 5.8 (a) to (h)) show that both dosage forms swelled extensively and that capsules swelled to a slightly greater extent than tablets. For both capsules and tablets dimensional changes in length were more pronounced than changes in diameter, therefore both dosage forms maintained a cylindrical shape during hydration. After 5hr hydration the capsule matrix had swollen to approximately 104% of its original length while the tablet matrix had swollen to approximately 92% of its initial length. Although the dimensions of the swollen bodies were not identical at equivalent time points, it is possible that when the diffusion pathway caused by the tortuosity of the swollen gel-like material is long, then differences between the dimensions of the swollen material formed become negligible. This could account for the equivalent release profiles observed. Alternatively, it is possible that the slightly greater swelling observed in hydrated capsules matrices could be balanced by the looser porous network formed resulting in a overall diffusional path length similar to that of tablet matrices.

Although tablet and capsule dissolution profiles were equivalent for the model drug diclofenac sodium, propranolol HCl and diltiazem HCl, figure 5.9 shows that the dissolution of benzamide from capsule matrices was faster than from tablet matrices. The difference was more pronounced at the first time point, at subsequent time points the differences between the percentage released from each dosage form decreased. It is

possible that a slight burst release from these matrices became significant because of the overall low drug loading. Alternatively, for a low dose solute differences in the diffusion pathway presented by tablet and capsule dosage forms may become apparent. A third explanation for the differences may be related to the role played by the model drugs themselves in determining their own release rates. Examination of the release profiles for propranolol HCl (figure 5.4) and diltiazem HCl (figure 5.5) shows that after a period of time the rate of dissolution began to rapidly decrease. After 9hr dissolution only approximately 58% of propranolol HCl was released and after 11hr approximately 42% of diltiazem HCl was released. This suggested that some type of interaction, developing as hydration progressed, was taking place. The effect of drugs on the release controlling properties of hydrophilic matrices has been well documented and there are a number of ways in which drugs are known to interfere with dissolution rates. Interactions of drugs with polysaccharides can occur through adsorption of drugs to the excipients (166,167) and in some cases this has been shown to affect the dissolution of drugs from tablets (76,168). Adsorption is the preferential partitioning of a drug to a solid liquid interface as opposed to the bulk and probably occurs to some extent in all excipients. The primary mechanism of interaction is thought to be through weak Van der Waals' attraction forces (169). This is known to occur between the amine groups of drug molecules and anionic regions of microcrystalline cellulose (167,170). Since XG is anionic and XG, LBG and glucose have many hydroxyl groups, the potential for hydrogen bonding with positively charged regions of drug molecules is high, especially when the polymer is highly hydrated. Hydrogen bonds however are weak and are unlikely to account for the interactions observed here. It has been shown that cationic drugs can adsorb onto the surface of MCC by an ion-exchange mechanism, due to the negatively charged MCC surface (170) and it is thought that cationic drugs can form complexes with sodium carboxymethylcellulose, an anionic hydrophilic material (76,171). It is possible that some type of covalent binding occurred between HP-based matrices and the cationic drugs, diltiazem HCl and propranolol HCl. Physicochemical interactions between the model drugs, benzamide and diclofenac sodium, and the excipients may also have occurred to a lesser extent. Although interactions can adversely effect dissolution they may also play a part in maintaining the integrity of the network. It was observed that after diltiazem HCl matrices had been exposed to the dissolution medium for a number of hours a solid, opaque mass had formed. After 24hr dissolution, a large proportion of the mass remained, indicating that a body was produced that had a high resistance to erosion. The

presence of propranolol HCl in HPMC matrices has been shown to be important in maintaining the structure of the gel network (172). The presence of soluble solutes in the matrix can also affect the swelling and hydration of hydrophilic matrices (28). The presence of a very water-soluble drug has been shown to produce faster and more extensive swelling possibly due to osmotic effects (165). Talukdar and Ringet (28) found that the dissolution of caffeine from HPMC matrices was faster than the dissolution of indomethacin sodium despite indomethacin sodium being 10 times more soluble than caffeine. The results were attributed to the greater degree of swelling that occurred in the indomethacin sodium matrices, which emphasises the fact that swelling is a principle rate-limiting factor for drug release. In cellulose ethers, the presence of solute may lower the thermal gelation temperature, which can result in a higher than expected viscosity due to polymer-polymer interactions and can extend drug dissolution times (6,82). Since LBG/XG solutions do not exhibit the properties of thermal gelation (39) then the presence of strongly ionic drugs will not affect the gelation of the matrix in this way. High levels of strongly ionic salts can however, compete with for available water in the gel layer and cause polymer dehydration. This can cause precipitation of the gel, resulting in matrix failure and premature dissolution (6,87). This has not yet been reported for XG or HP matrices. The potential for interaction between drugs and HP-based materials has not been investigated extensively but this work shows that drug/excipient interactions should be taken into consideration when formulating these matrices.

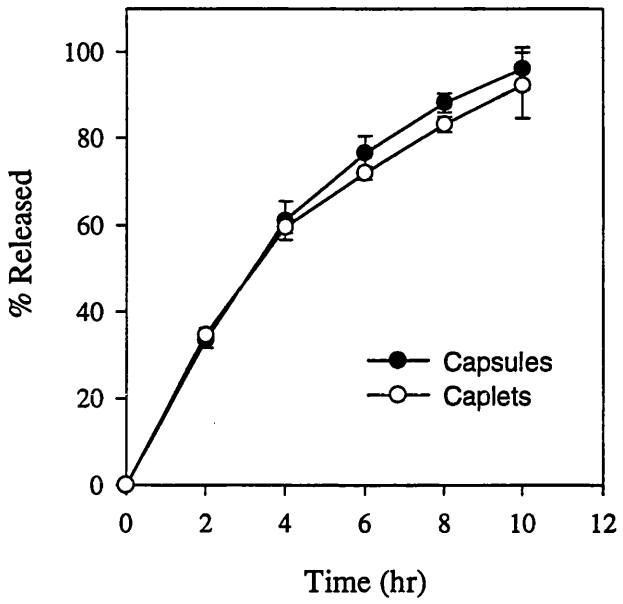

Figure 5.3 Dissolution of diclofenac sodium from capsule and tablet matrices containing the drug distributed intragranularly (paddle speed 50rpm, n=5)

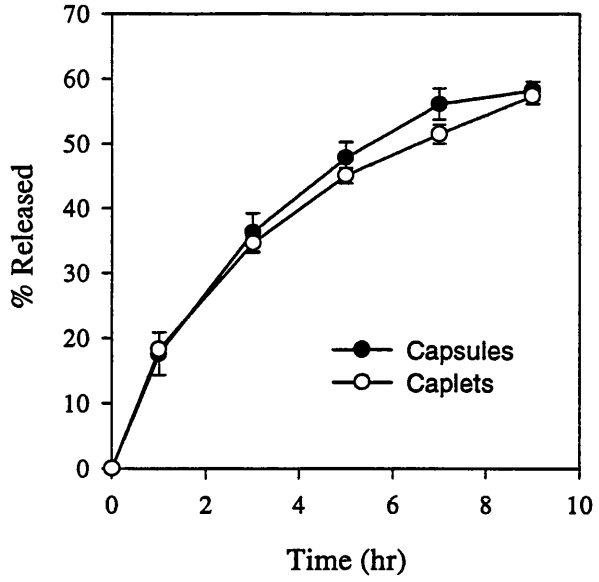

Figure 5.4 Dissolution of propranolol HCl from HP-based tablet and capsule matrices (paddle speed 50rpm, n=5)

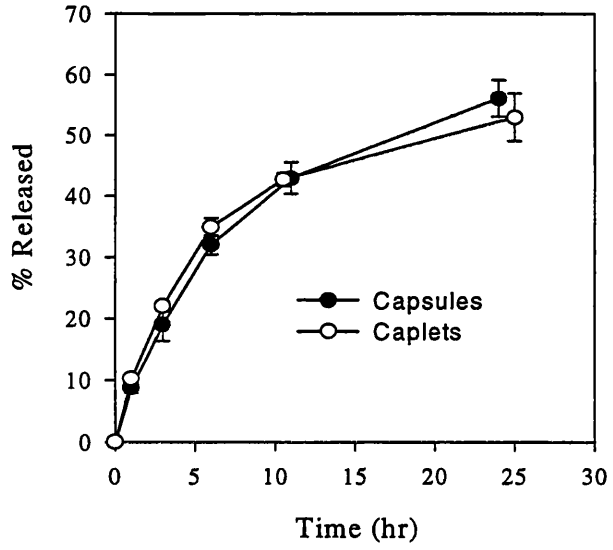

Figure 5.5 Dissolution of diltiazem HCl from HP-based tablet and capsule matrices (paddle speed 50rpm, n=5)

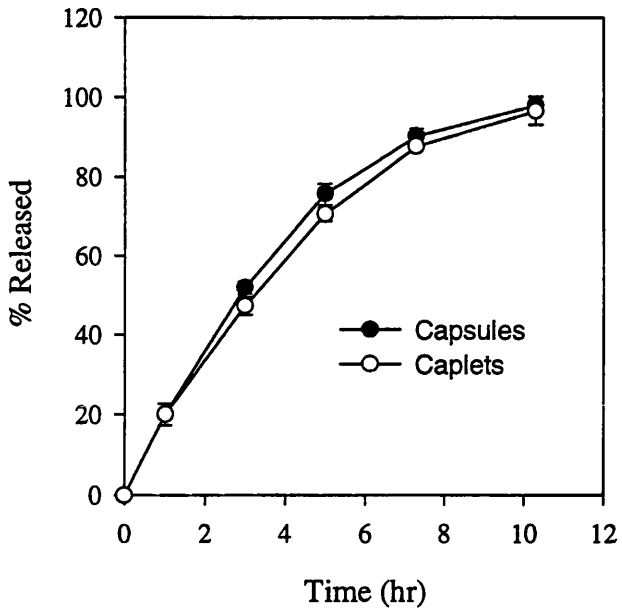

Figure 5.6 Dissolution of diclofenac sodium from HP-based matrices containing the drug distributed intragranularly
(paddle speed 100prm, n=5)

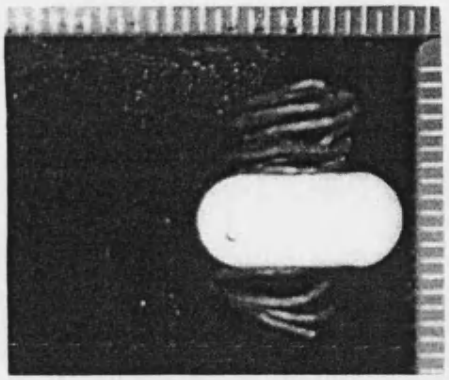

Figure 5.7 (a) t=0

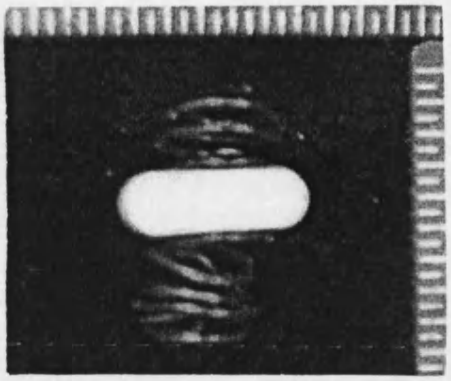

Figure 5.8 (a) t=0

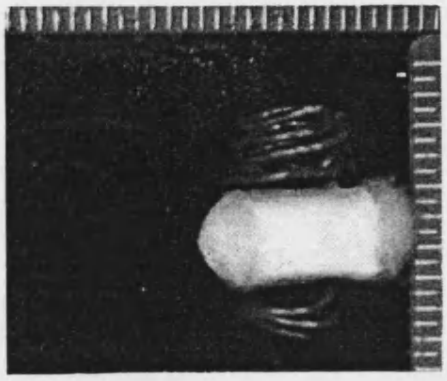

Figure 5.7 (b) t=10min

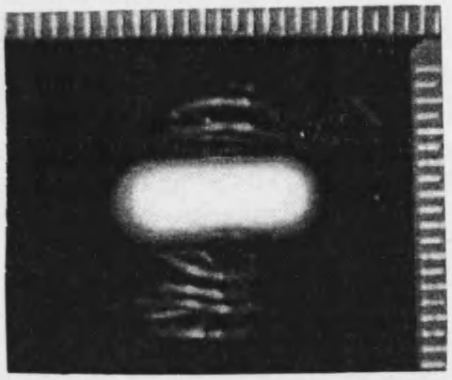

Figure 5.8 (b) t=10min

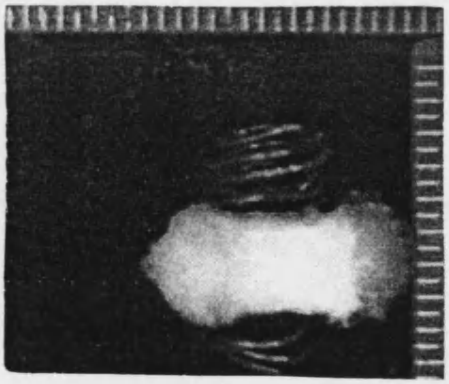

Figure 5.7 (c) t=30min

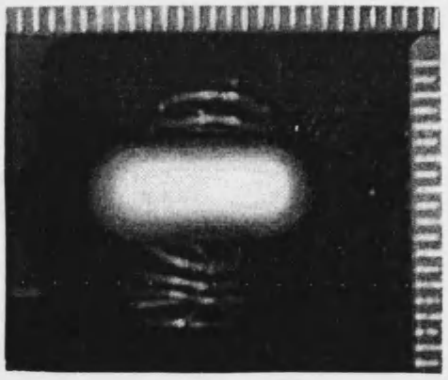

Figure 5.8 (c) t=30min

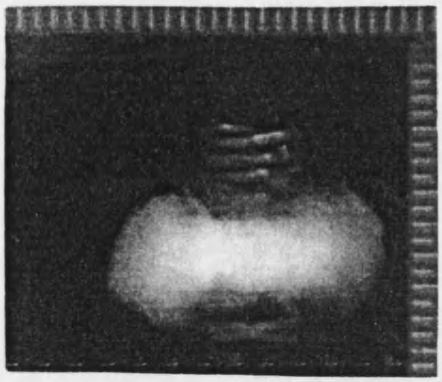

Figure 5.7 (d) t=1hr

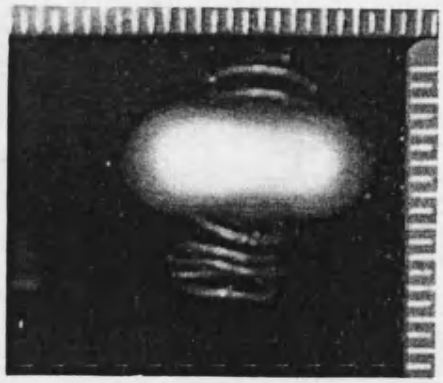

Figure 5.8 (d) t=1hr

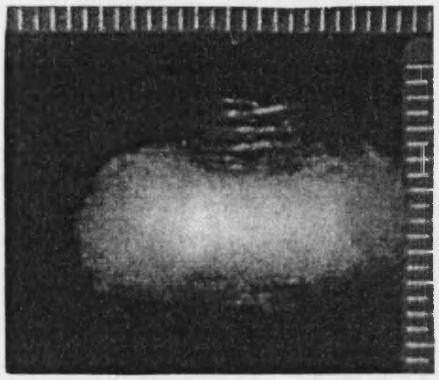

Figure 5.7 (e) t=2hr

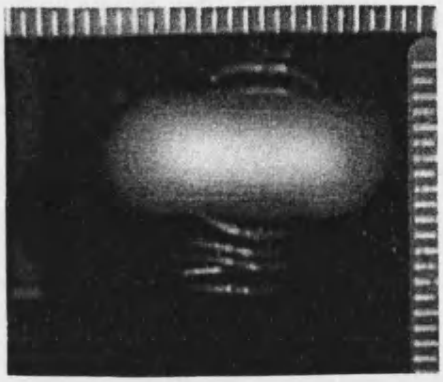

Figure 5.8 (e) t=2hr

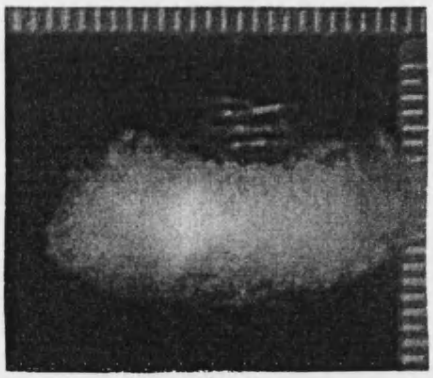

Figure 5.7 (f) t=3hr

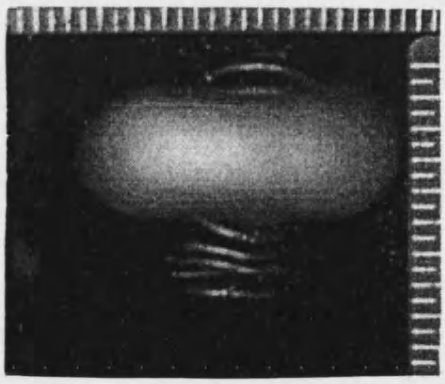

Figure 5.8 (f) t=3hr

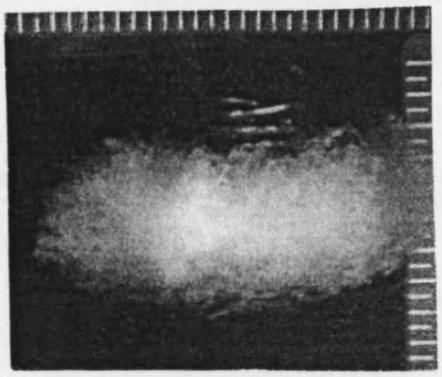

Figure 5.7 (g) t=4hr

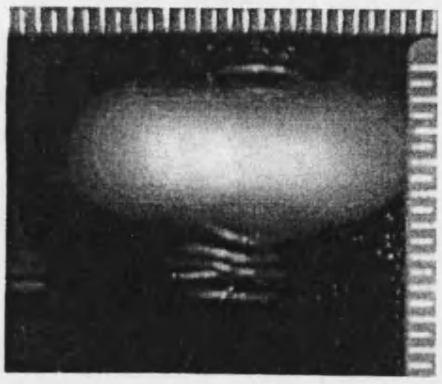

Figure 5.8 (g) t=4hr

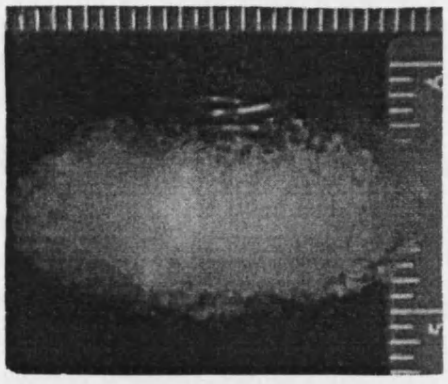

Figure 5.7 (h) t=5hr

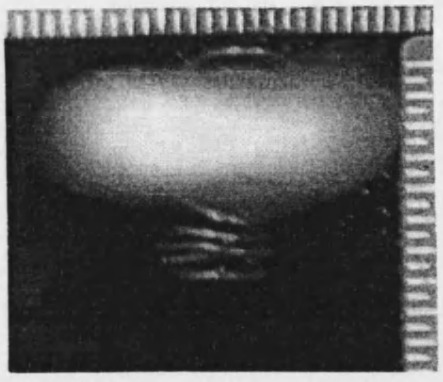

Figure 5.8 (h) t=5hr

Figure 5.7 (a) to (h) Digital images of of a hydrating capsule matrix

Figure 5.8 (a) to (h) Digital images of a hydrating tablet matrix

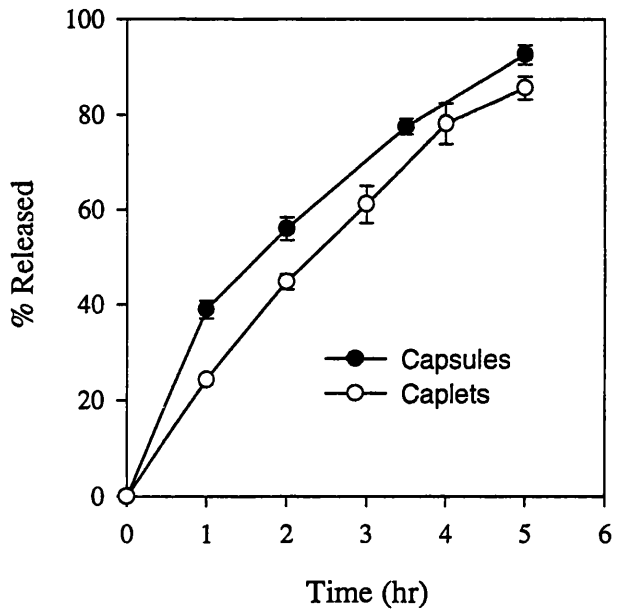

Figure 5.9 Dissolution of benzamide from HP-based tablet and capsule matrices (paddle speed 50rpm, n=5)

In order to produce HP-based compacts that have the strength required for pharmaceutical processing it is necessary to granulate the components using a high shear mixer (37). To determine whether high shear agglomeration of HP components was necessary to obtain material possessing high release retarding properties the dissolution of diclofenac sodium from matrix tablets prepared from a simple dry blend of HP-based components was examined. Figure 5.10 shows that no difference in release controlling action was observed between matrices that had been prepared by wet agglomeration and matrices that had been prepared by simply dry blending the three components. The synergistic reaction that occurs between XG and LBG may develop as the matrix hydrates and high shear agglomeration of the components may not be necessary to obtain a formulation with high release retarding ability. Although this observation was made for matrices containing diclofenac sodium, matrices containing model drugs other than diclofenac sodium may behave differently. Figure 5.10 also shows that, when the formulation contained diclofenac sodium distributed extragranularly, equivalent capsule and tablet release rates were still observed. This demonstrated the rapid rate of swelling in these matrices, which prevented drug near the surface of the tablet or capsule being released at an initially rapid rate.

Formulations containing diclofenac sodium distributed extragranularly contained HP-based material that had a median particle size of approximately 60μm while the formulation containing diclofenac sodium distributed intragranularly had a median particle size of 182μm. Both formulations were capable of sustaining the release of diclofenac sodium to the same degree for up to 10hr. This was interesting since Dhopeshwarker and Zatz (71) found that coarse sieve fractions of XG (74 to 177μm and 177 to 420μm) did not hydrate rapidly enough to sustain the release of acetominophen. In contrast, XG particles in the size range 40 to 70μm were found to sustain the release for more than 8hr. For HP-based formulations both coarse and fine particle sizes were found to provide sustained release of diclofenac sodium. This may be because of the presence of glucose in the formulation, which enhances wetting, thus ensuring that even coarser particles hydrate rapidly.

Simple monolithic swellable controlled release matrices are commonly associated with release rates that decrease with time, however, zero-order release kinetics have occasionally been reported (19). Release kinetics that approximated to zero-order for up to 70% drug release was observed from diclofenac sodium matrices that contained the drug incorporated extragranularly (r^2 ranged from 0.976 to 0.996) (figure 5.10). This was in contrast to release profiles from matrices that contained diclofenac sodium dispersed intragranularly, where time-dependent release was observed. In swellable matrix systems the most important rate-limiting parameters controlling linear release kinetics are polymer relaxation, gel erosion, polymer dissolution and the maintenance of gel layer thickness (5). The mechanism of drug release and factors influencing the release process from theses systems are complex, debatable and still in progress (5,173). Baveja *et al.* (19) have proposed that zero-order drug release will be observed when the swelling and erosion fronts become synchronised thereby maintaining a gel-like layer of constant thickness. Colombo *et al.* (17) suggested that when a diffusion layer exists the dissolved drug layer thickness is the reference element for drug release. The difference in release of diclofenac sodium from the formulation were the drug was dispersed intragranularly and from the formulation with the drug dispersed extragranularly were possibly due to a number of factors including; a change in drug solubility as a result of wet granulation; differences between the degree of drug/polymer interaction in each formulation; differences in the contribution of the drug to swelling and hydration in each formulation. Section 4.4.2 shows that the dissolution of benzamide from HP-based matrices followed zero-order kinetics. Although benzamide has a much higher aqueous solubility than diclofenac

sodium the difference in release kinetics can not be attributed to solubility alone (76), many other contributing factors are likely to determine the release kinetics.

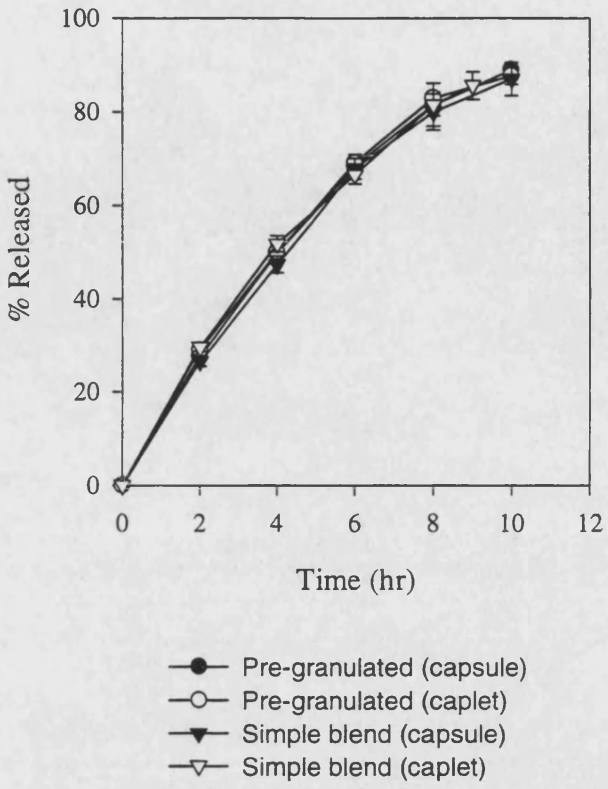

Figure 5.10 Dissolution of diclofenac sodium from a simple dry blended formulation and from a pre-granulated formulation presented in capsule and caplet form (paddle speed 50rpm, n=3)

One of the important characteristics of soluble hydrophilic matrices is the dependence of the release on hydrodynamic conditions. Ideally, formulations would show a lack of dependence on dissolution conditions, however, this is not always be the case. It has been suggested that the influence of stirring rate is negligible for releases according to the square root of time, that is where the release is diffusion controlled rather than erosion controlled (173). This is thought to be the situation in well hydrated, high viscosity polymers (173). It has been shown that for matrices containing low viscosity swellable materials, or matrices containing a low proportion of polymer, increasing hydrodynamic stress by raising the speed of revolution in a USP II paddle apparatus can increase dissolution rates as a result of accelerated polymer dissolution (27,156). Although no

difference in release of diclofenac sodium from HP-based matrices was observed when the paddle speed was increased to 100rpm, differences in dissolution might be observed using other methods of *in vitro* dissolution testing. It is possible that under conditions were a different type of stress is applied e.g., rotating basket method, then differences in release profiles between tablet and capsule dosage forms may be observed.

5.4.3 *Methocel K15M matrices*

Figure 5.11 shows the release of diclofenac sodium from tablet and capsule matrices prepared using Methocel K15M as a hydrophilic swellable matrix excipient. The grade of HPMC chosen was a high viscosity grade that has frequently been studied as a controlled release excipient (17,82,165) because of its high release retarding properties. The K grades are the fastest to hydrate among the HPMC family because the products have a lower amount of hydrophobic methoxyl substitution and a higher amount of the hydrophilic hydroxypropyl substitution (163). It can seen from figure 5.11 that equivalent release profiles from capsule and caplet matrices were observed when Methocel K15M was used as the rate controlling material. The release controlling ability of different grades of HPMC, including lower viscosity and less rapidly hydrating material, in capsule and tablet form would be further area of study. It is anticipated that equivalent release profiles might not be observed with HPMC grades and other hydrophilic swellable excipients that hydrate more slowly and which swell less extensively.

Figure 5.11 shows the release of diclofenac sodium from HP-based tablets and from Methocel K15M based tablets. These formulations were similar in excipient composition (see table 5.4), particle size and were prepared in a similar way. The HP-based formulation was found to release diclofenac sodium at a much slower rate than the Methocel K15M based formulation. After 7hr dissolution 95% of diclofenac sodium had been released from Methocel K15M based matrices, in comparison, 92% of drug was released from HP-based matrices after 10hr dissolution. It has been reported that the release retarding ability of XG is higher than HPMC (30,71). Some of the possible reasons for the differences were investigated by Talukdar and Kinget (29), who found that; (a) the diffusitivity of indomethacin, indomethacin sodium and caffeine was higher in hydrated gels of XG than in hydrated gels of HPMC; (b) the equilibrium moisture content of XG powder was higher than that of Methocel K4M when the two materials were stored under identical controlled humidity conditions. This suggested that XG was more

hydrophilic than HPMC; (c) the thickness of the outer layer of XG matrices was significantly higher than the thickness of the hydrated layer of a similar Methocel K4M matrix. It is possible that the differences observed between the release retarding properties of HMPC and HP-based matrices could be attributed to differences in hydrophilicity, extent of swelling and tortuosity of the swollen material. In combination, LBG, XG and glucose result in a material that has superior release controlling characteristics.

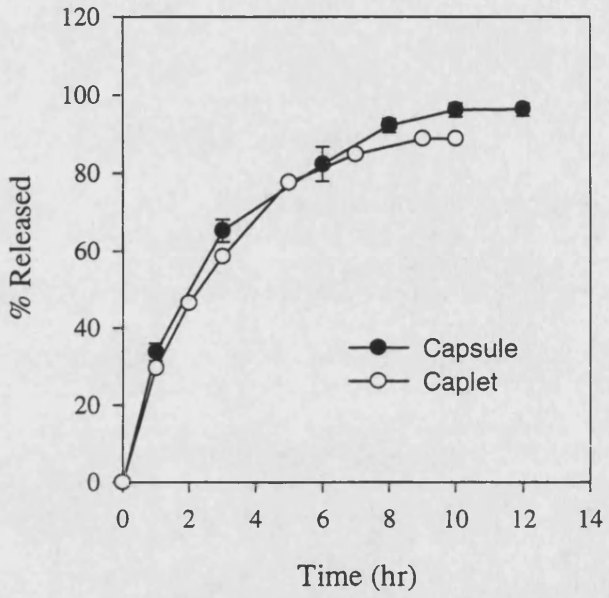

Figure 5.11 Dissolution of diclofenac sodium from Methocel K15M capsule and tablet matrices (paddle speed 50rpm, n=5)

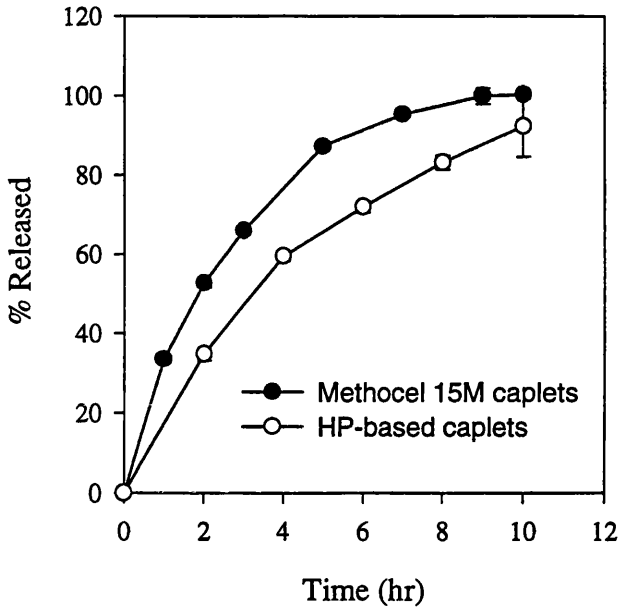

Figure 5.12 Dissolution of diclofenac sodium from Methocel K15M and HP-based tablet matrices (paddles speed 50rpm, n=5)

HPMC formulation	HP-based formulation
50% Methocel K15M	50% HP
45% glucose	45% glucose
5% diclofenac sodium	5% diclofenac sodium

Table 5.6 Formulation of Methocel K15M and HP-based diclofenac sodium matrices

5.4.4 *Mechanical strength of hydrated capsule and tablet matrices*

The outer layer of hydrated polymer matrices controls drug release by determining diffusion and erosion rates. To some extent drug release must be controlled by the physical and mechanical properties of this layer. The mechanical strength of the gelatinous layer surrounding hydrophilic matrices is not routinely investigated in the formulation of swellable matrices, the viscosity of the gelatinous layer being more commonly used to characterise release-controlling properties. A measure of mechanical strength was obtained by measuring the force required to move a probe into the hydrated

layer. Figure 5.13 shows the mechanical strength of swollen HP-based capsule and caplet matrices as a function of time. After 1 and 2 hr of swelling the gel-like material formed from the caplets had a much higher mechanical strength than the swollen body formed from the capsule matrices. At the subsequent time points the mechanical strength of the swollen material was similar in each case. This method of determining hydrated layer strength clearly differentiated between the two dosage forms. Although the propensity of the gels to true dissolution is certainly linked to the rheological properties of the materials it does not appear, at least in this instance, that the mechanical strength of the hydrated layer can be correlated to dissolution behaviour. Figures 5.14 and 5.15 show the penetrating force displacement curves for HP-based tablets and capsule matrices, respectively. The almost linear relationship between force and distance observed for both dosage forms was possibly due to the viscoelastic nature of the materials. As the probe penetrated the matrix the material flowed, like a viscous solution, around the indented probe. The absence of a sharp increase in force as the probe penetrated the core of the dosage form reflected the visual observation that the core had almost reached its glassy state after 1hr hydration.

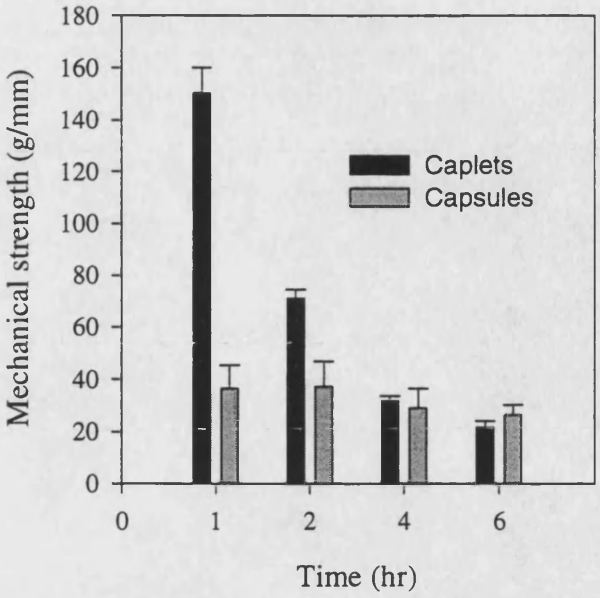

Figure 5.13 Mechanical strength of hyrated capsule and tablet matrices over a 6hr period

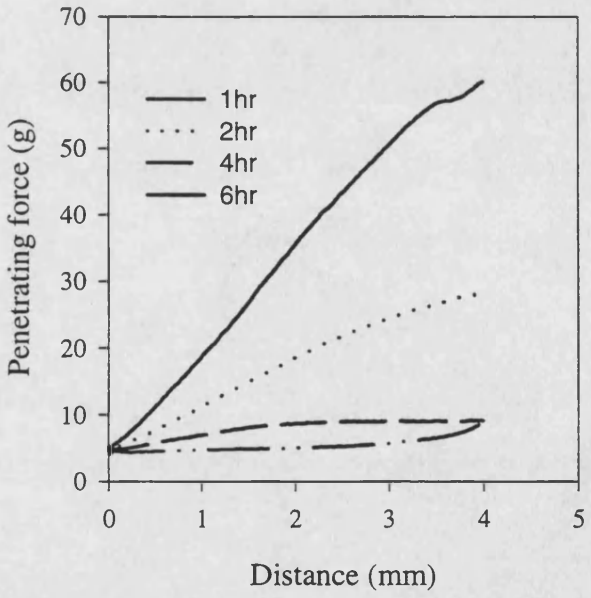

Figure 5.14 Penetrating force vs displacements curves for caplet matrices

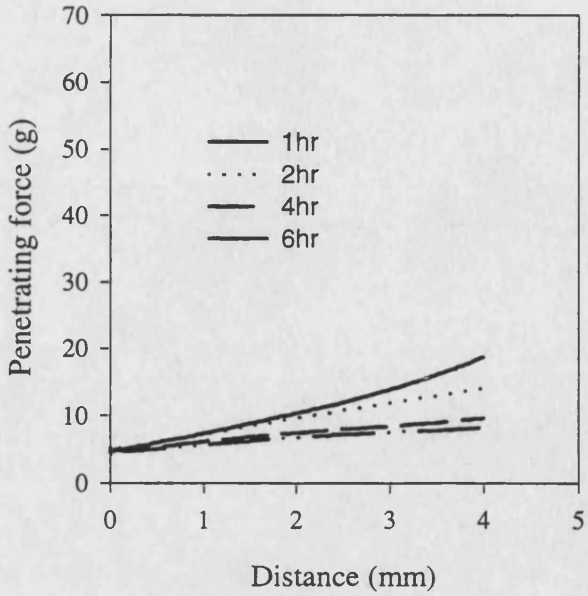

Figure 5.15 Penetrating force vs displacement curves for capsule matrices

5.5 Conclusion

Capsule and tablet matrices based on HP were found to control the *in vitro* release of three model drugs at equivalent rates. The findings of this study were of relevance to a concept of dosage form interchangeability proposed by the standards development division of the USP Pharmacoepia. The standards division deals with maintaining existing standards and introducing new standards and proposed revisions are published for public review and comment in the pharmaceutical form (PF). Proposals that are believed to be of most interest to health care practitioners are abstracted from PF and published as a newsletter 'standard issues for the health care practitioner'. In the January-February 1997 issue (174), the dissolution and bioavailability subcommittee of the standards division discussed the concept of functional interchangeability of solid oral dosage forms. The committee recommended that USP general notices and requirements include the following statement; 'Unless otherwise stated in the individual monograph, tablets and capsules prepared with the same active substance and of the same release rate classification (e.g. prompt release) are considered to be functionally interchangeable'.

This would mean that any specific USP solid oral dosage form could be dispensed regardless of whether it is formulated as a tablet or a capsule as long as three criteria are met:

(a) the articles contain the same active ingredient
(b) the articles contain the same amount of active ingredient
(c) the release characteristics are the same.

The practical implication of functionally interchangeability means that a practitioner could prescribe a medication in either capsule or tablet forms, depending on the patients needs and/or desires, as long as the two preparations contained the same drug in the same quantity and had equivalent release profiles. However, there would be no requirement for the tablets and capsules to contain the same excipients or for the formulations to be processed in the same way. Functional interchangeability could for example, exist between a hydrophilic matrix tablet and a capsule containing the drug formulated as controlled release pellets, even if the formulations contained different excipients and were processed in different ways. Since tablet and capsule matrices based on HP contained the same active ingredient, in the same quantity and had equivalent release profiles they could be considered functionally interchangeability. Additionally since they contained they same formulation, processed in the same way they could also be considered as pharmaceutically equivalent. Functionally interchangeability coupled with pharmaceutical equivalence is a concept that has not been reported until now.

6. Investigation of the gastro intestinal transit of a placebo heterodisperse polysaccharide-based formulation in capsule and tablet form using gamma scintigraphy

6.1 Introduction

HP-based capsule and tablet matrices were found to have equivalent release controlling action under the *in vitro* dissolution conditions employed. However, it could not be concluded on the basis of this that the dosage forms would be bioequivalent. In order to determine the bioavailability of solid oral dosage forms it is essential that experiments are carried out *in vivo*. The ultimate test of an oral dosage form is the pharmacokinetics of drug release. However, by studying the transit of a dosage form in the gastrointestinal tract (GIT) an indication of the likelihood of the dosage form meeting *in vivo* pharmacokinetic objectives may be obtained (105). Scintigraphic imaging of radiolabelled controlled release dosage forms provides a non-invasive method of studying their GI transit.

The primary aim of the gamma scintigraphy study was to assess the degree to which HP-based capsule and tablet matrices maintained their integrity as they passed down the GIT. This was difficult to predict from *in vitro* studies because of two main reasons. Firstly, the physicochemical characteristics of the GIT were likely to differ substantially from the conditions that the dosage forms were exposed to during *in vitro* dissolution tests. Physiological conditions in the GIT such as hydrodynamic flow and mechanical destructive forces that arise from digestive actions (grinding and crushing of GI contents) are difficult to predict and are reported to be highly variable (103). GI hydrodynamic flow around dosage forms is thought to be slow (103) and, based on dissolution studies, it was concluded that the erosion and fragmentation of tablets and capsules was unlikely to be highly sensitive to the hydrodynamic flow conditions in the GIT. However, destructive forces were likely to be important in determining the degree to which capsule and tablet dosage forms maintained their integrity. The presence of food in the GI tract stimulates more intense mechanical agitation than exists in the fasted state. In order to present the greatest challenge to dosage forms studies may be carried out in the fed state since greater destruction of dosage forms has been found to occur in the fed state as compared to the fasted state (177). Secondly, it was difficult to predict how the pH conditions and ionic strength of the contents of the GIT would affect

hydration and swelling of the matrices. Little is known about the effect of pH and ionic strength on hydration and swelling of HP-based matrices. Xanthan gum (XG) matrices are often regarded as being compatible with a wide range of salts, acids and bases (39,175) and the release of drugs from XG matrices has been found to be insensitive to changes in pH. Lu *et al.* (175) found that pH had no effect on theophylline release from a xanthan gum matrix in both 0.1N HCl and pH 6.8 phosphate buffer. The release of caffeine, a model whose solubility is independent of pH, was found to be similar in a range of phosphate buffers with pH between 5.8 and 7.4 (156). However, the rate of release was found to increase, as the ionic strength of the dissolution medium was increased (156). The presence of salts appeared to decrease the initial rate of hydration but once the tablet had hydrated the release rate in each solution was similar. Although dissolution studies under a range of pH conditions and ionic strengths may be of value in estimating the influence of these factors on the hydration and swelling of HP-based matrices it is possible that sensitivities observed *in vitro* could be of limited importance *in vivo* (60,104). This could be due to the transient characteristics of conditions in the GIT (60).

Since HP-based capsules and tablet dosage forms had initially different physical characteristics it was considered that this could result in differences between the GI transit of both dosage forms. Capsules had a lower bulk density than tablets, which could possibly affect the location of the dosage forms within the GIT. In a study comparing the GI transit of capsule formulations it was found that capsules with lower density remained in the fundus of the stomach whereas denser capsules sedimented to the more distal regions (179). However, capsule density has been shown to have only a minor effect on GI transit time (179). The presence of a gelatin shell could possibly influence the GI transit of capsule dosage forms. When tablets or capsules are swallowed they may adhere to the oesophageal membrane thus delaying oesophageal transit (178). It has been shown that capsules are less likely to stick than tablets, and that the quantity of water taken with the dosage form can affect the passage of tablets but not of capsules (178). Differences between the bioadhesive nature of each dosage form could also affect GI transit. Although XG is not thought to have bioadhesive properties (100), the effect of a gelatin shell on bioadhesion is not known. The effect of bioadhesion is however, likely to be of limited importance as it has been shown that the gastric emptying of some potentially adhesive formulations did not differ greatly from that of control materials (176).

The degree of destruction that capsules and tablets under go in the GIT is important since it is proposed that equivalent release profiles were observed *in vitro* because of similar diffusional path lengths existing within each swollen dosage form. Greater destruction of either dosage form presentation could increase the dissolution rate of a drug from the matrix by reduction of the diffusional path length. This is important since it is known that the bioavailability of many drugs is highly dependent on the rate of dissolution of the drug from the dosage form (182). From gamma scintigraphy studies the GI transit time of dosage forms and their position in the GIT may also be estimated. GI transit time and location is also important in relation to bioavailability since the absorption, and possibly the release, of drug from a controlled release formulation may depend in part on the location of the system within the GI tract (176) and/or GI transit time (176).

Gamma scintigraphy studies on hydrophilic matrix preparations have previously been carried out. Daly *et al.* (180) found good correlation between the *in vitro* and *in vivo* release of a non-absorbable water-soluble chelate labelled with technetium from HPMC matrices. Abrahamsson *et al.* (181) found that erosion of HM's based on HPMC in the stomach and small intestine was similar to the erosion measured *in vitro* using a USP dissolution apparatus II with paddles rotating at 50rpm. The use of Gamma scintigraphy to compare and evaluate the integrity and fate of pharmaceutically equivalent hydrophilic capsule and tablets matrices in man, has not previously been reported.

6.2 Materials

TIMERxE (Lot No. NS1101), a formulation containing 25% xanthan gum, 25% locust bean gum and 50% glucose was provided by Penwest Pharmaceutical Co. The material received was of a suitable quality for clinical use. Hard gelatin capsules, DAVCAPS DB size A, Swedish orange, were obtained from Capsugel, Bornem, Belgium. The capsules were of a suitable quality for clinical use. Diclofenac sodium (Lot No. 94-01342) was obtained from Heumann Pharma GmbH (Nurenberg, Germany). The resin used for the *in vitro* and *in vivo* study was Amberlite CG120, 100 to 200 mesh (Lot No. 344984/1), which was obtained from Fluka Chemika (Italy).

6.3 Method

The integrity and fate of a placebo HP-based formulation presented in tablet and capsule form was evaluated in six healthy male volunteers using the non-invasive technique of gamma scintigraphy. The study was carried out in two parts and involved radio-labelling the tablets (first part) and capsules (second part) with (1MBq) ^{111}In bound to amberlite resin, which was then swallowed by the volunteers. Using a gamma camera, placed in front of the volunteer, the position of the dosage forms in the GIT was ascertained. Prior to the Gamma scintigraphy, dissolution tests were carried out on tablets and capsules prepared from blend of TIMERxE, diclofenac sodium and amberlite resin. This was to establish if equivalent release profiles from tablets and capsules were observed in the presence of amberlite resin.

6.3.1 *In vitro validation*

7.5% diclofenac sodium was blended with 92.5% TIMERxE by geometric trituration (blend 1). Total batch size was 100g. 0.77% amberlite resin was incorporated into a proportion of the TIMERxE/diclofenac sodium blend by geometric trituration (blend 2). Each blend was filled into hard gelatin capsules giving a mean fill weight of 529 ± 5mg (n=4, blend 1) and 526 ± 7mg (n=3, blend 2). Each blend was also compacted into 5 × 16mm caplet shaped tablets using a single punch tablet press (Type F3, Manesty, Speke, Liverpool, U.K.) with a strain gauge fitted to the top punch. Compaction force was approximately 15kN, mean tablet weight was 522 ± 14mg (n=3, blend 1) and 525 ± 11mg (n=3, blend 2). Dissolution studies were carried out in 1000ml of distilled water heated to 37°C ± 0.2°C using a USP II dissolution apparatus (Type 8ST, GB Calerva Ltd., Dorset, U.K.) with paddles positioned 4cm above the point of curvature at the bottom of the vessel. Paddle speed was 50rpm. The dosage forms to be analysed were supported in stainless steel wire cages (approximately 3.5cm × 2.5cm), which allowed dissolution from all surfaces. Samples of dissolution medium (7.5ml) were manually removed at predetermined intervals and filtered through 1μm cellulose nitrate filters. UV absorbance at 274nm was determined using a diode array spectrophotometer (Type 8452A, Hewlett Packard, Palo Alto, CA). 7.5ml of distilled water, heated to approximately 37°C, was added after sampling to maintain constant volume. The absorbance of a solution of TIMERxE (500mg/l) was found to amount to 4% of total absorbance after 100% dissolution.

6.3.2.1 *Preparation of radiolabelled tablets*

100mg of amberlite resin CG-120 was weighed into a 10ml glass vial. The resin was washed 3 times with distilled water. As much water as possible was removed after washing using a Pasteur pipette. 0.3ml of an acidic solution of indium chloride (In^{111} Mallinckrodt Medical B.V., Petten, Holland), having an activity of 111MBq, was added to the resin, mixed and incubated at room temperature for 15min. The resin was washed twice with distilled water to remove excess radioactivity. Excess water was removed using a Pasteur pipette. Before the dosage forms were prepared the resin was dried in an oven at 65°C for approximately 45min then ground in a pestle and mortar. TIMERxE was blended with approximately 1% w/w radiolabelled resin using a pestle and mortar. Tablet and capsule dosage forms were prepared using the procedure described in section 6.3.1. The radioactivity of tablets and capsules was measured (CompuGamma CS, Turku, Finland) to ensure that each dosage form contained approximately 1 MBq of activity at the time of administration.

6.3.2.2 *Study protocol*

The study was approved by the Liverpool John Moores University Ethics Committee, the Liverpool Research Ethics Committee (Liverpool Royal University Hospital) and the DoH Administration of Radioactive Substances Advisory Committee (ARSAC). The gamma camera, accessories and computers used were tested and validated by the Nuclear Medicine Department of the Royal Liverpool University Hospital prior to use.

The study was a two-way, cross-over study with a wash out period of 14 days. The weight, height and year of birth of the 6 healthy male volunteers are detailed in table 6.1. Subject inclusion and exclusion criteria are detailed in appendix IV. The volunteers underwent a medical check up at the Medical Centre, JMU, Byrom Street for general health, and blood and urine samples were tested for absence of drugs of abuse. The use of tobacco, alcohol, prescription and over-the-counter drugs were not permitted 48hr prior to or during the study.

The volunteers abstained from food and fluids after 2200hr on the day before the study. The dosage form was swallowed followed by 150ml of cool water. Gamma scintigraphy images were acquired using a Siemens Gamma Camera (Model 750). Both

anterior and posterior images were recorded each over 180s. The position and movement of the dosage forms were noted using the Digital Operator Terminal (DOT) (Model 3219), which gave a real time image of the dosage forms on screen. The behaviour of the dosage forms was demonstrated and recorded by the presence and release of ^{111}In. Before anterior imaging began an external anatomical marker (consisting of a tablet or a capsule, depending on the study, containing 1MBq In-111, in a 2ml syringe) was held 2 fingers above the sternum notch for about 15s. The marker was then removed without volunteers' movement and imaging was continued for the 180s duration. After the last image, the camera was set up to record a dual isotope image in the energy levels suitable for In-111 and also Tc-99m. The volunteers were then given 150ml of orange juice containing 3MBq Tc-99m and a scan was carried out, which established the position of the stomach. The first image (0min) was recorded 30s after ingestion of the dosage form. Subsequent images were recorded at 30min intervals for 7hr. A light breakfast was consumed after the 90min image along with tea or coffee. Lunch was consumed after the 270min image. After lunch there was no restriction on water uptake (water, juice or pop).

The qualitative image processing was carried out using ICON, a computer package developed by Siemens. Each acquired image was processed sequentially from time 0 to 420min by displaying them and drawing the outline of the stomach (from the Tc-99m image) and also taking into account the position of the external marker. Both anterior and posterior images were examined. The location of the radioactivity on the image was recorded and comments were make on the appearance of the source. The number of sources, if more than one, and the presence of traces of activity around the main source or in the vicinity of the source were related to the break down of the matrix and erosion of the outer layer of gel structure of the matrix, respectively. The movement of each source was separately noted from the DOT, real time images.

Volunteer No.	Year of birth	Weight (Kg)	Height (cm)
1	1976	76	182
2	1975	75	184
3	1977	62	164
4	1970	65	173
5	1968	75	180
6	1953	80	175

Table 6.1 Year of birth, weight and height of volunteers

6.4 Results and discussion

6.4.1 *In vitro dissolution profiles*

Figures 6.1 and 6.2 show that similar release profiles of diclofenac sodium from TIMERxE based capsule and tablet matrices were observed in formulations prepared without amberlite resin and with amberlite resin, respectively. Statistical analysis using Student's t-test showed that there was no significant difference between the mean percentages released from tablet and capsule matrices at each time point. It was concluded that the presence of Amberlite resin was unlikely to cause differences between the GI transit of placebo TIMERxE dosage forms.

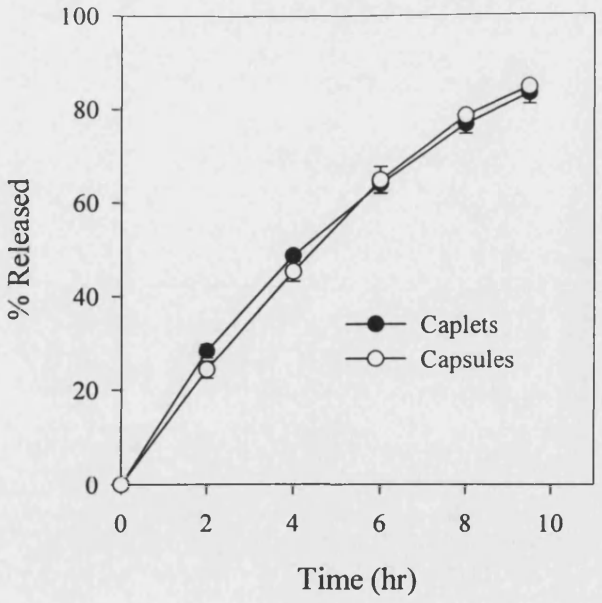

Figure 6.1 Dissolution of diclofenac sodium from TIMERxE caplet and capsule matrices (n=3)

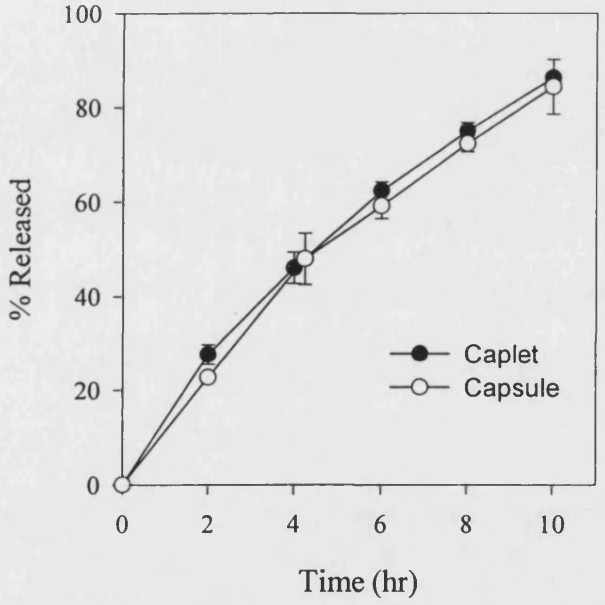

Figure 6.2 Dissolution of diclofenac sodium from TIMERxE capsule and caplet matrices containing amberlite resin (n=3)

6.4.2 *Qualitative evaluation of gamma scintigraphy images*

A qualitative description of the size, location, number of centres of activity observed and degree of dispersion of radioactivity in each image is given in appendix V. A summary of the 6 observations made on capsules and tablets is given in tables 6.2 and 6.3, respectively. Anterior images of the capsule and tablet administered to volunteer number 4, taken at time points 0, 30, 90, 180 and 390min are shown in appendix V.

The images taken 30s after ingestion of the dosage forms showed that both capsules and tablets remained intact after swallowing in all cases. In the majority of volunteers both dosage forms passed through the stomach within 30min, entering into the duodenum and small intestine. The images taken at 30min showed that the dosage forms had started to swell, indicating that rapid hydration of both capsules and tablets occurred in the GIT. This can be seen in the images presented in appendix V, were a central source is visible with some diffused activity around the perimeter of the source. It was noted that in all cases capsule matrices located at the upper part of the stomach compared to tablets, which settled in the lower part of the stomach. This is probably due to the lower bulk density of capsule matrices, which causes them to 'float' on the stomach contents. This confirms the findings of Muller-Lissner and Blum (179) who found that denser dosage forms sedimented to the more distal regions of the stomach while less dense dosage forms remained in the fundus of the stomach. Hydrodynamically balanced systems (HBS) are designed to 'float' in the stomach thereby increasing stomach residence time. It was observed here that the positioning of HP-based capsules did not increase stomach residence time relative to tablets and therefore HP-based capsule matrices are unlikely to be useful as HBS's.

Images taken of dosage forms in the SI and in the colon, showed that at a number of time points the radioactivity was concentrated at more than one position, indicating that the dosage forms had separated into two or more fragments. The time at which the presence of more than one source was first noted was identified in each case and the mean time of fragmentation was calculated for tablets and capsules (table 6.4). It can be seen that capsules tended to separate into two or more fragments earlier than tablets, with capsules fragmenting approximately 75min after ingestion and tablets fragmenting approximately 190min after ingestion. The 90min image of the capsule in volunteer 4 (appendix V) shows that the capsule separated into a smaller fragment and a larger fragment. However, in the 180min and 360min images the radiation appeared as a single

source because the fragments regrouped at the ileocaecal junction after 150min (not shown). Regrouping of fragments at the ICJ and at other areas of the GIT could be due to the high viscoelasticity of HP-based components, which may promote coalescence of separated fragments. The images of the tablet administered to volunteer 4 show that at 120min the tablet was observed as a large L-shaped source (not shown), which did not separate. Instead, fragmentation of the tablet occurred at 270min (not shown) but after 300min a single source was visible due to regrouping of the fragments. Fragmentation of capsules and tablets was noted in all volunteers at various positions along the SI and colon. The earlier fragmentation of capsule matrices could be related to the lower mechanical strength of these matrices and/or the effect of the gelatin shell. It had been found that after 1hr hydration at 37°C the force required to move a steel probe through a hydrated tablet was greater than 3 times the force required to move the probe through a hydrated capsule (see section 5.4.4). Digital images of hydrated matrices taken over a 5hr period (Chapter 5, figures 5.7(a) to (h) and 5.8(a) to (h)) showed that capsule matrices formed a looser gel structure than tablet matrices when the dosage forms were allowed to swell without restriction. The more diffuse structure formed in capsule matrices was presumably due to the initial high porosity of these matrices.

Table 6.2 Qualitative assessment of the *in vivo* behaviour of HP-based capsule matrices, summary of 6 observations

Time (min)	Stomach	Small intestine	Ileocaecal junction	Colon
0	Observed, Intact			
30		Swollen single unit		
60		2 fragments, moving		
90		1-2 fragments with dispersion*		
120		1-2 fragments with dispersion and residues**		
150		1-4 fragments with diffusion and erosion		
180		1-2 fragments, residues and erosion, collecting at ICJ		
210		Regrouping, generally appears as single unit, residues at ICJ		
240		Spreading, erosion and residues		
270			Mainly ICJ, ascending & transverse colon	
300			Mostly in colon, dispersion and residues	
330			Fragments still visible	
360			Mostly lower ascending colon	
390			More than 1 source, erosion and residues	
420			As above	

* Dispersion is evidence of erosion of the outer gel layer of the matrices

** Residues form a back track of activity. This can be adhesion or remains of eroded polymer

Table 6.3 Qualitative assessment of the *in vivo* behaviour of HP-based tablet matrices, summary of 6 observations

Time (min)	Stomach	Small intestine	Ileocaecal junction	Colon
0	Observed, intact			
30	Single unit, swollen			
60		Single fragments with swelling		
90		Mainly single unit with erosion		
120		Swollen, some intact, some with residues**. Mainly SI		
150		Mainly SI. 1-2 fragments, dispersion*		
180		Swollen, dispersing. Mainly SI		
210		1-3 fragments with diffusion		
240		1-2 fragments with diffusion		
270			1-2 fragments with diffusion	
300				Mainly colon, diffuse fragments
330				Mainly ascending colon, 1-2 sources with dispersion
360				As above
390				As above, more dispersion
420				Central source still visible, more dispersion

* Residues form a back track of activity. This can be adhesion or remains of eroded polymer
** Dispersion is evidence of erosion of the outer gel layer of the matrices

The mechanical stresses in the GIT could result in greater destruction of weaker gel structures and this may account for the earlier fragmentation of capsules. It was noted that capsules initially tended to separate into 2 fragments. This phenomenon may be partly due to the presence of a gelatin shell. The digital images of a hydrated capsule (figure 5.7 (a) to (h)) show that the gelatin shell dissolved firstly from either end of the capsule. At either end the capsule shell was one layer thick while in part of the centre two gelatin layers enclosed the granules. This meant that the gelatin shell at the centre dissolved more slowly and restricted swelling at the centre when swelling at both ends was unrestricted, resulting in the formation of a dumbbell structure. Figure 5.7 (d) shows the presence of the gelatin shell at the centre of the capsule after 1hr hydration and the more swollen material at the ends. The dumbbell structure was more prominent after 1hr hydration and this corresponded approximately to the time at which fragmentation was first noted in the GIT. It is possible that an area of low mechanical strength occurred between the well hydrated swollen material at the ends of the capsule and the less hydrated, less swollen material within the partly dissolved gelatin shell. This may have promoted separation of the ends of the capsule from the main body and may also explain why at later time points capsules tended to separate into 1-3 fragments while tablets separated into two fragments.

	Time to fragmentation (min)
Tablets	190 ± 77
Capsules	75 ± 37

Table 6.4 Time at which fragmentation of the dosage forms was first noted (n=6)

Images taken of the dosage forms in the small intestine, and later the colon, show dispersed activity around the main bulk of activity in both capsule and tablet matrices. This is evidence slow erosion of the outer layer of the matrices. As the hydrated polymer matrix swells and erodes, In-111 is carried away from the main source and this is observed as dispersed radioactivity. Residues of activity behind the main source were also noted in both dosage forms. These were likely to be the remains of eroded material left behind as the main fragments moved along the GIT. Alternatively, this may have

been material that had adhered to the mucosal lining. Without qualitative analysis of the images it is difficult to accurately estimate the degree of dispersion and diffusion around capsules and tablets matrices. Generally it appears that the degree of spreading and erosion was higher in the capsule matrices. In the images taken from volunteer 4 (appendix V) it can be seen that the area of the main source was greater in the capsule matrix as compared to the tablet matrix. The images, which are of the same magnification, show that the length of the main source of the capsule matrix at 180 and 390min was greater than that of the tablet matrix. Additionally, the radial spread of the swollen capsule was slightly greater than that of the tablets. The fact that the initial diameter of dry capsules was larger than that of tablets probably accounted in part for the differences in swollen diameter observed. The digital images of hydrated matrices (figures 5.7 (a) to (h) and figures 5.8 (a) to (h)) show that under *in vitro* testing conditions, where unrestricted swelling could occur, the length of swollen capsule matrices was greater than that of tablets at each time point. Similarly, the radial diameter of swollen capsules was greater than that of swollen tablets under *in vitro* conditions. This is important because although capsule matrices swelled more than tablets *in vitro,* equivalent release profiles were still observed. It was proposed that this was because (a) small differences in the degree of swelling between capsules and tablets became negligible when the overall tortuosity of the matrices was very large or (b) the looser porous network formed in capsule matrices compensated for the higher degree of swelling in these matrices causing the overall diffusional path length to be similar. It is therefore possible that capsule matrices and tablet matrices may have similar release controlling action in the GIT despite capsules spreading more than tablets. However, differences in the time and extent of fragmentation between capsule and tablets may largely affect dissolution because fragmentation will substantially decrease the diffusional path length and therefore increase dissolution.

Gamma scintigraphy images taken of the dosage forms in the lower part of the SI, the ascending and transverse colon, showed that both tablets and capsules maintained a degree of integrity through out GI transit. The 390min of the capsule administered to volunteer No.4 (appendix V) shows that the cylindrical shape of the capsule was still well defined. It was clear that coalescence of hydrated granules had occurred producing a continuous matrix that maintained the shape of the capsule in which the granules were initially contained. The image showed diffused radiation and residues that were left behind as the dosage form moved up the ascending colon. The final images, taken

420min after ingestion, showed that in all cases were a tablet had been administered a main source was still visible. When a capsule had been administered, a single source was still visible in 5 cases. The images in appendix V show that after 390min in the GIT the cylindrical shape of the capsule dosage form in volunteer no. 4 was still clearly visible and a concentrated source of radioactivity could be seen. Although capsules tended to fragment earlier than tablets the dosage forms appeared to undergo more similar degrees of fragmentation further down the GIT. This could be because the mechanical stresses further along the GI tract were less aggressive. Alternatively, the observations could again be related to the mechanical strength of the matrices. It had been found that the mechanical strength of hydrated matrices became more similar as hydration progressed (section 5.4.4). After 2 hours, hydrated capsules had half the mechanical strength of tablet matrices, while after 3 and 4 hours hydration the strength of both matrices was similar. It is possible that the propensity of the dosage forms to destruction was similar after a number of hour's hydration since the mechanical strengths were similar. Additionally, it had been found that after 2hr hydration the gelatin shell enclosing the capsules had dissolved and more uniform swelling of the matrix had occurred (figure 5.7 (e)). Uniform swelling of material comprising the capsule may have provided more resistance to fragmentation and destruction as compared to the more uneven swelling observed in the earlier stages of hydration.

The mean time for capsules and tablets to reach the small intestine, ileocaecal junction and colon was calculated (table 6.5). This showed that the GI transit times of tablets and capsules were roughly similar. Capsules appeared to have slightly more variable GI transit times than tablets. The degree of integrity that each dosage form maintained as it passed through the GI tract varied between volunteers (appendix V). For example, in volunteer No. 1 the capsule formulation remained in the small intestine and existed mainly as a single source with diffusion around it for up to 420min. In contrast, when the capsule formulation was administered to volunteer No. 6, extensive swelling and erosion occurred after 90min, spreading to the transverse colon by 270min. Generally, the degree of variation between subjects appeared to be higher for the capsule formulation than the tablet formulation. This could be due to the wide variation in gastric motility that can exist between individuals and the resultant effect of mechanical agitation on destruction of capsule dosage forms.

	Mean gastro-intestinal transit time ± S.D (min)	
	Tablets	Capsules
Stomach	0.5 ± 0	0.5 ± 0
Small intestine	40 ± 15	30 ± 0
Ileocaecal junction	182 ± 47	215 ± 106
Colon	255 ± 65	250 ± 96

Table 6.5 Mean gastro-intestinal transit time of tablet sand capsules (n=6)

From the gamma scintigraphy results a number of clear observations could be made concerning the GI transit of pharmaceutically equivalent HP-based tablets and capsules; (a) capsule matrices fragmented earlier than capsule matrices; (b) more spreading of activity was noted in capsule matrices; (c) the GI transit time of both dosage forms was similar. Quantitative evaluation of the images would be required to more accurately assess the extent of swelling/dispersion and erosion. The degree to which the differences in fragmentation and erosion will affect bioavailability from each matrix will depend upon the drug under consideration. The fundamental parameters controlling bioavailability are dissolution of the drug and its gastrointestinal permeability (182). Drugs selected for extended release products should have good gastrointestinal permeability and an extended site of absorption (183). Four physiological factors have been identified that can also affect the release and absorption of a drug from an extended release product (183). Firstly, the residence times at each GI site. There is increasing evidence that the absorption of many drugs is not confined to the small intestine and significant absorption may occur in the colon (183). Colonic residence times are substantially larger than those in the small intestine and this may result in substantial absorption. Secondly, the effective permeability coefficient. Drugs are considered to be optimally absorbed from the upper part of the small intestine. Indirect evidence suggests that permeability decreases with distance down the GIT. Thirdly, pH/buffer capacity of the intestinal fluid. Substantial hydrogen ion changes occur with distance down the GI tract. There is an initial rise in pH on exiting the stomach, with pH continuing to rise down the small intestine until the caecum is reached at which point a drop in the order of 1 unit appears to occur. The pH then rises gradually down the colon. These pH changes

can have dramatic effects on ionisable drugs altering the proportion of ionised to nonionised and hence solubility and permeability. Acidic drugs will tend to have lower solubilities high up the GIT, with solubility increasing down the GIT. With increased ionisation intestinal permeability should fall. In contrast, bases will loose solubility with transit down the GIT, but become more permeable. Fourthly, the potential for drug degradation at different sites. Many drugs are metabolised in the colon and this may reduce the amount available for absorption. All of above factors may affect the rate and extent of absorption of a drug from an extended release product. Amidon *et al.* (182) established a biopharmaceutical classification for drugs taking into account that gastropermeability and solubility were fundamental in determining bioavailability. The aim of the classification was to assist in correlating *in vitro* drug product dissolution and *in vivo* bioavailability for IR products. The classes were defined as: Case 1. High solubility-high permeability drugs. Case 2. Low-solubility-high permeability drugs. Case 3. High solubility-low permeability drugs. Case 4. Low solubility-low permeability drugs. A modified biopharmaceutical classification for ER drugs has also been proposed, which does not consider drugs having low gastropermeability since these are unlikely to be formulated as ER products (183):

Class I Solubility high and independent of site
- (a) permeability-high and independent of site
- (b) permeability dependent on site-narrow absorption window

Class II Solubility low and independent of site
- (a) permeability high and independent of site
- (b) permeability dependent on site-narrow absorption window

Class V Variable solubility and permeability

This classification may be useful when attempting to assess on the basis of gamma scintigraphy results whether two dosage forms are likely to be bioequivalent. Drug products can be considered bioequivalent when the rate and extent of absorption of the therapeutic moiety from each product does not differ significantly when the same molar dose of the therapeutic moiety is administered under similar experimental conditions (184). Considering that HP-based capsule matrices under go fragmentation and possibly erosion earlier that tablet matrices then it is possible that for drugs that have

a high solubility and are absorbed in the upper part of the GIT that bioavailability from capsule and tablet matrices may not be comparable. However, because fragments tend to regroup forming single units then it is possible that bioavailability from capsules and tablets may be more similar in the lower part of the GIT. Therefore, if a drug was primarily absorbed in the lower part of the small intestine and/or colon then it is more likely that bioequivalence would be observed. Unfortunately, information on regional variations in drug permeability along the GIT is limited. Additionally, the pH and ionic strength of the GIT contents are often variable and difficult to measure making it difficult to predict the extent of drug ionisation. Therefore, for drugs that do not have a high water-solubility and high gastrointestinal permeability it may still be necessary to carry out *in vivo* pharmacokinetic studies in order to establish if capsule and tablet matrices are bioequivalent. Drugs that are marketed as ER products represent a small subgroup of those that are administered orally to man. Of these compounds 63% may be chemically classified as weak bases, the majority of which are incorporated in salt form (183). As weak bases lose solubility as they pass down the GIT absorption becomes more dissolution/release-controlled (183). So for the majority of drugs that have been marketed as ER products an increase in dissolution rate would probably increase bioavailability.

The USP II dissolution apparatus with paddles rotating at 50rpm and 100rpm did not identify any differences between the *in vitro* erosion and fragmentation of capsules and tablets. By testing the dosage forms under conditions of greater mechanical stresses then differences that have been observed *in vivo* may become apparent *in vitro*. A suitable apparatus may be the USP III (Biodis) apparatus, which employs a reciprocating basket. Dissolution in media having a range of ionic strength and pH's may also help to discriminate between the dosage form presentations. If dissolution conditions are found which mimic more closely how the dosage forms fragment and erode in the GIT then *in vitro* dissolution profiles of capsules and tablets under these conditions can be obtained. If similar release profiles from pharmaceutical equivalent capsules and tablets under these conditions were observed then this would support the argument that capsules and tablets could potentially be functionally interchangeable.

7.0 Conclusions and further work

The *in vitro* dissolution profiles of model drugs from hydrophilic matrix tablets based on HP were found to be independent of the initial bulk physical characteristics of the tablets. This is a useful characteristic of HP-based tablets, as small changes in processing conditions are unlikely to affect the *in vitro* and possibly *in vivo* dissolution behaviour of the product. Thus, tablet matrices based on HP are robust formulations.

Functional interchangeability of pharmaceutically equivalent tablet and capsule matrices containing diclofenac sodium, diltiazem HCl and propranolol HCl was established *in vitro,* using a USP II rotating paddle method. The high release controlling action of capsule matrices containing loose, uncompacted granules was considered due to the rapid hydration of HP-based material and the tendency of hydrated particles to coalesce, forming a continues viscous elastic network that had a high resistance to erosion. Functional interchangeability was attributed to similar diffusional path lengths existing within hydrated tablet and capsule matrices, despite more extensive swelling of capsule matrices.

Clear images of the transit of pharmaceutically equivalent tablet and capsule matrices based on HP through the GIT of 6 male volunteers were obtained using the technique of gamma scintigraphy. The images showed that capsule matrices fragmented earlier in the GIT than tablet matrices and that the spreading of capsule matrices was more extensive as compared to tablets. However, regrouping of the fragments meant that capsules still maintained a high degree of integrity after 7hr in the GIT. The results suggested that further *in vitro* dissolution testing using more aggressive testing conditions may help to predict whether capsules and tablets are likely to be functionally interchangeable *in vivo.* The USP III apparatus should be evaluated as a dissolution test method. This employs a reciprocating basket, which is likely to subject the dosage forms to higher mechanical stresses. Additionally, swelling, hydration and drug release from capsule and tablet matrices in media having different pH values and ionic strengths requires investigation. Statistical analysis of the gamma scintigraphy is also required in order to effectively compare the spreading, fragmentation and erosion of HP-based capsules and tablets. Quantification of the degree of swelling *in vitro* would be useful for comparative purposes.

It was found that HP-based material had a greater release controlling action than Methocel K15M, when the two materials were used in equivalent amounts. Mechanical strength studies had also shown that matrices based on HP had a greater resistance to a penetrating probe than matrices based on Methocel K15M. Therefore, it might be expected that under similar *in vivo* conditions, capsules matrices based on cellulose ethers such as Methocel K15M may under go a higher of destruction in the GIT as compared to HP-based capsules. An evaluation of the release sustaining action of capsule matrices formulated using different grades of cellulose ethers and other commonly used hydrophilic excipients would be of interest. An assessment could then be made of the effectiveness of HP, relative to other hydrophilic excipients, in formulating hydrophilic capsule matrices. The levels of hydrophilic carrier required to ensure that a coherent swollen body is formed could also be assessed along with the effect of capsule size and capsule fill weight on the dissolution of model drugs from capsule matrices.

A clear difference in mechanical strength of capsule and tablet matrices based on HP was observed using the penetrating probe method described. The mechanical strength of hydrated matrices may correlate with the degree of destruction that the dosage forms encounter in the GIT. This could be further investigated. Alternative methods of assessing the mechanical and physical characteristics of hydrated matrices could be also evaluated.

Although the pore structure of HP-based matrices was easily quantified using mercury porosimetry no correlation was observed between tablet pore structure and release controlling action. However, the pore structure of tablets may be related to other physical characteristics of tablets such as hardness and friability. Similarly, the porous structure of granules may influence the physical properties of granules. Further evaluation of the effect of granule and tablet pore structure on the mechanical properties of these materials would be interesting.

The interaction between drugs and HP is an area that would warrant further investigation. The degree to which drugs are involved in maintaining a strong hydrophilic network in HP-based matrices is not known. The investigations carried out here indicated a potential interaction between propranolol HCl and diltiazem HCl with

HP. It is possible that this also would be observed with other cationic drugs and possibly anionic and non-ionic materials. These interactions may largely determine the rate of release of the drug from the matrix.

A clear difference in the release controlling action of TIMERxN and BHP-based material has been observed. To fully explain these differences further studies to investigate the effect of the tertiary components ethylcellulose and calcium sulphate on release controlling action is required. Additional investigation into the effect of wet and alcoholic granulation on dissolution profiles may be useful in understanding the differences in release controlling action observed. A further area of investigation would involve a study of the effect of tertiary components on interactions between drugs and HP matrix components.

This work also suggested that wet granulation of TIMERxN components was not necessary to obtain a material that had a high release controlling action. However, this observation was made with one drug substance only and further studies using a range of drug entities would be necessary to evaluate the release characteristics of matrices containing a simple dry blend of HP components.

Dissolution studies showed that granules contained, uncompacted in hard gelatin capsules produced a dosage form that had a high release controlling action *in vitro*. The gamma scintigraphy study showed that capsule matrices maintained a high degree of integrity as they passed through the GIT. This suggests that capsule matrices may also have a high release sustaining action *in vivo*. Additionally, the dosage form is simple to produce, can be processed using standard powder processing and encapsulation equipment and has a high capacity to incorporate active principles. An *in vivo* study to determine the pharmacokinetics of drug release from these matrices would be useful to assess the potential of capsule matrices as simple controlled release dosage forms.

Appendix I

Mercury porosimetry calibration data

	Pressure kNm^{-2}	Micromeritic specifications	Reference sample
Total intrusion volume (ml/g)	414000	0.55 ± 0.03	0.521
	207000	0.51 ± 0.03	0.483
Median pore diameter (μm)	414000	0.0075 ± 0.0005	0.0072
	207000	0.0076 ± 0.0005	0.0073

Appendix II

Yates method for calculating magnitude of factors and interactions

Yield	I	II	III
$y_{(1)}$	$y_{(1)} + y_a$	$(y_{(1)} + y_a) + (y_b + y_{ab})$	$[(y_{(1)} + y_a) + (y_b + y_{ab})] + [(y_c + y_{ac}) + (y_{bc} + y_{abc})]$
y_a	$y_b + y_{ab}$	$(y_c + y_{ac}) + (y_{bc} + y_{abc})$	$[(y_a - y_{(1)}) + (y_{ab} - y_b)] + [(y_{ac} - y_c) + (y_{abc} - y_{bc})]$
y_b	$y_c + y_{ac}$	$(y_a - y_{(1)}) + (y_{ab} - y_b)$	$[(y_b + y_{ab}) - (y_{(1)} + y_a)] + [(y_{bc} + y_{abc}) - (y_c + y_{ac})]$
y_{ab}	$y_{bc} + y_{abc}$	$(y_{ac} - y_c) + (y_{abc} - y_{bc})$	$[(y_{ab} - y_b) - (y_a - y_{(1)})] + [(y_{abc} - y_{bc}) - (y_{ac} - y_c)]$
y_c	$y_a - y_{(1)}$	$(y_b + y_{ab}) - (y_{(1)} + y_a)$	$[(y_c + y_{ac}) + (y_{bc} + y_{abc})] - [(y_{(1)} + y_a) + (y_b + y_{ab})]$
y_{ac}	$y_{ab} - y_b$	$(y_{bc} + y_{abc}) - (y_c + y_{ac})$	$[(y_{ac} - y_c) + (y_{abc} - y_{bc})] - [(y_a - y_{(1)}) + (y_{ab} - y_b)]$
y_{bc}	$y_{ac} - y_c$	$(y_{ab} - y_b) - (y_a - y_{(1)})$	$[(y_{bc} + y_{abc}) - (y_c + y_{ac})] - [(y_b + y_{ab}) - (y_{(1)} + y_a)]$
y_{abc}	$y_{abc} - y_{bc}$	$(y_{abc} - y_{bc}) - (y_{ac} - y_c)$	$[(y_{abc} - y_{bc}) - (y_{ac} - y_c)] - [(y_{ab} - y_b) - (y_a - y_{(1)})]$

Appendix III

Calibration plots of benzamide in water at 228nm

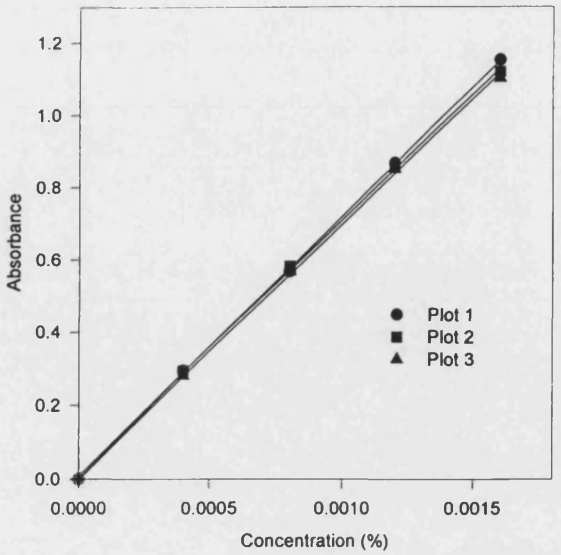

Calibration plots of diclofenac sodium in water at 273nm

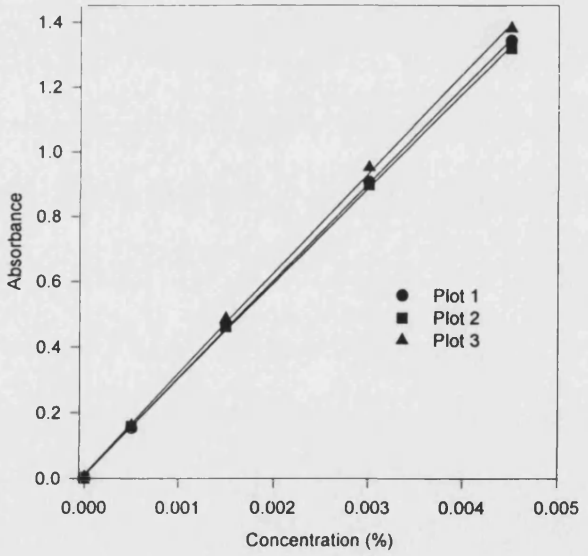

Calibration plots of diltiazem HCl in water at 236nm

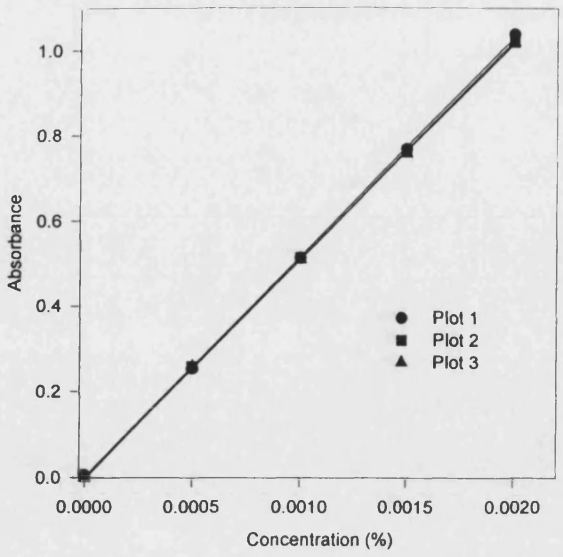

Calibration plots of propranolol HCl in water at 228nm

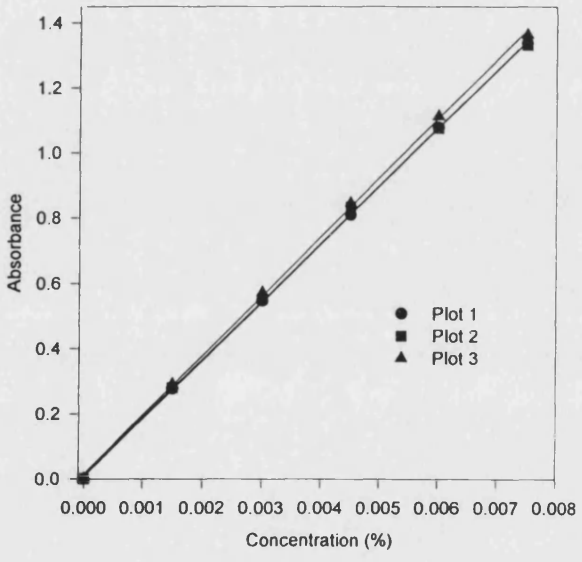

Calibration plots of frusemide in pH 5.8 phosphate buffer at 271nm

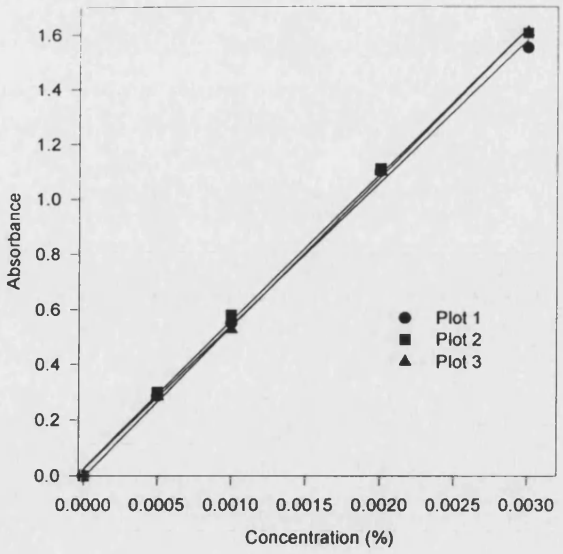

Appendix IV

Subject inclusion criteria:

Written and witnessed informed consent to participate in the trial given voluntarily

Healthy males between the ages of 18 and 45years

No clinically significant abnormal findings on the physical examination and medical history

No clinically significant abnormal laboratory values

Negative urine screen for alcohol and drugs of abuse

Body weight not more than 15% above or below the ideal weight for height an frame

Normal blood pressure measured after resting supine for 3min. Normal range 100 to 140mmHg systolic and 50 to 90mmHg diastolic

Normal heart rate in the range 50 to 90bpm

Able to communicate with the investigator and to comply with the requirements of the entire study

Subject exclusion criteria:

Participation in another trial within the past four weeks prior to or during the trial

History of alcohol or drug abuse within the last two years

History of allergic or adverse response to any of the polysaccharides used in this study

Any condition or disease, which in the opinion of the clinical investigator, would place the subject at undue risk, or interfere with the ability of the subject to complete the study

Abnormal diet, or substantial changes in eating habits in the past 30 days

Difficulty in swallowing capsules or tablets

Use of any alcoholic beverages within 48 hr of study initiation

Appendix V

Volunteer No. : 1

Tablet formulation

Time	Stomach	Small intestine	Ileocaecal Junction	Colon	Remarks
0	Observed				
30	Intact swollen				
60		Intact, swollen, bigger			
90		Two sources			
120		Two sources			
150		Two segments with dispersion in the image			
180		Segments regroup			Appears as 2 segments regrouped and behave as one unit
210		Dispersion in the image, one unit			
240		No movement, one unit and dispersing out			Possibly in ICJ
270			Segments are separating again	One segment in the ascending colon	
300				Clear image of dispersion of the tablets in the ascending colon, still 2 segments	
330				As above	
360				Still 2 pieces moving up in the ascending colon	
390				As above, more dispersion in the image observed	
420				As above, very little central activity, tablet broken down	

Volunteer No.: 1

Capsule formulation

Time	Stomach	Small intestine	Ileocaecal Junction	Colon	Remarks
0	Observed				Shape of capsule clearly seen
30		Swollen intact			
60		2 separate units, moving			
90		One fragment intact second diffusing out			
120		Static but diffusing, 2 fragments			
150		Static, 2 fragments with diffusion			
180		2 loose fragments			
210		Regrouping of fragments with diffusion radiating around it			
240		As above except more diffusion			
270		No movement, as above			
300		Appears as a single source with diffusion around it			
330		As above			
360		As above with more diffusion of radiation			
390		As above the source looks coherent			
420		As above			

Volunteer No.: 2

Tablet formulation

Time	Stomach	Small intestine	Ileocaecal Junction	Colon	Remarks
0	Observed				
30		Intact swollen			
60		Swollen, intact, much sharper view from posterior			
90		Intact, swollen			
120		Swollen further, intact			
150		As above			
180		As above but slowly diffusing			Could all be in ICJ
210		Traces of diffusion, intact			
240		As above			
270			Intact tablet, moving ahead leaving residues	Moving into ascending colon	
300				Ascending, 2 fragments observed with diffusion around them	
330				Moving up the as a single unit	
360				Single diffused unit moving up AC	
390				Tablet moving upwards in the AC leaving residues	
420				Bolus of activity halfway up ascending colon with trail of residues behind	

Volunteer No.: 2

Capsule formulation

Time	Stomach	Small intestine	Ileocaecal Junction	Colon	Remarks
0	Capsule observed intact, moving				
30		Moving single with swelling and residues			
60		2 fragments moving, posterior image of one unit			
90		Single unit with diffusion around it			
120		Vigorous movement of a single unit			
150		3 distinct fragments, SI or ICJ, with diffusion around	Possibly in ICJ		
180			Observed as 2 fragments ICJ/ASC colon leaving residues behind		
210				Regrouping of 2 fragments in ACJ/ASC colon	
240			Residues at ICJ	One fragment in AJC colon a clear 2nd fragment in the transverse colon	
270			Residues at ICJ	Residues at ICJ one fragment ASC and second at transverse colon	
300				As above, dispersion & residues	Dispersion and residues observed
330				As above	
360				As above with more dispersion and residues visible	
390				As above	
420				More evidence of dispersion of both fragments	

Volunteer No.: 3

Tablet formulation

Time	Stomach	Small intestine	Ileocaecal Junction	Colon	Remarks
0	Observed				
30		Observed, small swelling			
60		Intact with swelling			
90		Intact with swelling			
120		As above with larger image (swelling)			
150		Swelling with some dispersion but still intact			
180		Evidence of more dispersion of tablet	Moving into ICJ		
210			2 distinct segments well apart, 1 appears in ICJ/AC colon, the second in transverse colon		
240				2 segments regrouping in transverse colon	
270		Diffused image seen over the area		Still 2 segments with dispersion	
300			Diffused segment of tablet observed over the area		Part of the tablet in transverse colon
330			Extensive diffusion includes transverse colon		
360				Main bolus in AC+ bits in transverse colon	
390				As above	
420				As above	

Volunteer No.: 3

Capsule formulation

Time	Stomach	Small intestine	Ileocaecal Junction	Colon	Remarks
0	Observed, moving				
30		Single unit, seen as 2 due to moving			
60		Still single piece but moving, swelling			
90		Single unit with movement			
120		Single unit with some diffusion and swelling			
150		3-4 fragments with residues			
180		Regrouped and single unit image			
210		Single unit with diffusion around it			
240		Still in SI		Traces in AC but main unit in transverse colon	2 fragments, 1 moved ahead of the second
270*			Collecting at ICJ		Spread across SI down on left side of image
300			Anterior: low intensity image Posterior: high intensity image, 3 fragments		
330			As above		
360				Faint anterior image slight movement upwards	
390				As above	
420				As above	

*From 270min a collection of fragments with diffused radiation grouped together at ICJ and slowly empties into ascending colon

Volunteer No.: 4

Tablet formulation

Time	Stomach	Small intestine	Ileocaecal Junction	Colon	Remarks
0	Observed tablet, intact				
30		Swelling, single unit			
60		Single unit moved right down compared to marker			
90		Single unit with residues around it			
120		Large unit with residues around it			
150		Single unit with residues	Possibly at ICJ		
180		As above with trail of residues at the base of activity			
210		As above with more diffusion around			
240			2 fragments with diffusion around them		
270			Movement of 2 fragments with activity around them		
300			Appears as a single unit with some erosion		
330				The main single unit moving up the AC with residues behind	
360				In the AC with erosion, seen as a single unit	
390				Moving up the AC	
420				Still in the AC	

Volunteer No.: 4

Capsule formulation

Time	Stomach	Small intestine	Ileocaecal Junction	Colon	Remarks
0	Observed, intact				
30		Single unit very low position in abdomen			
60		2 fragments with movement			
90		Main unit still intact but erosion and residues observed			
120		2 fragments with residues around			Each fragment moving independently
150			Collecting as a single unit at the ICJ with residues to the right of image		
180				Spreading upwards into the AC (eroded)	
210				As above	
240				Moving up the AC as an eroded mass with 2 main fragments	
270				As above	
300				All at the lower end of the AC with sign of erosion around 1 or 2 main fragments (centre of source of radiation)	
330					
360					
390					
420					

Volunteer No.: 5

Tablet formulation

Time	Stomach	Small intestine	Ileocaecal Junction	Colon	Remarks
0	Observed intact				
30	Still in stomach, swollen				
60		Moving unit. Single tablet			Swollen
90		As above			Swollen
120		Lots of movement, more than 1 fragment			In fact is only one unit
150		Single unit with residues	Possibly at ICJ		
180			As above more diffusion		
210					
240			As above with more erosion		
270			As above		
300				Moving as two fragments in the AC	
330				Two clear fragments in AC with no movement	
360				Extensive erosion of the fragments in the AC	Two or more fragments
390				As above with more erosion	
420				Travelling up the AC	

Volunteer No.: 5

Capsule formulation

Time	Stomach	Small intestine	Ileocaecal Junction	Colon	Remarks
0	Observed with movement				
30		Moved down with swelling, single unit			
60		2 clear fragments			
90		Observed as a single unit (regrouping or superimposing)*			
120		Single unit with residues			
150		Single unit with extensive erosion			
180			Collection at ICJ with a single unit with residues around it		
210			As above, some movement		
240			As above with erosion and residues around it		
270			Stationary still one central source with residue around it		
300				At the lower end of the AC appears as one up to 360 min and then two units of fragments with extensive erosion and residues around the sources	
330					
360					
390					
420					

* 2 fragments possibly alongside each other thus seen as one source of activity

Volunteer No.: 6

Tablet formulation

Time	Stomach	Small intestine	Ileocaecal Junction	Colon	Remarks
0	Observed				
30		Movement, single unit			
60		Single unit with slight erosion			
90		Single unit with more erosion			
120		Movement as single unit into ICJ			
150				Erosion in AC, seen as a long extended source	
180				3 fragments along the AC colon	
210				Still 3 fragments with more diffused image (erosion)	
240				Fragments regrouped into 2 fragments	
270				As above with no movement	
300				2 fragments	In the upper part of AC with no movement
330				2 fragments	
360				More diffused image	
390				As above	
420				As above	

Volunteer No.: 6

Capsule formulation

Time	Stomach	Small intestine	Ileocaecal Junction	Colon	Remarks
0	Observed				
30	Main unit with some erosion in the stomach and small intestine				
60	Still the main fragment in the stomach with residues spread to right and left segments of SI				
90	Very little residues in stomach	Main unit and extensive spreading in the SI			
120		Spreading of activity around SI			
150		As above and collecting at the ICJ			
180				Spread of activity without evidence of a single fragment in the AC	
210				All in the AC	
240				AC as a mass	
270				Upper part of AC and start of transverse colon	
300				Spread of activity from AC to the end of the transverse colon	
330					
360					
390					
420					


0 min
30 min
90 min
180 min
360 min
Capsule formulation studied in volunteer no. 4
Speed

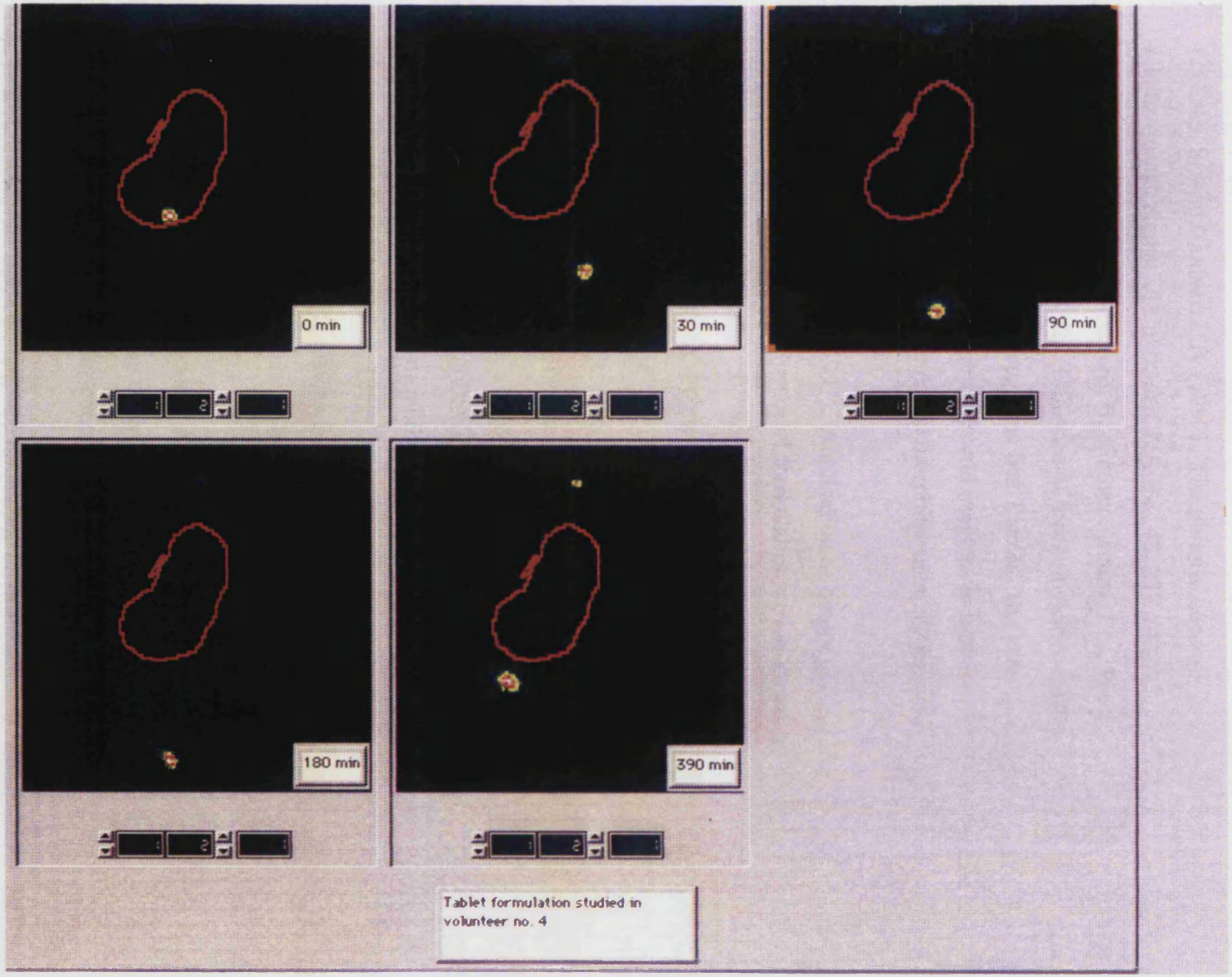
0 min
30 min
90 min
180 min
390 min
Tablet formulation studied in volunteer no. 4

References

(1) Lachman, L., Lieberman, H.A., and Kanig, J.L. (1986). The theory and practice of industrial pharmacy. **3rd** Philidelphia: Lea and Febiger. 0812109775.

(2) Saks, S., and Gardner, L.B. (1997). The pharmacoeconomic value of controlled release dosage forms. *J. Controlled Release.*, **48**, 237-242.

(3) Vazquez, M.J., Perez-Marcos, B., Gomez-Amoza, J.L., Martinez-Pacheco, R., Souto, C., and Concheiro, A. (1992). Influence of technological variables on release of drugs from hydrophilic matrices. *Drug Dev. Ind. Pharm.*, **18** (11&12), 1355-1375.

(4) Khan, M.Z. (1995). Recent trends and progress in sustained or controlled oral delivery of some water soluble drugs: morphine salts, diltiazem and captopril. *Drug Dev. Ind. Pharm.*, **21** (9), 1037-1070.

(5) Kim, H., and Fassihi, R. (1997). Application of binary polymer systems in drug release rate modulation. 2. Influence of formulation variables and hydrodynamic conditions on release kinetics. *J. Pharm. Sci.*, **86** (3), 323-328.

(6) Alderman, D.A. (1984). A review of cellulose ethers in hydrophilic matrices for oral controlled-release dosage forms. *Int. J. Pharm.*, **5** (3), 1-9.

(7) Langer, R., and Peppas, N.A. (1983). Chemical and physical structure of polymers as carriers for controlled release of bioactive agents: a review. *J. Macromol. Sci.*, **23**, 61-126.

(8) Melia, C.D., Binns, J.S., and David, S.T. (1985). Polymer hydration and drug distribution within gel layer hydrophilic matrix devices during drug release. *Int. J. Pharm. Tech. Prod. Manuf.*, **5**, 125P

(9) Rajabi-Siahboomi, A.R., Davies, M.C., and Melia, C.D. (1992). Probing the hydration of the surface gel layer in HMPC hydrophilic matrices. Proceed. 1st UKAPS Conference, STS, Cardiff. pp. 34

(10) Melia, C.D., Rajabi-Siahboomi, A.R., Hodsdon, A.C., Adler, J., and Mitchell, J.R. (1993). Structure and behaviour of hydrophilic matrix sustained release dosage forms: 1. The origin and mechanism of formation of gas bubbles in the hydrated surface layer. *Int. J. Pharm.*, **100**, 263-269.

(11) Hodsdon, A.C., Mitchell, J.R., Davies, M.C., and Melia, C.D. (1995). Structure and behaviour in hydrophilic matrix sustained release dosage forms: 3. The influence of pH on the sustained-release performance and internal gel structure of sodium alginate matrices. *J. Controlled Release.*, **33**, 143-152.

(12) Fan, L.T., and Singh, S.K. (1989). Controlled release. A quantitative treatment. Springer-Verlag.

(13) Ranga-Rao, K.V., and Padmalatha Devi, K. (1988). Swelling controlled-release systems: recent developments and applications. *Eur. J. Pharm. Biopharm.*, **48**, 1-13.

(14) Hussain, A.S., Johnson, R.D., Shivanand, P., and Zoglio, M.A. (1994). Effects of blending a nonionic and an anionic cellulose ether polymer on drug release from hydrophilic matrix capsules. *Drug Dev. Ind. Pharm.*, **20** (17), 2645-2657.

(15) Vazquez, M.J., Gomez-Amoza, J.L., Martinez-Pacheco, R., Souto, C., and Concheiro, A. (1995). Relationships between drug dissolution profile and gelling agent viscosity in tablets prepared with hydroxypropylmethylcellulose (HPMC) and sodium carboxymethylcellulose (NaCMC) mixtures. *Drug Dev. Ind. Pharm.*, **21** (16), 1859-1874.

(16) Shah, A.C., Britten, N.J., Olanoff, L.S., and Badalamenti, J.N. (1989). Gel-matrix systems exhibiting bimodal controlled release for oral drug delivery. *J. Controlled Release.*, **9**, 169-175.

(17) Colombo, P., Bettini, R., De Ascentiis, A., and Peppas, N.A. (1996). Analysis of the swelling and release mechanisms from drug delivery systems with emphasis on drug solubility and water transport. *J. Controlled Release.*, **39**, 231-237.

(18) Lee, P.I. (1991). Kinetic considerations of drug delivery from swelling-controlled and erosion/dissolution controlled systems. *Proced. Intern. Symp. Control. Rel. Bioact. Mater.*, **18**, 315-316.

(19) Baveja, S.K., Ranga-Rao, K.V., and Padmalatha Devi, K. (1987). Zero-order release hydrophilic matrix tablets of beta-adrenergic blockers. *Int. J. Pharm.*, **39**, 39-45.

(20) Lee, P.I. (1980). Diffusional release of a solute from a polymeric matrix: approximate analytical solutions. *J. Membr. Sci.*, **7**, 255-275.

(21) Higuchi, T. (1963). Mechanism of sustained-action medication. Theoretical analysis of rate of release of solid drugs dispersed in solid matrices. *J. Pharm. Sci.*, **52** (12), 1145-1149.

(22) Higuchi, W.I. (1962). Analysis of data on the medicament release from ointments. *J. Pharm. Sci.*, **51** (8), 802-804.

(23) Ritger, P.L., and Peppas, N.A. (1987). A simple equation for description of solute release II. Fickian and anomalous release from swellable devices. *J. Controlled Release.*, **5**, 37-42.

(24) Melia, C.D. (1991). Hydrophilic matrix sustained release systems based on polysaccharide carriers. *Critical Reviews in Therapeutic Drug Carrier Systems.*, **8** (4), 395-421.

(25) Sanchez, L., Torrado, S., and Lastres, J.L. (1995). Gelatinized/freeze-dried starch as excipient in sustained release tablets. *Int. J. Pharm.*, **115**, 201-208.

(26) Nigalaye, A.G., Adusumilli, P., and Bolton, S. (1990). Investigation of prolonged drug release from matrix formulations of chitosan. *Drug Dev. Ind. Pharm.*, **16** (3), 449-467.

(27) Mockel, J.E., and Lippold, B.C. (1993). Zero-order drug release from hydrocolloid matrices. *Pharm. Res.*, **10** (7), 1066-1069.

(28) Talukdar, M.M., and Kinget, R. (1995). Swelling and drug release behaviour of xanthan gum matrix tablets. *Int. J. Pharm.*, **120**, 63-72.

(29) Talukdar, M.M., Michoel, A., Rombaut, P., and Kinget, R. (1996). Comparative study on xanthan gum and hydroxypropylmethylcellulose as matrices for controlled-release drug delivery I. Compaction and in vitro drug release behaviour. *Int. J. Pharm.*, **129**, 233-241.

(30) Talukdar, M.M., and Kinget, R. (1997). Comparative study on xanthan gum and hydroxypropylmethylcellulose as matrices for controlled-release drug delivery. II. Drug diffusion in hydrated matrices. *Int. J. Pharm.*, **151**, 99-107.

(31) Te Wierik, G.H.P., Eissens, A.C., and Lerk, C.F. (1993). Preparation, characterisation and pharmaceutical application of linear dextrins: IV. Drug release from capsules and tablets containing amylodextrin. *Int. J. Pharm.*, **98**, 219-224.

(32) Perez-Marcos, B., Gutierrez, C., Gomez-Amoza, J.L., Martinez-Pacheco, R., Souto, C., and Concheiro, A. (1991). Usefulness of certain varieties of Carbomer in the formulation of hydrophilic furosemide matrices. *Int. J. Pharm.*, **67**, 113-121.

(33) Cooper, A.M., Doshi, D.H., and Paterl, M.V. (1995). In-vitro prolonged release of basic CNS componds from HPMC and Carbopol 974P hydrophilic matrices. *Proceed. Intern. Symp. Control. Rel. Bioact. Mater.*, **22**, 288-289.

(34) Baveja, S.K., Ranga-Rao, K.V., and Padmalatha Devi, K. (1988). Relationship between gum content and half-life of soluble beta blockers from hydrophilic matrix tablets. *Int. J. Pharm.*, **47**, 133-139.

(35) Mannion, R.O., Melia, C.D., Mitchell, J.R., Harding, S.E., and Green, A.P. (1984). Effects of xanthan/locust bean synergy on ibuprofen release from hydophophilic matrix tablets. *J. Pharm. Pharmacol.*, **43**, 76p

(36) Waaler, P.J., Andersen, M., Graffner, C., and Muller, B.W. (1992). Influence of compaction pressure on the properties of xanthan/guar gum matrix tablets. *Acta Pharm. Nord.*, **4** (3), 167-170.

(37) Tobyn, M.J., Staniforth, J.N., Baichwal, A.R., and McCall, T.W. (1996). Prediction of physical properties of a novel polysaccharide controlled release system. I. *Int. J. Pharm.*, **128**, 113-122.

(38) Staniforth, J.N., and Baichwal, A.R. (1993). Synergistically interacting heterodisperse polysaccharides: Function in achieving drug delivery. , 327-350. ACS Symposium series.

(39) Fitzpatrick, J.P. (1996). Xanthan gum in hydrophilic matrix drug delivery systems. *Excipients and delivery systems for pharmaceutical formulations.* , 123-132.

(40) Williams, P.A., and Phillips, G.O. (1995). Interactions in mixed polysaccharide systems. A.M. Stephen (ed.), *Food polysaccharides and their applications.* , 463-501. Marcel Dekker.

(41) Morris, V.J. (1995). Bacterial polysaccharides. A.M. Stephen (ed.), *Food polysaccharides and their applications.* , 431-375. Marcel Dekker.

(42) Atkins, E. (1990). Structure of microbial polysaccharides using x-ray diffraction. *Proceedings of the national research workshop on new biosynthetic biodegradable polymers from microorganisms.*, , 371-386.

(43) Rocks, J.K. (1971). Xanthan gum. *Food Technol.*, **25**, 476-483.

(44) Zatz, J.L. (1984). Viscosity of xanthan gum solutions at low shear rates. *J. Pharm. Sci.*, **73** (4), 468-471.

(45) Rol, F. (1973). Locust Bean Gum. R.L. Whistler & J.N. BeMiller (eds.), *Industrial Gums.* , 323-337. London: Academic press, inc. 0-12-746252-x.

(46) Dea, I.C.M., Allan, C.H., and McCleary, B.V. (1986). Effect of galactose-substitution-patterns on the inter-action properties of galactomannans. *Carbohydr. Res.*, **147**, 274-294.

(47) Craig, D.C., Kee, A., Tamburic, S., and Barnes, D. (1997). An investigation into the temperature dependence of the rheological synergy between xanthan gum and locust bean gum mixtures. *J. Biomater. Sci. Polymer Edn.*, **8** (5), 377-389.

(48) Copetti, G., Grassi, M., Lapasin, R., and Pricl, S. (1997). Synergistic gelation of xanthan gum with locust bean gum: a rheological investigation. *Glycoconjugate journal.*, **14**, 951-961.

(49) Whistler, R.L., and McCredie, R.J. (1959). Industrial gums. **1st** NY: Academic press, Inc.

(50) Tako, M., Asato, A., and Nakamura, S. (1984). Rheological aspects of the intermolecular interaction between xanthan and locust bean gum in aqueous media. *Agri. Biol. Chem.*, **48** (12), 2995-3000.

(51) Dea, I.C.M., Morris, E.R., Rees, D.A., Welsh, E.J., Barnes, H.A., and Price, J. (1977). *Carbohydr. Res.*, **57**, 249-272.

(52) Tako, M. (1991). Synergistic interaction between xanthan and tara-bean gum. *Carbohydr. Polym.*, **16**, 239-252.

(53) Cairns, P., Miles, M.J., and Morris, M.J. (1986). Intermolecular binding of xanthan gum and carob gum. *Nature.*, **322** (3), 89-90.

(54) Cairns, P., Miles, M.J., and Morris, V.J. (1987). X-ray fibre-diffraction studies of synergistic, binary polysaccharide gels. *Carbohydr. Res.*, **160**, 411-423.

(55) Morris, E.R., Rees, D.A., Young, G., Walkinshaw, M.D., and Darke, A. (1977). Order-disorder transition for a bacterial polysaccharide in solution. A role for polysaccharide conformation in recognition between *xanthomonas* pathogen and its plant host. *J. Mol. Biol.*, **110**, 1-16.

(56) Bos, M.A., Vennat, B., and Pourrat, A. (1994). Procyanidins gels: influence of ions on the gelification of carraghenan solutions. *Drug Dev. Ind. Pharm.*, **20** (10), 1821-1828.

(57) Lahaye, M., and Axelos, M.A.V. (1993). Gelling properties of water-soluble polysaccharides from proliferating marine green seaweed (Ulva spp.). *Carbohydr. Polym.*, **22**, 261-265.

(58) Hodsdon, A.C., Mitchell, J.R., Davies, M.C., and Melia, C.D. (1993). The influence of pH and calcium ions on the gel structure of sodium alginate hydrophilic matrix systems. *Proceed. Intern. Symp. Control. Rel. Bioact. Mater.*, **20**, 228-229.

(59) Stockwell, A.F., Davis, S.S., and Walker, S.E. (1986). In-vitro evaluation of alginate gel systems as sustained release drug delivery systems. *J. Controlled Release.*, **3**, 167-175.

(60) Abrahamsson, B., Alpsten, M., Bake, B., Larsson, A., and Sjogren, J. (1998). In vitro and in vivo erosion of two different hydrophilic gel matrix tablets. *Eur. J. Pharm. Biopharm.*, **46**, 69-75.

(61) Nakano, M., Ohmori, N., Ogata, A., Sugimoto, K., Tobino, Y., Iwaoku, R., and Juni, K. (1983). Sustained release of theophylline from hydroxypropylcellulose tablets. *Pharmaceutical Sciences.*, **72** (4), 378-380.

(62) Daly, P.B., Davis, S.S., and Kennerley, J.W. (1984). The effect of anionic surfactants on the release of chlorpheneramine from a polymer matrix tablet. *Int. J. Pharm.*, **18**, 201-205.

(63) Ford, J.L., Rubinstein, M.H., and Hogan, J.E. (1985). Propranolol hydrochloride and aminophylline release from matrix tablets containing hydroxypropylmethylcellulose. *Int. J. Pharm.*, **24**, 339-350.

(64) Sung, K.C., Nixon, P.R., Skoug, J.W., Ju, T.R., Gao, P., Topp, E.M., and Patel, M.V. (1996). Effect of formulation variables on drug and polymer release from HPMC-based matrix tablets. *Int. J. Pharm.*, **142**, 53-60.

(65) United States Pharmacopeial Convention. (1994). The United States Pharmcaoepia. **23rd** Rockville, MD: 0913595810.

(66) Mitchell, K., Ford, J.L., Armstrong, D.J., Elliott, P.N.C., Hogan, J.E., and Rostron, C. (1993). The influence of substitution type on the performance of methylcellulose and hydroxypropylmethylcellulose in gels and matrices. *Int. J. Pharm.*, **100**, 143-154.

(67) Bonferoni, M.C., Rossi, S., Ferrari, F., Bertoni, M., Sinistri, R., and Caramella, C. (1995). Characterisation of three hydroxypropylmethylcellulose substitution types: rheological properties and dissolution behaviour. *Eur. J. Pharm. Biopharm.*, **41** (4), 242-246.

(68) Dahl, T.C., Calderwood, T., Bormeth, A., Trimble, K., and Piepmeier, E. (1990). Influence of physio-chemical properties of hydroxypropylmethylcellulose on naproxen release from sustained release matrix tablets. *J. Controlled Release.*, **14**, 1-10.

(69) Ford, J.L., Rubinstein, M.H., McCaul, F., Hogan, J.E., and Edgar, P.J. (1987). Importance of drug type, tablet shape and added diluents on drug release kinetics from hydroxypropylmethylcellulose matrix tablets. *Int. J. Pharm.*, **40**, 223-234.

(70) Pagay, S.N. (1988). Use of buffers in matrix capsule formulations. *Drug Dev. Ind. Pharm.*, **14** (7), 875-894.

(71) Dhopeshwarker, V., and Zatz, J.L. (1993). Evaluation of xanthan gum in the preparation of sustained release matrix tablets. *Drug Dev. Ind. Pharm.*, **19** (9), 999-1017.

(72) Mitchell, K., Ford, J.L., Armstrong, D.J., Elliott, P.N.C., Hogan, J.E., and Rostron, C. (1993). The influence of particle size of hydroxypropylmethylcellulose K15M on its hydration and performance in matrix tablets. *Int. J. Pharm.*, **100**, 175-179.

(73) Shah, N., Railkar, A.S., Phuapradit, W., Zeng, F., Chen, A., Infeld, M.H., and Malick, A.W. (1996). Effect of processing techniques in controlling release rate and

mechanical strength of hydroxypropylmethylcellulose based hydrogel matrices. *Eur. J. Pharm. Biopharm.*, **42** (3), 183-187.

(74) Mosquera, M.J., Cuna, M., Souto, C., Concherio, A., Martinez-Pacheco, R., and Gomez-Amoza, J.L. (1996). Effects of hydroxymethylpropylcellulose (HPMC) moisture content on hydrochlothiazide release from HPMC-based tablets. *Int. J. Pharm.*, **135**, 147-149.

(75) Ford, J.L., Rubinstein, M.H., and Hogan, J.E. (1985). Dissolution of a poorly soluble drug, indomethacin, from hydroxypropylmethylcellulose controlled release tablets. *Proceed. Intern. Symp. Control. Rel. Bioact. Mater.*, **37**, 33P

(76) Ranga-Rao, K.V., Padmalatha Devi, K., and Buri, P. (1990). Influence of molecular size and water solubility of the solute on its release from swelling and erosion controlled polymeric matrices. *J. Controlled Release.*, **12**, 133-141.

(77) Baveja, S.K., Ranga-Rao, K.V., Singh, A., and Gombar, V.K. (1988). Release characteristics of some bronchodilators from compressed hydrophilic polymeric matrices and their correlation with molecular geometry. *Int. J. Pharm.*, **41**, 55-62.

(78) Tahara, K., Yamamoto, K., and Nishihata, T. (1996). Application of model-independent and model analysis for the investigation of effect of drug solubility on its release rate from hydroxypropyl methylcellulose sustained release tablets. *Int. J. Pharm.*, **133**, 17-27.

(79) Malamataris, S., and Ganderton, D. (1991). Sustained release from matrix systems comprising hydrophobic and hydrophilic (gel-forming) parts. *Int. J. Pharm.*, **70**, 69-75.

(80) Ford, J.L., Rubinstein, M.H., and Hogan, J.E. (1985). Formulation of sustained release promethazine hydrochloride tablets using hydroxypropylmethycellulose matrices. *Int. J. Pharm.*, **24**, 327-338.

(81) El-Arini, S.K., and Leuenberger, H. (1995). Modelling of drug release from polymer matrices: effect of drug loading. *Int. J. Pharm.*, **121**, 141-148.

(82) Mitchell, K., Ford, J.L., Armstrong, D.J., Elliott, P.N.C., Hogan, J.E., and Rostron, C. (1993). The influence of drugs on the properties of gels and swelling characteristics of matrices containing methylcellulose or hydroxypropylmethylcellulose. *Int. J. Pharm.*, **100**, 165-173.

(83) Lapidus, H., and Lordi, N.G. (1966). Some factors affecting the release of a water-soluble drug from a compressed hydrophilic matrix. *J. Pharm. Sci.*, **55** (8), 840-843.

(84) Efentakis, M., Viachou, M., and Choulis, N.H. (1997). Effects of excipients on swelling and drug release from compressed matrices. *Drug Dev. Ind. Pharm.*, **23** (1), 107-112.

(85) Pharm, A.T., and Lee, P.I. (1994). Probing the mechanisms of drug release from hydroxypropylmethylcellulose matrices. *Pharm. Res.*, **11** (10), 1379-1384.

(86) Touitou, E., and Donbrow, M. (1982). Influence of additives on (hydroxyethyl) methylcellulose properties: relation between gelation temperature change, compressed matrix integrity and drug release profile. *Int. J. Pharm.*, **11**, 131-148.

(87) Rajabi-Siahboomi, A.R., Davies, M.C., and Melia, C.D. (1994). Identification of active molecular structures in thermally dependent release behaviour of diclofenac sodium from HPMC matrices. *Proceed. Intern. Symp. Control. Rel. Bioact. Mater.*, **21**, 25-26.

(88) Feely, L.C., and Davis, S.S. (1988). The influence of polymeric excipients on drug release from hydroxypropylmethylcellulose matrices. *Int. J. Pharm.*, **44**, 131-139.

(89) Rizk, S., Guyot, J.C., Duru, C., and Gaudy, D. (1995). Influence of lubricant properties on compression behaviour and drug dissolution rate of scleroglucan hydrophilic matrix. *Int. J. Pharm.*, **126**, 57-63.

(90) Bansal, P., Ranga-Rao, K.V., Plakogiannis, F., and Roscoff, M. (1992). Hydophilic matrix for a water-soluble drug. *Proceed. Intern. Symp. Control. Rel. Bioact. Mater.*, **19**, 269-270.

(91) Bettini, R., Colombo, P., Catellani, P.L., and Vitali, T. (1994). Swelling and drug release in hydrogel matrices: Polymer viscosity and matrix porosity effects. *Eur. J. Pharm. Biopharm.*, **2**, 213-219.

(92) Korsmeyer, R.W., Gurny, R., Doelker, E., Buri, P., and Peppas, N.A. (1982). Mechanisims of potassium chloride release from compressed hydrophilic, polymeric matrices: effect of entrapped air. *J. Pharm. Sci.*, **72** (10), 1189-1191.

(93) Hashim, and Li Wan Po. (1987). Improving release characteristics of water-soluble drugs from sustained release hydrophilic matrices by in situ gas generation. *Int. J. Pharm.*, **35**, 201-209.

(94) Van der Veen, J., Te Wierik, G.H.P., Van der Wal, L., Eissons, A.C., and Lerk, C.F. (1994). Controlled release of theophylline monohydrate from amylodextrin tablets: *in vitro* observations. *Pharm. Res.*, **11** (4), 499-502.

(95) Rizk, S., Duru, C., Gaudy, D., Jacob, M., Colombo, P., and Massimo, G. (1994). Natural polymer hydrophilic matrix: influencing drug release factors. *Drug Dev. Ind. Pharm.*, **20** (16), 2563-2574.

(96) Kawashima, Y., Takeuchi, H., Hino, T., Niwa, T., Lin, T., and Sekigawa, F. (1993). Preparation of a sustained-release matrix tablet of acetaminophen with pulverised low-substituted hydroxypropylcellulose via dry granulation. *Chem. Pharm. Bull.*, **41** (10), 1827-1831.

(97) Te Wierik, G.H.P., Eissens, A.C., Bergsma, J., Arends-Scholte, A.W., and Bolhuis, G.K. (1997). A new generation starch product as excipient in pharmaceutical tablets III. Parameters affecting controlled drug release from tablets based on high surface area retrograded pregelatinised potato starch. *Int. J. Pharm.*, **157**, 181-187.

(98) Sheth, P.R., and Tossounian, J. (1984). The hydrodynamically balanced system (HBSTM)-A novel drug delivery system for oral use. *Drug Dev. Ind. Pharm.*, **10** (2), 313-339.

(99) Augsburger, L.L., and Ashraf, M. (1987). The effect of formulation and process variables on drug release from sustained release matrix capsules containing hydroxypropylcellulose, NF. *Pharm. Res.*, **4**, S-27

(100) Lehr, C., Bouwstra, J.A., Schacht, E., and Junginger, H.E. (1992). In vitro evaluation of mucoadhesive properties of chitosan and some other natural polymers. *Int. J. Pharm.*, **78**, 43-48.

(101) Khan, M.Z. (1996). Dissolution testing for sustained or controlled release oral dosage forms and correlation with in vivo data: challenges and opportunities. *Int. J. Pharm.*, **140**, 131-143.

(102) Fagan, P.P., Harrison, P.J., and Shankland, N. (1989). A correlation between cloud point and disintegration of hydroxyalkylcellulose controlled release matrices. *J. Pharm. Pharmacol.*, **41**, 25p

(103) Shameem, M., Katori, N., Aoyagi, N., and Kojima, S. (1995). Oral solid controlled release dosage forms: role of GI mechanical destructive forces and colonic release in drug absorption under fasted and fed conditions in humans. *Pharm. Res.*, **12**, 1049-1054.

(104) Butler, J., Devane, J., Fogarty, F., and Young, D. (1995). Lack of in vivo impact of ionic concentration on a HPMC formulation. *Pharm. Res.*, **12**, S-250

(105) Fell, J.T., and Digenis, G.A. (1984). Imaging and behaviour of solid oral dosage forms *in vivio*. *Int. J. Pharm.*, **22**, 1-15.

(106) Davis, S.S. (1985). The design and evaluation of controlled release systems for the gastrointestinal tract. *J. Controlled Release.*, **2**, 27-38.

(107) Brittain, H.G., Bogdanowich, S.J., Bugay, D.E., DeVincentis, J., Lewen, G., and Newman, A.W. (1991). Physical characterization of pharmaceutical solids. *Pharm. Res.*, **8** (8), 963-973.

(108) Ganderton, D., and Selkirk, A.B. (1969). The effect of granule properties on the pore structure of tablets of sucrose and lactose. *J. Pharm. Pharmacol.*, **22**, 345-353.

(109) Dees, P.J., and Polderman, J. (1981). Mercury porosimetry in pharmaceutical technology. *Powder Technol.*, **29**, 187-197.

(110) Van Brakel, J., Modry, S., and Svata, M. (1981). Mercury porosimetry: State of the art. *Powder Technol.*, **29**, 1-12.

(111) UK Compaction simulator group. (1996). Minutes of compaction simulator user groups meeting. **March 1996**

(112) Doelker, E. (1993). Comparative compaction properties of various microcrystalline cellulose types and generic products. *Drug Dev. Ind. Pharm.*, **19** (17&18), 2399-2471.

(113) Clarke, M.J., Potter, U.J., Gilpin, C., Tobyn, M.J., and Staniforth, J.N. (1998). Imaging of hygroscopic ultrafine pharmaceutical powders using low temperature and enviromental scanning electron microscopy. *Pharmacy and pharmacology communications.*, **4**, 419-425.

(114) Ganderton, D., and Selkirk, A.B. (1970). The effect of granule properties on the pore structure of tablets of sucrose and lactose. *J. Pharm. Pharmacol.*, **22**, 345-353.

(115) Carstensen, J.T., and Hou, X. (1985). The Athy-Heckel equation applied to granular agglomerates of basic tricalcium phosphate. *Powder Technol.*, **42**, 153-157.

(116) Washburn, E.W. (1921). Note on a method of determining the distribution of pore sizes in a porous material. *Proc. National Academy Sci.*, **7**, 115-116.

(117) Ganderton, D., and Hunter, B.M. (1971). A comparison of granules prepared by pan granulation and by massing and screening. *J. Pharm. Pharmacol.*, **23**, 1S-10S.

(118) Sheskey, P.J., and Williams, D.M. (1996). Comparison of low-shear and high-shear wet granulation techniques and the influence of percent water addition in the preparation of a controlled-release matrix tablet containing HPMC and a high-dose, highly water-soluble drug. *Pharmaceutical Technology.*, , 80-92.

(119) Dullien, F.A. (1981). Wood's metal porosimetry and its relation to mercury porosimetry. *Powder Technol.*, **29**, 109-116.

(120) Westermarck, S., Juppo, A.M., Kervinen, L., and Yliruusi, J. (1998). Pore structure and surface area of mannitol powder, granules and tablets determined with mercury porosimetry and nitrogen adsorption. *Eur. J. Pharm. Biopharm.*, **46**, 61-68.

(121) Brakel, J.V., Modry, S., and Svata, M. (1981). Mercury porosimetry: state of the art. *Powder Technol.*, **29**, 1-12.

(122) Brunauer, S., and Emmett, P.H. (1937). The use of low temperature Van der Waals adsorbtion isotherms in determining the surface area of various adsorbents. *J. Am. Chem Soc.*, **59**, 1553-1564.

(123) Newman, A.W. (1995). Micromeritics. H.G. Brittain (ed.), *Physical characterisation of pharmaceutical solids.* , 253-280. New York: Marcel Dekker, Inc. 0-8247-9372-2.

(124) Wade, A., and Weller, P.J. (1994). Handbook of pharmaceutical excipients. **2nd** Washington and London: American Pharmaceutical Association and the Pharmaceutical Press. 0-85369-305-6.

(125) Pesonen, T., and Paronen, P. (1986). Evaluation of a new cellulose material as binding agent for direct compression of tablets. *Drug Dev. Ind. Pharm.*, **12** (11-13), 2091-2111.

(126) Alderborn, G., and Wikberg, M. (1996). J. Warbrick (ed.), *Pharmaceutical powder compaction technology.* Marcel Dekker Inc.

(127) Zuurman, K., Riepma, K.A., Bolhuis, G.K., Vromans, H., and Lerk, C.F. (1994). The relationship between bulk density and compactibility of lactose granulations. *Int. J. Pharm.*, **102**, 1-9.

(128) Selkirk, A.B., and Ganderton, D. (1970). The influence of wet and dry granulation methods on the pore structure of lactose tablets. *J. Pharm. Pharmacol.*, **22** (suppl.), 86S-94S.

(129) Wikberg, M., and Alderborn, G. (1991). Compression characteristics of granulated materials. IV. The effect of granule porosity on the fragmentation propensity and the compactibility of some granulations. *Int. J. Pharm.*, **69**, 239-253.

(130) Tapper, G.I., and Lindberg, N.O. (1986). The granulation of some lactose qualities with different particle size distributions in a domestic-type mixer. *Acta Pharm. Suec.*, **23**, 47-56.

(131) Healey, J.N.C., Humphreys-Jones, J.F., and Walters, V. (1973). The effects of granule porosity and strength on the porosity, air permeability and tensile strength of tablets. *J. Pharm. Pharmacol.*, **25**, 110P

(132) Juppo, A.M., and Yliruusi, J. (1994). Effect of amount of granulation liquid on total pore volume and pore size distribution of lactose, glucose and mannitol granules. *Eur. J. Pharm. Biopharm.*, **40** (5), 299-309.

(133) Juppo, A.M. (1996). Porosity parameters of lactose, glucose and mannitol tablets obtained by mercury porosimetry. *Int. J. Pharm.*, **129**, 1-12.

(134) Wikberg, M., and Alderborn, G. (1992). Compression characteristics of granulated materials, assessed by mercury penetration, of compacts of two lactose granulations with different fragmentation propensities. *Int. J. Pharm.*, **84**, 191-195.

(135) Juppo, A.M., Kervinen, L., Yliruusi, J., and Kristoffersson, E. (1995). Compression of lactose, glucose and mannitol granules. *J. Pharm. Pharmacol.*, **47**, 543-549.

(136) Davies, O.L. (1993). *The design and analysis of industrial experiments.* Cambridge: Royal Society of Chemistry. 0851861377.

(137) Nokhodchi, A., Ford, J.L., Rowe, P.H., and Rubinstein, M.H. (1996). The effects of compression rate and force on the compaction properties of different viscosity grades of hydroxypropylmethylcellulose 2208. *Int. J. Pharm.*, **129**, 21-31.

(138) Malamataris, S., and Talukdar, M.M. (1994). Effect of particle size and sorbed moisture on the tensile strength of some tableted hydroxypropylmethylcellulose (HPMC) polymers. *Int. J. Pharm.*, **104**, 115-123.

(139) Wade, A. (1980). Pharmaceutical handbook. **19th** London: The Pharmaceutical Society of Great Britain. 0853691304.

(140) Jaegerskou, A., Holm, P., Schaefer, T., and Kristensen, H., G. (1984). Granulation in high speed mixers Part 3: effects of process variables on intragranular porosity. *Pharm. Ind.*, **46** (3), 310-314.

(141) Augsburger, L.L., and Vappala, M.K. (1996). Theory of granulation. D.M. Parikh (ed.), *Handbook of granulation technology.* , 7-23. NY: Marcel Dekker. 0-8247-9882-1.

(142) Wikberg, M., and Alderborn, G. (1990). Compression characteristics of granulated materials II. Evaluation of granule fragmentation during compression by tablet permeability and porosity measurements. *Int. J. Pharm.*, **62**, 229-241.

(143) Wells, J.I., and Walker, C.V. (1983). The influence of granulating fluids upon granule and tablet properties: the role of secondary binding. *Int. J. Pharm.*, **15**, 97-111.

(144) Ritala, M., Holm, P., and Kristensen, A. (1988). Influence of liquid bonding strength on power consumption during granulation in a high shear mixer. *Drug Dev. Ind. Pharm.*, **14** (8), 1041-1060.

(145) Rekhi, G.S., and Vuppala, M.K. (1997). D.M. Parikh (ed.), *Handbook of pharmaceutical granulation technology.* , 389 Marcel Dekker Inc.

(146) Nystrom, C., and Karehill, P. (1996). The importance of intermolecular bonding forces and the concept of bonding surface area. G. Alderborn & C. Nystrom (eds.), *Pharmaceutical powder compaction technology.* , 17-53. NY: Marcel Dekker. 0-8247-9376-5.

(147) Van der Voort Maarschalk, K., Vromans, H., Bolhuis, G.K., and Lerk, C.F. (1996). The effect of viscoelasticity and tabletting speed on consolidation and relaxation of a viscoelastic material. *Eur. J. Pharm. Biopharm.*, **42** (1), 49-55.

(148) Roberts, R.J., and Rowe, R.C. (1985). The effect of punch velocity on the compaction of a variety of materials. *J. Pharm. Pharmacol.*, **37**, 377-384.

(149) Vromans, H., Bolhuis, G.K., Lerk, C.F., Kussendrager, K.D., and Bosch, H. (1986). Studies on tableting properties of lactose VI. Consolidation and compaction of spray dried amorphous lactose. *Acta Pharm. Suec.*, **23**, 231-240.

(150) Roberts, R.J., and Rowe, R.C. (1986). The effect on the relationship between punch velocity and particle size on the compaction behaviour of materials with varying deformation mechanisms. *J. Pharm. Pharmacol.*, **38** (8), 567-571.

(151) Juppo, A.M. (1996). Change in porosity parameters of lactose, glucose and mannitol granules caused by low compression force. *Int. J. Pharm.*, **130**, 149-157.

(152) Train, D. (1957). Transmission of forces through a powder mass during the process of pelleting. *Transactions of the Institution of Chemical Engineers.*, **35**, 258-266.

(153) Budavari, S. (1996). The Merck index. **12th** NJ: Merck Research Laboratories. 0911910-12-3.

(154) Lund, W. (1994). The Pharmaceutical Codex. **12th** London: Royal Pharmaceutical Society of Great Britain. 0-085369-290-4.

(155) Durrani, M.J., Todd, R., Whitaker, R.W., Greenberg, E., and Benner, S.C. (1992). Polymer concentration effects on carbopol 934P tablets for controlled release. *Proceed. Intern. Symp. Control. Rel. Bioact. Mater.*, **19**, 1237

(156) Talukdar, M.M., and Plazier-Vercammen, J. (1993). Evaluation of xanthan gum as a hydrophilic matrix for controlled-release dosage form preparations. *Drug Dev. Ind. Pharm.*, **19** (9), 1037-1046.

(157) Lee, P.I. (1985). Kinetics of drug release from hydrogel matrices. *J. Controlled Release.*, **2**, 277-288.

(158) Leuenberger, H., Imanidis, G., and Usteri, M. (1987). Monitoring the granulation process by power consumption measurement. *Acta Pharm. Suec.*, **24** (2), 57-58.
(159) Bonny, J.D., and Leuenberger, H. (1991). Matrix type controlled release systems: I. Effect of percolation on drug dissolution kinetics. *Pharmaceutic Acta Helvetiae.*, **66** (5-6), 160-164.
(160) Carabello, I., Millan, M., and Rabasco, A.M. (1996). Relationship between drug percolation threshold aand particle size in matrix tablets. *Pharm. Res.*, **13** (3), 387-390.
(161) Khankari, R.K., and Hontz, J. (1997). Binders and solvents. D.M. Parikh (ed.), *Handbook of pharmaceutical granulation technology.* , 59-73. NY: Marcel Dekker. 0-8247-9882-1.
(162) Chen, G., and Hao, W. (1998). In vitro performance of floating sustained release capsule of verapamil. *Drug Dev. Ind. Pharm.*, **24** (11), 1067-1072.
Colorcon. (1998). Methocel K15M Premium. Technical literature.

(164) Lee, P.I., and Peppas, N.A. (1987). Prediction of polymer dissolution in swellable controlled-release systems. *J. Controlled Release.*, **6**, 207-215.
(165) Pharm, A.T., and Lee, P.I. (1993). Probing the mecahnism of drug release from hydroxypropylmethylcellulose (HMPC) matrices. *Proceed. Intern. Symp. Control. Rel. Bioact. Mater.*, **20**, 339-340.
(166) Lin, S., and Perng, R. (1992). Adsorption and desorption of indomethacin on cellulose-like biopolymers: chitin and chitosan. *Chem. Pharm. Bull.*, **40** (4), 1058-1060.
(167) Rivera, S.L., and Ghodbane, S. (1994). In vitro adsorption-desorption of famotidine on microcrystalline cellulose. *Int. J. Pharm.*, **108**, 31-38.
(168) Aly, S.A.S., and Udeala, O.K. (1987). Drug excipient interaction: effect of adsorption of oxytetracycline hydrochloride by some tablet excipients on the dissolution profile of the tablets. *S.T.P.Pharma.*, **3** (1), 23-27.
(169) Al-nimry, S., Assaf, S.M., Jalal, I.M., and Najib, N.M. (1997). Adsorption of ketotifen onto some pharmaceutical excipients. *Int. J. Pharm.*, **149**, 115
(170) Okada, S., Nakahara, H., and Isaka, H. (1987). Adsorption of drugs on microcrystalline cellulose suspended in aqueous solutions. *Chem. Pharm. Bull.*, **35**, 761-768.
(171) Hogan, J.E., Ford, J.L., Dabbagh, M.A., and Rubinstein, M.H. (1994). Release of propranolol HCl from mixed cellulose matrices. *Proceed. Intern. Symp. Control. Rel. Bioact. Mater.*, **21**, 732-733.

(172) Mitchell, K., Ford, J.L., Armstrong, D.J., Elliott, P.N.C., Rostron, C., and Hogan, J.E. (1993). The influence of concentration on the release of drugs from gels and matrices containing Methocel. *Int. J. Pharm.*, **100**, 155-163.

(173) Lindner, W.D., and Lippold, B.C. (1995). Drug release from hydrocolloid embeddings with high or low susceptibility to hydrodynamic stress. *Pharm. Res.*, **12** (11), 1781-1785.

(174) www.usp.org/pubs/newspf/news034a.htm. (1997). USP Pharmaceutical Forum. Standard issues for the health care practitioner. **Issue No. 34**

(175) Fu Lu, M., Woodward, L., and Borodkin, S. (1991). Xanthan gum and alginate based controlled release theophylline formulations. *Drug Dev. Ind. Pharm.*, **17** (14), 1987-2004.

(176) Harris, D., Fell, J.T., Sharma, H.L., and Taylor, D.C. (1990). GI transit of potential bioadhesive formulation in man: A scintographic study. *J. Controlled Release.*, **12**, 45

(177) Davis, S.S., Khosla, R., Wilson, C.G., and Washington, N. (1987). Gastrointestinal transit of a controlled-release pellets formulation of tiaprofenic acid and the effect of food. *Int. J. Pharm.*, **35**, 253-258.

(178) Hey, H., Jorgensen, F., Sorensen, K., Hasssssselbalch, H., and Wamberg, T. (1982). Oesophageal transit of six commonly used tablets and capsules. *British medical journal.*, **285**, 1717-1719.

(179) Muller-Lissner, S.A., and Blum, A.L. (1981). The effect of specific gravity and eating on gastric emptying of slow release capsules. *New England Jouranl of Medicine.*, **304** (22), 1365-1366.

(180) Daly, P.B., Davis, S.S., Frier, M., Kennerley, J.W., and Wilson, J.W. (1982). Scintigraphic assessment of the *in vivo* dissolution rate of a sustained release tablet. *Int. J. Pharm.*, **10**, 17-24.

(181) Abrahamsson, B., Alpsten, M., Hugossnon, M., Jonsson, U.E., Sundgren, M., Svenhenden, A., and Tolli, J. (1993). Absorption, gastrointestinal Transit, and tablet erosion of felodipine extended release (ER) tablets. *Pharm. Res.*, **10** (5), 709-714.

(182) Amidon, G.L., Lennernas H., Shah, V.P., Crison, J.R. (1995). Theoretical basis for a biopharmaceutic drug classification-the correlation of in vitro drug product dissolution and in vivo bioavailability. *Pharm.Res.* **12** (3), 413-420.

(183) Corrigan, O.I (1997). The biopharmaceutic drug classification and drugs administered in extended release (ER) formulations. *In vitro-in vivo correlations*. Young,

D. Devane, J.D. and Butler,J (eds). Advances in experimental medicine and biology Volume 423. 111-128 N.Y: Plenum Publishing Corporation. 0-306-45600-1.

(184) Approved drug products with therapeutic equivalence, 19th edition, April 1999. Centre for drug evaluation and research. Food and Drug Administration.